# 3.0 THERMAL EVALUATION

This chapter identifies and describes the principal thermal design aspects of the Advanced Test Reactor (ATR) Fresh Fuel Shipping Container (FFSC). Further, this chapter presents the evaluations that demonstrate the thermal safety of the ATR FFSC package[1] and compliance with the thermal requirements of 10 CFR 71[2] when transporting a payload consisting of either an assembled, un-irradiated ATR fuel element or a payload of loose, un-irradiated ATR fuel plates. The loose fuel element plates may be either flat or rolled to the geometry required for assembly into a fuel element.

Specifically, all package components are shown to remain within their respective temperature limits under the normal conditions of transport (NCT). Further, per 10 CFR §71.43(g), the maximum temperature of the accessible package surfaces is demonstrated to be less than 122 °F for the maximum decay heat loading, an ambient temperature of 100 °F, and no insolation. Finally, the ATR FFSC package is shown to retain sufficient thermal protection following the HAC free and puncture drop scenarios to maintain all package component temperatures within their respective short term limits during the regulatory fire event and subsequent package cool-down.

## 3.1 Description of Thermal Design

The ATR FFSC package, illustrated in Figure 1.2-1 through Figure 1.2-5 from Section 1.0, *General Information*, consists of three basic components: 1) a Body assembly, 2) a Closure assembly, and 3) either a Fuel Handling Enclosure (FHE) or a Loose Fuel Plate Basket (LFPB). The FHE is configured to house an assembled ATR fuel element, while the LFPB is configured to house loose ATR fuel element plates. The maximum gross weight of the package loaded with an FHE and ATR fuel element is approximately 280 pounds. The maximum gross weight of the package loaded with a LFPB containing its maximum payload is approximately 290 pounds.

The ATR FFSC is designed as a Type AF packaging for transportation of an ATR fuel element or a bundle of loose ATR fuel element plates. The packaging is rectangular in shape and is intended to be transported in racks of multiple packages by highway truck. Since the payload generates essentially no decay heat, the worst case thermal conditions will occur with an individual package fully exposed to ambient conditions. The package performance when configured in a rack of multiple packages will be bounded by that seen for an individual package.

The principal components of the packaging are shown in Figure 1.2-1 and described in more detail below. With the exception of minor components, all steel used in the ATR FFSC

---

[1] In the remainder of this chapter, the term 'packaging' refers to the assembly of components necessary to ensure compliance with the regulatory requirements, but does not include the payload. The term 'package' includes both the packaging components and the payload of ATR fuel.

[2] Title 10, Code of Federal Regulations, Part 71 (10 CFR 71), *Packaging and Transportation of Radioactive Material*, 01-01-03 Edition.

packaging is Type 304 stainless steel. Components are joined using full-thickness fillet welds and full and partial penetration groove welds.

## 3.1.1 Design Features

The primary heat transfer mechanisms within the ATR FFSC are conduction and radiation, while the principal heat transfer from the exterior of the packaging is via convection and radiation to the ambient environment. The Body and Closure assemblies serve as the primary impact and thermal protection for the FHE or the LFPB and their enclosed payloads of an ATR fuel element or loose fuel plates. The FHE and LFPB provide additional thermal shielding of their enclosed payloads during the transient HAC event.

There is no pressure relief system included in the ATR FFSC packaging design. The portions of the packaging that are not directly vented to atmosphere do not contain out-gassing materials. The package insulation is the only non-metallic component located in the enclosed volumes of the package and it is fabricated of a ceramic fiber. The Closure assembly is not equipped with either seals or gaskets so that potential out-gassing of the neoprene material used in ATR fuel tray and the plastic bag material used as a protective sleeve for the fuel element will readily vent without significant pressure build-up in the payload cavity.

The principal thermal design features of each package component are described in the following paragraphs.

### 3.1.1.1 ATR FFSC Body

The ATR FFSC body is a stainless steel weldment that is approximately 73 inches long and 8 inches square and weighs about 230 lbs (empty). It consists of two nested shells; the outer shell is fabricated of a square stainless steel tube with a 3/16 inch wall thickness, while the inner shell is fabricated from a 6 inch diameter, 0.120 inch wall, stainless steel tube. Three, 1-inch thick stiffening plates (i.e., ribs) are secured to the inner shell by fillet welds at four equally spaced intervals. The ribs are not mechanically attached to the outer shell. Instead, a nominal 0.06 inch air gap exists between the ribs and the outer shell, with a larger nominal gap existing at the corners of the ribs. These design features help to thermally isolate the inner shell from the outer shell during the HAC event.

Further thermal isolation of the inner shell is provided by ceramic fiber thermal insulation which is wrapped around the inner shell between the ribs and by the 28 gauge stainless steel sheet used as a jacket material over the insulation. The insulation is applied in two 0.5-inch thick layers in order to permit over-lapping joints between the layers and prevents direct line-of-sight between the inner shell and the jacket should the insulation shift under normal or accident conditions. The stainless steel jacket maintains the insulation around the inner shell and provides a relatively low emissivity barrier to radiative heat exchange between the insulation and the outer sleeve. The insulation jacket is pre-formed to the design shape and dimensions prior to installation. As such, the potential for inadvertent compression of the insulation during installation is minimized.

Once assembled, the inner shell, ribs, and the jacketed insulation wrap are slid as a single unit into the outer shell and secured to closure plates at both ends by welding. Thermal insulation is built into the bottom end closure plate of the packaging, while the ATR FFSC closure (see below) provides thermal insulation at the top end closure.

Cross-sectional views showing key elements of the ATR FFSC body are provided in Figure 1.2-2 and Figure 1.2-3. Figure 1.2-2 illustrates a cross sectional view at the top end closure of the package and 1.2-3 presents a similar cross sectional view of the package at the bottom end closure.

#### 3.1.1.2 ATR FFSC Closure

The ATR FFSC closure engages with the body using a bayonet style engagement via four uniformly spaced lugs on the closure that engage with four slots in the mating body feature. The closure incorporates 1 inch of ceramic fiber thermal insulation to provide thermal protection and is designed to permit gas to easily vent through the interface between the closure and the body. The closure weighs approximately 10 pounds and is equipped with a handle to facilitate use with gloved hands.

A cross sectional view of the ATR FFSC closure is illustrated in Figure 1.2-4.

#### 3.1.1.3 Fuel Handling Enclosure (FHE)

The Fuel Handling Enclosure (FHE) is a hinged, aluminum weldment used to protect the ATR fuel element from damage during loading and unloading operations. It is fabricated of thin wall (i.e., 0.09 inch thick) 5052-H32 aluminum sheet and features a hinged lid and neoprene rub strips to minimize fretting of the fuel element side plates where they contact the FHE. The surface of the FHE is neither anodized nor coated, but is left as an 'unfinished' aluminum sheet. Figure 1.2-1 presents an illustration of the FHE.

#### 3.1.1.4 ATR FFSC Loose Fuel Plate Basket (LFPB)

The Loose Fuel Plate Basket (LFPB) serves to maintain the fuel plates within a defined dimensional envelope during transport. The four identical machined segments are machined from a billet of 6061-T651 aluminum and are joined by threaded fasteners (see Figure 1.2-6). A variable number of ATR fuel plates may be housed in the basket, with the maximum payload weight being limited to 20 lbs. or less. The empty weight of the loose fuel plate basket is approximately 30 lbs. Like the FHE, the surface of the LFPB is neither anodized nor coated, but is left with its 'as machined' finish.

### 3.1.2 Content's Decay Heat

The ATR FFSC is designed as a Type AF packaging for transportation of an un-irradiated ATR fuel element or a bundle of loose, un-irradiated ATR fuel plates. The decay heat associated with un-irradiated ATR fuel is negligible. Therefore, no special devices or features are needed or utilized in the ATR FFSC packaging to dissipate the decay heat. Section 1.2.2, *Contents*, provides additional details.

### 3.1.3 Summary Tables of Temperatures

Table 3.1-1 provides a summary of the package component temperatures under normal and accident conditions. The temperatures for normal conditions are based on an analytical model of

the ATR FFSC package for extended operation with an ambient temperature of 100°F and a diurnal cycle for the insolation loading. The temperatures for accident conditions are based on an analytical model of the ATR FFSC package with the worst-case, hypothetical pre-fire damage as predicted based on drop tests using full-scale certification test units (CTUs).

The results for NCT conditions demonstrate that significant thermal margin exists for all package components. This is to be expected since the only significant thermal loads on the package arise from insolation and ambient temperature changes. The payload dissipates essentially zero decay heat. Further, the evaluations for NCT demonstrate that the package skin temperature will be below the maximum temperature of 122°F permitted by 10 CFR §71.43(g) for accessible surface temperature in a nonexclusive use shipment when transported in a 100°F environment with no insolation.

The results for HAC conditions also demonstrate that the design of the ATR FFSC package provides sufficient thermal protection to yield component temperatures that are significantly below the acceptable limits defined for each component. While the neoprene rubber and polyethylene plastic material used to protect the ATR fuel element from damage are expected to reach a sufficient temperature level during the HAC fire event to induce some level of thermal degradation (i.e., melting, charring, the chemical breakdown of the materials into 2 or more substances, etc.), the loss of these components is not critical to the safety of the package. See Sections 3.2.2, *Technical Specifications of Components*, and 3.4.3.1, *Maximum HAC Temperatures*, for more discussion.

## 3.1.4 Summary Tables of Maximum Pressures

Table 3.1-2 presents a summary of the maximum pressures achieved under NCT and HAC conditions. Since the ATR FFSC package is a vented package, both the maximum normal operating pressure (MNOP) and the maximum pressure developed within the payload compartment under the HAC condition are 0 psig.

Although the volume between the outer and inner shells is sealed, it does not contain organic or other materials that may outgas or thermally degrade. Therefore, the maximum pressure that may develop within the space will be limited to that achieved due to ideal gas expansion. The maximum pressure rise under NCT will be less than 4 psig, while the pressure rise under HAC conditions will be 38 psig.

**Table 3.1-1** – Maximum Temperatures for NCT and HAC Conditions

| Location / Component | NCT Hot Conditions | Accident Conditions | Maximum Allowable ① | |
|---|---|---|---|---|
| | | | Normal | Accident |
| ATR Fuel Element Fuel Plate | 147°F | 690°F | 400°F | 1,100°F |
| ATR Fuel Element Side Plate | 148°F | 786°F | 400°F | 1,100°F |
| Neoprene Rub Strips/Polyethylene Bag | 151°F ② | 975°F ② | 225°F | N/A |
| Fuel Handling Enclosure (FHE) | 151°F | 975°F | 400°F | 1,100°F |
| Loose Fuel Plate Basket (LFPB) | 151°F ② | 712°F | 400°F | 1,100°F |
| Inner Shell | 157°F | 1,377°F | 800°F | 2,700°F |
| Ceramic Fiber Insulation, Body | | | | |
| - Maximum | 185°F | 1,411°F | 2,300°F | 2,300°F |
| - Average | 151°F | 1,176°F | 2,300°F | 2,300°F |
| Ceramic Fiber Insulation, Closure | | | | |
| - Maximum | 145°F | 1,376°F | 2,300°F | 2,300°F |
| - Average | 144°F | 1,254°F | 2,300°F | 2,300°F |
| Closure | 145°F | 1,402°F | 800°F | 2,700°F |
| Outer Shell | 186°F | 1,427°F | 800°F | 2,700°F |

Table Notes:

① Maximum allowable temperatures are defined in Section 3.2.2, *Technical Specifications of Components.*

② Component temperature assumed to be equal to that of the FHE.

**Table 3.1-2** – Summary of Maximum Pressures

| Condition | Fuel Cavity Pressure | Outer/Inner Shell Cavity Pressure |
|---|---|---|
| NCT Hot | 0 psi gauge | 4 psi gauge |
| HAC Hot | 0 psi gauge | 38 psi gauge |

# 3.2 Material Properties and Component Specifications

The ATR FFSC is fabricated primarily of Type 304 stainless steel, 5052-H32 and 6061-T651 aluminum, ceramic fiber insulation, and neoprene rubber. The payload materials include 6061-T6 and/or 6061-0 aluminum, and uranium aluminide ($UAl_x$). A polyethylene plastic bag is used as a protective sleeve over the ATR fuel element.

## 3.2.1 Material Properties

Table 3.2-1 presents the thermal properties for Type 304 stainless steel and 5052-H32 aluminum from Table TCD of the ASME Boiler and Pressure Vessel Code[3]. Since the HAC analysis requires thermal properties in excess of the maximum temperature point of 400°F provided in Table TCD for 5052-H32 aluminum, the property values for 1100°F (i.e., the approximate melting point for aluminum) are assumed to be the same as those at 400°F. This approach is appropriate for estimating the temperature rise within the fuel basket during the HAC event since the thermal conductivity of aluminum alloys tends to decrease with temperature while the specific heat tends to increase. The density values listed in the table are taken from an on-line database[4]. Properties between the tabulated values are calculated via linear interpolation within the heat transfer code.

Table 3.2-2 presents the thermal properties for the ATR fuel element. For analysis purposes, the material used for the side plates, covers, and fuel cladding are assumed to be 6061-0 aluminum. The thermal properties for the fuel plates are determined as a composite of the cladding and the fuel core materials based on the geometry data for the ATR fuel element[5] and the thermal properties for the ATR fuel element materials[6]. The details of the computed values are presented in Section 3.5.2.4, *Determination of Composite Thermal Properties for ATR Fuel Plates*. For simplicity, the thermal properties are assumed to be constant with temperature based on the use of conservatively high thermal conductivity and conservatively low specific heat values. This approach maximizes the heat transfer into the fuel components during the HAC event, while under-estimating the ability of the components to store the heat.

The thermal properties for the non-metallic materials used in the ATR FFSC are presented in Table 3.2-3. The thermal properties for neoprene rubber are based on the *Polymer Data Handbook*[7], while the thermal properties for the ceramic fiber insulation are based on the Unifrax Durablanket® S insulation product[8] with a nominal density of 6 $lb/ft^3$. The thermal properties are for the uncompressed material in both cases. Although the package design requires that the insulation blanket be compressed by up to 20% at the quadrant points, ignoring the compression for the purposes of the thermal modeling and using the thermal properties for the uncompressed material at all locations provides a conservative estimate of the package's

---

[3] American Society of Mechanical Engineers (ASME) Boiler and Pressure Vessel Code, Section II, *Materials, Part D – Properties*, Table TCD, Material Group J, 2001 Edition, 2002 and 2003 Addenda, New York

[4] Matweb, Online Material Data Sheets, www.matweb.com.

[5] *ATR Mark VII Fuel Element Assembly*, INEEL Drawing No. DWG-405400, Rev-19.

[6] *Thermophysical And Mechanical Properties Of ATR Core Materials*, Report No. PG-T-91-031, August 1991, EG&G Idaho, Inc.

[7] *Polymer Data Handbook*, Oxford University Press, Inc., 1999.

[8] Unifrax DuraBlanket S ceramic fiber insulation, Unifrax Corporation, Niagara Falls, NY.

performance under the HAC condition. This conclusion arises from the fact that the insulation's thermal conductivity decreases with density for temperatures above approximately 500°F (see Table 3.2-3). For example, the thermal conductivity of 8 pcf insulation at 1000°F and 1400°F is 0.0814 and 0.1340 Btu/hr-ft-°F, respectively, versus the 0.0958 and 0.1614 Btu/hr-ft-°F values for 6 pcf insulation at the same temperatures. While compression will increase conductivity below 500°F, ignoring the effects of compression for NCT conditions has an insignificant effect since the peak package temperatures occur in the vicinity of the ribs and are therefore unaffected by a local increase in the thermal conductivity of the insulation. Further, large thermal margins exist for the NCT conditions.

The thermal properties for air presented in Table 3.2-4 are derived from curve fits[9]. Because the thermal conductivity of air varies significantly with temperature, the computer model calculates the thermal conductivity across air spaces as a function of the mean film temperature. All void spaces within the ATR FFSC package are assumed to be filled with air at atmospheric pressure.

Table 3.2-5 and Table 3.2-6 present the assumed emissivity ($\varepsilon$) for each radiating surface and the solar absorptivity ($\alpha$) value for the exterior surface. The emissivity of 'as-received' Type 304 stainless steel has been measured[10] as 0.25 to 0.28, while the emissivity of weathered Type 304 stainless steel has been measured[11] from 0.46 to 0.50. For the purpose of this analysis, an emissivity of 0.30 is assumed for the emittance from all interior radiating stainless steel surfaces, while the emissivity for the exterior surfaces of the package is assumed to be 0.45. The solar absorptivity of Type 304 stainless steel is approximately 0.52[12]. Under HAC conditions, the outside of the package is assumed to attain an emissivity of 0.8 in compliance with 10 CFR §71.73(c)(4) and to have a solar absorptivity of 0.9 to account for the possible accumulation of soot.

The 5052-H32 aluminum sheet used to fabricate the FHE will be left with a plain finish while the 6061-T651 billets used to fabricate the Loose Fuel Plate Basket will have a machined surface. The emissivity for either type of finish can be expected to be low (i.e., 0.10 or lower)[12] however, for conservatism, an emissivity of 0.25[12] representative of a heavily oxidized surface is assumed for this evaluation. The 6061-0 aluminum used for the ATR fuel components are assumed to have a surface coating of boehmite ($Al_2O_3H_2O$). A 25 μm boehmite film will exhibit a surface emissivity of approximately 0.92[13]. While a fresh fuel element may have a lower surface emissivity, the use of the higher value will provide a conservative estimate of the temperatures achieved during the HAC event.

The ceramic fiber insulation has a surface emissivity of approximately 0.90[12] based on a

---

[9] Rohsenow, Hartnett, and Cho, *Handbook of Heat Transfer*, 3rd edition, McGraw-Hill Publishers, 1998, curve fit equations on pp 2.4.

[10] Frank, R. C., and W. L. Plagemann, *Emissivity Testing of Metal Specimens.* Boeing Analytical Engineering coordination sheet No. 2-3623-2-RF-C86-349, August 21, 1986. Testing accomplished in support of the TRUPACT-II design program.

[11] *"Emissivity Measurements of 304 Stainless Steel"*, Azzazy, M., prepared for Southern California Edison, September 6, 2000, Transnuclear File No. SCE-01.0100.

[12] G. G. Gubareff, J. E. Janssen, and R. H. Torborg, *Thermal Radiation Properties Survey*, 2nd Edition, Honeywell Research Center, 1960.

[13] *Heat Transfer in Window Frames with Internal Cavities*, PhD Thesis for Arild Gustavsen, Norwegian University of Science and Technology, Trondheim, Norway, September 2001.

combination of the material type and surface roughness. The same emissivity is assumed for the neoprene rubber.

## 3.2.2 Technical Specifications of Components

The materials used in the ATR FFSC that are considered temperature sensitive are the aluminum used for the FHE, the LFPB, and the ATR fuel, the neoprene rubber, and the polyethylene wrap used as a protective sleeve around the ATR fuel element. Of these materials, only the aluminum used for the ATR fuel is considered critical to the safety of the package. The other materials either have temperature limits above the maximum expected temperatures or are not considered essential to the function of the package.

Type 304 stainless steel has a melting point above 2,700°F[4], but in compliance with the ASME B&PV Code[14], its allowable temperature is limited to 800°F if used for structural purposes. However, the ASME temperature limit generally applies only to conditions where the material's structural properties are relied on for loads postulated to occur in the respective operating mode or load combination (such as the NCT and HAC free drops). Since the package is vented to atmosphere, no critical structural condition exists following the HAC free drop events and, as such, the appropriate upper temperature limit is 800°F for normal conditions and 2,700°F for accident conditions

Aluminum (5052-H32, 6061-0/6061-T6) has a melting point of approximately 1,100°F[4] however for strength purposes the normal operational temperature should be limited to 400°F[3].

The ceramic fiber insulation has a manufacturer's recommended continuous use temperature limit of 2,300°F[8]. There is no lower temperature limit.

The polyethylene plastic wrap used as a protective sleeve around the ATR fuel element has a melting temperature of approximately 225 to 250°F[4]. For the purposes of this analysis, the lower limit of 225°F is used. As a thermoplastic, the polyethylene wrap will melt and sag onto the fuel element when exposed to temperatures in excess of 250°F. Further heating could lead to charring (i.e., oxidation in the absence of open combustion) and then thermal decomposition into its volatile components. Thermal decomposition will begin at approximately 750°F. Unpiloted, spontaneous ignition could occur at temperatures of approximately 650°F[15] or higher. The plastic wrap is approximately 7 inches wide (when pressed flat), 67.5 inches long, and weights approximately 3 oz. Per NUREG-1805[16] calculators, if ignited, a polyethylene bag weighting 3 oz. and with a surface area of 6.56 ft$^2$ would be consumed within 4.5 seconds. Loss of the plastic wrap is of no consequence to the thermal safety of the ATR FFSC since its effect on conductive and radiative heat transfer is negligible.

The neoprene rub strips used to minimize fretting of the fuel element side plates have a continuous temperature rating of 200 to 250°F and a short term (i.e., 0.5 hour or less) temperature

---

[14] American Society of Mechanical Engineers (ASME) Boiler & Pressure Vessel Code, Section III, *Rules for Construction of Nuclear Facility Components*, Division 1, Subsection NB, *Class 1 Components*, & Subsection NG, *Core Support Structures*, 2001 Edition, 2002 Addendum.

[15] Troitzsch, J., *Plastics Flammability Handbook*, 2nd Edition, Oxford University Press, New York, 1990.

[16] NUREG-1805, Fire Dynamics Tools, Nuclear Regulatory Commission, Washington, DC.

limit of approximately 525°F [17]. For the purposes of this analysis, a limit of 225°F is used for NCT conditions, while a peak temperature of 525°F is assumed for HAC conditions before thermal degradation begins. Since neoprene is a thermoset polymer, it will not melt, but decompose into volatiles as it degrades. Loss of the neoprene rub strips is of no consequence to the thermal safety of the ATR FFSC.

The minimum allowable service temperature for all ATR FFSC components is below -40 °F.

[17] Parker O-Ring Handbook, ORD 5700/USA, 2001, www.parker.com.

**Table 3.2-1** – Thermal Properties of Package Metallic Materials

| Material | Temperature (°F) | Thermal Conductivity (Btu/hr-ft-°F) | Specific Heat (Btu/$lb_m$-°F) | Density ($lb_m/in^3$) |
|---|---|---|---|---|
| Stainless Steel Type 304 | 70 | 8.6 | 0.114 | 0.289 |
| | 100 | 8.7 | 0.115 | |
| | 200 | 9.3 | 0.119 | |
| | 300 | 9.8 | 0.123 | |
| | 400 | 10.4 | 0.126 | |
| | 500 | 10.9 | 0.128 | |
| | 600 | 11.3 | 0.130 | |
| | 700 | 11.8 | 0.132 | |
| | 800 | 12.2 | 0.133 | |
| | 1000 | 13.2 | 0.136 | |
| | 1200 | 14.0 | 0.138 | |
| | 1400 | 14.9 | 0.141 | |
| | 1500 | 15.3 | 0.142 | |
| Aluminum Type 5052-H32 | 70 | 79.6 | 0.214 | 0.097 |
| | 100 | 80.8 | 0.216 | |
| | 150 | 82.7 | 0.219 | |
| | 200 | 84.4 | 0.222 | |
| | 250 | 85.9 | 0.225 | |
| | 300 | 87.2 | 0.227 | |
| | 350 | 88.4 | 0.229 | |
| | 400 | 89.6 | 0.232 | |
| | 1100 ① | 89.6 | 0.232 | |

Notes:

① Values for 1100°F are assumed equal to values at 400°F.

## Table 3.2-2 – Thermal Properties of ATR Fuel Materials

| Material | Temperature (°F) | Thermal Conductivity (Btu/hr-ft-°F) | Specific Heat (Btu/$lb_m$-°F) | Density ($lb_m/in^3$) |
|---|---|---|---|---|
| Aluminum Type 6061-0 | 32 | 102.3 | - | 0.0976 |
| | 62 | - | 0.214 | |
| | 80 | 104.0 | - | |
| | 170 | 107.5 | - | |
| | 260 | 109.2 | 0.225 | |
| | 350 | 109.8 | - | |
| | 440 | 110.4 | 0.236 | |
| | 530 | 110.4 | - | |
| | 620 | 109.8 | 0.247 | |
| | 710 | 108.6 | - | |
| | 800 | 106.9 | 0.258 | |
| | 890 | 105.2 | - | |
| | 980 | 103.4 | 0.269 | |
| | 1080 | 101.1 | 0.275 | |
| ATR Fuel Plate 1① | - | 46.6 | 0.193 | 0.120 |
| ATR Fuel Plates 2 to 18① | - | 69.6 | 0.210 | 0.112 |
| ATR Fuel Plate 19① | - | 38.9 | 0.188 | 0.122 |

Notes:

① Values determined based on composite value of aluminum cladding and fuel core material (see Appendix 3.2.5.4). Thermal conductivity value is valid for axial and circumferential heat transfer within fuel plate.

## Table 3.2-3 – Thermal Properties of Non-Metallic Materials

| Material | Temperature (°F) | Thermal Conductivity (Btu/hr-ft-°F) | Specific Heat (Btu/$lb_m$-°F) | Density ($lb_m/ft^3$) | Comments |
|---|---|---|---|---|---|
| Neoprene① | --- | 0.11 | 0.52 | 76.8 | |
| Ceramic Fiber Insulation② | 70 | 0.0196 | 0.28 | 6 | |
| | 200 | 0.0238 | | | |
| | 400 | 0.0343 | | | |
| | 600 | 0.0499 | | | |
| | 800 | 0.0703 | | | |
| | 1000 | 0.0958 | | | |
| | 1200 | 0.1262 | | | |
| | 1400 | 0.1614 | | | |
| | 1600 | 0.2017 | | | |
| Ceramic Fiber Insulation②③ | 70 | 0.0300 | 0.28 | 8 | |
| | 200 | 0.0313 | | | |
| | 400 | 0.0369 | | | |
| | 600 | 0.0463 | | | |
| | 800 | 0.0620 | | | |
| | 1000 | 0.0814 | | | |
| | 1200 | 0.1053 | | | |
| | 1400 | 0.1340 | | | |
| | 1600 | 0.1669 | | | |

Notes:

① Conductivity value represents uncompressed neoprene.

② Conductivity values are for uncompressed insulation. Compression of the material will increase the thermal conductivity for temperatures below approximately 500°F where conduction dominates and decrease the thermal conductivity for temperatures above 500°F where heat transfer via radiation dominates.

③ 8 pcf ceramic fiber insulation is not used in the ATR FFSC Package. Data is provided for comparison purposes to demonstrate the effect of insulation compression on thermal conductivity.

## Table 3.2-4 – Thermal Properties of Air

| Temperature (°F) | Density $lb_m/in^3$ [1] | Specific Heat (Btu/$lb_m$-°F) | Dynamic Viscosity ($lb_m$ /ft-hr) | Thermal Conductivity (Btu/hr-ft-°F) | Prandtl Number [2] | Coef. Of Thermal Exp. ($°R^{-1}$) [3] |
|---|---|---|---|---|---|---|
| -40 | Use Ideal Gas Law w/ Molecular wt = 28.966 | 0.240 | 0.03673 | 0.0121 | Compute as $Pr = c_p\mu / k$ | Compute as $\beta = 1/(°F+459.67)$ |
| 0 | | 0.240 | 0.03953 | 0.0131 | | |
| 50 | | 0.240 | 0.04288 | 0.0143 | | |
| 100 | | 0.241 | 0.04607 | 0.0155 | | |
| 200 | | 0.242 | 0.05207 | 0.0178 | | |
| 300 | | 0.243 | 0.05764 | 0.0199 | | |
| 400 | | 0.245 | 0.06286 | 0.0220 | | |
| 500 | | 0.248 | 0.06778 | 0.0240 | | |
| 600 | | 0.251 | 0.07242 | 0.0259 | | |
| 700 | | 0.253 | 0.07680 | 0.0278 | | |
| 800 | | 0.256 | 0.08098 | 0.0297 | | |
| 900 | | 0.259 | 0.08500 | 0.0315 | | |
| 1000 | | 0.262 | 0.08887 | 0.0333 | | |
| 1200 | | 0.269 | 0.09620 | 0.0366 | | |
| 1400 | | 0.274 | 0.10306 | 0.0398 | | |
| 1500 | | 0.277 | 0.10633 | 0.0412 | | |

Table Notes:

1) Density computed from ideal gas law as $\rho = PM/RT$, where R= 1545.35 ft-lbf/lb-mole-R, T= temperature in °R, P= pressure in $lbf/ft^2$, and M= molecular weight of air. For example, at 100°F and atmospheric pressure of $14.69 lbf/in^2$, $\rho = (14.69*144\ in^2/ft^2*28.966\ lbm/lb\text{-}mole)/1545.35*(100+459.67) = 0.071\ lbm/ft^3 = 4.099x10^{-5}\ lbm/in^3$.

2) Prandtl number computed as $Pr = c_p\mu / k$, where $c_p$ = specific heat, $\mu$ = dynamic viscosity, and k = thermal conductivity. For example, at 100°F, $Pr = 0.241*0.04607/0.0155 = 0.72$.

3) Coefficient of thermal expansion is computed as the inverse of the absolute temperature. For example, at 100°F, $\beta = 1/(100+459.67) = 0.00179$.

## Table 3.2-5 – NCT Thermal Radiative Properties

| Material | Assumed Conditions | Assumed Emissivity (ε) | Absorptivity (α) |
|---|---|---|---|
| Outer Shell, Exterior Surfaces (Type 304 Stainless Steel) | Weathered | 0.45 | 0.52 |
| Outer Shell, Interior Surface and Inner Shell (Type 304 Stainless Steel) | 'As- Received' | 0.3 | --- |
| Ceramic Fiber Insulation & Neoprene | --- | 0.90 | --- |
| Fuel Handling Enclosure and Loose Fuel Plate Basket (6061-T651 &5052-H32 Aluminum) | Oxidized | 0.25 | --- |
| ATR Fuel Side Plates and Fuel Cladding (6061-0 Aluminum) | Boehmite film | 0.92 | --- |
| Ambient Environment | --- | 1.00 | N/A |

## Table 3.2-6 – HAC Thermal Radiative Properties

| Material | Assumed Conditions | Assumed Emissivity (ε) | Absorptivity (α) |
|---|---|---|---|
| Outer Shell, Exterior Surfaces (Type 304 Stainless Steel) | Sooted/Oxidized | 0.80 | 0.90 |
| Outer Shell, Interior Surface and Inner Shell (Type 304 Stainless Steel) | Slightly Oxidized | 0.45 | --- |
| Ceramic Fiber Insulation & Neoprene | --- | 0.90 | --- |
| Fuel Handling Enclosure and Loose Fuel Plate Basket (6061-T651 &5052-H32 Aluminum) | Oxidized | 0.25 | --- |
| ATR Fuel Side Plates and Fuel Cladding (6061-0 Aluminum) | Boehmite film | 0.92 | --- |
| Ambient Environment | --- | 1.00 | N/A |

# 3.3 Thermal Evaluation for Normal Conditions of Transport

This section presents the thermal evaluation of the ATR FFSC for normal conditions of transport (NCT). Under NCT, the package will be transported horizontally. This establishes the orientation of the exterior surfaces of the package for determining the free convection heat transfer coefficients and insolation loading. While the package would normally be transported in tiered stacks of multiple packages, the evaluation for NCT is conservatively based on a single, isolated package since this approach will yield the bounding maximum and minimum temperatures achieved by any of the packages. Further, the surface of the transport trailer is conservatively assumed to prevent heat exchange between the package and the ambient. Thus, the bottom of the ATR FFSC is conservatively treated as an adiabatic surface.

The details of the thermal modeling used to simulate the ATR FFSC package under NCT conditions are provided in Appendix 3.5.2, *Analytical Thermal Model.*

## 3.3.1 Heat and Cold

### 3.3.1.1 Maximum Temperatures

The maximum temperature distribution for the ATR FFSC occurs with a diurnal cycle for insolation loading and an ambient air temperature of 100°F, per 10 CFR §71.71(c)(1). The evaluation of this condition is conducted as a transient using the thermal model of an undamaged ATR FFSC described in Appendix 3.5.2.1, *Description of Thermal Model for NCT Conditions.* Figure 3.3-1 and Figure 3.3-2 illustrate the expected heat-up transient for an ATR FFSC loaded with an ATR fuel element. The transient analysis assumes a uniform temperature condition of 70°F for all components prior to loading and exposure to the specified NCT condition at time = 0. The figures demonstrate that the ATR FFSC package will respond rapidly to changes in the level of insolation and will reach it peak temperatures within the first day or two after loading. Table 3.3-1 presents the maximum temperatures reached for various components of the package. As seen from the table, all components are within in their respective temperature limits. Figure 3.3-3 illustrates the predicted temperature distribution within the ATR FFSC package at the time of peak temperature.

The maximum temperature distribution for the ATR FFSC without insolation loads occurs with an ambient air temperature of 100°F. Since the package payload dissipates essentially zero watts of decay heat, the thermal analysis of this condition represents a trivial case and no thermal calculations are performed. Instead, it is assumed that all package components achieve the 100°F temperature under steady-state conditions. The resulting 100°F package skin temperature is below the maximum temperature of 122°F permitted by 10 CFR §71.43(g) for accessible surface temperature in a nonexclusive use shipment.

No specific thermal analysis is presented for the ATR FFSC package loaded with the Loose Fuel Plate Basket since a similar package temperature distribution will occur under all NCT conditions.

#### 3.3.1.2 Minimum Temperatures

The minimum temperature distribution for the ATR FFSC occurs with a zero decay heat load and an ambient air temperature of -40°F per 10 CFR §71.71(c)(2). The thermal analysis of this condition also represents a trivial case and no thermal calculations are performed. Instead, it is assumed that all package components achieve the -40°F temperature under steady-state conditions. As discussed in Section 3.2.2, *Technical Specifications of Components*, the -40°F temperature is within the allowable operating temperature range for all ATR FFSC package components.

### 3.3.2 Maximum Normal Operating Pressure

The payload cavity of the ATR FFSC is vented to the atmosphere. As such, the maximum normal operating pressure (MNOP) for the package is 0 psig.

While the volume between the outer and inner shells is sealed, it does not contain organic or other materials that may outgas or thermally degrade. Therefore, the maximum pressure that may develop within the space will be limited to that achieved due to ideal gas expansion. Assuming a temperature of 70°F at the time of assembly and a maximum operating temperature of 190°F (based on the outer shell temperature, see Table 3.3-1, conservatively rounded up), the maximum pressure rise within the sealed volume will be less than 4 psi.

## **Table 3.3-1** - Maximum Package NCT Temperatures

| Location / Component | NCT Hot Conditions | Maximum Allowable ① |
|---|---|---|
| ATR Fuel Element Fuel Plate | 147°F | 400°F |
| ATR Fuel Element Side Plate | 148°F | 400°F |
| Neoprene Rub Strips/Polyethylene Bag | 151°F ② | 225°F |
| Fuel Handling Enclosure (FHE) | 151°F | 400°F |
| Loose Fuel Plate Basket (LFPB) | 151°F ② | 400°F |
| Inner Shell | 157°F | 800°F |
| Ceramic Fiber Insulation, Body<br>- Maximum<br>- Average | <br>185°F<br>151°F | <br>2,300°F<br>2,300°F |
| Ceramic Fiber Insulation, Closure<br>- Maximum<br>- Average | <br>145°F<br>144°F | <br>2,300°F<br>2,300°F |
| Closure | 145°F | 800°F |
| Outer Shell | 186°F | 800°F |

Table Notes:
① The maximum allowable temperatures under NCT conditions are provided in Section 3.2.2, Technical Specifications of Components.
② Component temperature assumed to be equal to that of the FHE.

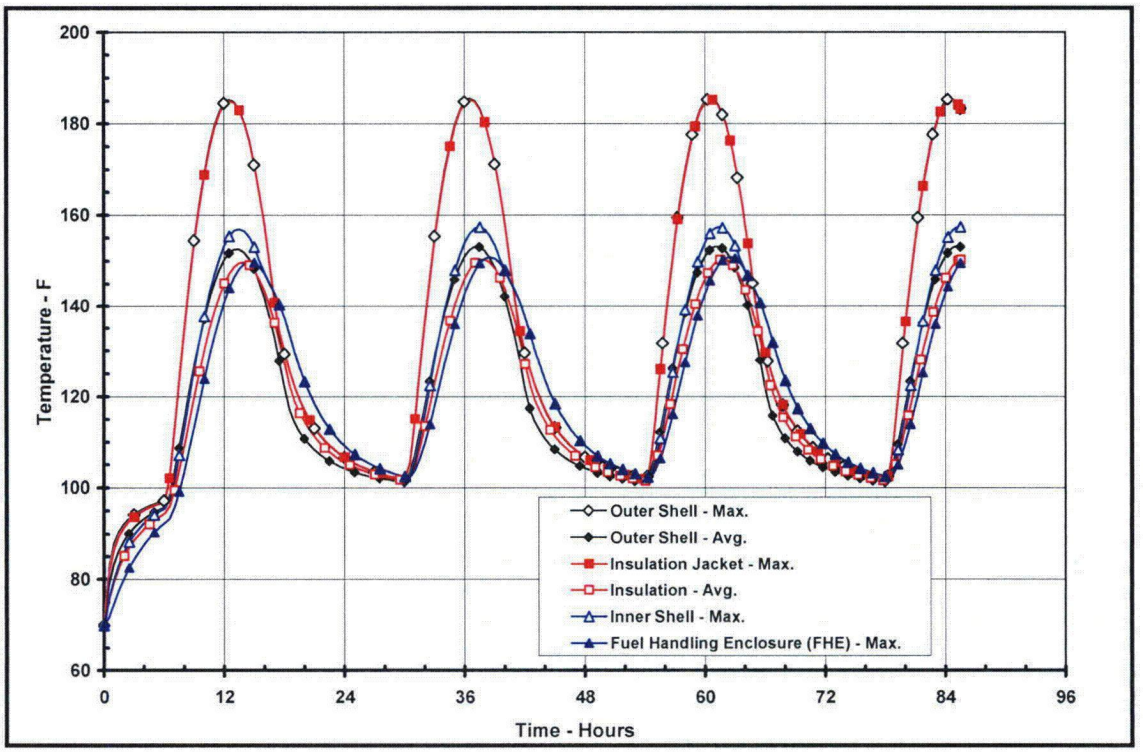


**Figure 3.3-1** – ATR FFSC Package Heat-up, NCT Hot Conditions

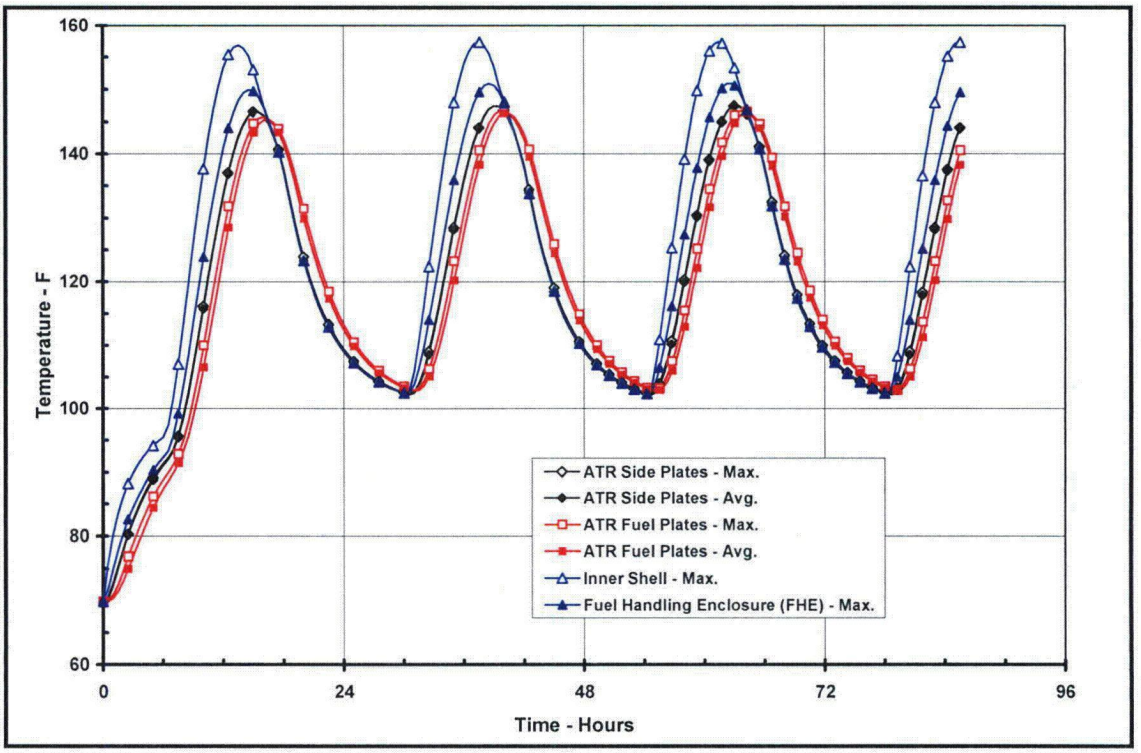


**Figure 3.3-2** – ATR Fuel Element Heat-up, NCT Hot Conditions

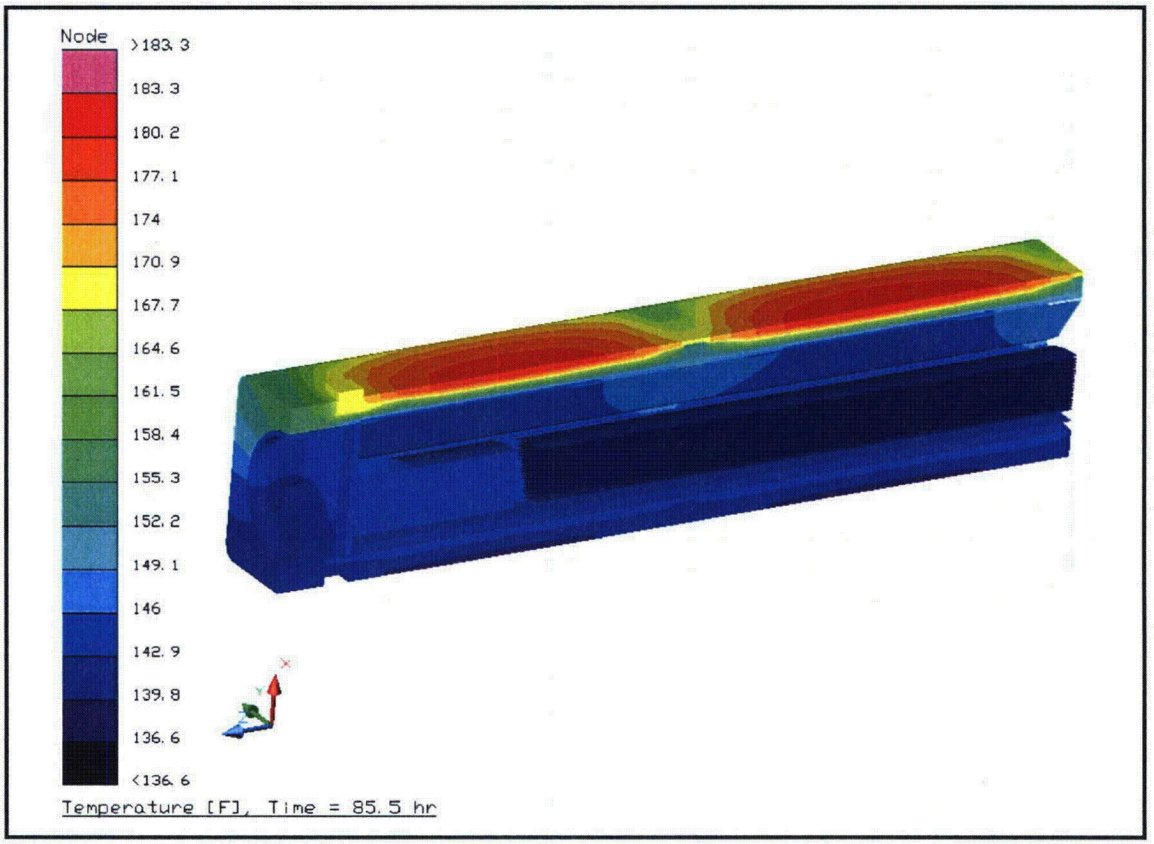


**Figure 3.3-3** – Package NCT Temperature Distribution

# 3.4 Thermal Evaluation for Hypothetical Accident Conditions

This section presents the thermal evaluation of the ATR FFSC package under the hypothetical accident condition (HAC) specified in 10 CFR §71.73(c)(4) based on an analytical thermal model of the ATR FFSC. The analytical model for HAC is a modified version of the quarter symmetry NCT model described in Section 3.5.2.1, *Description of Thermal Model for NCT Conditions*, with the principal model modifications consisting of simulating the expected package damage resulting from the drop events that are assumed to precede the HAC fire and changing the package surface emissivities to reflect the assumed presence of soot and/or surface oxidization.

Physical testing using full scale certified test units (CTUs) is used to establish the expected level of damage sustained by the ATR FFSC package from the 10 CFR 71.73 prescribed free and puncture drops that are assumed to precede the HAC fire event. Appendix 2.12.1, *Certification Tests on CTU-1* and Appendix 2.12.2, *Certification Tests on CTU-2* provide the configuration and initial conditions of the test articles, the test facilities and instrumentation used, and the test results. Section 3.5.2.2, *Description of Thermal Model for HAC Conditions*, provides an overview of the test results, the rationale for selecting the worst-case damage scenario, and the details of the thermal modeling used to simulate the package conditions during the HAC fire event.

## 3.4.1 Initial Conditions

The initial conditions assumed for the package prior to the HAC event are described below in terms of the modifications made to the NCT thermal model to simulate the assumed package conditions prior to and during the HAC event. These modifications are:

- Simulated the worst-case damage arising from the postulated HAC free and puncture drops as described in Section 3.5.2.2, *Description of Thermal Model for HAC Conditions*,
- Assume an initial, uniform temperature distribution of 100°F based on a zero decay heat package at steady-state conditions with a 100°F ambient with no insolation. This assumption complies with the requirement of 10 CFR §71.73(b)[2] and NUREG-1609[18],
- Increased the emissivity of the external surfaces from 0.45 to 0.8 to account for possible soot accumulation on the surfaces, per 10 CFR §71.73(c)(4),
- Increased the emissivity of the interior surfaces of the outer shell from 0.30 to 0.45 to account for possible oxidization of the surfaces during the HAC event,

Following the free and puncture bar drops, the ATR FFSC package is assumed come to rest in a horizontal position prior to the initiation of the fire event. Since the package geometry is essentially symmetrical about its axial axis, there are no significant thermal differences whether the

[18] NUREG-1609, *Standard Review Plan for Transportation Packages for Radioactive Material*, §3.5.5.1, U.S. Regulatory Commission, Office of Nuclear Materials Safety and Standards, March 1999.

package is right-side up, up-side down, or even on its end. The potential for the ATR fuel element payload being re-positioned depending upon the package orientation is not significant to the peak temperatures developed under HAC conditions given the modeling approach used to compute the heat transfer from the inner shell to the ATR fuel element. Therefore, the peak package temperatures predicted under this evaluation are representative of those achieved for any package orientation.

## 3.4.2 Fire Test Conditions

The fire test conditions analyzed to address the 10 CFR §71.73(c) requirements are as follows:

- The initial ambient conditions are assumed to be 100°F ambient with no insolation,
- At time = 0, a fully engulfing fire environment consisting of a 1,475°F ambient with an effective emissivity of 0.9 is used to simulate the average flame temperature of the hydrocarbon fuel/air fire event. Since a 1,475°F flame temperature with an effective emissivity of 0.9 is equivalent to a 1,425°F flame temperature with a effective emissivity of 1.0, this evaluation uses an ambient temperature of 1,475°F for all convection based heat transfer calculations, while an ambient temperature of 1,425°F is used for all radiation based heat transfer calculations,
- The convection heat transfer coefficients between the package and the ambient during the 30-minute fire event are based on an average gas velocity[19] of 10 m/sec. Following the 30-minute fire event the convection coefficients are based on still air,
- The ambient condition of 100°F with insolation is assumed following the 30-minute fire event. Since a diurnal cycle is used for insolation, the evaluation assumes that the 30-minute fire begins at noon so as to maximize the insolation heating during the post-fire cool down period. A solar absorptivity of 0.9 is assumed for the exterior surfaces to account for potential soot accumulation on the package surfaces.

The transient analysis is continued for 11.5 hours after the end of the 30-minute fire to ensure that the peak package temperatures are captured..

## 3.4.3 Maximum Temperatures and Pressure

### 3.4.3.1 Maximum HAC Temperatures

The outer shell and the ceramic fiber insulation provide thermal protection to the ATR FFSC package during the HAC fire event. The level of thermal protection can be seen via the thermal response curves presented in Figure 3.4-1 and Figure 3.4-2. As illustrated in the figures, while the exterior of the package quickly rises to nearly the temperature of the fire, the heat flow to the

[19] Schneider, M.E and Kent, L.A., *Measurements Of Gas Velocities And Temperatures In A Large Open Pool Fire, Heat and Mass Transfer in Fire* - HTD Vol. 73, 1987, ASME, New York, NY.

FHE and its enclosed ATR fuel element payload is sufficiently restricted that the maximum temperatures of both the FHE and the ATR fuel element are well below the melting point of aluminum. This result occurs despite the conservative assumption of direct contact between the FHE and the inner shell at 3 locations (e.g., the equivalent of four locations for a full model).

This level of thermal protections is further illustrated by the perspective views presented in Figure 3.4-3 and Figure 3.4-4 of the temperature distribution in the ATR FFSC package after 30 minutes of exposure to the HAC fire and at the point when the peak ATR fuel element temperature is attained (approximately 22 minutes after the end of the fire). The figures show that the ceramic fiber insulation limits the elevated temperatures resulting from the fire event to regions adjacent to the outer shell. The assumed absence of the ceramic fiber insulation adjacent to the ribs as a result of the pre-fire free drop event can be seen in each figure.

A similar thermal performance is seen for the package when loaded with the Loose Fuel Plate Basket (LFPB). Figure 3.4-5 presents the thermal response curve, while Figure 3.4-6 and Figure 3.4-7 present perspective views of the temperature distribution in the ATR FFSC package after 30 minutes of exposure to the HAC fire and at the point when the peak LFPB temperature is attained (approximately 22 minutes after the end of the fire). A lower maximum temperature is achieved in the LFPB vs. that seen for the FHE because of the higher thermal mass associated with the LFPB. Further, since the LFPB is modeled without its payload of loose fuel plates, these results will bound those seen for a LFPB with a payload.

Table 3.4-1 presents the component temperatures seen prior to the fire, at the end of the 30-minute fire event, and the peak temperature achieved during the entire simulated HAC thermal event. As seen, all temperatures are within their allowable limit. It is expected that the neoprene rub strips and the polyethylene bag used as a protective sleeve for the ATR fuel element will thermally degrade due to the level of temperature achieved. In the case of the polyethylene bag, the bag is expected to melt and sag onto the fuel element when exposed to temperatures in excess of 250°F. Further heating will lead to charring and then thermal decomposition into its volatile components. While spontaneous ignition is unexpected under the unpiloted conditions, the effect would be minimal since, per NUREG-1805[16], if ignited, a polyethylene bag weighting 3 oz. and with a surface area of 6.56 $ft^2$ would be consumed within 4.5 seconds. As a thermoset polymer, the neoprene is expected to simply decompose into volatiles as it thermally degrades. These components are not critical to the safety of the package and any out-gassing associated with their thermal degradation will not contribute to package pressurization since package is vented.

### 3.4.3.2 Maximum HAC Pressures

The payload cavity of the ATR FFSC is vented to the atmosphere. As such, the maximum pressure achieved under the HAC event will be 0 psig.

Although the volume between the outer and inner shells is sealed, it does not contain organic or other materials that may outgas or thermally degrade. Assuming a temperature of 70°F at the time of assembly and a maximum temperature of 1,427°F (based on the outer shell temperature, see Table 3.4-1), the maximum pressure rise within the sealed volume due to ideal gas expansion will be less than 38 psig. This level of pressurization will occur for only a few minutes and then quickly reduce as the package cools.

## 3.4.4 Maximum Thermal Stresses

The temperature difference between the inner and outer shells during the HAC event (see the average inner and outer shell temperatures presented in Figure 3.4-1) will result in differential thermal expansion between the shells. This differential thermal expansion is expected to peak at approximately 6 minutes after the initiation of fire exposure when the average outer shell temperature is 1,294°F and the average inner shell temperature is 188°F. Based on the differential thermal expansion for Type 304 stainless steel[20] the change in length is computed as:

$$DTE = \Delta L_{OuterShell} - \Delta L_{InnerShell} = [\alpha_{OS}(T_{OS} - 70) - \alpha_{IS}(T_{IS} - 70)]L = 0.9 \text{ inches}$$

where:

$\alpha_{OS}$ = 10.7($10^{-6}$) in/in/°F at 1,300 °F
$\alpha_{IS}$ = 8.9($10^{-6}$) in/in/°F at 200 °F
$T_{OS}$ = 1,294 °F
$T_{IS}$ = 188 °F
L = 73 inches (conservatively for both shells)

After 6 minutes of exposure to the fire the difference in shell lengths will decrease as the inner shell heats up. The differential expansion will reach 0-inches approximately 7 minutes after the end of the fire event when the inner and outer shells reach thermal equilibrium and then go negative as the outer shell continues to cool faster than the inner shell. The largest negative thermal differential expansion achieved is approximately 0.25-inches.

The result of this variation in differential thermal expansion may take one of three forms:

1) the outer shell buckles outward,
2) the outer shell buckles inward, or
3) the weld attaching the inner shell to either the closure plate or the bottom end plate will fail and permit the outer shell and the affected plate to move freely.

While in reality, a square tube is likely to buckle inward on two of the four faces and outward on the remaining two faces simultaneously, the two buckling modes are treated independently for the purposes of this evaluation. The possibility of the outer shell buckling outwards is the assumption upon which the thermal modeling presented in Section 3.5.2.2, *Description of Thermal Model for HAC Conditions* is based. This mode is seen as likely given the level of metal softening that will occur with the outer shell quickly reaching over 1,200°F and the expected pressurization of the void space between the inner and outer shells. Buckling the outer shell in this fashion will act to lower the rate of inward heat transfer. As such, ignoring the outer shell's displacement due to differential thermal expansion, as assumed by the HAC thermal modeling, yields conservatively high package temperatures.

The second possibility is that the outer shell buckles inward under the differential thermal expansion. Should this occur, the maximum deflection would be 0.9-inches/2 = 0.45-inches assuming a zero length deflection and only one buckle along the length of the outer shell. In

[20] American Society of Mechanical Engineers (ASME) Boiler and Pressure Vessel Code, Section II, *Materials, Part D – Properties*, 2001 Edition, 2002 and 2003 Addenda, New York ,Table TE-1, Group 3. Coefficient B = 8.9x$10^{-6}$ inches/inch/°F at 200°F and 10.7x$10^{-6}$ inches/inch/°F at 1,300°F.

reality, the actual deflection would measure perhaps 0.33-inches after properly accounting for the curvature in the buckled section. Since this level of deflection would still leave 0.5-inches or more of insulation separating the inner shell from the outer shell, no significant impact on the predicted peak HAC temperatures will occur.

The final possibility which the differential thermal expansion may manifest itself is in the failure of the one of the welds attaching the inner shell to the closure and bottom end plates. If this occurs, besides releasing any potential pressure buildup in the void between the inner and outer shells, the outer shell and the associated end plate will extend away from the inner shell at the point of the weld failure. The size of the gap will maximize at about 0.9-inches and then decrease. Since the insulation jacket is cut out to fit around the hardware used to index the packages to one another, the insulation jacket and the underlying insulation will be pulled in the same direction as the outer shell, thus preventing the creation of a gap between the interface of the insulation wrap and the end plate. Even if such a gap would occur, no direct exposure of cavity within the inner shell to the outer shell surfaces will result since the closure plugs at each end of the package are longer than the predicted movement under differential thermal expansion. Instead, the likely and worst case scenario is that the movement of the outer shell, the insulation jacket, and the insulation will create a gap of approximately 0.9-inches at the interface between the first support rib and the insulation. Combining this gap with an insulation shift of up to 1.75-inches at this same locations due to a pre-fire, 30-foot end drop (see Section 3.5.2.2, *Description of Thermal Model for HAC Conditions*) could result in a scenario where there is a 0.9-inch gap between the support rib and the insulation jacket and up to a 0.9 + 1.75 = 2.65-inch gap between the support rib and the end of the insulation wrap. A sensitivity thermal analysis of this geometry showed that the peak inner shell temperature reported in Table 3.4-1 remained bounding, while the maximum temperature of the ATR fuel element increased by less than 25°F. This modest change in temperature occurs because there is little difference in temperature between the outer shell and the stainless steel insulation wrap. Since this level of temperature increase is well within the thermal margins apparent from Table 3.4-1, the potential thermal impact due to the package geometry displacement under differential thermal expansion is seen as being not significant to the safety of the package.

## Table 3.4-1 – HAC Temperatures

| Location / Component | Pre-fire | End of Fire | Peak | Maximum Allowable ① |
|---|---|---|---|---|
| ATR Fuel Element Fuel Plate | 100°F | 540°F | 690°F | 1,100°F |
| ATR Fuel Element Side Plate | 100°F | 643°F | 786°F | 1,100°F |
| Neoprene Rub Strips/ Polyethylene Bag | 100°F | 973°F | 975°F | N/A |
| Fuel Handling Enclosure (FHE) | 100°F | 973°F | 975°F | 1,100°F |
| Loose Fuel Plate Basket (LFPB) | 100°F | 547°F | 712°F | 1,100°F |
| Inner Shell | 100°F | 1,377°F | 1,377°F | 2,700°F |
| Ceramic Fiber Insulation, Body | | | | |
| - Maximum | 100°F | 1,411°F | 1,411°F | 2,300°F |
| - Average | 100°F | 1,176°F | 1,176°F | 2,300°F |
| Ceramic Fiber Insulation, Closure | | | | |
| - Maximum | 100°F | 1,376°F | 1,376°F | 2,300°F |
| - Average | 100°F | 1,254°F | 1,254°F | 2,300°F |
| Closure | 100°F | 1,402°F | 1,402°F | 2,700°F |
| Outer Shell | 100°F | 1,427°F | 1,427°F | 2,700°F |

Table Notes:

① The maximum allowable temperatures under HAC conditions are provided in Section 3.2.2, Technical Specifications of Components.

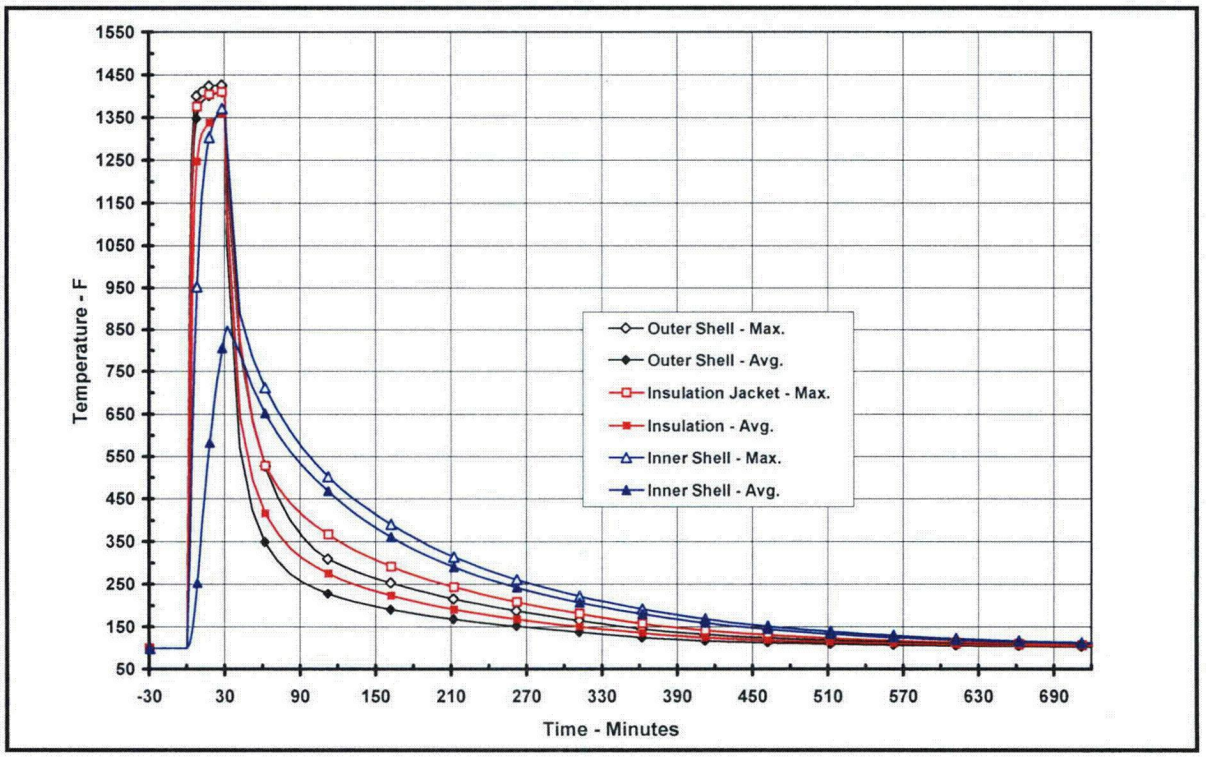


**Figure 3.4-1** – ATR FFSC Package Thermal Response to HAC Event

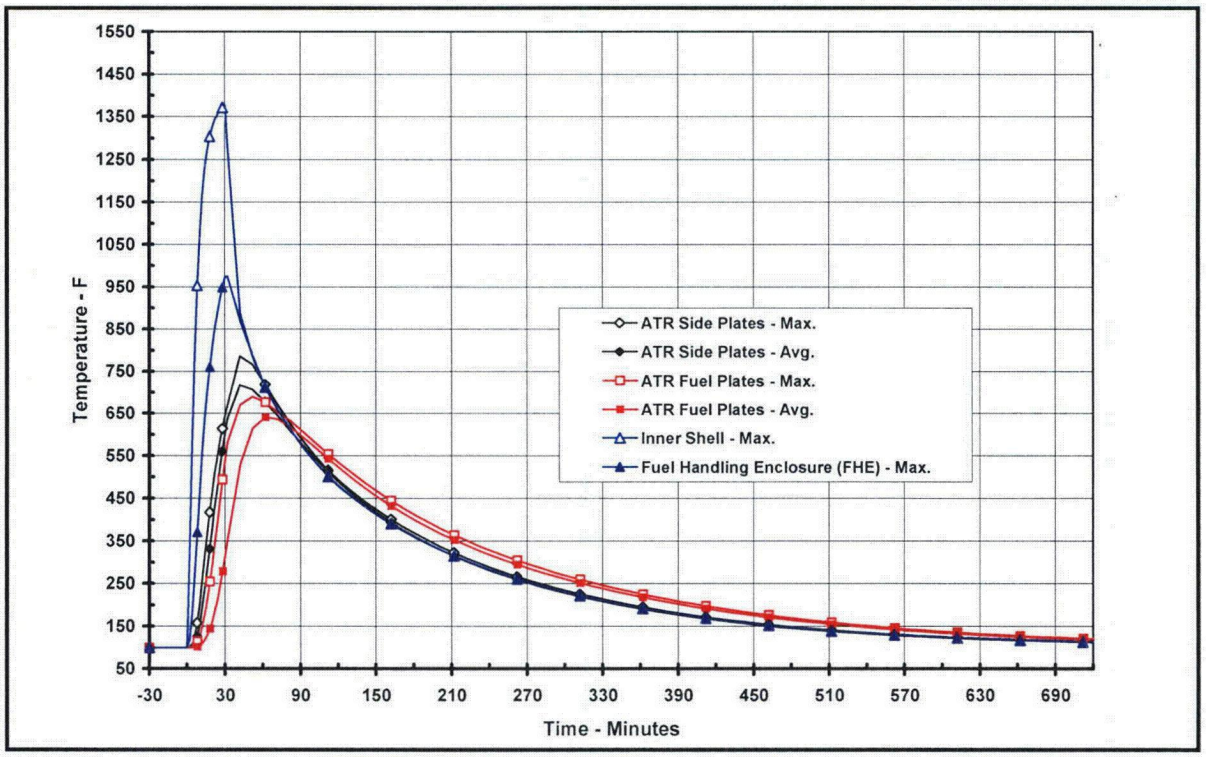


**Figure 3.4-2** – ATR Fuel Element Thermal Response to HAC Event

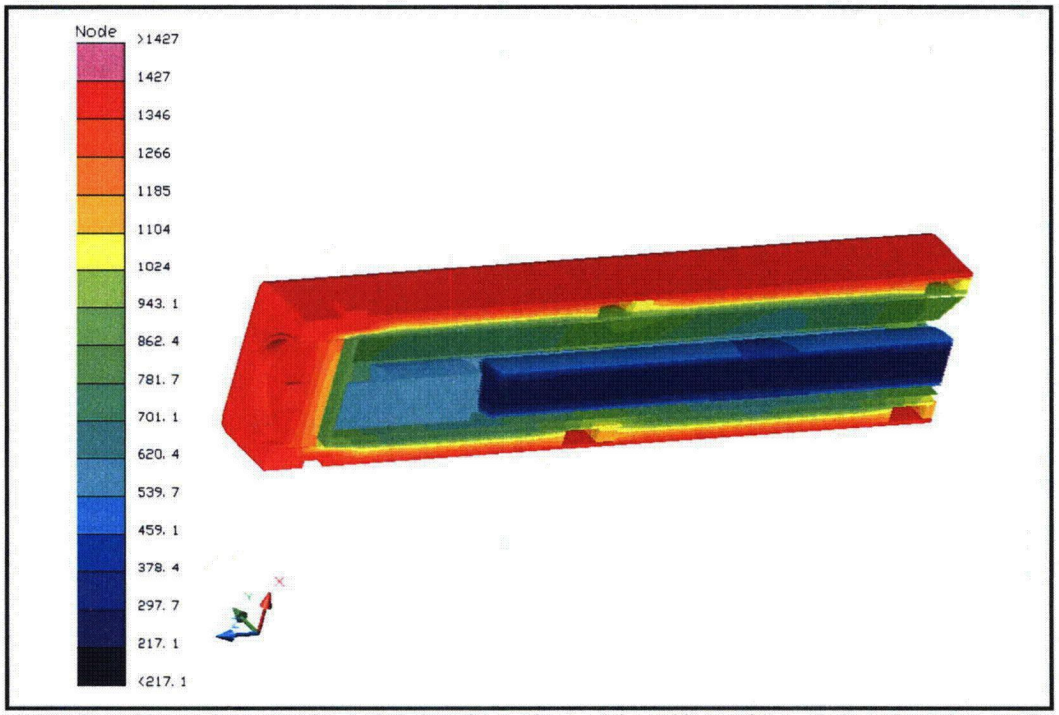


(Note: the positive x-axis is oriented towards the top of the package and the positive z-axis towards the package closure end)

**Figure 3.4-3** –Temperature Distribution at End of HAC 30-Minute Fire

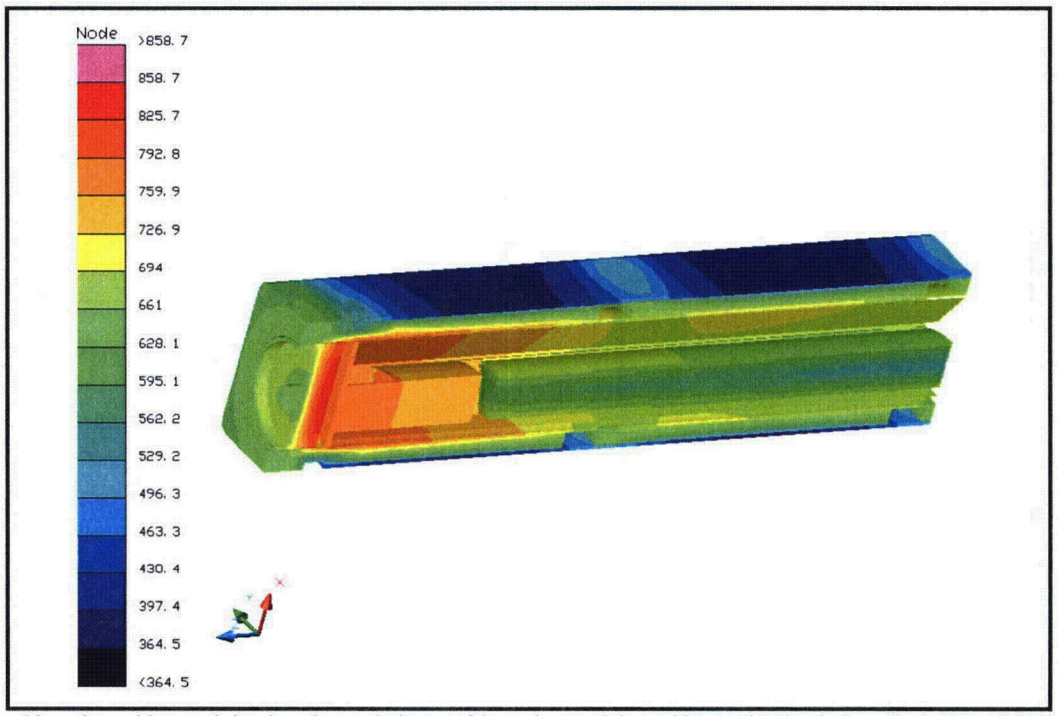


(Note: the positive x-axis is oriented towards the top of the package and the positive z-axis towards the package closure end)

**Figure 3.4-4** –Temperature Distribution at Peak ATR Fuel Element Temperature

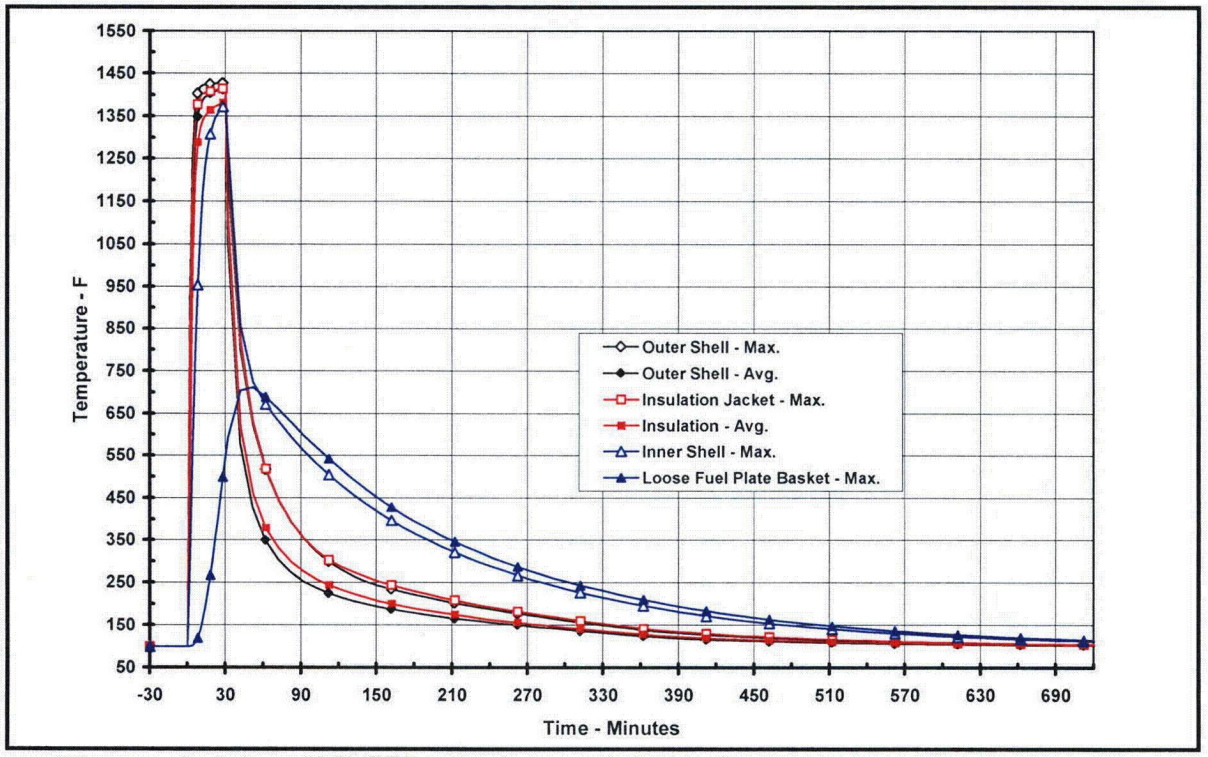


**Figure 3.4-5** – ATR FFSC Package with LFPB Thermal Response to HAC Event

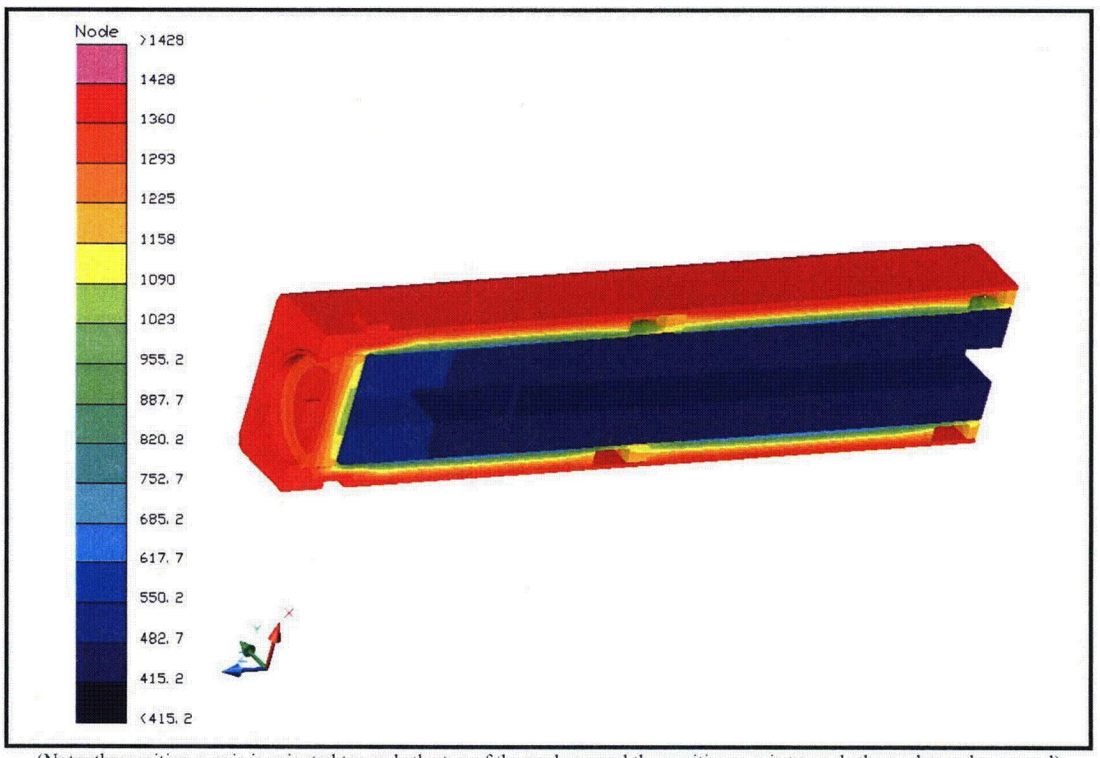


(Note: the positive x-axis is oriented towards the top of the package and the positive z-axis towards the package closure end)

**Figure 3.4-6** – FFSC-LFPB Temperature Distribution at End of HAC Fire

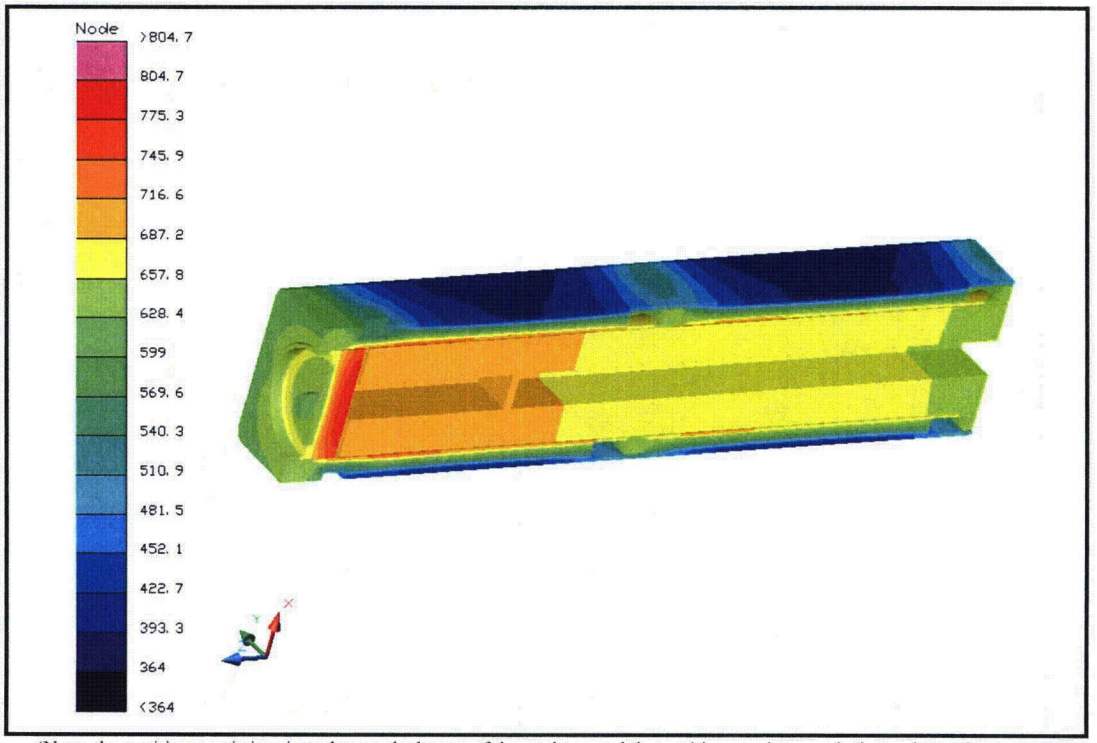


(Note: the positive x-axis is oriented towards the top of the package and the positive z-axis towards the package closure end)

**Figure 3.4-7** – FFSC-LFPB Temperature Distribution at Peak LFPB Temperature

# 3.5 Appendices

3.5.1 Computer Analysis Results

3.5.2 Analytical Thermal Model

## 3.5.1 Computer Analysis Results

Due to the size and number of the output files associated with each analyzed condition, results from the computer analysis are provided on a CD-ROM.

## 3.5.2 Analytical Thermal Model

The analytical thermal model of the ATR FFSC package was developed for use with the Thermal Desktop®[21] and SINDA/FLUINT[22] computer programs. These programs are designed to function together to build, exercise, and post-process a thermal model. The Thermal Desktop® computer program is used to provide graphical input and output display function, as well as computing the radiation exchange conductors for the defined geometry and optical properties. Thermal Desktop® is designed to run as an AutoCAD® application. As such, all of the CAD tools available for generating geometry within AutoCAD® can be used for generating a thermal model. In addition, the use of the AutoCAD® layers tool presents a convenient means of segregating the thermal model into its various elements.

The SINDA/FLUINT computer program is a general purpose code that handles problems defined in finite difference (i.e., lumped parameter) and/or finite element terms and can be used to compute the steady-state and transient behavior of the modeled system. Although the code can be used to solve any physical problem governed by diffusion-type equations, specialized functions used to address the physics of heat transfer and fluid flow make the code primarily a thermal code.

The SINDA/FLUINT and Thermal Desktop® computer programs have been validated for safety basis calculations for nuclear related projects[23].

Together, the Thermal Desktop® and SINDA/FLUINT codes provide the capability to simulate steady-state and transient temperatures using temperature dependent material properties and heat transfer via conduction, convection, and radiation. Complex algorithms may be programmed into the solution process for the purposes of computing heat transfer coefficients as a function of the local geometry, gas thermal properties as a function of species content, temperature, and pressure, or, for example, to estimate the effects of buoyancy driven heat transfer as a function of density differences and flow geometry.

### 3.5.2.1 Description of Thermal Model for NCT Conditions

A 3-dimensional, one-quarter symmetry thermal model of the ATR FFSC is used for the NCT evaluation. The model simulates one-quarter of the package, extending from the closure to the axial centerline of the package. Symmetry conditions are assumed about the package's vertical axis and at the axial centerline. This modeling choice captures the full height of the package

---

[21] Thermal Desktop®, Version 4.8, Cullimore & Ring Technologies, Inc., Littleton, CO, 2005.

[22] SINDA/FLUINT, Systems Improved Numerical Differencing Analyzer and Fluid Integrator, Version 4.8, Cullimore & Ring Technologies, Inc., Littleton, CO, 2005.

[23] Software Validation Test Report for Thermal Desktop® and SINDA/FLUINT, Version 4.8, Packaging Technology, Inc., File No. TR-VV-05-001, Rev. 1.

components and allows the incorporation of the varying insolation loads that will occur at the top and sides of the package. Program features within the Thermal Desktop® computer program automatically compute the various areas, lengths, thermal conductors, and view factors involved in determining the individual elements that make up the thermal model of the complete assembly.

Figure 3.5-1 and Figure 3.5-2 illustrate the 'solid' and 'hidden line' views of the package thermal model. The model simulates one-half of the closure end half of the package (i.e., symmetry is assumed about the package's vertical plane) and extends approximately 36.5 inches in the axial direction (e.g., from closure to the mid-point of the center support rib). As seen from the figure, the modeling captures the various components of the packaging, including the index lug and mating pocket used to align the stacked packages, the recessed exterior surface area of the package closure, the FHE, and the ATR fuel element. Also captured, but not easily seen in the figure due to the scale of the figures, are the nineteen (19) individual fuel plates that comprise the ATR fuel element.

The model is composed of solid and plate type elements representing the various package components. Thermal communication between the various components is via conduction, radiation, and surface-to-surface contact. Since the ATR FFSC Package dissipates essentially no decay heat, the peak temperatures internal to the package are driven by the external heating occurring during NCT and HAC conditions. While the potential for developing convective flows within the air filled cavity between the outer shell and the insulation jacket is small due to the cavity dimensions, if convective heat transfer was to develop it could raise the peak temperatures developed under either NCT or HAC conditions since it would reduce the thermal resistance to heat flowing inward from the outer shell. To address this possibility, the thermal conductivity associated with the air overpack nodes in the lower quadrant of the package are increased by a factor of 2 from that for conduction as a means of simulating the type of enhanced heat transfer that convection would cause. The affected nodes are limited to those in the lower quadrant of the package since, in the assumed horizontal orientation of the package under both NCT and HAC conditions, the buoyancy forces associated with convection will tend to drive the flow in this portion of the package in a circular motion, but would only produce a stratified temperature layer in the upper quadrant.

A total of approximately 8,050 nodes, 2,800 planar elements, and 3,700 solid elements are used to simulate the modeled components. In addition, one boundary node is used to represent the ambient environment for convection purposes and a second boundary node is used to represent the ambient temperature for the purpose of radiation heat transfer.

Figure 3.5-3 and Figure 3.5-4 illustrate the quarter symmetry thermal models of the FHE and the ATR fuel element. The FHE thermal model uses planar elements to represent the 0.09 inch thick sides of the enclosure, while solid elements are used to represent the 0.25 inch thick end cap. Heat transfer between the FHE and the inner shell of the package is modeled as a combination of radiation and conduction across the air-filled void space, as well as via direct contact along 3 edges of the FHE. The contact conductance simulates the physical contact between an impact deformed FHE and the inner shell. Figure 3.5-5 illustrates a cross-section through the combined modeling for the inner shell, the FHE, and the ATR fuel element. The left side of the figure illustrates the placement of the thermal nodes (indicated by the small circles) used to simulate each of the components, the use of curved elements to represent the 19 fuel plates, and the

assumed points of direct contact between the FHE and the inner shell. The right side of the figure includes depiction of the solid elements that are used to simulate the air voids in and around the FHE. The heat transfer between the FHE and the ATR fuel element is computed as conductance through the 0.125 inch thick neoprene rub strips (see Figure 3.5-5) and radiation and conductance through the air voids.

The heat transfer due to direct contact conservatively assumes the FHE has been deformed as a result of the HAC drop event to create 'flat' areas measuring 0.5 inches wide at the lower 2 points of contact, 0.75 inches wide at the top, and extending the entire length of the FHE. Although this type of damage would only occur for the HAC condition (if it occurs at all), it is conservatively assumed for the NCT modeling as well. A conservatively high contact conductance[24] of 1 Btu/min-in$^2$-°F is assumed.

A detailed model of the ATR fuel element is used to simulate the heat transfer within the fuel element and between the fuel element and the FHE. The detailed thermal model, illustrated in Figure 3.5-4 and Figure 3.5-5, includes a separate representation of each composite fuel plate, the side plates (including the cutouts), and the upper end box casting. Heat transfer between the individual fuel plates is simulated via conduction and radiation across the air space separating the plates. The curvature and separation distance between the plates is based on the information presented in Section 3.5.2.4, *Determination of Composite Thermal Properties for ATR Fuel Plates*. Each quarter segment of the fuel plates is represented by four thermal nodes in the circumferential direction and 16 nodes along its length.

The thermal modeling for the Loose Fuel Plate Basket uses the same model for the ATR FFSC, but replaces the thermal modeling of the FHE and the ATR fuel element with the thermal modeling for the Loose Fuel Plate Basket depicted in Figure 3.5-6. Approximately 500 nodes, 280 planar elements, and 530 solids are used to simulate the basket. Since the payload for the basket may contain a variable number and size of fuel plates, the thermal modeling is based on an empty basket. This approach is conservative since the addition of a payload will serve to increase the thermal mass of the basket and, thus, reduce its temperature rise under the transient conditions associated with the HAC event. Since the un-irradiated fuel plates have essentially zero decay heat, there will be no temperature rise between the loose fuel plates and the basket. As such, modeling of the loose fuel plate payload is both unnecessary and conservative for the purposes of this evaluation.

The heat transfer from the exterior surfaces of the ATR FFSC is modeled as a combination of convection and radiation exchange. Appendix 3.5.2.3, *Convection Coefficient Calculation*, presents the methodology used to compute the convection coefficients from the various surfaces. The radiation exchange is computed using a Monte Carlo, ray tracing technique and includes the affect of reflection and/or transmission, according to the optical properties assigned to each surface (see Section 3.2.1, *Material Properties*).

In addition, heating of the exterior surfaces due to solar insolation is assumed using a diurnal cycle. A sine wave model is used to simulate the variation in the applied insolation on the surfaces of the package over a 24-hour period, except that when the sine function is negative, the

[24] Rohsenow, Hartnett, and Ganic, *Handbook of Heat Transfer Fundamentals*, 2nd Edition, 1985, Curve 16, Figure 8, Chapter 4.

insolation level is set to zero. The timing of the sine wave is set to achieve its peak at 12 pm and peak value of the curve is adjusted to ensure that the total energy delivered matched the regulatory values. As such, the total energy delivered in one day by the sine wave solar model is given by:

$$\int_{6\cdot hr}^{18\cdot hr} Q_{peak}\cdot\sin\left(\frac{\pi\cdot t}{12\cdot hr}-\frac{\pi}{2}\right)dt=\left(\frac{24\cdot hr}{\pi}\right)\cdot Q_{peak}$$

Using the expression above for the peak rate of insolation, the peak rates for top and side insolation may be calculated as follows:

$$Q_{top}=\left(800\frac{cal}{cm^2}\right)\cdot\left(\frac{\pi}{24\,hr}\right) \qquad Q_{top}=2.68\frac{Btu}{hr\text{-}in^2}=0.0447\frac{Btu}{min\text{-}in^2}$$

$$Q_{side}=\left(200\frac{cal}{cm^2}\right)\cdot\left(\frac{\pi}{24\,hr}\right) \qquad Q_{sside}=0.67\frac{Btu}{hr\text{-}in^2}=0.0112\frac{Btu}{min\text{-}in^2}$$

Conversion factors of 1 cal/cm$^2$-hr = 0.0256 Btu/hr-in$^2$ are used in the above calculations. These peak rates are multiplied by the sine function and the solar absorptivity for Type 304 stainless steel (i.e., 0.52) to create the top and side insolation values as a function of time of day.

### 3.5.2.2 Description of Thermal Model for HAC Conditions

The thermal evaluations for the hypothetical accident condition (HAC) are conducted using an analytical thermal model of the ATR FFSC. The HAC thermal model is a modified version of the quarter symmetry NCT model described in Section 3.5.2.1, *Description of Thermal Model for NCT Conditions*, with the principal model modifications consisting of simulating the expected package damage resulting from the drop events that are assumed to precede the HAC fire and changing the package surface emissivities to reflect the assumed presence of soot and/or surface oxidization.

Physical testing using full scale certified test units (CTUs) is used to establish the expected level of damage sustained by the ATR FFSC package from the 10 CFR 71.73 prescribed free and puncture drops that are assumed to precede the HAC fire event. Appendix 2.12.1, *Certification Tests on CTU-1* and Appendix 2.12.2, *Certification Tests on CTU-2* document the configuration and initial conditions of the test articles, the test facilities, the instrumentation used, and the test results. The drop tests covered a range of hypothetical free drop orientations and puncture bar drops. The results from both sets of CTU drop tests showed the following:

1) The worst case physical damage to the exterior of the package occurs from a CG over corner drop. The resulting damage (depicted in Figure 3.5-7) is thermally insignificant in that there is no breach in the outer shell and the compaction of the underlying insulation is minor and offset by an increase in the gap between the outer shell and the insulation in other areas.

2) The oblique, CG over side puncture bar drop caused a 0.5 inch indentation to the side of the package at the center of the impact region and less near the edges. No tearing of the outer shell occurred.

3) The end drops caused the ceramic fiber insulation to slide axially between each set of ribs, as depicted in Figure 3.5-9. The amount of re-positioning varied from approximately 1 to 1.75 inches and results in the compression of the insulation in the axial direction by 6 to 10%. No compression or shifting of the insulation in the radial direction was noted from the drop tests. While the insulation jacket showed some crimping at the edges, it was essentially undamaged.

Based on the above observations, the NCT was modified for the HAC evaluations via the following steps:

1) A 1.85 inch long segment of insulation was removed between each set of ribs. This degree of insulation re-positioning/compression conservatively bounds the maximum observed distance of 1.75 inches. Heat transfer across the vacated segments of insulation is then computed as radiation and conduction across an air filled space. Figure 3.5-10 illustrates the change made to the NCT thermal model to capture the expected insulation re-positioning. The change in the insulation's thermal conductivity as a result of the compression is conservatively ignored since thermal conductivity decreases with density at temperatures in excess of approximately 500°F (see Table 3.2-3).

2) All other geometric aspects of the NCT thermal model are assumed to be unchanged for the HAC evaluations since the observed damage to the outer shell resulting from the free and puncture drops has a superficial impact to the thermal protection offered by the ATR FFSC to the HAC fire event.

3) The surface emissivities for the various components of the package are revised as presented in Table 3.2-6 vs. that given in Table 3.2-5.

### 3.5.2.3 Convection Coefficient Calculation

The convective heat transfer coefficient, $h_c$, has a form of: $h_c = Nu\frac{k}{L}$, where k is the thermal conductivity of the gas at the mean film temperature and L is the characteristic length of the vertical or horizontal surface.

Natural convection from each surface is computed based on semi-empirical relationships using the local Rayleigh number and the characteristic length for the surface. The Rayleigh number is defined as:

$$Ra_L = \frac{\rho^2 g_c \beta L^3 \Delta T}{\mu^2} \times Pr$$

where:

$g_c$ = gravitational acceleration, 32.174 ft/s$^2$
$\beta$ = coefficient of thermal expansion, °R$^{-1}$
$\Delta T$ = temperature difference, °F
$\rho$ = density of air at the film temperature, lb$_m$/ft$^3$
$\mu$ = dynamic viscosity, lb$_m$/ft-s
Pr = Prandtl number = ($c_p$ $\mu$) / k
L = characteristic length, ft
$k$ = thermal conductivity at film temperature
$c_p$ = specific heat, Btu/lb$_m$-hr-°F
$Ra_L$ = Rayleigh #, based on length 'L'

Note that k, $c_p$, and $\mu$ are each a function of air temperature as taken from Table 3.2-4. Values for $\rho$ are computed using the ideal gas law, $\beta$ for an ideal gas is simply the inverse of the absolute temperature of the gas, and Pr is computed using the values for k, $c_p$, and $\mu$ from Table 3.2-4. Unit conversion factors are used as required to reconcile the units for the various properties used.

The natural convection from a discrete vertical surface is computed using Equation 6.39 to 6.42 of Rohsenow, et. al. [25], which is applicable over the range 1 < Rayleigh number (Ra) < $10^{12}$:

$$Nu^T = \overline{C}_L Ra^{1/4}$$

$$\overline{C}_L = \frac{0.671}{\left(1 + (0.492/Pr)^{9/16}\right)^{4/9}}$$

$$Nu_L = \frac{2.8}{\ln(1 + 2.8/Nu^T)}$$

$$Nu_t = C_t^V Ra^{1/3}$$

$$C_t^V = \frac{0.13\,Pr^{0.22}}{\left(1 + 0.61\,Pr^{0.81}\right)^{0.42}}$$

[25] Rohsenow, Hartnett, and Ganic, *Handbook of Heat Transfer Fundamentals*, 2rd edition, McGraw-Hill Publishers, 1985.

$$Nu = \frac{h_c L}{k} = \left[(Nu_L)^6 + (Nu_t)^6\right]^{1/6}$$

Natural convection from horizontal surfaces is computed from Equations 4.39 and 4.40 of Rohsenow, et. al.[25], and Equations 3.34 to 3.36 of Guyer [26], where the characteristic dimension (L) is equal to the plate surface area divided by the plate perimeter. For a heated surface facing upwards or a cooled surface facing downwards and Ra > 1:

$$Nu = \frac{h_c L}{k} = \left[(Nu_L)^{10} + (Nu_t)^{10}\right]^{1/10}$$

$$Nu_L = \frac{1.4}{\ln\left(1 + 1.677/\left(\overline{C_L} Ra^{1/4}\right)\right)}$$

$$\overline{C_L} = \frac{0.671}{\left[1 + (0.492/Pr)^{9/16}\right]^{4/9}}$$

$$Nu_t = 0.14 Ra^{1/3}$$

For a heated surface facing downwards or a cooled surface facing upwards and $10^3 < Ra < 10^{10}$, the correlation is as follows:

$$Nu = Nu_L = \frac{2.5}{\ln\left(1 + 2.5/Nu^T\right)}$$

$$Nu^T = \frac{0.527}{\left(1 + (1.9/Pr)^{9/10}\right)^{2/9}} Ra^{1/5}$$

The forced convection coefficients applied during the HAC fire event are computed using the relationships in Table 6-5 of Kreith[27] for a flat surface, where the characteristic dimension (L) is equal to the length along the surface and the free stream flow velocity is V. The heat transfer coefficient is computed based on the local Reynolds number, where the Reynolds number is defined as:

$$Re_L = \frac{V \times \rho \times L}{\mu}$$

For Reynolds number (Re) < $5 \times 10^5$ and Prandtl number (Pr) > 0.1:

$$Nu = 0.664\, Re_L^{0.5}\, Pr^{0.33}$$

For Reynolds number (Re) > $5 \times 10^5$ and Prandtl number (Pr) > 0.5:

$$Nu = 0.036\, Pr^{0.33}\left[Re_L^{0.8} - 23{,}200\right]$$

Given the turbulent nature of the 30-minute fire event, a characteristic length of 0.25 feet is used for all surfaces to define the probable limited distance for boundary growth.

[26] Guyer, E.C., *Handbook of Applied Thermal Design*, McGraw-Hill, Inc., 1989.

[27] Kreith, Frank, *Principles of Heat Transfer*, 3rd edition, Harper & Row, 1973.

### 3.5.2.4 Determination of Composite Thermal Properties for ATR Fuel Plates

The ATR fuel plates are a composite material consisting of a fissile fuel matrix sandwiched within aluminum cladding. For the purposes of this calculation, the fuel composite is treated as a homogenous material with lumped thermal properties as defined below. This modeling approach is justified since the thermal gradient within the fuel element will be very low given that the un-irradiated fuel has essentially no decay heat.

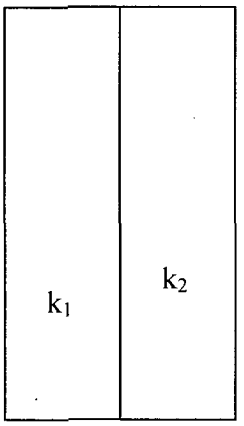


Because of the thinness of the plates, the average conductivity is required only for the axial and circumferential direction. Conductivity through the plates is not required as this analysis assumes a zero temperature gradient in that direction. Mean density and specific heat values are also defined below.

Circumferential and Axial Conductivity

Ignoring the affect of curvature, the heat flow can be written as,

$$q = -\Delta x \Delta z\, \bar{k} \frac{\Delta T}{\Delta y} = -\Delta x_1 \Delta z\, k_1 \frac{\Delta T}{\Delta y} - \Delta x_2 \Delta z\, k_2 \frac{\Delta T}{\Delta y} \quad \text{where}$$

$$\Delta x = \sum_i \Delta x_i$$

From which,

$$\bar{k} = \frac{\Delta x_1 k_1 + \Delta x_2 k_2}{\Delta x}$$

Mean Density

The mean density of the fuel plates is computed from:

$$Mass = \Delta x \Delta y \Delta z\, \bar{\rho} = \Delta x_1 \Delta y \Delta z\, \rho_1 + \Delta x_2 \Delta y \Delta z\, \rho_2 \text{, from which we get } \bar{\rho} = \frac{\Delta x_1 \rho_1 + \Delta x_2 \rho_2}{\Delta x}$$

Mean Specific Heat

In the same manner used to define the mean density, the mean specific heat for the fuel plates is computed as;

$$\bar{\rho}\, \bar{c}_p \Delta x \Delta y \Delta z = \rho_1 c_{p_1} \Delta x_1 \Delta y \Delta z + \rho_2 c_{p_2} \Delta x_2 \Delta y \Delta z \text{ from which we get, } \bar{c}_p = \frac{\rho_1 c_{p_1} \Delta x_1 + \rho_2 c_{p_2} \Delta x_2}{\bar{\rho}\, \Delta x}$$

The thermal properties for the individual plates making up the ATR fuel element are computed using the above approach and thermophysical and geometric data[28,29] for the ATR fuel element.

Based on these data sources, the radius of the inner plate is 3.015 inches, while the radius of the outer plate is 5.44 inches. The gap between the plates is 0.078 inches. The thickness of the aluminum cladding is 0.015 inches.

While the thermal properties for the aluminum cladding and the fissile fuel matrix material will vary with temperature, for the purposes of this evaluation, fixed material properties are assumed in order to simplify the calculation. To provide conservatism for this modeling approach conservatively low value is assumed for the specific heat for each component, while a conservatively high thermal conductivity value is used. This methodology will result in over-predicting the temperature rise within the composite material during the HAC fire event.

The thermal properties used in this calculation are:

1) Aluminum cladding thermal conductivity = 191 W/m-K, conservatively high value from [28], page 18
2) Fissile fuel matrix ($UAl_x$) = 14.47 W/m-K, conservatively high based on equation 2.3 from [28], at 300K
3) Aluminum cladding density = 2702 kg/m$^3$, from [28], page 16
4) Fissile fuel matrix ($UAl_x$) density = 3680 kg/m$^3$, from [28], Table 2.5, average density
5) Aluminum cladding specific heat = 1034 J/kg-K, from [28], Table 3.2, mean value at 600K
6) Fissile fuel matrix ($UAl_x$) specific heat = 708 J/kg-K, from [28], Table 2.4, average value at 600K

Table 3.5-1 presents the composite thermal conductivity, specific heat, and density values for each of the nineteen (19) fuel plates making up the ATR fuel element. These composite values are based on the thermal property values given above and the geometry depicted in Figure 3.5-11.

[28] *Thermophysical And Mechanical Properties Of ATR Core Materials*, Report No. PG-T-91-031, August 1991, EG&G Idaho, Inc.

[29] *ATR Mark VII Fuel Element Assembly*, INEEL Drawing No. DWG-405400, Rev-19.

## Table 3.5-1 – Composite Fuel Plate Thermal Properties

| Plate | Plate Thickness, in | UAlx Thickness, in | Axial & Circumferential Conductivity (W/m-K) | Inner radius, in | Outer radius, in | Mean radius, in | Mean density, kg/m^3 | Mean specific heat, J/(kg K) |
|---|---|---|---|---|---|---|---|---|
| 1 | 0.08 | 0.05 | 80.7 | 3.015 | 3.095 | 3.055 | 3313.3 | 807.7 |
| 2 | 0.05 | 0.02 | 120.4 | 3.173 | 3.223 | 3.198 | 3093.2 | 878.9 |
| 3 | 0.05 | 0.02 | 120.4 | 3.301 | 3.351 | 3.326 | 3093.2 | 878.9 |
| 4 | 0.05 | 0.02 | 120.4 | 3.429 | 3.479 | 3.454 | 3093.2 | 878.9 |
| 5 | 0.05 | 0.02 | 120.4 | 3.557 | 3.607 | 3.582 | 3093.2 | 878.9 |
| 6 | 0.05 | 0.02 | 120.4 | 3.685 | 3.735 | 3.710 | 3093.2 | 878.9 |
| 7 | 0.05 | 0.02 | 120.4 | 3.813 | 3.863 | 3.838 | 3093.2 | 878.9 |
| 8 | 0.05 | 0.02 | 120.4 | 3.941 | 3.991 | 3.966 | 3093.2 | 878.9 |
| 9 | 0.05 | 0.02 | 120.4 | 4.069 | 4.119 | 4.094 | 3093.2 | 878.9 |
| 10 | 0.05 | 0.02 | 120.4 | 4.197 | 4.247 | 4.222 | 3093.2 | 878.9 |
| 11 | 0.05 | 0.02 | 120.4 | 4.325 | 4.375 | 4.350 | 3093.2 | 878.9 |
| 12 | 0.05 | 0.02 | 120.4 | 4.453 | 4.503 | 4.478 | 3093.2 | 878.9 |
| 13 | 0.05 | 0.02 | 120.4 | 4.581 | 4.631 | 4.606 | 3093.2 | 878.9 |
| 14 | 0.05 | 0.02 | 120.4 | 4.709 | 4.759 | 4.734 | 3093.2 | 878.9 |
| 15 | 0.05 | 0.02 | 120.4 | 4.837 | 4.887 | 4.862 | 3093.2 | 878.9 |
| 16 | 0.05 | 0.02 | 120.4 | 4.965 | 5.015 | 4.990 | 3093.2 | 878.9 |
| 17 | 0.05 | 0.02 | 120.4 | 5.093 | 5.143 | 5.118 | 3093.2 | 878.9 |
| 18 | 0.05 | 0.02 | 120.4 | 5.221 | 5.271 | 5.246 | 3093.2 | 878.9 |
| 19 | 0.1 | 0.07 | 67.4 | 5.349 | 5.449 | 5.399 | 3386.6 | 786.0 |

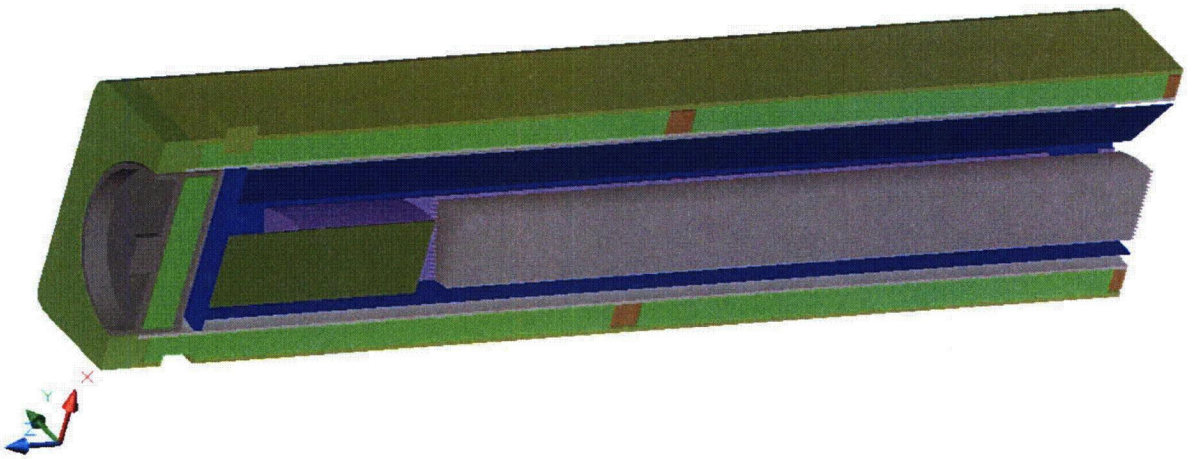

(Note: the positive x-axis is oriented towards the top of the package and the positive z-axis towards the package closure end)

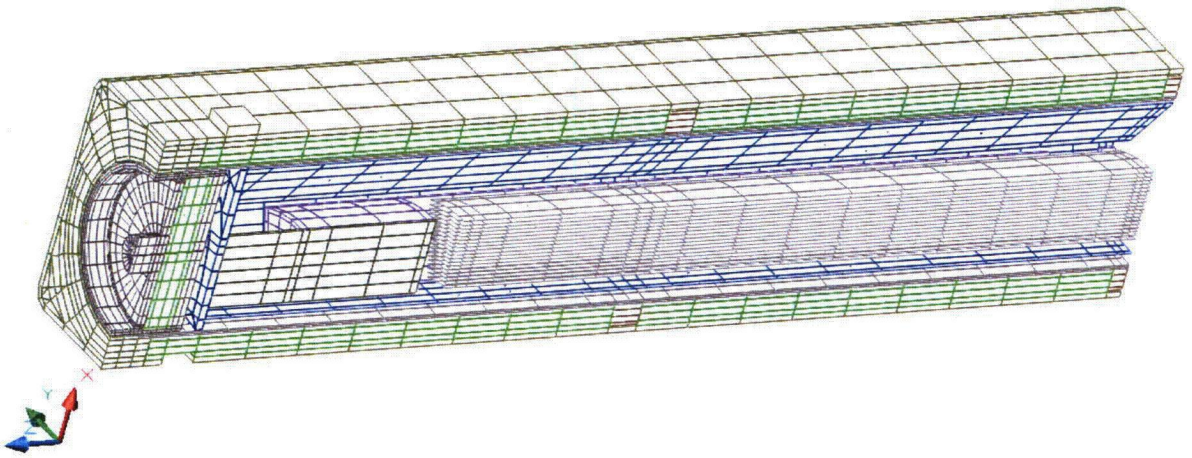

(Note: the positive x-axis is oriented towards the top of the package and the positive z-axis towards the package closure end)

**Figure 3.5-1** – 'Solid' and & 'Hidden Line' Views of Package Quarter Symmetry Thermal Model

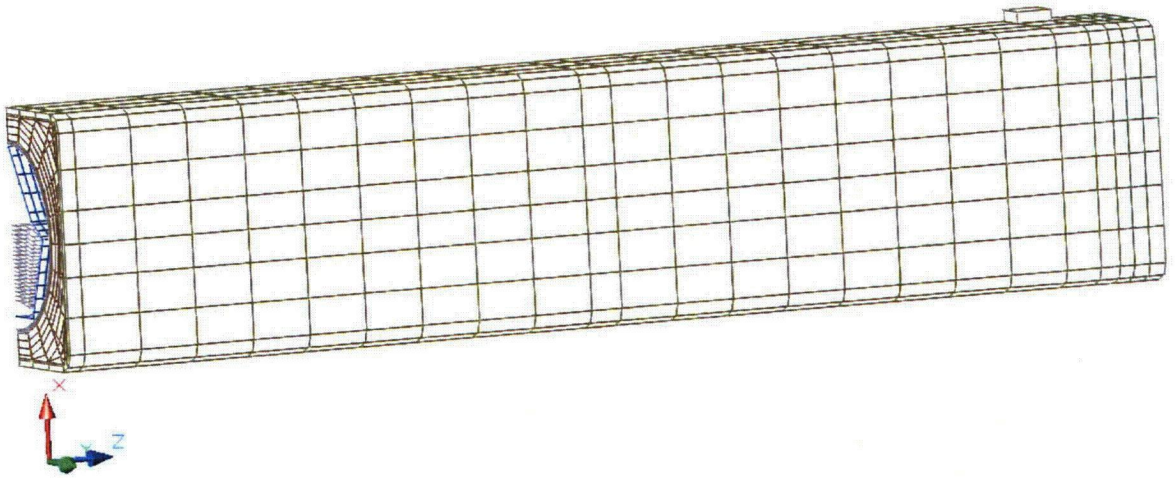


(Note: the positive x-axis is oriented towards the top of the package and the positive z-axis towards the package closure end)

**Figure 3.5-2** – Reverse, 'Hidden Line' View of Package Quarter Symmetry Thermal Model

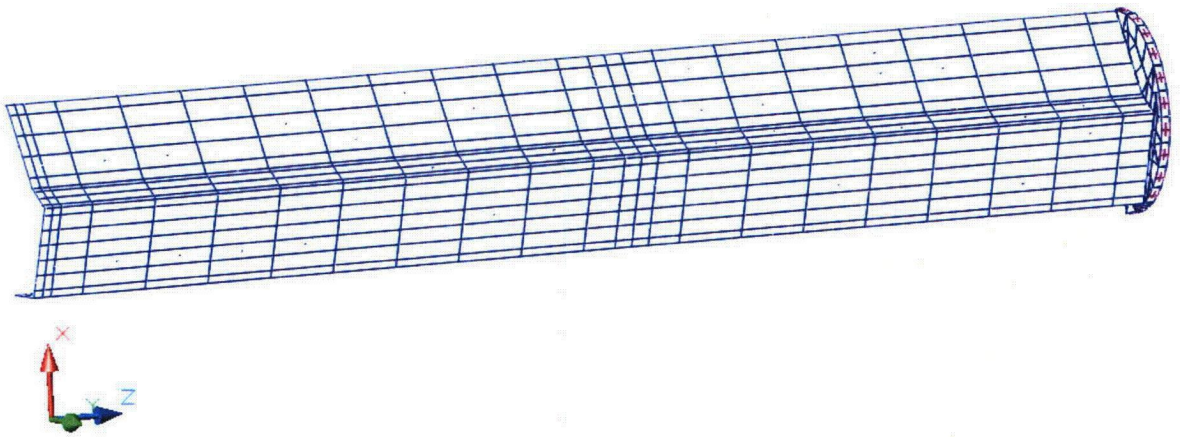


(Note: the positive x-axis is oriented towards the top of the package and the positive z-axis towards the package closure end)

**Figure 3.5-3** – Reverse, 'Hidden Line' View of FHE Quarter Symmetry Thermal Model

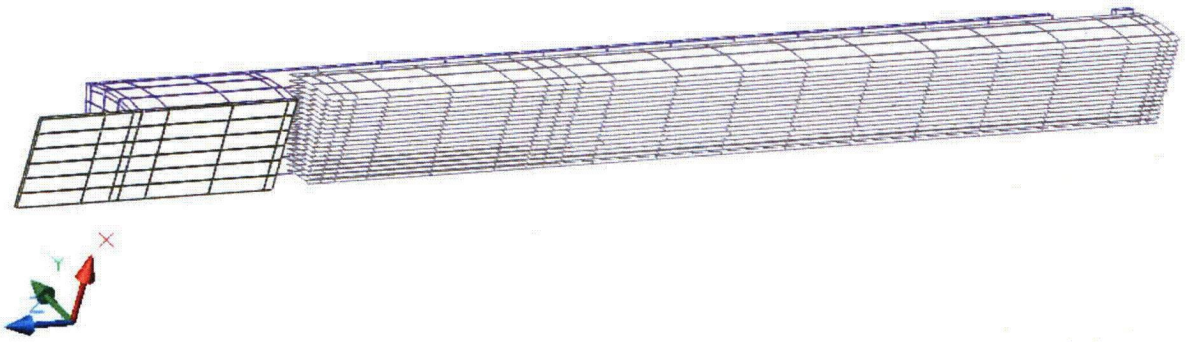


ATR Fuel Element Modeling, View Along Centerline of Element

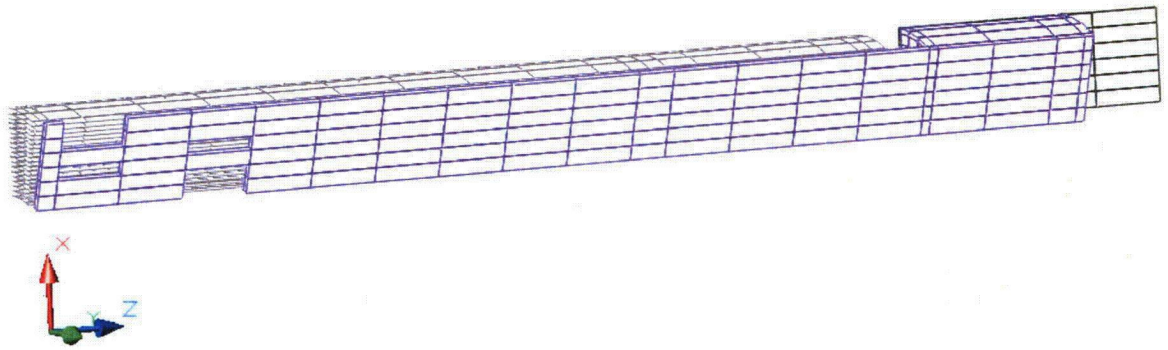


ATR Fuel Element Modeling, View Along Outside of Element

(Note: the positive x-axis is oriented towards the top of the package and the positive z-axis towards the package closure end)

**Figure 3.5-4** – Centerline and Side Views of ATR Fuel Element Thermal Model

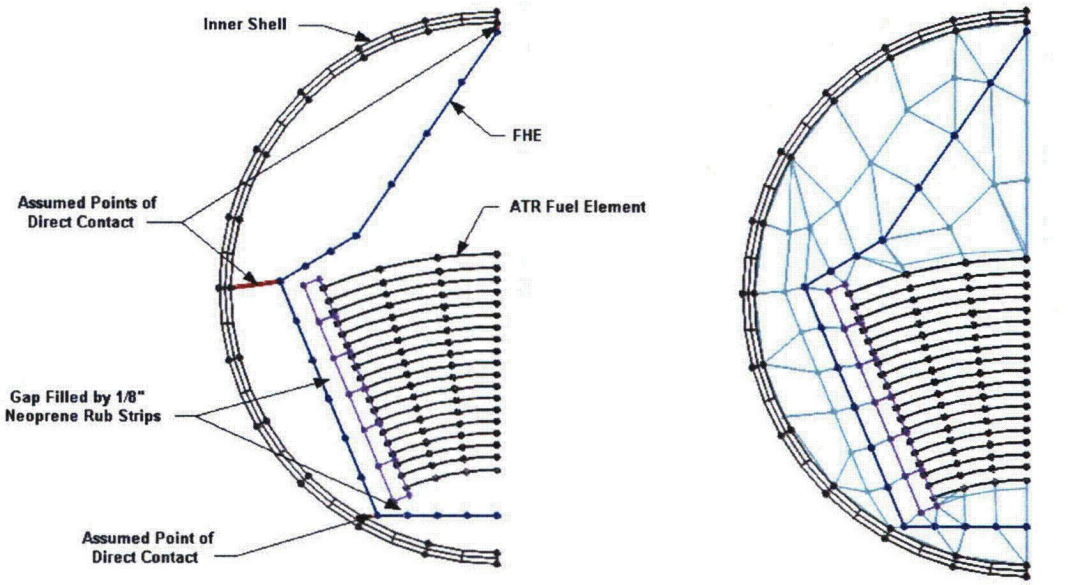


Modeling Showing Direct Contact

Modeling with 'Solid' Elements for Air

**Figure 3.5-5** – Thermal Model of ATR Fuel Element and FHE within Inner Shell

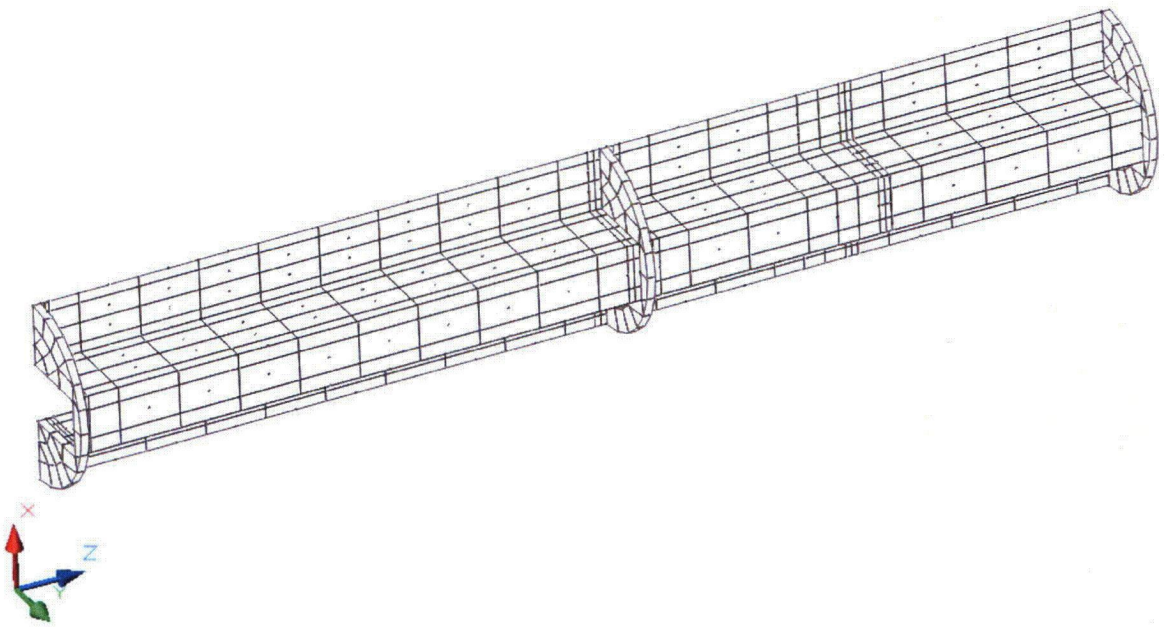


(Note: the positive x-axis is oriented towards the top of the package and the positive z-axis towards the package closure end)

**Figure 3.5-6** – Thermal Model of Loose Fuel Plate Basket (LFPB)

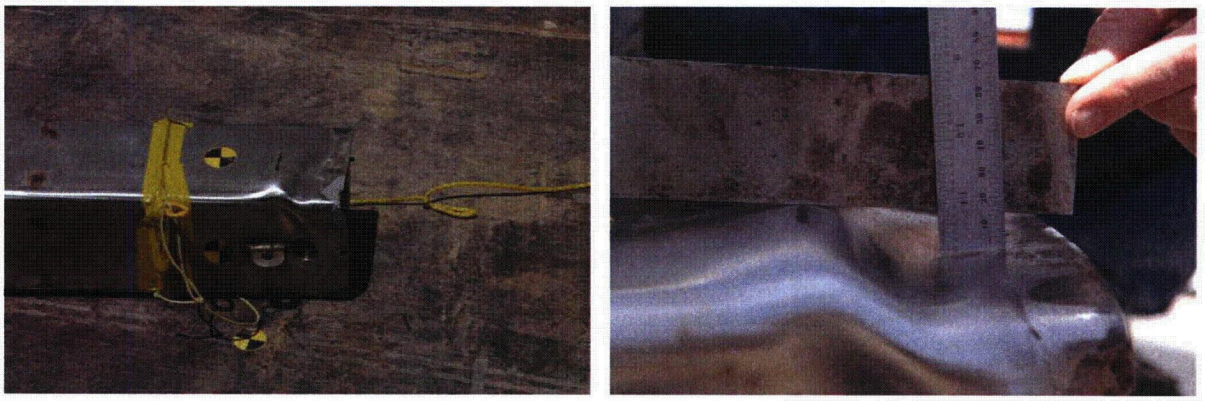

**Figure 3.5-7** – Worst Case Package Damage Arising from Corner Drop

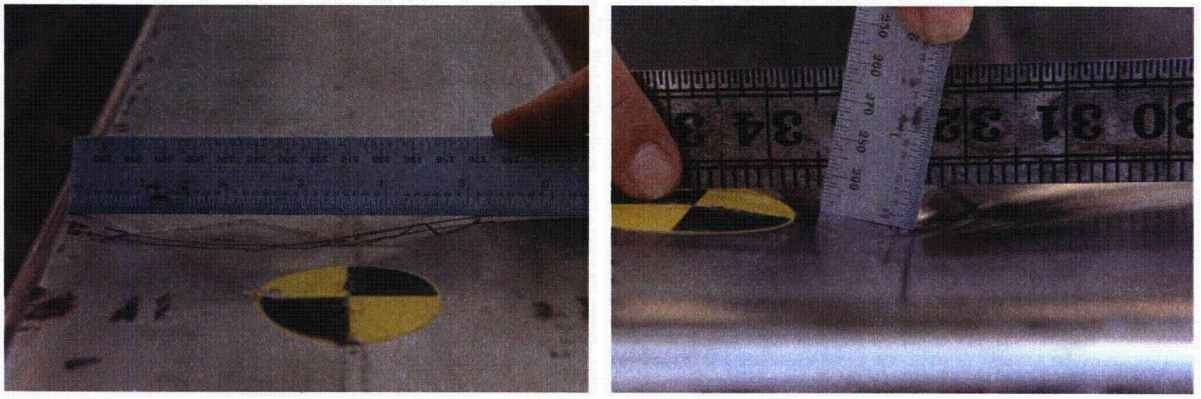

**Figure 3.5-8** – Worst Case Package Damage Arising from Oblique Puncture Drop

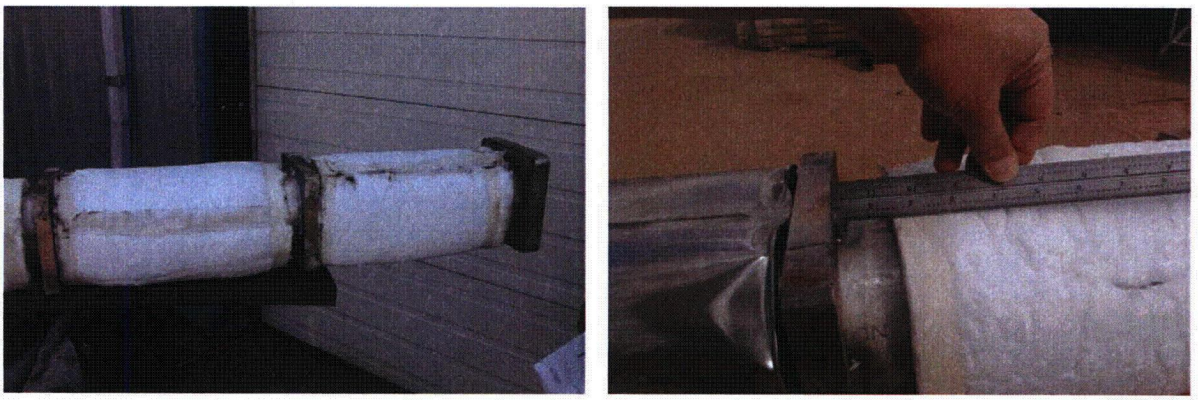

**Figure 3.5-9** – Insulation Re-positioning Arising from End Drop

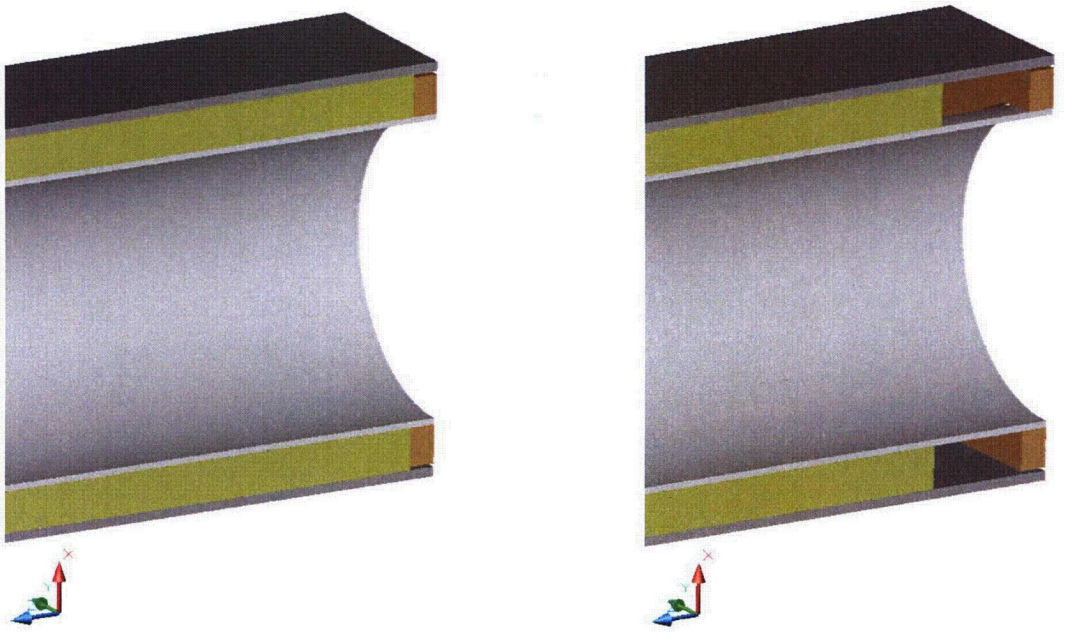

Insulation Modeling for NCT Conditions

Insulation Modeling for HAC Conditions

**Figure 3.5-10** – Thermal Modeling of Insulation Re-positioning for HAC Conditions

*Figure Withheld Under 10 CFR 2.390*

**Figure 3.5-11** – ATR Fuel Element Cross Section

# 4.0 CONTAINMENT

## 4.1 Description of the Containment System

The containment function of the ATR FFSC is to confine the ATR fuel element within the packaging during Normal Conditions of Transport (NCT) and Hypothetical Accident Conditions (HAC).

The body is a stainless steel weldment that consists of two nested shells. The outer shell is an 8-in square stainless steel tube with a 3/16-in thick wall, and the inner shell is a 6-in diameter stainless steel tube with a 0.120-in thick wall. Components are joined using full-thickness fillet welds (i.e., fillet welds whose leg size is nominally equal to the lesser thickness of the parts joined) and full and partial penetration groove welds. The end of the body is welded closed with 0.88-in plate.

The lid end of the package is closed with a simple closure device. The closure engages with the body using a bayonet style design. There are four lugs, uniformly spaced on the closure, that engage with four slots in the mating body fixture. The closure is secured by two retracting spring loaded pins, rotating the closure through 45°, and releasing the spring loaded pins such that the pins engage with the mating holes on the body. When the pins are properly engaged with the mating holes the closure is locked and cannot be removed unintentionally.

The containment boundary is defined as the boundary of the cavity formed by the closure and inner stainless steel tube. For criticality control purposes, the fuel element must remain within this boundary during NCT and HAC. No seals or gaskets are utilized within the package.

To prevent unauthorized operation, a small post on the closure is drilled to receive a tamper indicating device (TID) wire. An identical post is located on the body and is also drilled for the TID wire. For ease in operation, there are two TID posts on the body. There are only two possible angular orientations for the closure installation and the duplicate TID post on the body enables TID installation in both positions.

### 4.1.1 Type A Fissile Packages

The ATR FFSC is classified as a Type A Fissile package. The Type A Fissile package is constructed and prepared for shipment so that there is no loss or dispersal of the radioactive contents, and no significant increase in external surface radiation levels, and no substantial reduction in the effectiveness of the packaging during normal conditions of transport. The fissile material is contained within the containment boundary. Chapter 6.0, *Criticality Evaluation*, demonstrates that the package remains subcritical under normal and hypothetical accident conditions.

The ATR FFSC contains four radioactive isotopes: U-234, U-235, U-236, and U-238. The $A_2$ value for U-235 and U-238 is unlimited, while the minimum $A_2$ value for U-234 and U-236 is 0.16 Ci for slow lung absorption. To compute the mixture $A_2$, the maximum value of 1200 g U-235 is assumed, with a low weight fraction of 90% to maximize the mass of uranium. Therefore, the total mass of uranium is 1200/0.9 = 1333 g U. The maximum weight percents of U-234 (1.2%) and U-236 (0.7%) are assumed to maximize the mass of these isotopes. The balance is treated as U-238. For this conservative isotopic mix, the mixture $A_2$ is 0.164 Ci. The

package activity for this mixture is 0.103 Ci (mostly due to U-234); therefore, the package contains approximately $0.6A_2$.

### 4.1.2 Type B Packages

The content of the ATR FFSC package is high-enriched uranium with approximately $0.6A_2$ for release purposes. As a fissile package the ATR FFSC must meet the release rates for Type B packages when required by the total amount of radioactive material. However, because the $A_2$ value of the contents is less than 1 $A_2$, the package is classified as Type A and there are no release limits except as necessary for criticality control.

## 4.2 Containment under Normal Conditions of Transport

The ATR fuel element is confined within the packaging under NCT. This is verified by full-scale testing, as discussed in Section 2.6, *Normal Conditions of Transport*. The test units survived the NCT drop tests with minimal damage to the packaging and no damage to the fuel elements. The maximum internal pressure in the package does not exceed atmospheric pressure because the closure is not sealed with a gasket or other sealing material. Because the ATR FFSC is a Type A Fissile package, leakage rate testing is not required.

## 4.3 Containment under Hypothetical Accident Conditions

The radioactive material contents of the ATR FFSC package must meet the containment requirements of 10 CFR §71.55(e) such that the package would be subcritical under the HAC.

The test program demonstrates that the package contains the ATR fuel element and loose fuel plates under the HAC events sufficient to maintain criticality control. The full-scale HAC drop tests summarized in Section 2.7, *Hypothetical Accident Conditions*, confirm the HAC performance of the package. The closure remained intact throughout all the drop sequences, and the fuel element remained confined within the inner stainless steel tube. The non-fissile end boxes on the fuel element shattered as expected but the fueled portion of the element remained intact and retained its geometry. There was no dispersal of fissile material. The criticality evaluation presented in Section 6.0, *Criticality Evaluation*, evaluates the contents in the most reactive credible configuration and with water moderation as required.

Because the ATR FFSC package is a Type A Fissile package and the contents are less than 1 $A_2$, the performance requirements of 10 CFR §71.51 do not apply.

## 4.4 Leakage Rate Tests for Type B Packages

The ATR FFSC is a Type A Fissile package; therefore, this section does not apply.

# 5.0 SHIELDING EVALUATION

Compliance of the ATR FFSC with respect to the dose rate limits established by 10 CFR §71.47[1] for normal conditions of transport (NCT) or 10 CFR §71.51(a)(2) for hypothetical accident conditions (HAC) are satisfied when limiting the package to the contents specified in Section 1.2.2, *Contents*, and verified by measurement.

Prior to transport, the ATR FFSC shall be monitored for both gamma and neutron radiation to demonstrate compliance with 10 CFR §71.47. Although the ATR FFSC will likely be shipped exclusive use, dose rates will be sufficiently low to allow non-exclusive use transport, if desired.

Shielding materials are not specifically provided by the ATR FFSC. Because the contents are essentially unshielded, the HAC dose rates at one meter will not be significantly different from the NCT dose rates at one meter. This result ensures that the post-HAC, allowable dose rate of 1 rem/hr a distance of one meter from the package surface per 10 CFR §71.51(a)(2) will be met.

[1] Title 10, Code of Federal Regulations, Part 71 (10 CFR 71), *Packaging and Transportation of Radioactive Material.*

# 6.0 CRITICALITY EVALUATION

The following analyses demonstrate that the Advanced Test Reactor Fresh Fuel Shipping Container (ATR FFSC) complies with the requirements of 10 CFR §71.55[1] and §71.59. Based on a 5x5 array of damaged packages, the Criticality Safety Index (CSI), per 10 CFR §71.59, is 4.0.

## 6.1 Description of Criticality Design

### 6.1.1 Design Features Important for Criticality

A comprehensive description of the ATR FFSC is provided in Section 1.2, *Packaging Description*, and in the drawings in Appendix 1.3.2, *Packaging General Arrangement Drawings*. This section summarizes those design features important for criticality.

No poisons are utilized in the package. For the fuel element payload, the separation provided by the packaging (outer tube minimum flat-to-flat dimension of 7.9-in, inner tube maximum inner diameter of 5.814-in), along with the limit on the number of packages per shipment, is sufficient to maintain criticality safety. For the loose plate payload, in addition to the design features noted above, moderation of the loose plates is controlled by the loose plate basket, which confines the fuel plates to a rectangular area.

### 6.1.2 Summary Table of Criticality Evaluation

The upper subcritical limit (USL) for ensuring that the ATR FFSC (single package or package array) is acceptably subcritical, as determined in Section 6.8, *Benchmark Evaluations*, is:

$$USL = 0.9209$$

The package is considered to be acceptably subcritical if the computed $k_{safe}$ ($k_s$), which is defined as $k_{effective}$ ($k_{eff}$) plus twice the statistical uncertainty ($\sigma$), is less than or equal to the USL, or:

$$k_s = k_{eff} + 2\sigma \leq USL$$

The USL is determined on the basis of a benchmark analysis and incorporates the combined effects of code computational bias, the uncertainty in the bias based on both benchmark-model and computational uncertainties, and an administrative margin. The results of the benchmark analysis indicate that the USL is adequate to ensure subcriticality of the package.

The packaging design is shown to meet the requirements of 10 CFR 71.55(b) when the package is limited to either one 1200 g U-235 ATR fuel element, or 600 g U-235 in the form of ATR loose fuel plates. Moderation by water in the most reactive credible extent is utilized in both the NCT and HAC analyses. In the single package NCT models, full-density water fills the accessible cavity, while in the single package HAC models, full-density water fills all cavities. In the fuel element models, the most reactive credible configuration is utilized by maximizing the gap between the fuel plates. Maximizing this gap maximizes the moderation and hence the

[1] Title 10, Code of Federal Regulations, Part 71 (10 CFR 71), *Packaging and Transportation of Radioactive Material*.

reactivity because the system is under moderated. In the loose plate model, no credit is taken for the dunnage plates and the optimal pitch and fuel arrangement is utilized. In all single package models, 12-in of water reflection is utilized.

In the NCT and HAC array cases, partial moderation is considered to maximize array interaction effects. A 9x9x1 array is utilized for the NCT array, while a 5x5x1 array is utilized in the HAC array. In all array models, 12-in of water reflection is utilized.

The maximum results of the ATR fuel element criticality calculations are summarized in Table 6.1-1. The maximum calculated $k_s$ is 0.8284, which occurs for the optimally moderated NCT array case. The NCT array is more reactive than the HAC array because the NCT array is larger, and moderation is allowed in both conditions. In this case, the fuel element is moderated with full-density water, the inner tube is moderated with 0.3 $g/cm^3$ water, and void is modeled between the insulation and outer tube.

The maximum results of the loose plate basket criticality calculations are summarized in Table 6.1-2. The maximum calculated $k_s$ is 0.7747, which occurs for the optimally moderated NCT array case. The NCT array is more reactive than the HAC array because the NCT array is larger, and moderation is allowed in both conditions. In this case, the loose fuel plate basket is moderated with full-density water, the inner tube is moderated with 0.5 $g/cm^3$ water, and void is modeled between the insulation and outer tube.

It may be noted when comparing Table 6.1-1 and Table 6.1-2 the fuel element payload is more reactive than the loose plate basket payload.

**Table 6.1-1** – Summary of Criticality Evaluation (Fuel Element Payload)

| **Normal Conditions of Transport (NCT)** | |
|---|---|
| Case | $k_s$ |
| Single Unit Maximum | 0.4126 |
| 9x9 Array Maximum | 0.8284 |
| **Hypothetical Accident Conditions (HAC)** | |
| Case | $k_s$ |
| Single Unit Maximum | 0.4425 |
| 5x5 Array Maximum | 0.7360 |
| USL = 0.9209 | |

**Table 6.1-2** – Summary of Criticality Evaluation (Loose Plate Payload)

| **Normal Conditions of Transport (NCT)** | |
|---|---|
| Case | $k_s$ |
| Single Unit Maximum | 0.4020 |
| 9x9 Array Maximum | 0.7747 |
| **Hypothetical Accident Conditions (HAC)** | |
| Case | $k_s$ |
| Single Unit Maximum | 0.4363 |
| 5x5 Array Maximum | 0.6979 |
| USL = 0.9209 | |

## 6.1.3 Criticality Safety Index

A 5x5 array (2N = 25, or N = 12.5) is utilized for the HAC array calculations, while a 9x9 array (5N = 81, or N = 16.2) is utilized for the NCT array calculations. Therefore, the 10 CFR §71.59 criticality safety index is computed with the smaller value of N, or 50/N = 50/12.5 = 4.0. With a CSI = 4.0, a maximum of twenty-five (25) packages are allowed per exclusive use shipment. The CSI is the same regardless of payload.

# 6.2 Fissile Material Contents

The package can accommodate either (i) one ATR Mark VII fuel element, or (ii) a loose plate basket filled with ATR Mark VII fuel plates.

## 6.2.1 Fuel Element

Four different ATR Mark VII fuel element types are available: standard (7F), non-borated (7NB), non-borated hybrid (7NBH), and non-fueled plate 19 (YA). These fuel element types are described in Section 1.2.2, *Contents*. The 7NB fuel element is the only fuel element that does not contain boron, and is conservatively utilized in the criticality analysis.

Each fuel element contains up to 1200 g U-235, enriched up to 94 wt.%. The U-235 mass per plate is provided in Table 6.2-1. These values are generated by scaling up the U-235 loading for a 1075 g U-235 fuel element, as the 1200 g limit has been selected to envelope future increases in the loading. The weight percents of the remaining uranium isotopes are 1.2 wt.% U-234 (max), 0.7 wt.% U-236 (max), and 5.0-7.0 wt.% U-238. Each fuel element contains 19 curved fuel plates. Fuel plate 1 has the smallest radius, while fuel plate 19 has the largest radius, as shown in Figure 6.2-1. The as-modeled fuel element is shown in Figure 6.2-2. The fuel "meat" is uranium aluminide ($UAl_x$) mixed with additional aluminum. In the following paragraphs, the details of the fuel element are provided.

The key fuel element dimensions and tolerances utilized in the criticality models are summarized on Figure 6.2-1. Fuel plate 1 is nominally 0.080-in thick, fuel plates 2 through 18 are nominally 0.050-in thick, and fuel plate 19 is nominally 0.100-in thick. The plate thickness tolerance is +0.000/-0.002-in for all plates. The fuel meat is nominally 0.02-in thick for all 19 plates. The plate cladding material is aluminum ASTM B 209, 6061-0. Fuel element side plates are fabricated of ASTM B 209, aluminum alloy 6061-T6 or 6061-T651. All aluminum alloys are modeled as pure aluminum. The fuel element side plates have a minimum thickness of 0.182-in. Channels 2 through 10 have a width of 0.078 ± 0.007-in, while channels 11 through 19 have a width of 0.077 +0.008/-0.006-in. These tolerances represent average and not localized channel width. For an actual fuel element, the channel width may exceed these tolerances in localized areas.

The arc length of the fuel meat changes from plate to plate. This arc length varies based on the distance from the edge of the fuel meat to the fuel element side plate, as defined for each plate on Figure 6.2-1. This dimension is 0.245-in (max)/0.145-in (min) for fuel plates 1 and 19, 0.145-in (max)/0.045-in (min) for fuel plates 2 through 17, and 0.165-in (max)/0.065-in (min) for fuel plate 18. The smaller this dimension, the larger the arc length of the fuel meat.

The active fuel length varies between a minimum of 47.245-in (= 49.485 – 2*1.12) and a maximum of 48.775-in (= 49.515 – 2*0.37) for all fuel plates.

It is demonstrated in Section 6.4.1.2.1, *Fuel Element Payload Parametric Evaluation*, that reactivity increases with increasing meat arc length. Therefore, the arc length is modeled at the maximum value. To determine the number densities of the fuel meat, it is first necessary to compute the volume of the fuel meat. The volume of the fuel meat for each plate is the maximum arc length of the meat multiplied by the fuel length (48-in) and meat thickness (0.02-

in). The fuel length and meat thickness are treated as fixed quantities in all fuel element models, and the use of these dimensions is justified in Section 6.4.1.2.1.

The fuel meat volume for each of the 19 fuel plates is provided in Table 6.2-1. The mass of U-235 per plate utilized in the analysis is also provided in Table 6.2-1. The U-235 gram density for each fuel plate is also computed. Note that the U-235 gram density is higher in the inner plates compared to the outer plates.

The fuel itself is a mixture of $UAl_x$ and aluminum. The density of this mixture is proportional to the U-235 gram density, as shown in Table 6.2-2. These data are perfectly linear, and a linear fit of the data is $\rho_2 = 0.8733\rho_1 + 2.5357$, where $\rho_2$ is the total gram density of the mixture, and $\rho_1$ is the gram density of the U-235 in the mixture. This equation is used to compute the total mixture gram density provided as the last column in Table 6.2-1.

From the fuel volumes, U-235 gram densities, and total mixture densities provided in Table 6.2-1, the number densities for the fuel region of each fuel plate may be computed. These number densities are provided in Table 6.2-3. The U-235 weight percent is assumed to be the maximum value of 94%. Representative weight percents of 0.6% and 0.35% are assumed for U-234 and U-236, respectively, and the balance (5.05%) is modeled as U-238.

## 6.2.2 Loose Fuel Plates

The loose plate basket may transport up to 600 g of U-235 in the form of ATR Mark VII fuel plates. These plates are described in Section 6.2.1, *Fuel Element*, although the loose plates may be flat as well as curved. The widths of the fuel meat for flat plates are the same as the fuel meat arc lengths provided in Table 6.2-1.

Because an integer number of plates will be transported, for computational purposes it is useful to modify the mass of U-235 per plate so that the total U-235 mass per package adds to 600 g. The column labeled "Number of Plates to 600 g" in Table 6.2-4 is simply the total desired mass (600 g) divided by the mass of U-235 per plate (from Table 6.2-1) and gives an estimate of the number of plates of each type required to reach 600 g U-235. Detailed models are developed for only four plates: 3, 5, 8, and 15. It is demonstrated in the analysis that it is sufficient to bound all of the plates by modeling these four. The number of plates modeled and the modeled mass of U-235 per plate are provided as the last two columns in Table 6.2-4.

In fuel element calculations, it has been determined that the fuel element is the most reactive when the arc length of the fuel "meat" is maximized. Therefore, all loose plate models utilize fuel plates with maximized fuel meat arc length. Also, because it has been determined that nominal fuel meat thickness (0.02-in) and nominal active fuel length (48.0-in) may be utilized with negligible effect on the reactivity, all loose plate models utilize these nominal dimensions. The overall plate thickness tolerance is +0.000/-0.002-in, and the loose plates are modeled at the minimum thickness of 0.048-in by reducing the cladding thickness by 0.001-in.

The number densities utilized in the models are provided in Table 6.2-5. These number densities are computed using the same method utilized in the fuel element models, although the U-235 mass per plate has been slightly adjusted as necessary so that the models always have 600 g U-235.

The active fuel length is modeled as 48-in for all fuel plates, consistent with the treatment of the fuel elements. The axial regions outside the active fuel region are conservatively ignored. The width of cladding from the fuel meat to the edge of the plate is modeled as 0.045-in for all of the fuel plates, which is the minimum dimension from the fuel meat to the fuel element support structure. The actual plates are wider than modeled because the plates extend into the fuel element support structure and this additional width is neglected.

**Table 6.2-1** – Fuel Element Volume and Gram Densities

| Plate | Fuel Meat Arc Length (cm) | Fuel Meat Volume ($cm^3$) | U-235 Mass Per Plate (g) | U-235 density, $\rho_1$ ($g/cm^3$) | Total $UAl_x$ + Al Density, $\rho_2$ ($g/cm^3$) |
|---|---|---|---|---|---|
| 1 | 4.2247 | 26.2 | 27.1 | 1.04 | 3.44 |
| 2 | 5.0209 | 31.1 | 32.5 | 1.04 | 3.45 |
| 3 | 5.2764 | 32.7 | 43.2 | 1.32 | 3.69 |
| 4 | 5.5319 | 34.3 | 45.1 | 1.32 | 3.69 |
| 5 | 5.7873 | 35.8 | 58.2 | 1.62 | 3.95 |
| 6 | 6.0427 | 37.4 | 60.9 | 1.63 | 3.96 |
| 7 | 6.2982 | 39.0 | 63.6 | 1.63 | 3.96 |
| 8 | 6.5536 | 40.6 | 66.3 | 1.63 | 3.96 |
| 9 | 6.8090 | 42.2 | 69.0 | 1.64 | 3.96 |
| 10 | 7.0644 | 43.8 | 71.7 | 1.64 | 3.97 |
| 11 | 7.3198 | 45.3 | 74.3 | 1.64 | 3.97 |
| 12 | 7.5752 | 46.9 | 77.0 | 1.64 | 3.97 |
| 13 | 7.8306 | 48.5 | 79.7 | 1.64 | 3.97 |
| 14 | 8.0860 | 50.1 | 82.4 | 1.64 | 3.97 |
| 15 | 8.3414 | 51.7 | 85.2 | 1.65 | 3.98 |
| 16 | 8.5968 | 53.2 | 71.4 | 1.34 | 3.71 |
| 17 | 8.8521 | 54.8 | 73.6 | 1.34 | 3.71 |
| 18 | 9.0058 | 55.8 | 60.1 | 1.08 | 3.48 |
| 19 | 8.9039 | 55.1 | 58.7 | 1.06 | 3.47 |
| Total | -- | 824.5 | 1200.0 | -- | -- |

**Table 6.2-2** – Fuel Density Equation

| U-235 Density ($g/cm^3$) $\rho_1$ | Total Fuel Density ($g/cm^3$) $\rho_2$ |
|---|---|
| 1.00 | 3.409 |
| 1.30 | 3.671 |
| 1.60 | 3.933 |
| Linear Fit: $\rho_2 = 0.8733\rho_1 + 2.5357$ | |

## Table 6.2-3 – Fuel Element Number Densities

| Plate | U-234 (atom/b-cm) | U-235 (atom/b-cm) | U-236 (atom/b-cm) | U-238 (atom/b-cm) | Aluminum (atom/b-cm) | Total (atom/b-cm) |
|---|---|---|---|---|---|---|
| 1 | 1.7026E-05 | 2.6560E-03 | 9.8475E-06 | 1.4089E-04 | 5.2187E-02 | 5.5010E-02 |
| 2 | 1.7156E-05 | 2.6763E-03 | 9.9226E-06 | 1.4196E-04 | 5.2153E-02 | 5.4998E-02 |
| 3 | 2.1711E-05 | 3.3869E-03 | 1.2557E-05 | 1.7966E-04 | 5.0974E-02 | 5.4574E-02 |
| 4 | 2.1618E-05 | 3.3724E-03 | 1.2503E-05 | 1.7889E-04 | 5.0998E-02 | 5.4583E-02 |
| 5 | 2.6648E-05 | 4.1571E-03 | 1.5413E-05 | 2.2051E-04 | 4.9696E-02 | 5.4115E-02 |
| 6 | 2.6746E-05 | 4.1724E-03 | 1.5470E-05 | 2.2132E-04 | 4.9670E-02 | 5.4106E-02 |
| 7 | 2.6790E-05 | 4.1791E-03 | 1.5495E-05 | 2.2168E-04 | 4.9659E-02 | 5.4102E-02 |
| 8 | 2.6830E-05 | 4.1854E-03 | 1.5518E-05 | 2.2201E-04 | 4.9649E-02 | 5.4098E-02 |
| 9 | 2.6867E-05 | 4.1911E-03 | 1.5539E-05 | 2.2232E-04 | 4.9639E-02 | 5.4095E-02 |
| 10 | 2.6901E-05 | 4.1965E-03 | 1.5559E-05 | 2.2260E-04 | 4.9630E-02 | 5.4092E-02 |
| 11 | 2.6933E-05 | 4.2015E-03 | 1.5577E-05 | 2.2287E-04 | 4.9622E-02 | 5.4089E-02 |
| 12 | 2.6963E-05 | 4.2061E-03 | 1.5595E-05 | 2.2311E-04 | 4.9614E-02 | 5.4086E-02 |
| 13 | 2.6990E-05 | 4.2105E-03 | 1.5611E-05 | 2.2334E-04 | 4.9607E-02 | 5.4083E-02 |
| 14 | 2.7017E-05 | 4.2145E-03 | 1.5626E-05 | 2.2356E-04 | 4.9600E-02 | 5.4081E-02 |
| 15 | 2.7077E-05 | 4.2239E-03 | 1.5661E-05 | 2.2406E-04 | 4.9585E-02 | 5.4075E-02 |
| 16 | 2.2037E-05 | 3.4377E-03 | 1.2746E-05 | 1.8235E-04 | 5.0889E-02 | 5.4544E-02 |
| 17 | 2.2037E-05 | 3.4377E-03 | 1.2745E-05 | 1.8235E-04 | 5.0889E-02 | 5.4544E-02 |
| 18 | 1.7683E-05 | 2.7586E-03 | 1.0228E-05 | 1.4633E-04 | 5.2016E-02 | 5.4949E-02 |
| 19 | 1.7487E-05 | 2.7279E-03 | 1.0114E-05 | 1.4470E-04 | 5.2067E-02 | 5.4967E-02 |

## Table 6.2-4 – Loose Plate Data

| Plate | Number of Plates to 600 g U-235 | Modeled Number of Plates | Modeled U-235 Mass Per Plate (g) |
|---|---|---|---|
| 1 | 22.12 | - | - |
| 2 | 18.47 | - | - |
| 3 | 13.89 | 14 | 42.9 |
| 4 | 13.30 | - | - |
| 5 | 10.32 | 10 | 60.0 |
| 6 | 9.84 | - | - |
| 7 | 9.43 | - | - |
| 8 | 9.05 | 9 | 66.7 |
| 9 | 8.70 | - | - |
| 10 | 8.37 | - | - |
| 11 | 8.07 | - | - |
| 12 | 7.79 | - | - |
| 13 | 7.53 | - | - |
| 14 | 7.28 | - | - |
| 15 | 7.04 | 7 | 85.7 |
| 16 | 8.40 | - | - |
| 17 | 8.16 | - | - |
| 18 | 9.99 | - | - |
| 19 | 10.22 | - | - |

**Table 6.2-5** – Loose Plate Number Densities (as-modeled)

| Plate | U-234 (atom/b-cm) | U-235 (atom/b-cm) | U-236 (atom/b-cm) | U-238 (atom/b-cm) | Aluminum (atom/b-cm) | Total (atom/b-cm) |
|---|---|---|---|---|---|---|
| 3 | 2.1539E-05 | 3.3600E-03 | 1.2458E-05 | 1.7823E-04 | 5.1018E-02 | 5.4591E-02 |
| 5 | 2.7492E-05 | 4.2887E-03 | 1.5901E-05 | 2.2749E-04 | 4.9477E-02 | 5.4037E-02 |
| 8 | 2.6975E-05 | 4.2081E-03 | 1.5602E-05 | 2.2322E-04 | 4.9611E-02 | 5.4085E-02 |
| 15 | 2.7249E-05 | 4.2508E-03 | 1.5760E-05 | 2.2548E-04 | 4.9540E-02 | 5.4059E-02 |

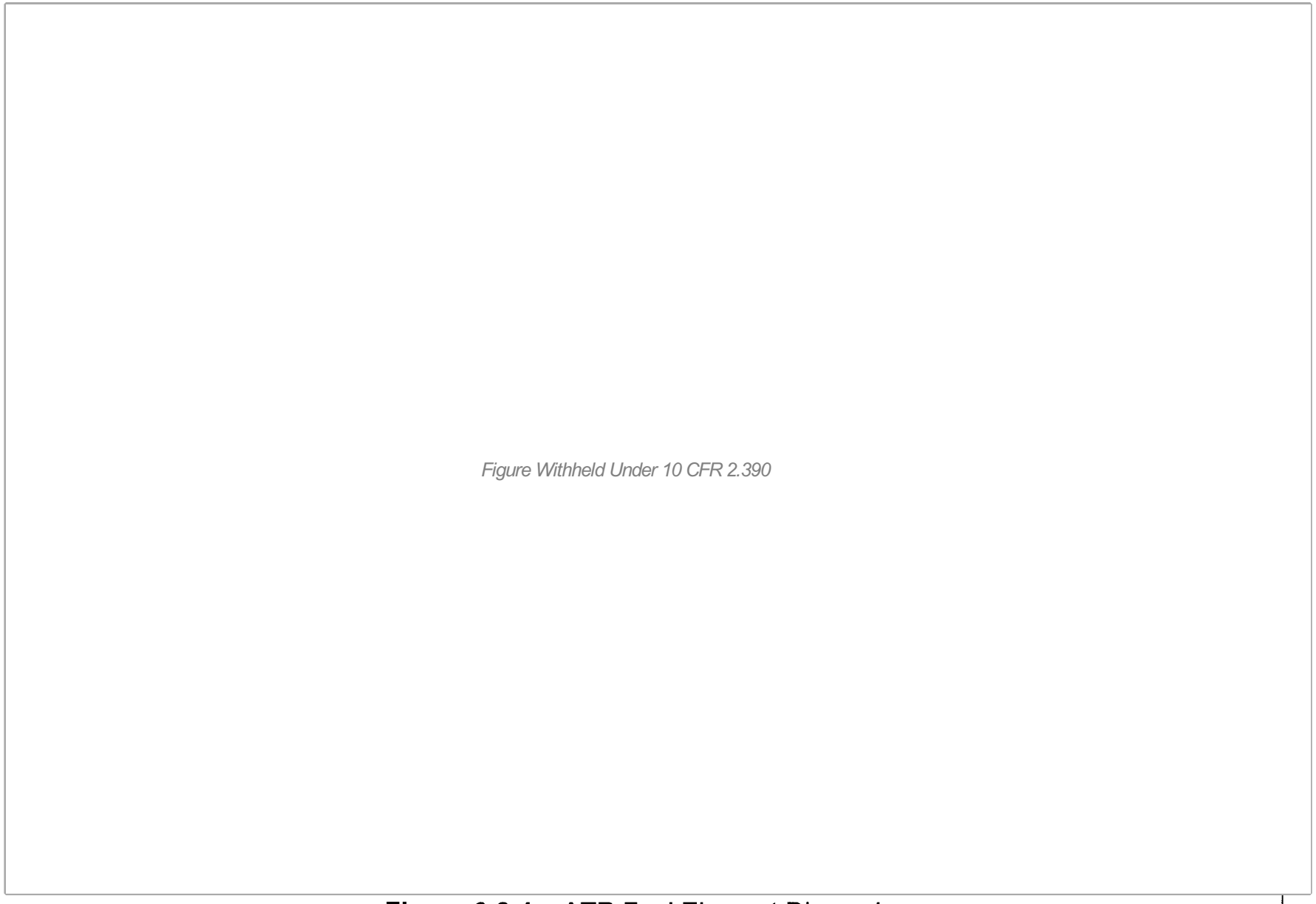


**Figure 6.2-1** – ATR Fuel Element Dimensions

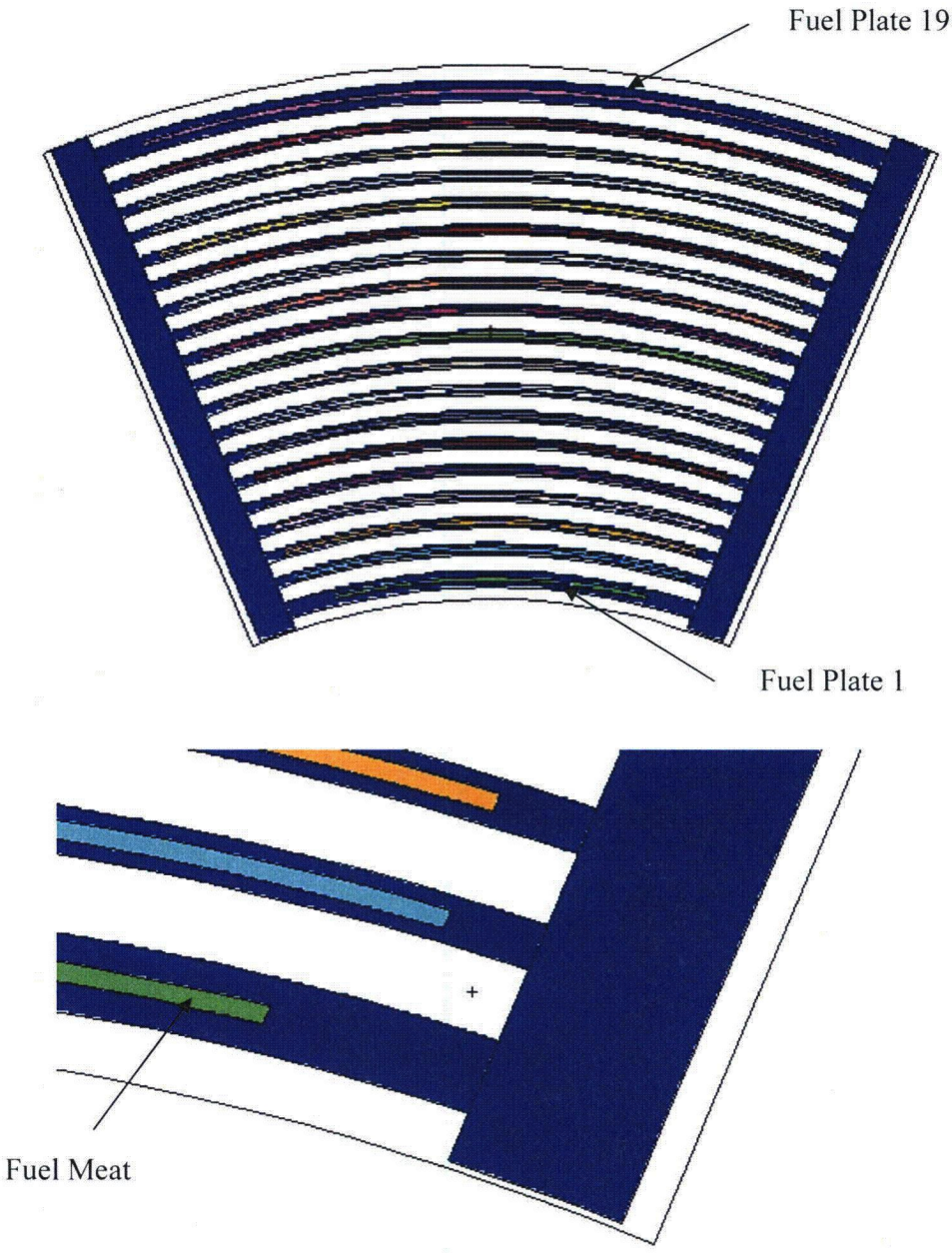


**Figure 6.2-2** – Fuel Element Model

# 6.3 General Considerations

Criticality calculations for the ATR FFSC are performed using the three-dimensional Monte Carlo computer code MCNP5[2]. Descriptions of the fuel assembly geometric models are given in Section 6.3.1, *Model Configuration*. The material properties for all materials used in the models are provided in Section 6.3.2, *Material Properties*. The computer code and cross section libraries used are provided in Section 6.3.3, *Computer Codes and Cross-Section Libraries*. Finally, the most reactive configuration is provided in Section 6.3.4, *Demonstration of Maximum Reactivity*.

## 6.3.1 Model Configuration

Models are developed for both the fuel element and loose plate basket payloads.

### 6.3.1.1 Fuel Element Payload

The model configuration is relatively simple. Most packaging details are conservatively ignored, particularly at the ends. Because the package is long and narrow, array configurations will stack only in the lateral directions (e.g., 5x5x1). Therefore, the end details, for both the package and the fuel element, are conservatively ignored external to the active fuel region, and these end regions are simply modeled as full-density water.

The package consists of two primary structural components, a circular inner tube and a square outer tube, as shown in Appendix 1.3.2, *Packaging General Arrangement Drawings*. The inner tube has a nominal outer diameter of 6-in and a nominal thickness of 0.12-in. The outer tube has a nominal outer dimension of 8-in and a nominal thickness of 0.188-in. A layer of insulating material 1-in thick is wrapped around the inner tube.

For the inner tube, tolerances are based upon ASTM A269[3]. The tolerance on the outer diameter (OD) is ± 0.030-in, and the tolerance on the wall thickness is ±10%. Tolerances are selected to minimize the spacing between the fuel elements in the array configuration. This spacing is minimized using the maximum OD and minimum wall thickness. Using the minimum wall thickness also reduces parasitic neutron absorption in the steel. Therefore, the modeled tube OD is 6.03-in, the modeled wall thickness is 0.108-in, and the modeled tube ID is 5.814-in.

For the outer tube, the wall thickness tolerance is ±10% based upon ASTM A554[4] (the tolerance for the optional use of ASTM A240[5] also falls within this value). Using the minimum wall thickness of 0.169-in reduces parasitic neutron absorption in the steel. Reactivity in the array cases is maximized by minimizing the outer dimensions of the square. A bounding tolerance of

[2] MCNP5, "*MCNP – A General Monte Carlo N-Particle Transport Code, Version 5; Volume II: User's Guide*," LA-CP-03-0245, Los Alamos National Laboratory, April, 2003.

[3] ASTM A269-02a, *Standard Specification for Seamless and Welded Austenitic Stainless Steel Tubing for General Service*.

[4] ASTM A554-03, *Standard Specification for Welded Stainless Steel Mechanical Tubing*.

[5] ASTM A240-03, *Standard Specification for Chromium and Chromium-Nickel Stainless Steel Plate, Sheet, and Strip for Pressure Vessels and for General Applications*.

0.1-in is assumed for this dimension, for a modeled OD of 7.9-in. The as-fabricated packages will meet this tolerance.

In the NCT single package models, the inner tube, insulation, and outer tube are modeled explicitly, as shown in Figure 6.3-1 and Figure 6.3-2. Although negligible water ingress is expected during NCT, the inner cavity of the package is assumed to be flooded with water because the package lid does not contain a seal. However, the region between the insulation and the outer tube will remain dry because water cannot enter this region. The Fuel Handling Enclosure (FHE) is conservatively ignored. Modeling the FHE would decrease water reflection in the single package model. However, the neoprene along the sides of the FHE is modeled explicitly using a thickness of 1/8-in. Because neoprene will reduce the reactivity due to parasitic absorption in chlorine, chlorine is removed from the neoprene, and the density is reduced accordingly. In the model, the fuel element is conservatively positioned at the radial center of the inner tube to maximize neutron reflection. The package is reflected with 12-in of full-density water.

The HAC single package model is essentially the same as the NCT single package model. Damage in the drop tests was shown to be negligible and concentrated at the ends of the package (See Section 2.12.1). As the ends of the package are not modeled, this end damage does not affect the modeling. The various side drops resulted in only minor localized damage to the outer tube, and no observable bulk deformation of the package. Therefore, the minor damage observed will not impact the reactivity. The insulation is replaced with full-density water, and the region between the insulation and outer tube is also filled with full-density water (see Figure 6.3-3). The treatment of the FHE is the same as the NCT single package model. Cases are developed both with and without the FHE neoprene, and with and without chlorine in the neoprene.

As a result of the drop tests, limited damage to the fuel element was observed. The bottom end box sheared off from the main body, although this condition has no effect on the criticality models because the fuel element is not modeled beyond the active fuel region. Limited damage to the fuel element plates was observed at the ends, although this damage is over a short length in a region of low reactivity worth. Slight localized buckling of the fuel plates was also observed in the region of the fuel element side plate vent openings, as the fuel plates are not as well supported in these regions. Because the observed fuel element damage is minor and will have only a negligible effect on reactivity, no damaged fuel element models are developed.

In the NCT array models, a 9x9x1 array is utilized. Although the FHE would survive NCT events with no damage, the FHE is conservatively ignored and the fuel elements are pushed toward the center of the array. Because the fuel elements are transported in a thin (~0.01-in) plastic bag, this plastic bag is assumed to act as a boundary for partial moderation effects. The plastic bag is not modeled explicitly, because it is too thin to have an appreciable effect on the reactivity. Therefore, it is postulated that the fuel element channels may fill with full-density water, while the region between the fuel element and inner tube fills with variable density water. The partial moderation effects that could be achieved by modeling the FHE explicitly are essentially addressed by the partial moderation analysis using the plastic bag. Also, modeling the FHE explicitly would result in the fuel elements being significantly pushed apart, which is a less reactive condition. Axial movement of the fuel elements is not considered because axial

movement would increase the effective active height of the system and reduce the reactivity due to increased leakage. The presence of chlorine-free neoprene is also considered.

In the HAC array models, a 5x5x1 array is utilized. The HAC array models are essentially the same as the NCT array models, except additional cases are developed to determine the reactivity effect of allowing variable density water in the region between the inner and outer tubes. Cases are also developed with and without the insulation, and with and without chlorine-free neoprene. The FHE is conservatively ignored for the reasons stated in the previous paragraph. Because the NCT and HAC models are very similar and the NCT models utilize a larger array, the NCT array models are more reactive than the HAC array models.

The detailed moderation assumptions for the array cases are discussed more fully in Section 6.5, *Evaluation of Package Arrays under Normal Conditions of Transport*, and Section 6.6, *Package Arrays under Hypothetical Accident Conditions*.

### 6.3.1.2 Loose Plate Basket Payload

The NCT and HAC single package models are shown in Figure 6.3-4 and Figure 6.3-5, respectively. The NCT and HAC packaging models, including tolerances, are consistent with the values used in the fuel element analysis. The difference is that the aluminum loose plate basket and payload of fuel plates is inserted into the cavity. The loose plate basket does not contain neoprene.

The dimensions of the loose plate basket are provided on the packaging general arrangement drawings. The wall thickness of the basket in the central rectangular region is 0.19 ± 0.06-in. The cavity width is 4.5 ± 0.06-in, and the cavity height is 1.62 ± 0.06-in. The basket wall thickness is modeled at the minimum thickness of 0.13-in to minimize absorption in the aluminum. The inner dimensions of the basket are modeled at the maximum values of 4.56-in x 1.68-in to maximize the volume available for moderation. The radial supports are neglected in the MCNP models.

In the actual loaded configuration, the loose plates are bundled so that the plates are in close contact, and aluminum dunnage plates are used to fill the void space to prevent lateral movement. In the criticality models, the dunnage plates are conservatively ignored. Modeling the dunnage plates would severely restrict the volume available for water moderation. Because no dunnage plates are modeled, the fuel plates are allowed to arrange in the most reactive geometry, including non-regular pitches. Flat plates are modeled rather than curved plates because flat plates are much simpler to model. It is demonstrated that flat plates and curved plates are neutronically equivalent.

Axial movement of the fuel plates is not considered, because this motion would be negligible and is precluded by the basket design, which has a cavity length of 50.5-in. The fuel plates are approximately 49.5-in long, although only the 48-in active length is modeled.

In the NCT and HAC single package models, the fuel basket is centered in the cavity to maximize water reflection, and all water is at full density to maximize moderation and reflection.

In the NCT array analysis, four different plate types are examined: 3, 5, 8, and 15. Plate type 5 is shown to be the most reactive. A number of both regular and non-regular pitches are utilized

in order to find the most reactive condition. Plate type 5 is used in all single package and array analyses.

In the NCT array models, a 9x9x1 array is utilized. Water is assumed to be present inside the cavity at a density that maximizes reactivity. To bound any potential damage to the loose plate basket, the rectangular region of each basket is pushed toward the radial center of the array until contact is made with the circular tube. This geometry is not considered credible because the ribs will maintain concentricity between the basket and cavity.

In the HAC array models, a 5x5x1 array is utilized. Water is assumed to be present inside the cavity and between the inner and outer tubes at a density that maximizes reactivity. The detailed moderation assumptions for the array cases are discussed more fully in Section 6.5, *Evaluation of Package Arrays under Normal Conditions of Transport*, and Section 6.6, *Package Arrays under Hypothetical Accident Conditions.*

The fuel plates are modeled as undamaged in both the NCT and HAC models. As a result of the drop tests, limited buckling of the fuel plates was observed at the end, although this damage is over a short length in a region of low reactivity worth. Because the observed fuel plate damage is minor and will have only a negligible effect on reactivity, no damaged fuel plate models are developed. Also, any anticipated damage is bounded because the most reactive pitch is modeled for both uniform and non-uniform conditions, and the damaged condition is essentially a subset of the conditions already modeled.

## 6.3.2 Material Properties

The fuel meat compositions are provided in Table 6.2-3 and Table 6.2-5 for the fuel element and loose plates, respectively. The fuel plate cladding is aluminum alloy 6061-0, while the side plates may be either aluminum alloy 6061-T6 or 6061-T651. From a criticality perspective, these alloys are essentially aluminum, and in the MCNP models all aluminum alloy structural materials are modeled as pure aluminum with a density of 2.7 g/cm$^3$. The material properties of the remaining packaging and moderating materials are described in the following paragraphs.

The inner and outer tubes of the package are constructed from stainless steel 304. Although MCNP is used in the calculations, the standard compositions for stainless steel 304 are obtained from the SCALE material library[6], which is a standard set accepted for use in criticality analyses. The stainless steel composition and density utilized in the MCNP models are provided in Table 6.3-1.

The insulation material utilized in the NCT models has a density of 6 pounds per cubic foot (0.096 g/cm$^3$). The insulation is composed of $Al_2O_3$ and $SiO_2$ in approximately equal quantities, with small (<1 wt%) quantities of other minor constituents. It is assumed in this analysis that the material is simply 50% $Al_2O_3$ and 50% $SiO_2$ by weight and the impurities are neglected. Insulation material properties are provided in Table 6.3-2.

[6] *Standard Composition Library*, NUREG/CR-0200, Rev. 6, Volume 3, Section M8, ORNL/NUREG/CSD-2/V3/R6, September 1998.

Neoprene ($C_4H_5Cl$) has a density of 1.23 g/cm$^3$, and the chemical composition is provided in Table 6.3-3. Because chlorine is a neutron absorber, for models in which the chlorine has been deleted, a density of 0.737 g/cm$^3$ is utilized.

Water is modeled with a density ranging up to 1.0 g/cm$^3$ and the chemical formula $H_2O$. The S($\alpha$,$\beta$) card LWTR.60T is used to simulate hydrogen bound to oxygen in water.

## 6.3.3 Computer Codes and Cross-Section Libraries

MCNP5 v1.30 is used for the criticality analysis[7]. All cross sections utilized are at room temperature (293.6 K). The uranium isotopes utilize preliminary ENDF/B-VII cross section data that are considered by Los Alamos National Laboratory to be more accurate than ENDF/B-VI cross sections. ENDF/B-V cross sections are utilized for chromium, nickel, and iron because natural composition ENDF/B-VI cross sections are not available for these elements. The remaining isotopes utilize ENDF/B-VI cross sections. Titles of the cross sections utilized in the models have been extracted from the MCNP output and provided in Table 6.3-4. As discussed in Section 6.3.2, the S($\alpha$,$\beta$) card LWTR.60T is also used to simulate hydrogen bound to water.

Cases are run with a minimum 2500 neutrons per generation for 250 generations, skipping the first 50. The 1-sigma uncertainty is approximately 0.001 for most cases.

## 6.3.4 Demonstration of Maximum Reactivity

Fuel Element Payload

The reactivities of the NCT and HAC single package cases are small, with $k_s < 0.5$.

The NCT and HAC array cases are similar. For the NCT array, a 9x9x1 array is utilized, while in the HAC array, a smaller 5x5x1 array is utilized. Because negligible damage was observed in the drop tests, the package dimensions are the same between the NCT and HAC models. Dimensions of both the fuel element and packaging are selected to maximize reactivity, and close-water reflection is utilized. In the fuel element, the fuel meat width and channel width are maximized, as this condition is the most reactive. In both NCT and HAC array cases, flooding with partial moderation is allowed in the central cavity, and the fuel elements are pushed toward the center of the array. In the fuel element models, the FHE is not modeled explicitly because the FHE would increase the fuel element spacing and decrease the reactivity. Any partial moderation effects of the FHE are essentially addressed by the partial moderation analysis for the fuel element itself.

In the NCT array models, insulation is modeled between the inner and outer tubes, while in the HAC array models, this region may have water, void, or insulation. In both sets of models, chlorine-free neoprene is modeled adjacent to the fuel element side plates, although the effect on the reactivity is small. No models in which the neoprene is allowed to decompose and homogeneously mix with the water are developed, as this scenario is already bounded by the variable water density search.

[7] MCNP5, "*MCNP – A General Monte Carlo N-Particle Transport Code, Version 5; Volume II: User's Guide*," LA-CP-03-0245, Los Alamos National Laboratory, April 2003.

The NCT array is more reactive than the HAC array, primarily because the NCT array is significantly larger. The most reactive case (Case D4) results in a $k_s = 0.8284$, which is below the USL of 0.9209.

Loose Plate Basket Payload

The reactivities of the NCT and HAC single package cases are small, with $k_s < 0.5$.

To facilitate model preparation, only four different plate types are examined: 3, 5, 8, and 15. The fuel meat width is maximized in all loose plate models, as this condition has been shown to maximize reactivity. For simplicity, plate types are not mixed in the same model. An optimum pitch search is performed to determine the most reactive condition. Both regular and non-regular pitches are examined. Plate 5 is the most reactive because its small width allows this plate to "double stack" along the width of the basket, resulting in a higher level of moderation compared to the larger plates. Plates 1 through 4 are smaller than Plate 5, but the low uranium loading of these plates results in a higher number of plates to achieve 600 g U-235, and the larger number of plates results in less moderation. In actual practice, plates of any type may be combined in a single loose plate basket, although random combinations of plates would be less reactive than modeling all plates as type 5.

The actual loose plate basket may accept either flat or curved plates. However, plates are modeled as flat rather than curved to facilitate model preparation. It is demonstrated that flat plates are neutronically equivalent to curved plates.

The array geometry and modeling assumption for the loose plate basket payload are similar to those described above for the fuel element payload. The NCT array is more reactive than the HAC array, primarily because the NCT array is significantly larger. The most reactive NCT configuration is with full-water density between the fuel plates, a water density of 0.5 g/cm$^3$ between the basket and the inner pipe, and void between the insulation and the outer tube. The axial regions beyond the active fuel are modeled as water to maximize reflection. The most reactive case (Case LG5) results in a $k_s = 0.7747$, which is below the USL of 0.9209. Note that the most reactive loose plate basket case is less reactive than the most reactive fuel element payload case.

**Table 6.3-1** – SS304 Composition

| Component | Wt.% |
|---|---|
| C | 0.08 |
| Si | 1.0 |
| P | 0.045 |
| Cr | 19.0 |
| Mn | 2.0 |
| Fe | 68.375 |
| Ni | 9.5 |
| Density = 7.94 g/cm$^3$ | |

**Table 6.3-2** – Insulation Composition

| Component | Wt.% |
|---|---|
| Al | 26.5 |
| Si | 23.4 |
| O | 50.2 |
| Density = 0.096 g/cm$^3$ | |

**Table 6.3-3** – Neoprene Composition

| Component | Wt.% |
|---|---|
| H | 5.7 |
| C | 54.3 |
| Cl | 40.0 |
| Density = 1.23 g/cm$^3$ | |

**Table 6.3-4** – Cross Section Libraries Utilized

| Isotope/Element | Cross Section Label (from MCNP output) |
|---|---|
| 1001.62c | 1-h-1 at 293.6K from endf-vi.8 njoy99.50 |
| 6000.66c | 6-c-0 at 293.6K from endf-vi.6 njoy99.50 |
| 8016.62c | 8-o-16 at 293.6K from endf-vi.8 njoy99.50 |
| 13027.62c | 13-al-27 at 293.6K from endf-vi.8 njoy99.50 |
| 14000.60c | 14-si-nat from endf/b-vi |
| 15031.66c | 15-p-31 at 293.6K from endf-vi.6 njoy99.50 |
| 17000.66c | 17-cl-0 at 293.6K from endf-vi.0 njoy99.50 |
| 24000.50c | njoy |
| 25055.62c | 25-mn-55 at 293.6K from endf/b-vi.8 njoy99.50 |
| 26000.55c | njoy |
| 28000.50c | njoy |
| 92234.69c | 92-u-234 at 293.6K from t16 u234la4 njoy99.50 |
| 92235.69c | 92-u-235 at 293.6K from t16 u235la9d njoy99.50 |
| 92236.69c | 92-u-236 at 293.6K from t16 u236la2d njoy99.50 |
| 92238.69c | 92-u-238 at 293.6K from t16 u238la8h njoy99.50 |

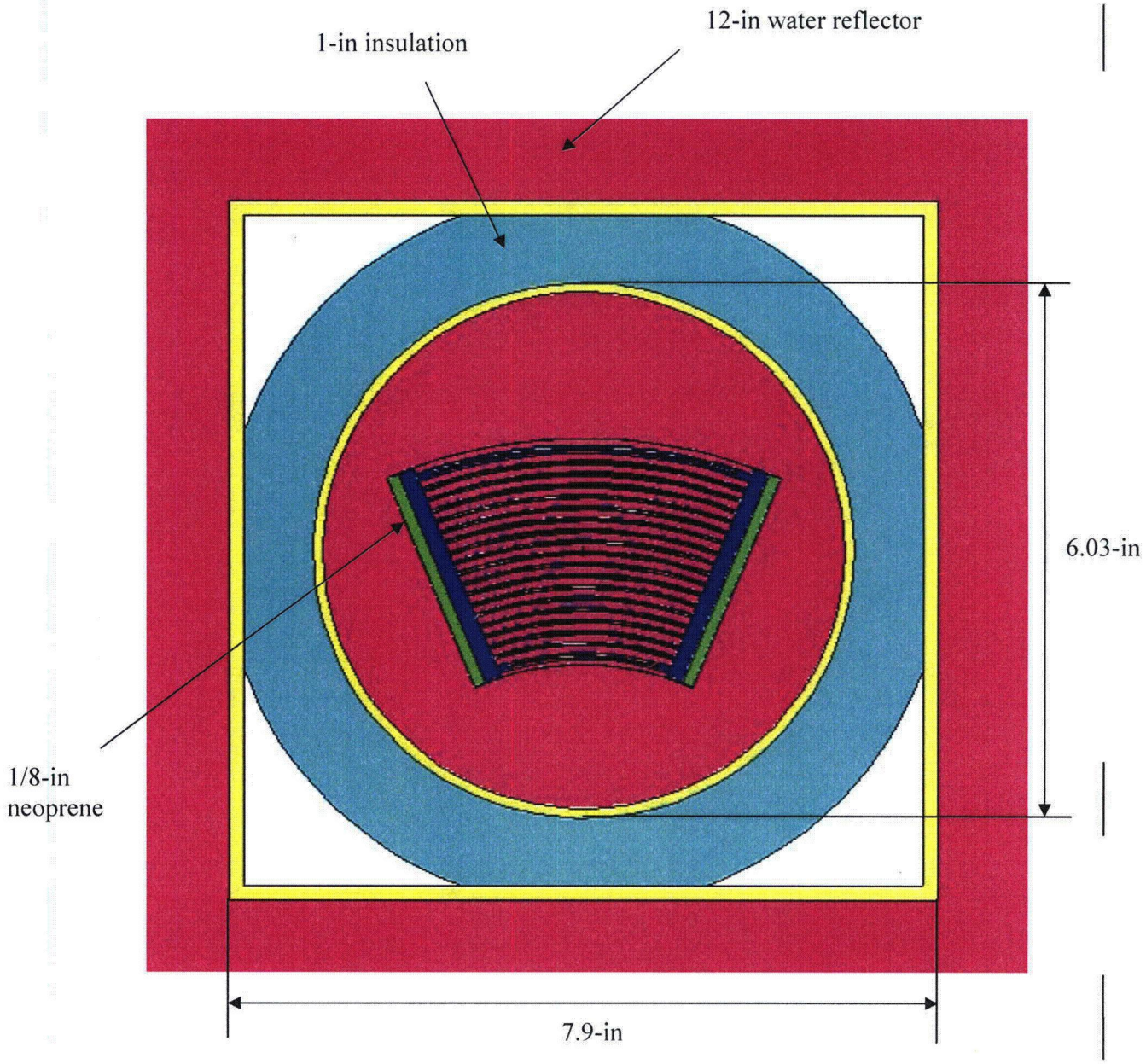


**Figure 6.3-1** – NCT Single Package Model, Fuel Element (planar view)

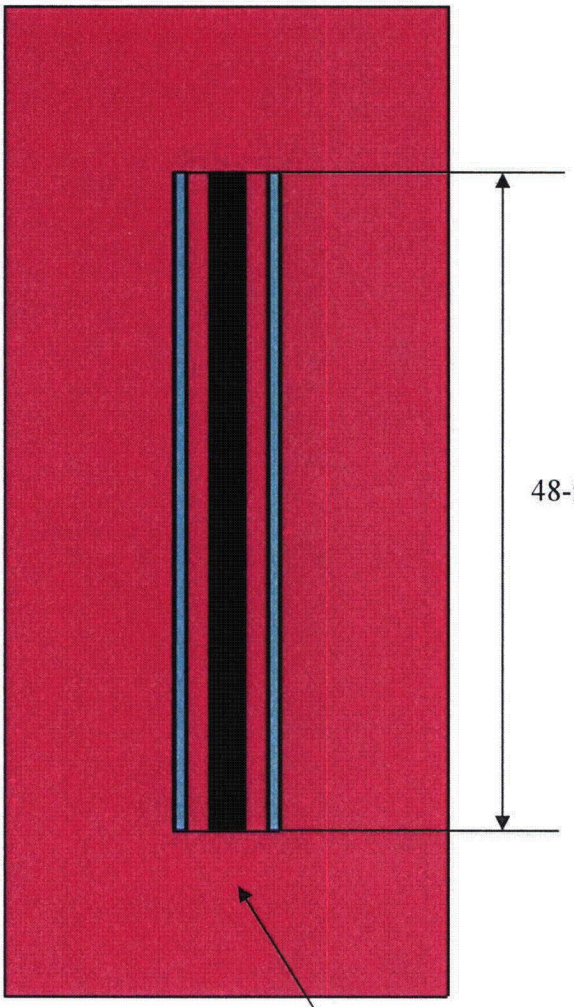


**Figure 6.3-2** – NCT Single Package Model, Fuel Element (axial view)

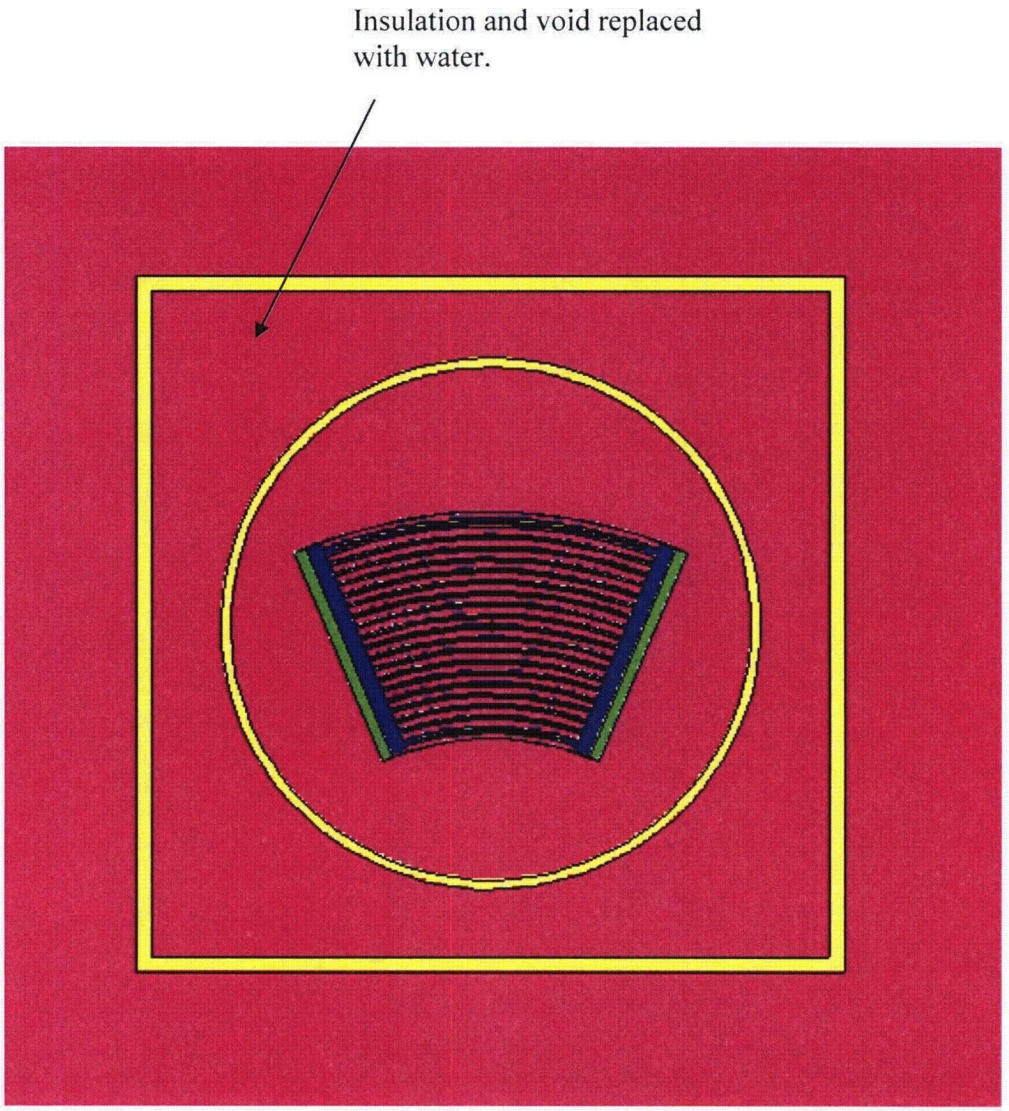


**Figure 6.3-3** – HAC Single Package Model, Fuel Element (planar view)

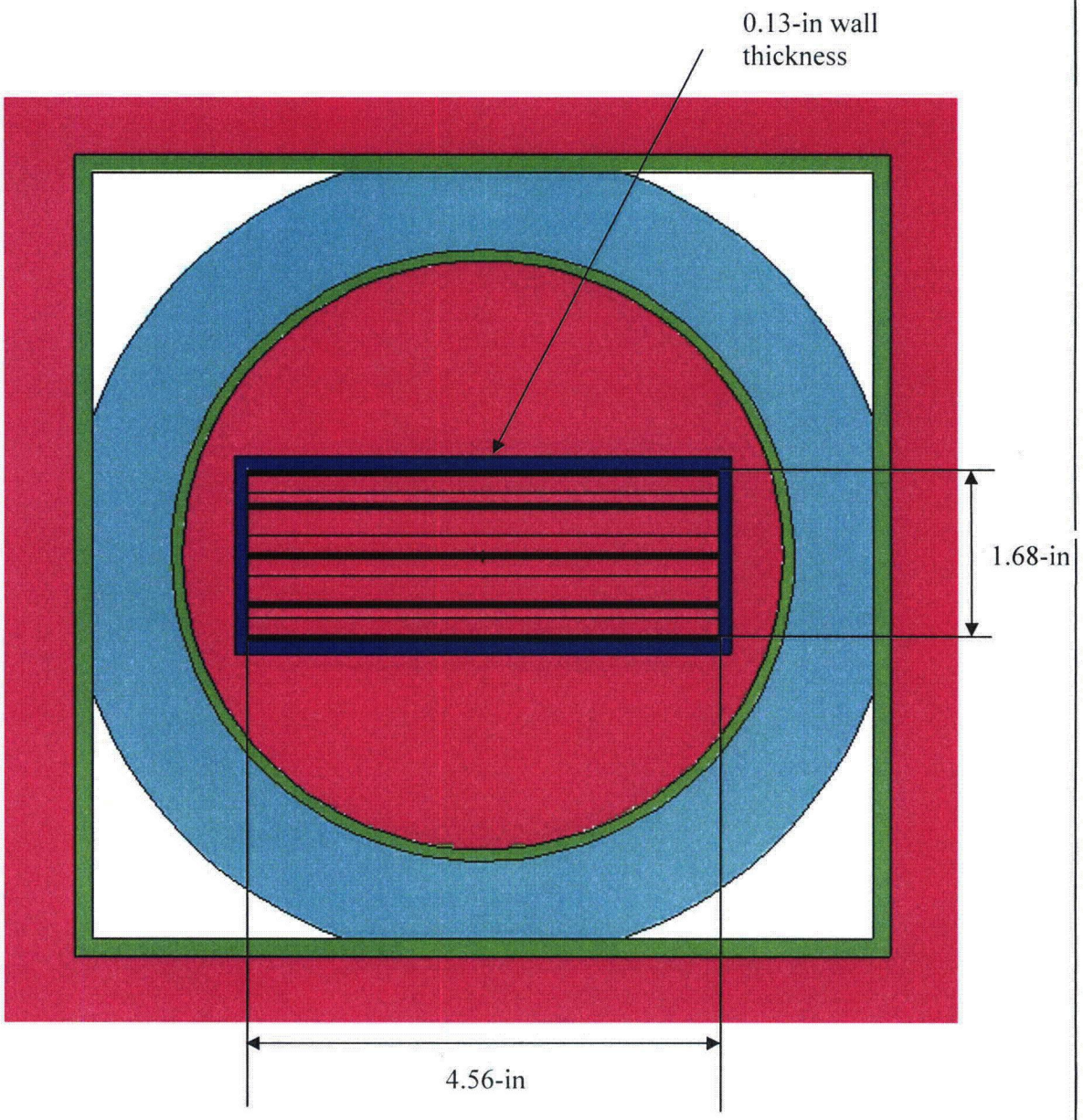


**Figure 6.3-4** – NCT Single Package Model, Basket (planar view)

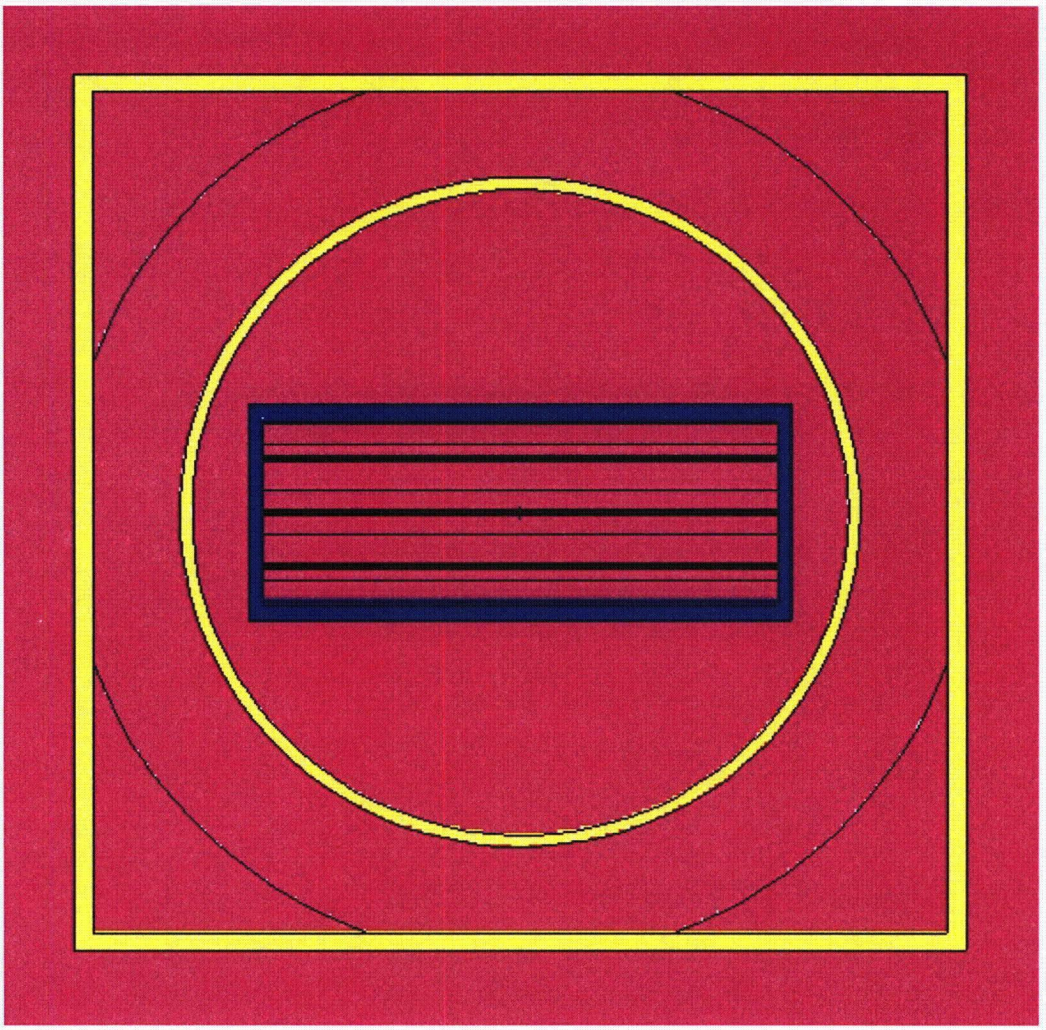

Case LB3

**Figure 6.3-5** – HAC Single Package Model, Basket (planar view)

# 6.4 Single Package Evaluation

Compliance with the requirements of 10 CFR §71.55 is demonstrated by analyzing an optimally moderated damaged and undamaged, single-unit ATR FFSC. The figures and descriptions provided in Section 6.3.1, *Model Configuration*, describe the basic geometry of the single-unit models.

## 6.4.1 Single Package Configuration

### 6.4.1.1 NCT Configuration

#### 6.4.1.1.1 Fuel Element Payload

The geometry of the NCT single package configuration is discussed in Section 6.3.1, *Model Configuration*. The inner tube is flooded with full-density water. The fuel element geometry is consistent with the most reactive fuel element model, including tolerances, as determined in Section 6.4.1.2.1, *Fuel Element Payload Parametric Evaluation*. Consistent with the most reactive HAC single package model, neoprene from the FHE is modeled at the sides of the fuel element. Chlorine is conservatively removed from the neoprene because chlorine acts as a poison. The package is reflected with 12-in of water. The reactivity is low, with $k_s = 0.41262$. This result is below the USL of 0.9209. Results are provided in Table 6.4-1.

#### 6.4.1.1.2 Loose Plate Basket Payload

The selection of the bounding fuel plate and development of the various plate arrangements are presented in conjunction with the NCT array analysis in Section 6.5.1.2, *Loose Plate Basket Payload*. It is determined that Plate 5 may be used as a bounding plate type for criticality purposes. Because the aluminum dunnage has not been credited, the plates are allowed to become arranged in the most reactive configuration within the loose plate container. The most reactive fuel plate arrangements determined in the NCT array analysis are used in the NCT single package analysis. The NCT single package models are reflected with 12-in of water.

The 10 Type 5 plates are modeled as 5 plates of double fuel meat width to allow two plates to be present side by side. The top and bottom plates are in contact with the fuel basket inner surfaces, and the center plate is always in the center of the basket. The two off-center plates are shifted in 0.1-cm increments away from the center plate so that the pitch is non-regular. When the pitch is non-regular, the maximum pitch is given as a "max" value in the results table.

A figure showing the general NCT model geometry is provided in Figure 6.3-4. Results are provided in Table 6.4-2. Six cases are run, with small variations in the plate arrangement. The maximum reactivity occurs for Case LA4, with $k_s = 0.40199$. This result is below the USL of 0.9209. The pitch of this case is non-regular. The top, center, and bottom plates are centered in the lattice locations with a base pitch of 1.036-cm, while the off-center plates are shifted 0.3-cm from the center plate. Note that the most reactive NCT array case peaks with the off-center plates shifted 0.2-cm rather than 0.3-cm, although this difference is most likely due to statistical fluctuation.

### 6.4.1.2 HAC Configuration

#### 6.4.1.2.1 Fuel Element Payload Parametric Evaluation

Prior to development of a single package model, a parametric analysis is performed to determine the impacts of various fuel element tolerances on the reactivity. This parametric analysis considers the effects of a number of parameters, such as fuel meat arc length, fuel meat thickness, channel width, and active fuel length.

Because the ATR fuel element is complex, with 19 unique fuel plates and 19 unique fuel material descriptions, performing this parametric study on an actual fuel element would be cumbersome. Rather, the approach utilized is to perform the parametric study on a system of 19 identical flat plates. This geometry mimics the ATR fuel element to determine trends in the data. Note that the reactivity of the 19 flat plate model is not identical to the reactivity of an actual ATR fuel element due to geometrical and material differences, although the trends are the same. The most reactive model variations are then incorporated into the ATR fuel element model.

In the parametric models, 1200 g U-235 is equally distributed between 19 identical flat plates. The base configuration consists of plates with a fuel meat width of 2.65-in (6.7355 cm; the average nominal meat arc length), active fuel height of 48-in, fuel meat thickness of 0.02-in, fuel cladding thickness of 0.015-in (total plate thickness of 0.050-in), and fuel channel thickness of 0.078-in. The geometry of Case B1 is shown in Figure 6.4-1. A total of 12 parametric models are developed, as summarized below.

| Case ID | Case Description |
|---|---|
| B1 | Base case |
| B2 | Increase width of fuel meat by 0.1-in |
| B3 | Decrease width of fuel meat by 0.1-in |
| B4 | Increase thickness of fuel meat by 0.002-in |
| B5 | Decrease thickness of fuel meat by 0.002-in |
| B6 | Increase thickness of fuel meat by 0.002-in but decrease the cladding thickness to maintain a nominal plate thickness |
| B7 | Decrease thickness of fuel meat by 0.002-in but increase the cladding thickness to maintain a nominal plate thickness |
| B8 | Increase water channel thickness to maximum of 0.085-in |
| B9 | Increase water channel thickness to maximum of 0.085-in by reducing the cladding thickness |
| B10 | Decrease active fuel length to 47.0-in |
| B11 | Reduce cladding thickness to the minimum value of 0.008-in |
| B12 | Combine cases B2 and B9 |

In Cases B2 through B12, each case is identical to the base case B1 with the exception of the changes identified in the table above. The pitch, which is the sum of the plate thickness and

channel thickness, is treated as a dependant variable and is allowed to vary as the independent parameters are changed. For example, in Case B5, decreasing the thickness of the fuel meat decreases the pitch, although the channel thickness remains constant. The detailed model description of the parametric cases is summarized in Table 6.4-3.

The results of the parametric analysis are summarized in Table 6.4-4. Because the uncertainty in the calculation is ~0.001, a difference of at least 0.002 (2 milli-k, abbreviated mk) between the various cases is required in order to distinguish a real effect from statistical fluctuation. The results indicate a reactivity increase of 4.3 mk for Case B2, when the width of the fuel meat is increased, and a decrease of 5.4 mk for Case B3, when the width of the fuel meat is decreased. Therefore, reactivity increases when the width of the fuel meat is maximized.

The nominal thickness of the fuel meat is 0.02-in. No tolerance on the fuel meat is defined because the fuel plates are fabricated using a rolling process. A thickness tolerance of 0.002-in (±10%) is assumed for computational purposes. In Cases B4 and B5, the fuel meat thickness is adjusted for constant channel thickness and variable pitch, while for Cases B6 and B7 the fuel meat thickness is adjusted for constant plate thickness and nominal pitch. The reactivity fluctuations are within 2 mk in all four cases, and it is concluded that a nominal fuel meat thickness of 0.02-in is acceptable for modeling purposes.

In Case B8, the water channel thickness is increased to the maximum value of 0.085-in (increase in pitch), while in Case B9 the water channel thickness is increased to the maximum by artificially reducing the cladding thickness (nominal pitch). Both cases B8 and B9 show large reactivity gains of 9.6 and 12.9 mk, respectively, indicating that reactivity is maximized when the water channel thickness is maximized.

In Case B10, the active fuel length is reduced to a lower bound value of 47.0-in. The reactivity increase is within statistical fluctuation. It may be inferred that increasing the active fuel length would also result in a reactivity effect within statistical fluctuation.

In Case B11, the cladding is reduced to the minimum value of 0.008-in, and the reactivity increases by 5.5 mk. This reactivity gain is likely due to the more compact geometry, as the pitch reduces considerably. This scenario is not directly applicable to an ATR fuel element because the pitch is fixed by the side plates and such a minimum pitch is not possible.

The only cases that show a statistically significant increase are B2, B8, B9, and B11. In Case B12, the increased fuel meat width of Case B2 and increased channel width of Case B9 are combined. This model geometry bounds Case B8, and Case B11 is incorporated in an approximate manner because the cladding thickness has been reduced to accommodate the larger channel. The reactivity of Case B12 represents an increase of 19.5 mk over base Case B1.

#### 6.4.1.2.2 Fuel Element Payload

The geometry of the HAC single package configuration is discussed in Section 6.3.1, *Model Configuration*. Based on the parametric evaluation, three HAC single package ATR fuel element models are developed in order to verify the trends indicated in the parametric analysis: (1) Case C1, a nominal (base) model, (2) Case C2, a conservative model with the increased channel width consistent with Case B9, and (3) Case C3, an optimized model with both increased channel width and increased meat arc length. In all three models, the FHE neoprene is ignored and a nominal pitch is utilized (i.e., the centerline radial locations of the 19 plates are the

same in each model). Note that in Cases C1 and C2, the fuel number densities are computed using nominal fuel meat arc lengths and thus do not correspond to the values in Table 6.2-3. In the increased channel width models, the channel width is increased by removing cladding. This approach is highly conservative, because it is unlikely (if not impossible) to maximize the channel width between each plate. In an actual fuel element, maximizing the channel width between two plates would likely minimize the channel width between the next two plates, as the overall plate thickness is held to a rather tight tolerance.

The HAC single package results are provided in Table 6.4-5. As expected from the parametric analysis, Case C2 is more reactive than Case C1 (by 13.7 mk), and Case C3 is more reactive than Case C1 (by 17.2 mk). Therefore, it may be concluded that reactivity is maximized in the ATR fuel element by maximizing the fuel meat arc length and maximizing the channel width between the fuel plates. This optimized fuel element is used in all models using the fuel element payload (including NCT single package, NCT array, and HAC array models).

In Cases C1, C2, and C3, the neoprene of the FHE is ignored and treated as full-density water. In Cases C4 and C5, the effect of neoprene is evaluated. Neoprene is a hydrocarbon with the chemical formula $C_4H_5Cl$. Neoprene is present on the FHE and is used to cushion the fuel element. In Case C4, 1/8-in of neoprene is modeled along the sides of the fuel element (see Figure 6.3-3). The small strips of neoprene above and below the fuel element are neglected because these strips are of insufficient mass to affect the reactivity in any appreciable manner. Inclusion of the neoprene has a pronounced negative effect on the reactivity, presumably due to absorption in the chlorine. In Case C5, the chlorine is deleted from the neoprene, and the density is reduced accordingly. Eliminating the chlorine from the neoprene may be postulated to be a result of decomposition during a fire, although such a scenario is not credible. Case C5 is slightly more reactive than Case C3, although the effect may simply be statistical fluctuation. It may be concluded that chlorine-free neoprene has a negligible effect on the reactivity.

Because the fuel may be transported inside of a plastic bag, it is conservatively assumed that the water density inside of the inner tube can vary independently of the water density inside of the fuel element. To maximize neutron reflection, full-density water is always modeled inside of the tube external to the fuel element, and the fuel element is centered laterally within the tube. In Cases C6 through C10, Case C5 is run with a range of water densities between the fuel plates, and maximum water density in all other regions of the model. Reactivity drops as the water density is reduced between the fuel plates, indicating that the system is under moderated.

Case C5 is the most reactive, with $k_s = 0.44248$. This result is below the USL of 0.9209.

#### 6.4.1.2.3 Loose Plate Basket Payload

The selection of the bounding fuel plate and development of the various plate arrangements are presented in conjunction with the NCT array analysis in Section 6.5.1.2, *Loose Plate Basket Payload*. The most reactive fuel plate arrangements determined in the NCT array analysis are used in the HAC single package analysis. This arrangement will also be the most reactive in the HAC single package models because both the NCT and HAC models are flooded and behave in a similar manner.

A figure showing the general HAC model geometry is provided in Figure 6.3-5. Results are provided in Table 6.4-6. Six cases are run, with small variations in the plate arrangement. The

maximum reactivity occurs for Case LB3, with $k_s = 0.43629$. This result is below the USL of 0.9209. The pitch of this case is non-regular. The top, center, and bottom plates are centered in the lattice locations with a base pitch of 1.036-cm, while the off-center plates are shifted 0.2-cm from the center plate.

## 6.4.2 Single Package Results

Following are the tabulated results for the single package cases. The most reactive configurations are listed in boldface.

**Table 6.4-1** – NCT Single Package Results, Fuel Element

| NCT Case | | | | | |
|---|---|---|---|---|---|
| Case ID | Filename | Moderator Density ($g/cm^3$) | $k_{eff}$ | $\sigma$ | $k_s$ ($k+2\sigma$) |
| **A1** | **NS_M100** | **1.0** | **0.41068** | **0.00097** | **0.41262** |

**Table 6.4-2** – NCT Single Package Results, Loose Plate Basket

| Case ID | Filename | Pitch (cm) | $k_{eff}$ | $\sigma$ | $k_s$ ($k+2\sigma$) |
|---|---|---|---|---|---|
| LA1 | NS_N5P52 | 1.036 | 0.39898 | 0.00091 | 0.40080 |
| LA2 | NS_N5P52A | 1.136 (max) | 0.39847 | 0.00096 | 0.40039 |
| LA3 | NS_N5P52B | 1.236 (max) | 0.39856 | 0.00097 | 0.40050 |
| **LA4** | **NS_N5P52C** | **1.336 (max)** | **0.40007** | **0.00096** | **0.40199** |
| LA5 | NS_N5P52D | 1.436 (max) | 0.39881 | 0.00095 | 0.40071 |
| LA6 | NS_N5P52E | 1.491 (max) | 0.39751 | 0.00095 | 0.39941 |

## Table 6.4-3 – Parametric Analysis Input Data, Fuel Element

| Parameter | B1 | B2 | B3 | B4 | B5 | B6 |
|---|---|---|---|---|---|---|
| Fuel Arc (cm) | 6.7355 | 6.9895 | 6.4815 | 6.7355 | 6.7355 | 6.7355 |
| Meat thickness (in) | 0.02 | 0.02 | 0.02 | 0.022 | 0.018 | 0.022 |
| Active fuel height (in) | 48 | 48 | 48 | 48 | 48 | 48 |
| Channel (in) | 0.078 | 0.078 | 0.078 | 0.078 | 0.078 | 0.078 |
| Cladding (in) | 0.015 | 0.015 | 0.015 | 0.015 | 0.015 | 0.014 |
| Total plate (in) | 0.050 | 0.050 | 0.050 | 0.052 | 0.048 | 0.050 |
| Pitch (in) | 0.128 | 0.128 | 0.128 | 0.130 | 0.126 | 0.128 |
| Volume ($cm^3$) | 41.7164 | 43.2895 | 40.1432 | 45.8880 | 37.5447 | 45.8880 |
| U-235 (g) | 63.2 | 63.2 | 63.2 | 63.2 | 63.2 | 63.2 |
| U-235 density ($g/cm^3$) | 1.51 | 1.46 | 1.57 | 1.38 | 1.68 | 1.38 |
| UAlx+Al density ($g/cm^3$) | 3.86 | 3.81 | 3.91 | 3.74 | 4.00 | 3.74 |
| N U-234 | 2.4865E-05 | 2.3962E-05 | 2.5840E-05 | 2.2605E-05 | 2.7628E-05 | 2.2605E-05 |
| N U-235 | 3.8789E-03 | 3.7380E-03 | 4.0309E-03 | 3.5263E-03 | 4.3099E-03 | 3.5263E-03 |
| N U-236 | 1.4382E-05 | 1.3859E-05 | 1.4945E-05 | 1.3074E-05 | 1.5980E-05 | 1.3074E-05 |
| N U-238 | 2.0576E-04 | 1.9828E-04 | 2.1382E-04 | 1.8705E-04 | 2.2862E-04 | 1.8705E-04 |
| N U-Al | 5.0157E-02 | 5.0391E-02 | 4.9905E-02 | 5.0742E-02 | 4.9442E-02 | 5.0742E-02 |
| Total | 5.4281E-02 | 5.4365E-02 | 5.4190E-02 | 5.4491E-02 | 5.4024E-02 | 5.4491E-02 |

| Parameter | B7 | B8 | B9 | B10 | B11 | B12 |
|---|---|---|---|---|---|---|
| Fuel Arc (cm) | 6.7355 | 6.7355 | 6.7355 | 6.7355 | 6.7355 | 6.9895 |
| Meat thickness (in) | 0.018 | 0.02 | 0.02 | 0.02 | 0.02 | 0.02 |
| Active fuel height (in) | 48 | 48 | 48 | 47 | 48 | 48 |
| Channel (in) | 0.078 | 0.085 | 0.085 | 0.078 | 0.078 | 0.085 |
| Cladding (in) | 0.016 | 0.015 | 0.0115 | 0.015 | 0.008 | 0.0115 |
| Total plate (in) | 0.050 | 0.050 | 0.0430 | 0.050 | 0.036 | 0.0430 |
| Pitch (in) | 0.128 | 0.135 | 0.128 | 0.128 | 0.114 | 0.128 |
| Volume ($cm^3$) | 37.5447 | 41.7164 | 41.7164 | 40.8473 | 41.7164 | 43.2895 |
| U-235 (g) | 63.2 | 63.2 | 63.2 | 63.2 | 63.2 | 63.2 |
| U-235 density ($g/cm^3$) | 1.68 | 1.51 | 1.51 | 1.55 | 1.51 | 1.46 |
| UAlx+Al density ($g/cm^3$) | 4.00 | 3.86 | 3.86 | 3.89 | 3.86 | 3.81 |
| N U-234 | 2.7628E-05 | 2.4865E-05 | 2.4865E-05 | 2.5394E-05 | 2.4865E-05 | 2.3962E-05 |
| N U-235 | 4.3099E-03 | 3.8789E-03 | 3.8789E-03 | 3.9615E-03 | 3.8789E-03 | 3.7380E-03 |
| N U-236 | 1.5980E-05 | 1.4382E-05 | 1.4382E-05 | 1.4688E-05 | 1.4382E-05 | 1.3859E-05 |
| N U-238 | 2.2862E-04 | 2.0576E-04 | 2.0576E-04 | 2.1014E-04 | 2.0576E-04 | 1.9828E-04 |
| N U-Al | 4.9442E-02 | 5.0157E-02 | 5.0157E-02 | 5.0020E-02 | 5.0157E-02 | 5.0391E-02 |
| Total | 5.4024E-02 | 5.4281E-02 | 5.4281E-02 | 5.4232E-02 | 5.4281E-02 | 5.4365E-02 |

**Table 6.4-4** – Parametric Analysis Results, Fuel Element

| Case ID | Filename | $k_{eff}$ | σ | $k_s$ (k+2σ) | Δ from B1 (mk) |
|---|---|---|---|---|---|
| B1 | P1 | 0.46601 | 0.00096 | 0.46793 | -- |
| B2 | P2 | 0.47015 | 0.00102 | 0.47219 | 4.3 |
| B3 | P3 | 0.46045 | 0.00102 | 0.46249 | -5.4 |
| B4 | P5 | 0.46403 | 0.00101 | 0.46605 | -1.9 |
| B5 | P4 | 0.46442 | 0.00111 | 0.46664 | -1.3 |
| B6 | P10 | 0.46753 | 0.00105 | 0.46963 | 1.7 |
| B7 | P9 | 0.46683 | 0.00101 | 0.46885 | 0.9 |
| B8 | P6 | 0.47528 | 0.00112 | 0.47752 | 9.6 |
| B9 | P7 | 0.47879 | 0.00100 | 0.48079 | 12.9 |
| B10 | P8 | 0.46704 | 0.00106 | 0.46916 | 1.2 |
| B11 | P11 | 0.47123 | 0.00108 | 0.47339 | 5.5 |
| B12 | P12 | 0.48534 | 0.00104 | 0.48742 | 19.5 |

**Table 6.4-5** – HAC Single Package Results, Fuel Element

| Case ID | Filename | Water Density Between Plates ($g/cm^3$) | $k_{eff}$ | σ | $k_s$ (k+2σ) |
|---|---|---|---|---|---|
| C1 | HS_M100_NOM | 1.0 | 0.42274 | 0.00095 | 0.42464 |
| C2 | HS_M100_TOL | 1.0 | 0.43639 | 0.00099 | 0.43837 |
| C3 | HS_M100_TOLW | 1.0 | 0.43991 | 0.00097 | 0.44185 |
| C4 | HS_M100_TOLW_N1 | 1.0 | 0.41002 | 0.00102 | 0.41206 |
| **C5** | **HS_M100_TOLW_N2** | **1.0** | **0.44040** | **0.00104** | **0.44248** |
| C6 | HS_M050 | 0.5 | 0.35396 | 0.00088 | 0.35572 |
| C7 | HS_M060 | 0.6 | 0.36994 | 0.00095 | 0.37184 |
| C8 | HS_M070 | 0.7 | 0.38607 | 0.00099 | 0.38805 |
| C9 | HS_M080 | 0.8 | 0.40411 | 0.00102 | 0.40615 |
| C10 | HS_M090 | 0.9 | 0.42092 | 0.00096 | 0.42284 |

**Table 6.4-6** – HAC Single Package Results, Loose Plate Basket

| Case ID | Filename | Pitch (cm) | $k_{eff}$ | σ | $k_s$ (k+2σ) |
|---|---|---|---|---|---|
| LB1 | HS_N5P52 | 1.036 | 0.43263 | 0.00097 | 0.43457 |
| LB2 | HS_N5P52A | 1.136 (max) | 0.43350 | 0.00092 | 0.43534 |
| **LB3** | **HS_N5P52B** | **1.236 (max)** | **0.43443** | **0.00093** | **0.43629** |
| LB4 | HS_N5P52C | 1.336 (max) | 0.43388 | 0.00096 | 0.43580 |
| LB5 | HS_N5P52D | 1.436 (max) | 0.43328 | 0.00091 | 0.43510 |
| LB6 | HS_N5P52E | 1.491 (max) | 0.43169 | 0.00089 | 0.43347 |

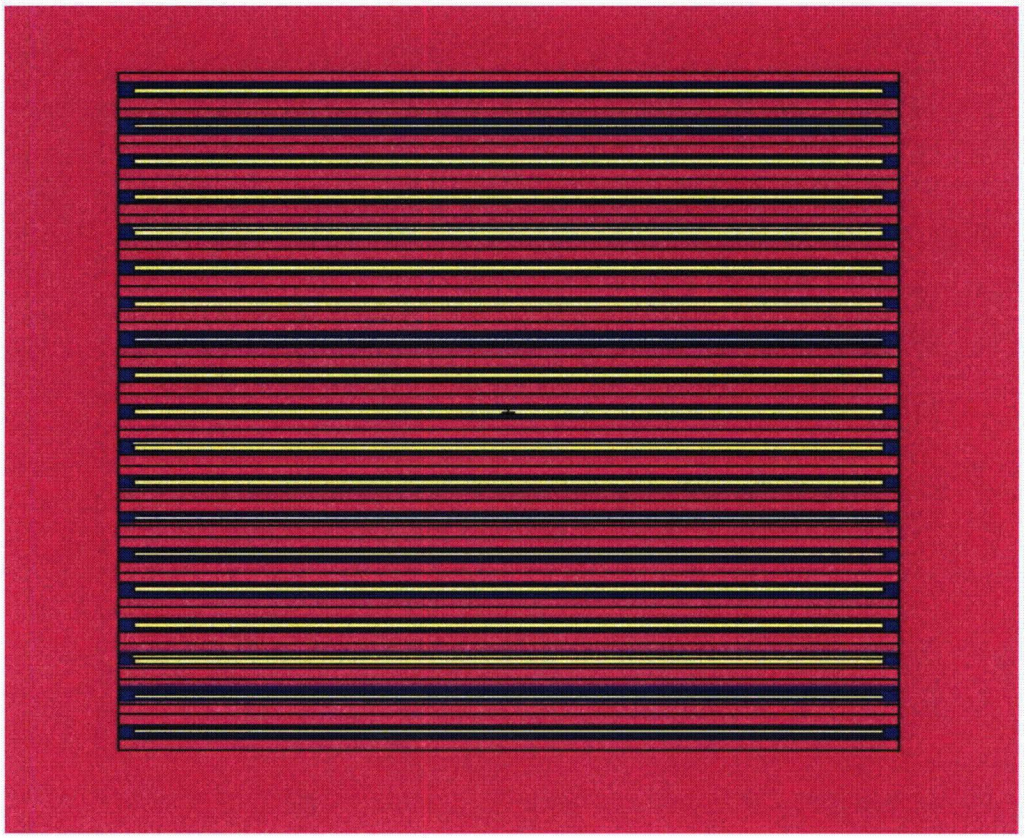

**Figure 6.4-1** – Base Parametric Model (Case B1)

# 6.5 Evaluation of Package Arrays under Normal Conditions of Transport

## 6.5.1 NCT Array Configuration

### 6.5.1.1 Fuel Element Payload

The NCT array model is a 9x9x1 array of the NCT single package model, see Figure 6.5-1. Although an 8x8x1 array is of sufficient size to justify a CSI = 4.0, the larger 9x9x1 array is utilized simply for modeling convenience. Neoprene is modeled without chlorine in all models. It is demonstrated in Section 6.6.1.1, *Fuel Element Payload*, that chlorine-free neoprene may have a slight positive effect on the reactivity, although the effect is small. The entire array is reflected with 12-in of full-density water.

The fuel elements are pushed to the center of the array and rotated to minimize the distance between the fuel elements. This geometry is not feasible for NCT, because the FHE would force the fuel elements to remain in the center of the package, although the FHE does allow rotation. Therefore, it is conservative to ignore the FHE to minimize the separation distance. In addition, a small notch is added to the neoprene so that the fuel element may be translated to the maximum extent without interfering with the inner tube geometry. This notch is not present in the single package models.

Two calculational series are developed. In Series 1, the water density is fixed at 1.0 g/cm$^3$ between the fuel plates and the water density is allowed to vary inside the inner tube. Series 2 is the same as Series 1, although the density within the fuel plates is at a reduced density of 0.9 g/cm$^3$. Void is always present between the insulation and the outer tube, as this region is water-tight. The results are provided in Table 6.5-1.

Reactivity is at a maximum for Case D4, which has full-density water between the fuel plates, and 0.3 g/cm$^3$ water inside the inner tube, with $k_s$ = 0.82839. As expected, the reactivity drops when the water density between the fuel plates is reduced, as the system is under moderated. The maximum result is far below the USL of 0.9209.

As a point of interest, an additional case (Case D12) is developed in which the fuel elements are centered in the cavity and not rotated, using the moderation assumptions of Case D4 (see the lower figure of Figure 6.5-1). The reactivity drops by 18.5 mk, which essentially represents the additional conservatism of pushing the fuel elements to the center of the array.

### 6.5.1.2 Loose Plate Basket Payload

The NCT array model is a 9x9x1 array of the NCT single package model. For the NCT single package cases, it was sufficient to laterally center the fuel basket within the inner tube to maximize reflection by the water in the tube. However, in the NCT array configuration, it is expected that reactivity would be maximized by pushing the fuel baskets to the center of the array, as shown in the top sketch of Figure 6.5-2. The fuel elements may be packed closer by rotating them as shown in the figure. Therefore, unless otherwise noted, all NCT array models have the baskets pushed toward the center of the array. Although this assumption bounds any

anticipated basket damage, this arrangement is not credible, because the structural ribs that center the baskets within the inner tube will not deform in this manner.

The loose plate payload consists of 19 different plate types. Each plate type has a different width and uranium mass, although the lengths are the same. Each plate may be either flat or curved, for a total of 19*2 = 38 different variations. However, flat and curved plates will not be mixed in the same basket (to facilitate packaging). Within each loose plate basket, any combination of plate types may be present, with the only limitation that the total U-235 mass present in the basket must not exceed 600 g.

Clearly, there are a large number of possible combinations of plates that may be present within the basket. The objective is to determine a simplified configuration that bounds any random collection of plates. Fortunately, calculations may be performed using only flat plates, because the neutronic behavior of flat and curved plates is demonstrated to be nearly identical. Therefore, the flat plate results also apply to the curved plates. Flat plates allow easy geometry setup using MCNP repeated structures, while curved plates generally cannot be modeled using repeated structures unless the plate pitch is rather large.

Basic data for the 19 plate types are provided in Table 6.2-1. It is not necessary to model each of the 19 different plate types. Rather, from examination of these data, a subset of plates is selected for further analysis. Plates 5 through 15 have a U-235 density of approximately 1.64 g/cm$^3$, while the remaining plates have a significantly lower U-235 density. Plate 5 is the smallest plate in this range, and Plate 15 is the largest plate in this range; both are selected for further evaluation. Plate 8 is also selected as a representative plate between these two extremes, and should result in reactivity values between Plate 5 and 15. It is demonstrated that the smaller plate configuration (Plate 5) is more reactive than the larger plate configurations (Plates 8 and 15). Plate 3 is also selected for further evaluation because it is smaller than Plate 5, although the reduced U-235 density will result in a larger number of plates.

For simplicity, only one plate type is modeled within each basket. Randomly mixing different plate types would result in a less reactive condition that the most reactive single plate configuration. Also, number densities of the selected plates have been slightly adjusted so that the total mass of U-235 is always 600 g. For plates 5, 8, and 15, the number densities are increased, while for plate 3 the number densities are decreased.

Four initial series of calculations are performed, one series for each of the four plate types under consideration. The goal of these initial calculations is to simply determine the bounding plate type. Once the bounding plate type has been determined, additional series of calculations are performed on the bounding plate type. For all of the initial models, full-density water is modeled between the plates, 0.3 g/cm$^3$ water is modeled between the plate array and basket (this region is not present once the plate array fills the entire basket area), 0.3 g/cm$^3$ water is modeled between the basket and inner tube, and insulation/void is modeled between the inner and outer tubes. The water density of 0.3 g/cm$^3$ is selected based upon the most reactive moderation condition of the ATR fuel element analysis, and will be optimized once the bounding plate is selected.

**Fuel Plate 5 Series:** Fuel plate 5 is the first plate type examined. Ten plates are required to achieve a mass of 600 g U-235. The plate arrangements for a number of the configurations are shown in Figure 6.5-3 through Figure 6.5-5. Results are provided in Table 6.5-2. In cases LC1 through LC9, the plates are arranged in a 1x10 array at the center of the basket. Reactivity is

low when the pitch is small, and reactivity increases as the pitch increases. In cases LC10 and LC11, the reactivity increases as the plates are alternately shifted to the right and left because moderation increases. In case LC12, plates are alternately shifted up and down until they contact each other.

Because fuel plate 5 is rather narrow, it is possible to further increase the moderation by modeling the plates in a 2x5 array in cases LC13 through LC29. Because the plate is slightly too wide to fit two side-by-side, the two side-by-side plates are modeled as a single plate by doubling the fuel meat width. The reactivity continues to increase with increasing pitch. Case LC19 has the largest reactivity obtained with a constant pitch.

However, moderation can be further increased if a non-regular pitch is utilized. In cases LC20 through LC29, non-regular pitches are examined. In these cases, the plates at the top, center, and bottom of the basket remain fixed, while the two off-center plates are shifted away from the center plate in 0.1-cm increments. Because the pitches in these cases are non-regular, the pitches provided in the results table are noted as "max" values. Case LC21 is the most reactive, with $k_s$=0.76806, although the reactivity gain resulting from a non-regular pitch is relatively small and within statistical fluctuation. For case LC21, the top, center, and bottom plates are centered in the lattice locations with a base pitch of 1.036 cm, while the off-center plates are shifted 0.2-cm from the center plate (maximum pitch of 1.236 cm).

**Fuel Plate 8 Series:** Nine plates are required to achieve a mass of 600 g U-235. The plate arrangements for a number of configurations are shown in Figure 6.5-6 and Figure 6.5-7. Results are provided in Table 6.5-3. Considerably fewer cases are generated compared to fuel plate 5 because it has been established that the plates are highly under moderated when packed tightly.

In cases LD1 through LD3, the plates are modeled in a simple 1x9 array. In cases LD4 though LD11, the plates are alternately shifted left and right to increase moderation. In cases LD6 through LD11, the top, bottom, and center plates remain fixed, while the remaining plates are progressively shifted up or down in 0.1-cm increments. Case LD7 is the most reactive, with $k_s$=0.75241, although the reactivity is less than the most reactive plate 5 case. For case LC7, the base lattice pitch is 0.574-cm, and the off-center plates are shifted 0.2-cm from the center plate.

**Fuel Plate 15 Series:** Seven plates are required to achieve a mass of 600 g U-235. The plate arrangements for a number of the configurations are shown in Figure 6.5-8. Results are provided in Table 6.5-3. Using the same methodology as plates 5 and 8, case LE8 is the most reactive, with $k_s$=0.74548. This case also features a non-regular pitch. For case LE8, the base lattice pitch is 0.804 cm, and the off-center plates are shifted 0.1 cm from the center plate.

Comparing the maximum $k_s$ values for plates 5, 8, and 15, plate 5 is the most reactive ($k_s$=0.76806), plate 15 is the least reactive ($k_s$=0.74548), and plate 8 falls between the two ($k_s$=0.75241). In fact, the reactivities of plates 8 and 15 are fairly close, despite the difference in the width and number of plates. Plate 5 is somewhat more reactive than either plate 8 or 15, most likely because its narrow width allows "double stacking" of this plate along the width of the basket, which results in a more advantageous moderation and geometry conditions. Therefore, the trend is that for a fixed U-235 mass per basket, the smaller plates are more reactive than the larger plates.

Of course, plates 1 through 4 are smaller than plate 5. However, these plates have a lower U-235 density so that more plates are required to achieve 600 g U-235. More plates would provide less volume for moderation, so it is expected that plate 5 would bound plates 1 through 4. This is confirmed by running several cases for plate 3.

**Fuel Plate 3 Series:** Fourteen plates are required to achieve a mass of 600 g U-235. The plate arrangements for the configurations are shown in Figure 6.5-9. Results are provided in Table 6.5-3. All cases are for a 2x7 arrangement and non-regular pitches, as similar arrangements have been shown to be the most reactive for the other plates. Two side-by-side plates are modeled as a single plate with double fuel meat width, consistent with the treatment of the Type 5 plate. Case LF2 is the most reactive, with $k_s$=0.75904, although this case is less reactive than the Type 5 plate. For case LF2, the pitch is 0.796 cm.

**Criticality Analysis Using Plate 5:** From the analysis of plate types 3, 5, 8, and 15, Type 5 is shown to be the most reactive. Therefore, the remaining analysis uses only this plate type. An additional two series of cases are performed using fuel plate 5 in which the water densities in the various model regions are allowed to vary. The primary regions of interest are within the basket and between the basket and the inner tube.

In Series 1, full-density water is modeled within the basket, while the water density between the basket and the inner tube is varied from 0 to 1.0 g/cm$^3$. The results are provided in Table 6.5-4. The maximum reactivity occurs for Case LG5, with $k_s$ = 0.77469. A water density of 0.5 g/cm$^3$ within the inner tube is utilized in the most reactive case.

In Series 2, the water density inside the basket is reduced to 0.9 g/cm$^3$, while the water density between the basket and the inner tube is varied from 0 to 1.0 g/cm$^3$. The reactivity clearly drops when reduced density water is modeled inside the basket.

Several miscellaneous cases are run to validate the assumptions noted above. In Case LJ1, the most reactive case (Case LG5) is run with the fuel baskets centered inside of the tubes (see the lower sketch of Figure 6.5-2). The reactivity drops as the fuel elements are pushed apart, $k_s$ = 0.76237 for Case LJ1, compared to $k_s$ = 0.77469 for Case LG5.

It has been implicitly assumed the maximum reactivity is obtained for the maximum fissile mass of 600 g U-235. In general, the maximum allowable fissile loading is not necessarily the most reactive condition if the volume of fissile material is so large that little volume is available for moderating material. That is not the case for the loose plate analysis, as the fuel plates are thin and only a small number of plates are required to achieve a mass of 600 g U-235. Removing plates might increase moderation slightly as water is added to the system, although reducing the fissile mass more than compensates for the additional moderation and lowers the reactivity. To demonstrate this effect, the arrangement of Case LC9, which has ten type 5 plates in a 1x10 evenly spaced array (see Figure 6.5-3), is repeated with ten, nine, eight, and seven evenly spaced plates (Cases LJ2, LJ3, LJ4, and LJ5, see Figure 6.5-10) with an inner tube water density of 0.5 g/cm$^3$. The reactivity drops as each successive plate is removed (0.62333 for Case LJ2 to 0.57579 for Case LJ5), despite the fact that the plates are spaced farther and farther apart and moderation is improved. If plates are removed from the most reactive models, for which the pitch is already non-regular to maximize reactivity, the reactivity drop resulting from removing plates would be more pronounced.

It is stated that modeling the plates as flat is neutronically equivalent to modeling the plates as curved. This modeling assumption is verified by modeling both flat and curved plates with a constant pitch of 0.80 cm. This pitch is selected because it is large and constant and the curved plates may be modeled with repeated structures. Case LJ6 is the flat plate model, and Case LJ7 is the curved plate model. Case LJ6 is geometrically identical to case LC13 (see Figure 6.5-4) except the water density inside the basket is 1.0 g/cm$^3$ between the plate array and the basket. Case LJ7 is shown in Figure 6.5-10. Flat plate Case LJ6 has $k_s$=0.73021, while curved plate Case LJ7 has $k_s$=0.73022. The difference between these cases is negligible, and the statement that flat plates are neutronically equivalent to curved plates is verified.

In conclusion, Case LG5 is the most reactive loose plate basket model, with $k_s$ = 0.77469. This result is below the USL of 0.9209. Case LG5 has fully moderated fuel plates, 0.5 g/cm$^3$ water inside the inner tube, and fuel plate baskets that have been rotated and moved to the center of the array.

## 6.5.2 NCT Array Results

The results for the NCT array cases are provided in the following table. The most reactive configuration is listed in boldface.

## Table 6.5-1 – NCT Array Results, Fuel Element Payload

| Case ID | Filename | Water Density Between Tubes ($g/cm^3$) | Water Density Inside Inner Tube ($g/cm^3$) | Water Density Between Plates ($g/cm^3$) | $k_{eff}$ | $\sigma$ | $k_s$ ($k+2\sigma$) |
|---|---|---|---|---|---|---|---|
| **Series 1: Variable water density inside inner tube, full density water between plates.** | | | | | | | |
| D1 | NA_P000 | 0 | 0 | 1.0 | 0.76716 | 0.00120 | 0.76956 |
| D2 | NA_P010 | 0 | 0.1 | 1.0 | 0.80349 | 0.00123 | 0.80595 |
| D3 | NA_P020 | 0 | 0.2 | 1.0 | 0.81928 | 0.00112 | 0.82152 |
| **D4** | **NA_P030** | **0** | **0.3** | **1.0** | **0.82605** | **0.00117** | **0.82839** |
| D5 | NA_P040 | 0 | 0.4 | 1.0 | 0.82149 | 0.00119 | 0.82387 |
| D6 | NA_P050 | 0 | 0.5 | 1.0 | 0.81420 | 0.00118 | 0.81656 |
| D7 | NA_P060 | 0 | 0.6 | 1.0 | 0.80521 | 0.00108 | 0.80737 |
| D8 | NA_P070 | 0 | 0.7 | 1.0 | 0.79216 | 0.00121 | 0.79458 |
| D9 | NA_P080 | 0 | 0.8 | 1.0 | 0.78130 | 0.00132 | 0.78394 |
| D10 | NA_P090 | 0 | 0.9 | 1.0 | 0.76905 | 0.00120 | 0.77145 |
| D11 | NA_P100 | 0 | 1.0 | 1.0 | 0.75603 | 0.00124 | 0.75851 |
| D12 | NA_P030C | 0 | 0.3 | 1.0 | 0.80743 | 0.00122 | 0.80987 |
| **Series 2: Variable water density inside inner tube, 0.9 $g/cm^3$ density water between plates.** | | | | | | | |
| E1 | NA_M90P000 | 0 | 0 | 0.9 | 0.72938 | 0.00111 | 0.73160 |
| E2 | NA_M90P010 | 0 | 0.1 | 0.9 | 0.77108 | 0.00120 | 0.77348 |
| E3 | NA_M90P020 | 0 | 0.2 | 0.9 | 0.79299 | 0.00116 | 0.79531 |
| E4 | NA_M90P030 | 0 | 0.3 | 0.9 | 0.79943 | 0.00123 | 0.80189 |
| **E5** | **NA_M90P040** | **0** | **0.4** | **0.9** | **0.80192** | **0.00108** | **0.80408** |
| E6 | NA_M90P050 | 0 | 0.5 | 0.9 | 0.79378 | 0.00108 | 0.79594 |
| E7 | NA_M90P060 | 0 | 0.6 | 0.9 | 0.78539 | 0.00111 | 0.78761 |
| E8 | NA_M90P070 | 0 | 0.7 | 0.9 | 0.77658 | 0.00118 | 0.77894 |
| E9 | NA_M90P080 | 0 | 0.8 | 0.9 | 0.76496 | 0.00117 | 0.76730 |
| E10 | NA_M90P090 | 0 | 0.9 | 0.9 | 0.75315 | 0.00121 | 0.75557 |
| E11 | NA_M90P100 | 0 | 1.0 | 0.9 | 0.74334 | 0.00126 | 0.74586 |

**Table 6.5-2** – NCT Array Results, Pitch Variations, Plate 5

| Case ID | Filename | Pitch (cm) | $k_{eff}$ | σ | $k_s$ (k+2σ) |
|---|---|---|---|---|---|
| LC1 | NA_N5P08 | 0.160 | 0.41955 | 0.00093 | 0.42141 |
| LC2 | NA_N5P10 | 0.200 | 0.44783 | 0.00091 | 0.44965 |
| LC3 | NA_N5P12 | 0.240 | 0.47653 | 0.00104 | 0.47861 |
| LC4 | NA_N5P14 | 0.280 | 0.50372 | 0.00104 | 0.50580 |
| LC5 | NA_N5P16 | 0.320 | 0.53109 | 0.00103 | 0.53315 |
| LC6 | NA_N5P18 | 0.360 | 0.55470 | 0.00109 | 0.55688 |
| LC7 | NA_N5P20 | 0.400 | 0.57669 | 0.00104 | 0.57877 |
| LC8 | NA_N5P22 | 0.440 | 0.59930 | 0.00111 | 0.60152 |
| LC9 | NA_N5P23 | 0.460 | 0.61120 | 0.00102 | 0.61324 |
| LC10 | NA_N5P23A | 0.460 | 0.69108 | 0.00118 | 0.69344 |
| LC11 | NA_N5P23B | 0.460 | 0.74866 | 0.00109 | 0.75084 |
| LC12 | NA_N5P23C | 0.460 | 0.74714 | 0.00102 | 0.74918 |
| LC13 | NA_N5P40 | 0.800 | 0.71462 | 0.00107 | 0.71676 |
| LC14 | NA_N5P42 | 0.840 | 0.72319 | 0.00108 | 0.72535 |
| LC15 | NA_N5P44 | 0.880 | 0.73353 | 0.00102 | 0.73557 |
| LC16 | NA_N5P46 | 0.920 | 0.74169 | 0.00107 | 0.74383 |
| LC17 | NA_N5P48 | 0.960 | 0.74962 | 0.00112 | 0.75186 |
| LC18 | NA_N5P50 | 1.000 | 0.75920 | 0.00109 | 0.76138 |
| LC19 | NA_N5P52 | 1.036 | 0.76423 | 0.00118 | 0.76659 |
| LC20 | NA_N5P52A | 1.136 (max) | 0.76520 | 0.00102 | 0.76724 |
| **LC21** | **NA_N5P52B** | **1.236 (max)** | **0.76582** | **0.00112** | **0.76806** |
| LC22 | NA_N5P52C | 1.336 (max) | 0.76393 | 0.00107 | 0.76607 |
| LC23 | NA_N5P52D | 1.436 (max) | 0.76254 | 0.00096 | 0.76446 |
| LC24 | NA_N5P52E | 1.493 (max) | 0.75949 | 0.00093 | 0.76135 |
| LC25 | NA_N5P67 | 1.540 (max) | 0.75942 | 0.00101 | 0.76144 |
| LC26 | NA_N5P67A | 1.640 (max) | 0.75508 | 0.00105 | 0.75718 |
| LC27 | NA_N5P67B | 1.740 (max) | 0.74803 | 0.00106 | 0.75015 |
| LC28 | NA_N5P67C | 1.840 (max) | 0.73839 | 0.00107 | 0.74053 |
| LC29 | NA_N5P67D | 1.940 (max) | 0.72412 | 0.00105 | 0.72622 |

**Table 6.5-3** – NCT Array Results, Pitch Variations, Plates 8, 15, and 3

| Case ID | Filename | Pitch (cm) | $k_{eff}$ | σ | $k_s$ (k+2σ) |
|---|---|---|---|---|---|
| **Plate 8** | | | | | |
| LD1 | NA_N8P22 | 0.440 | 0.60412 | 0.00106 | 0.60624 |
| LD2 | NA_N8P24 | 0.480 | 0.62588 | 0.00106 | 0.62800 |
| LD3 | NA_N8P26 | 0.518 | 0.64309 | 0.00112 | 0.64533 |
| LD4 | NA_N8P26A | 0.518 | 0.74015 | 0.00102 | 0.74219 |
| LD5 | NA_N8P29 | 0.574 | 0.74719 | 0.00105 | 0.74929 |
| LD6 | NA_N8P29A | 0.674 (max) | 0.74875 | 0.00112 | 0.75099 |
| **LD7** | **NA_N8P29B** | **0.774 (max)** | **0.75035** | **0.00103** | **0.75241** |
| LD8 | NA_N8P29C | 0.874 (max) | 0.74896 | 0.00099 | 0.75094 |
| LD9 | NA_N8P29D | 0.974 (max) | 0.74574 | 0.00102 | 0.74778 |
| LD10 | NA_N8P29E | 1.074 (max) | 0.74373 | 0.00092 | 0.74557 |
| LD11 | NA_N8P29F | 1.174 (max) | 0.73494 | 0.00106 | 0.73706 |
| **Plate 15** | | | | | |
| LE1 | NA_N15P32 | 0.640 | 0.68653 | 0.00107 | 0.68867 |
| LE2 | NA_N15P34 | 0.690 | 0.70200 | 0.00113 | 0.70426 |
| LE3 | NA_N15P34A | 0.690 | 0.73590 | 0.00114 | 0.73818 |
| LE4 | NA_N15P34B | 0.790 (max) | 0.74090 | 0.00110 | 0.74310 |
| LE5 | NA_N15P34C | 0.890 (max) | 0.74003 | 0.00111 | 0.74225 |
| LE6 | NA_N15P34D | 0.970 (max) | 0.74209 | 0.00108 | 0.74425 |
| LE7 | NA_N15P40 | 0.804 | 0.74153 | 0.00115 | 0.74383 |
| **LE8** | **NA_N15P40A** | **0.904 (max)** | **0.74322** | **0.00113** | **0.74548** |
| LE9 | NA_N15P40B | 1.004 (max) | 0.74089 | 0.00118 | 0.74325 |
| LE10 | NA_N15P40C | 1.104 (max) | 0.73801 | 0.00100 | 0.74001 |
| **Plate 3** | | | | | |
| LF1 | NA_N3P40 | 0.796 | 0.75062 | 0.00102 | 0.75266 |
| **LF2** | **NA_N3P40A** | **0.796** | **0.75696** | **0.00104** | **0.75904** |
| LF3 | NA_N3P40B | 0.896 (max) | 0.75655 | 0.00107 | 0.75869 |
| LF4 | NA_N3P40C | 0.996 (max) | 0.75365 | 0.00094 | 0.75553 |
| LF5 | NA_N3P40D | 1.096 (max) | 0.75155 | 0.00106 | 0.75367 |

## Table 6.5-4 – NCT Array Results, Plate 5

| Case ID | Filename | Water Density Between Tubes ($g/cm^3$) | Water Density Inside Inner Tube ($g/cm^3$) | Water Density Between Plates ($g/cm^3$) | $k_{eff}$ | $\sigma$ | $k_s$ ($k+2\sigma$) |
|---|---|---|---|---|---|---|---|
| **Series 1: Variable water density inside inner tube, full-density water in basket.** | | | | | | | |
| LG1 | NA_N5P000 | 0 | 0 | 1.0 | 0.66797 | 0.00097 | 0.66991 |
| LG2 | NA_N5P010 | 0 | 0.1 | 1.0 | 0.71859 | 0.00100 | 0.72059 |
| LG3 | NA_N5P020 | 0 | 0.2 | 1.0 | 0.74925 | 0.00104 | 0.75133 |
| LC21 | NA_N5P52B | 0 | 0.3 | 1.0 | 0.76582 | 0.00112 | 0.76806 |
| LG4 | NA_N5P040 | 0 | 0.4 | 1.0 | 0.77225 | 0.00117 | 0.77459 |
| **LG5** | **NA_N5P050** | **0** | **0.5** | **1.0** | **0.77251** | **0.00109** | **0.77469** |
| LG6 | NA_N5P060 | 0 | 0.6 | 1.0 | 0.76738 | 0.00099 | 0.76936 |
| LG7 | NA_N5P070 | 0 | 0.7 | 1.0 | 0.75998 | 0.00100 | 0.76198 |
| LG8 | NA_N5P080 | 0 | 0.8 | 1.0 | 0.75086 | 0.00114 | 0.75314 |
| LG9 | NA_N5P090 | 0 | 0.9 | 1.0 | 0.74066 | 0.00111 | 0.74288 |
| LG10 | NA_N5P100 | 0 | 1.0 | 1.0 | 0.72764 | 0.00111 | 0.72986 |
| **Series 2: Variable water density inside inner tube, reduced density water in basket.** | | | | | | | |
| LH1 | NA_N5M090P000 | 0 | 0 | 0.9 | 0.63496 | 0.00098 | 0.63692 |
| LH2 | NA_N5M090P010 | 0 | 0.1 | 0.9 | 0.69390 | 0.00093 | 0.69576 |
| LH3 | NA_N5M090P020 | 0 | 0.2 | 0.9 | 0.72793 | 0.00095 | 0.72983 |
| LH4 | NA_N5M090P030 | 0 | 0.3 | 0.9 | 0.74560 | 0.00108 | 0.74776 |
| LH5 | NA_N5M090P040 | 0 | 0.4 | 0.9 | 0.75402 | 0.00108 | 0.75618 |
| **LH6** | **NA_N5M090P050** | **0** | **0.5** | **0.9** | **0.75480** | **0.00109** | **0.75698** |
| LH7 | NA_N5M090P060 | 0 | 0.6 | 0.9 | 0.75429 | 0.00110 | 0.75649 |
| LH8 | NA_N5M090P070 | 0 | 0.7 | 0.9 | 0.74414 | 0.00100 | 0.74614 |
| LH9 | NA_N5M090P080 | 0 | 0.8 | 0.9 | 0.73639 | 0.00104 | 0.73847 |
| LH10 | NA_N5M090P090 | 0 | 0.9 | 0.9 | 0.72573 | 0.00095 | 0.72763 |
| LH11 | NA_N5M090P100 | 0 | 1.0 | 0.9 | 0.71549 | 0.00107 | 0.71763 |
| **Miscellaneous Cases** | | | | | | | |
| LJ1 | NA_N5P050C | 0 | 0.5 | 1.0 | 0.76003 | 0.00117 | 0.76237 |
| LJ2 | NA_N5P23_10 | 0 | 0.5 | 1.0 | 0.62119 | 0.00107 | 0.62333 |
| LJ3 | NA_N5P23_9 | 0 | 0.5 | 1.0 | 0.60657 | 0.00106 | 0.60869 |
| LJ4 | NA_N5P23_8 | 0 | 0.5 | 1.0 | 0.59251 | 0.00114 | 0.59479 |
| LJ5 | NA_N5P23_7 | 0 | 0.5 | 1.0 | 0.57369 | 0.00105 | 0.57579 |
| LJ6 | NA_N5P40_F | 0 | 0.5 | 1.0 | 0.72815 | 0.00103 | 0.73021 |
| LJ7 | NA_N5P40_C | 0 | 0.5 | 1.0 | 0.72810 | 0.00106 | 0.73022 |

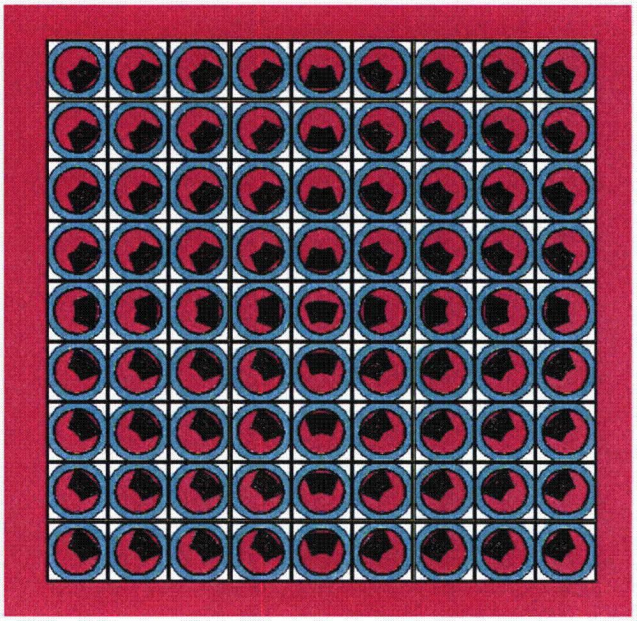

Pushed to center of array

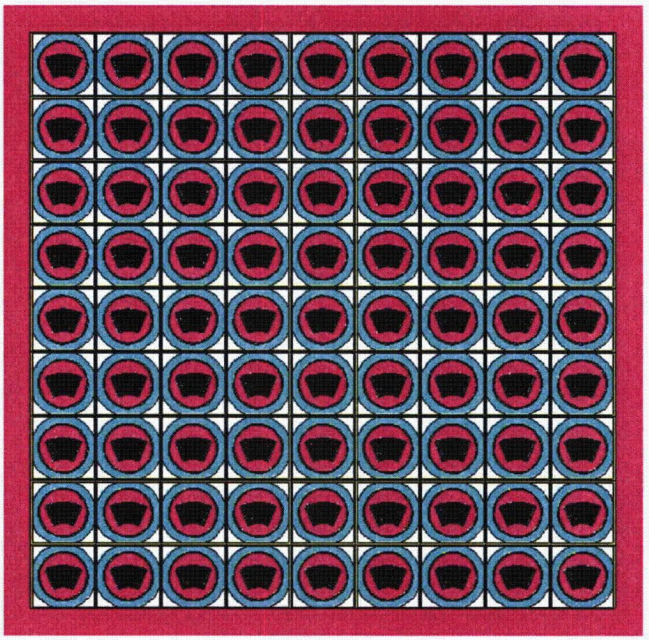

Centered in each tube (D12)

**Figure 6.5-1** – NCT Array Geometry, Fuel Element Payload

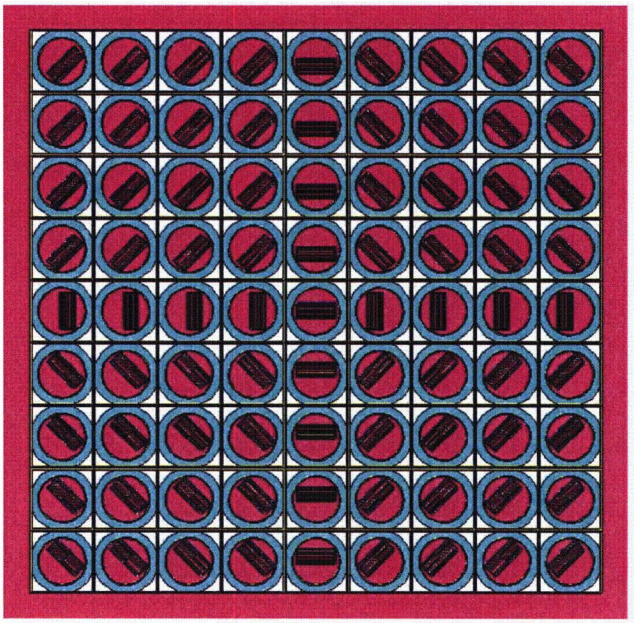

Pushed to center of array

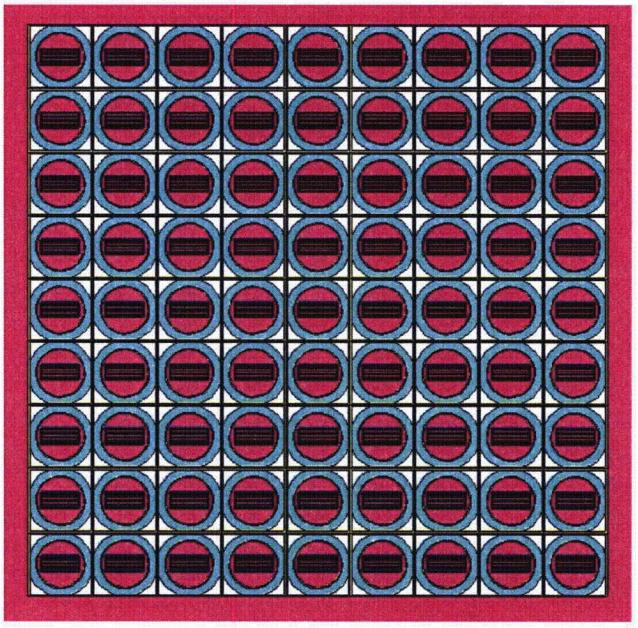

Centered in each tube (LJ1)

**Figure 6.5-2** – NCT Array Geometry, Loose Plate Basket Payload

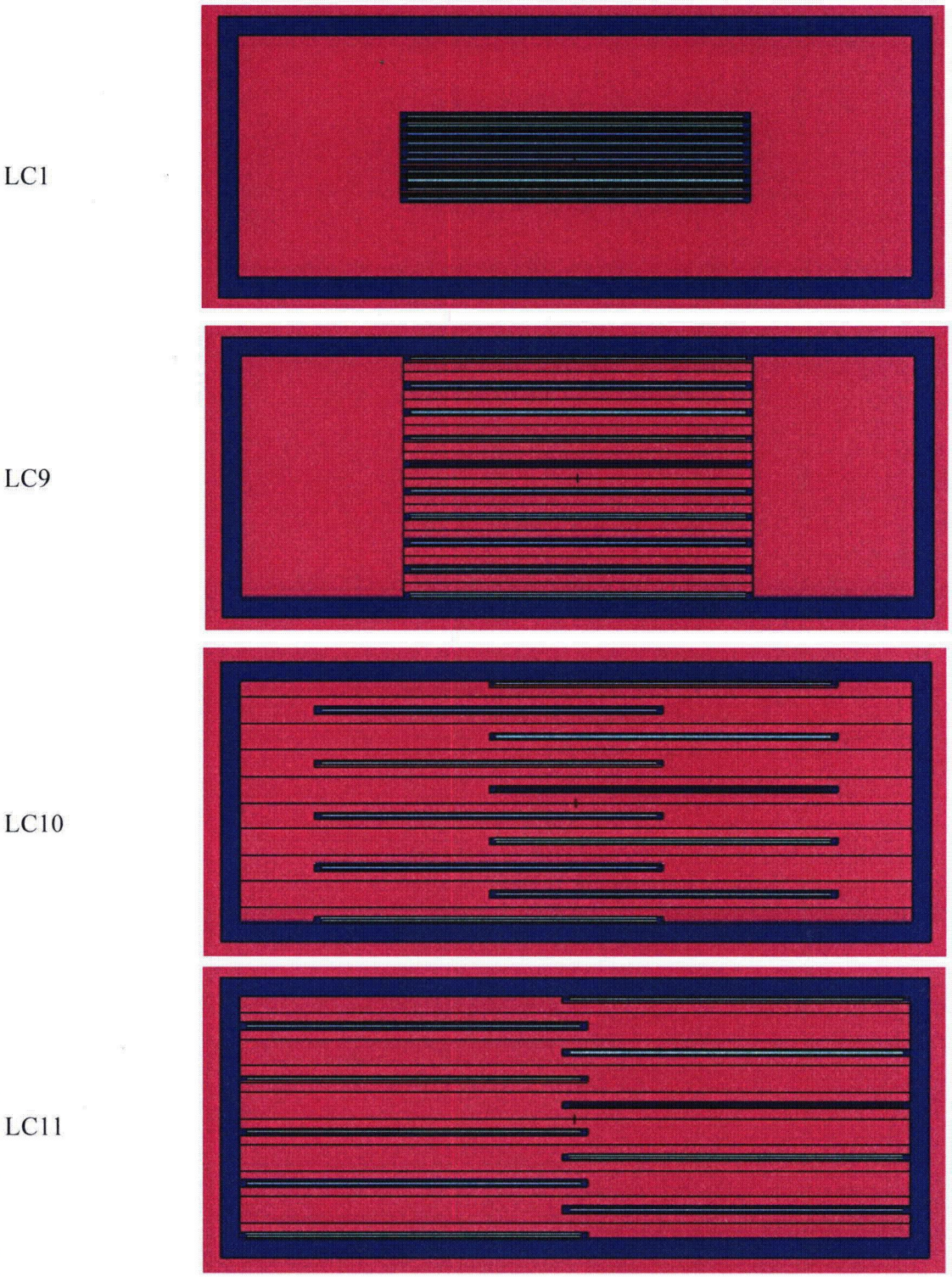


**Figure 6.5-3** – NCT Array Geometry, Plate 5 (LC1, LC9, LC10, LC11)

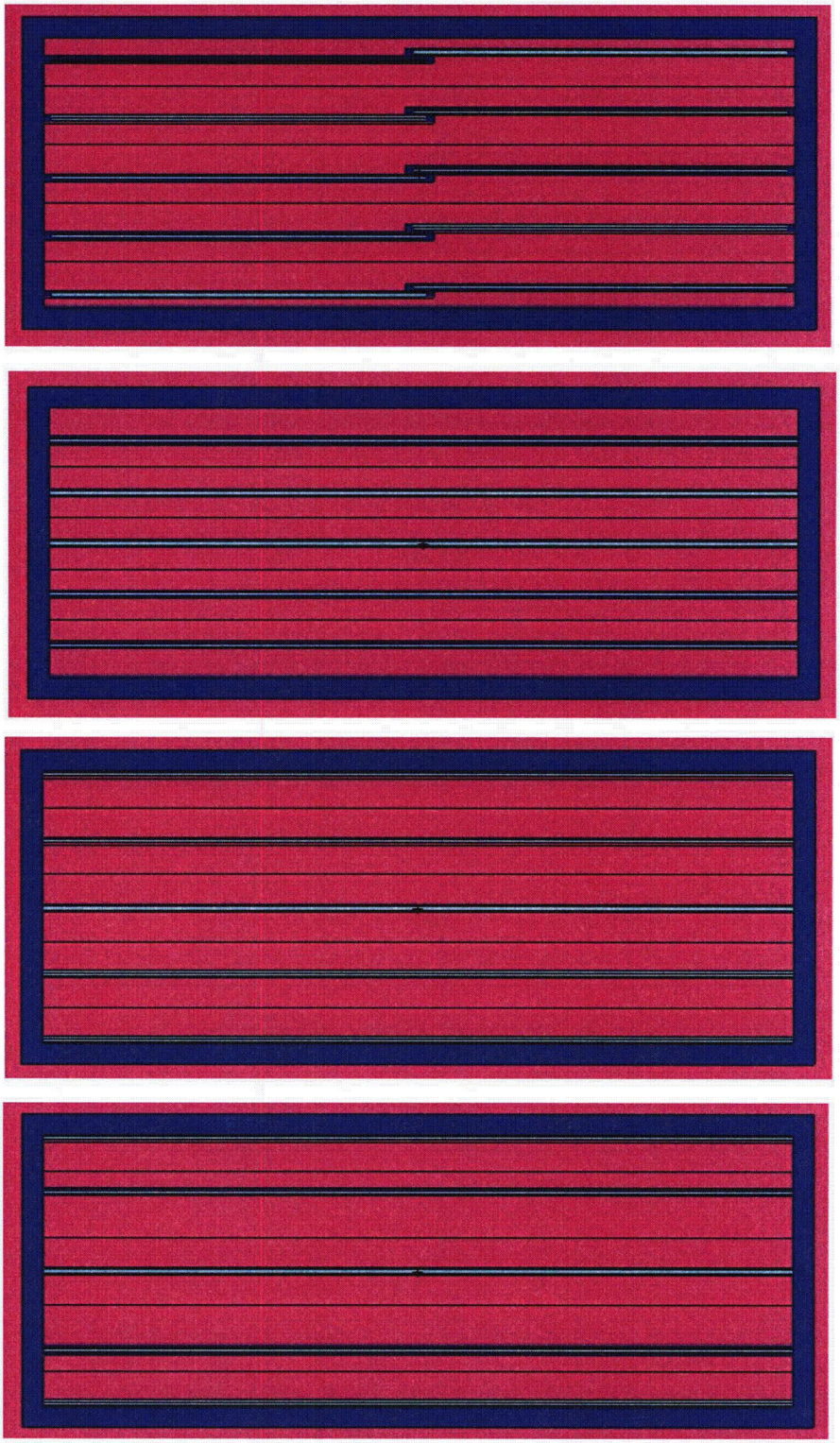


**Figure 6.5-4** – NCT Array Geometry, Plate 5 (LC12, LC13, LC19, LC21)

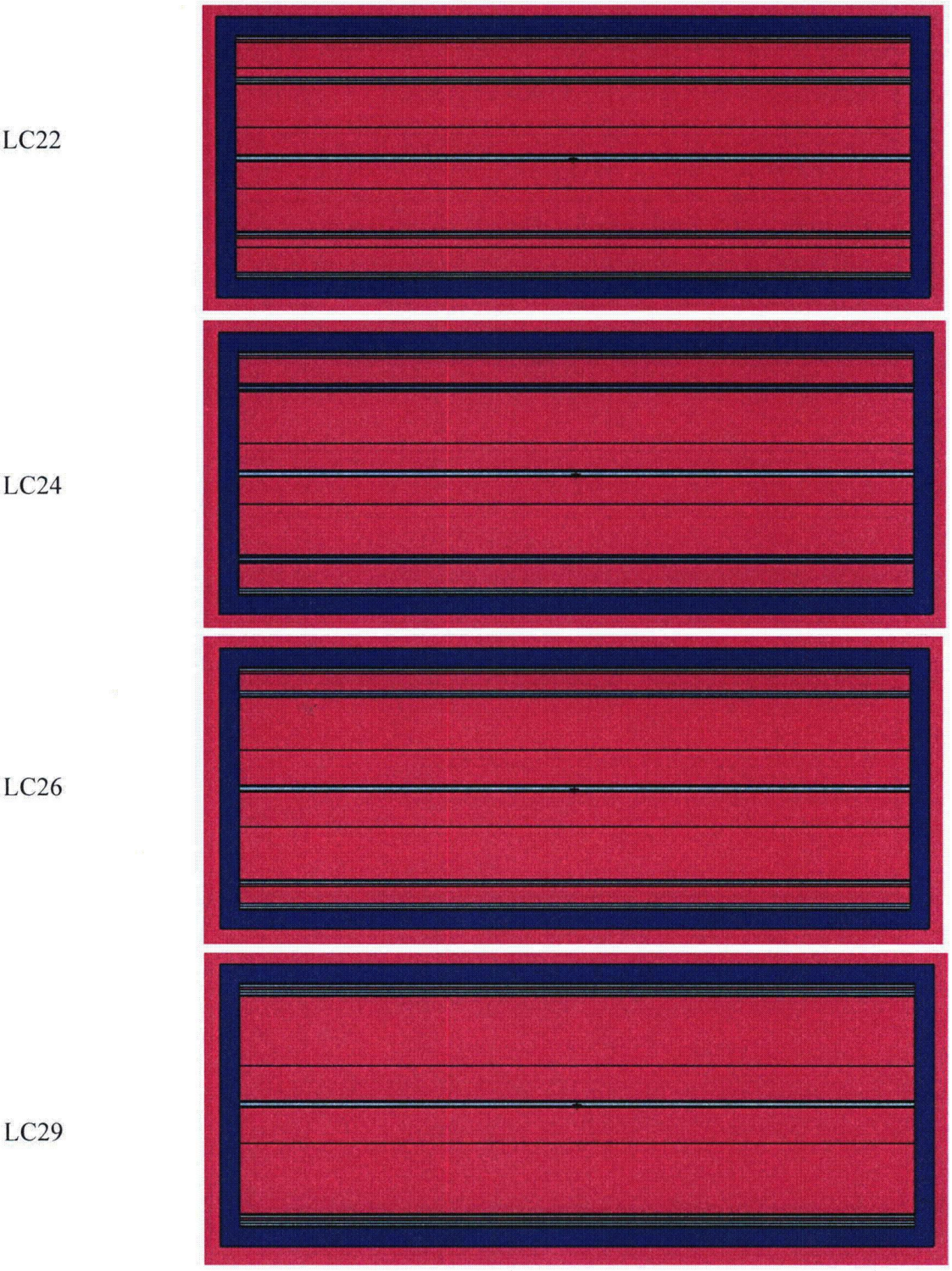


**Figure 6.5-5** – NCT Array Geometry, Plate 5 (LC22, LC24, LC26, LC29)

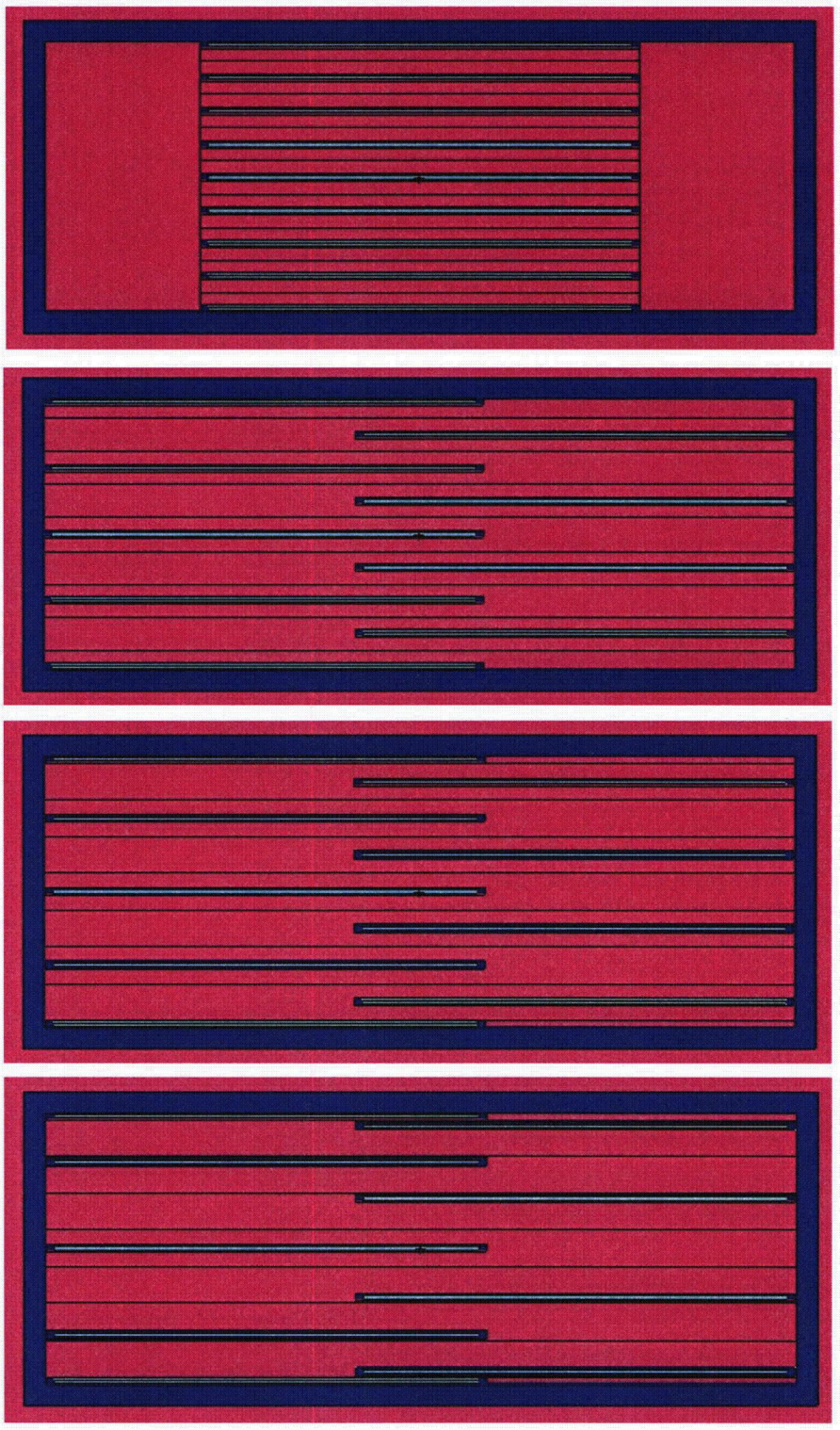


**Figure 6.5-6** – NCT Array Geometry, Plate 8 (LD3, LD4, LD5, LD7)


**Figure 6.5-7** – NCT Array Geometry, Plate 8 (LD8, LD9, LD10, LD11)

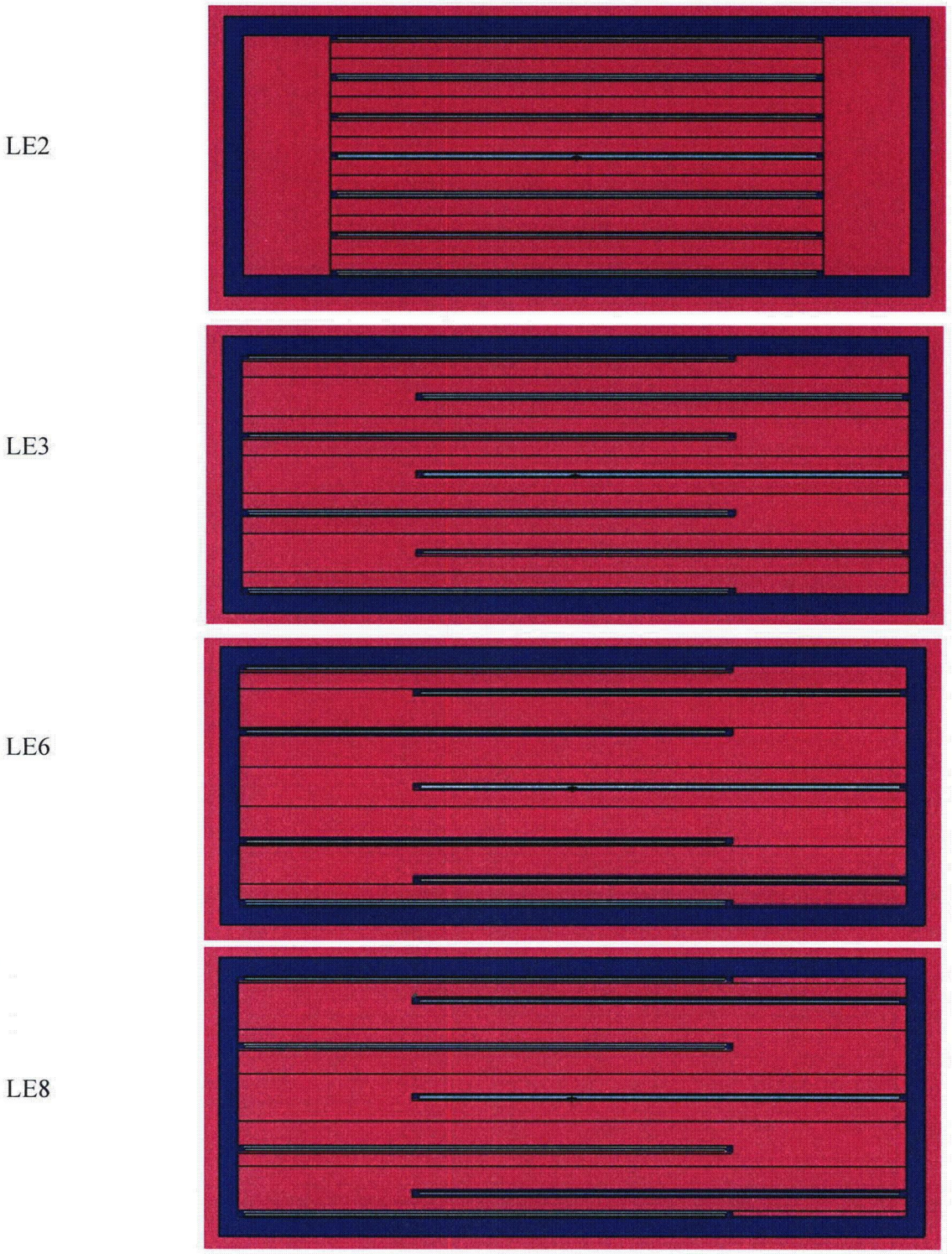


**Figure 6.5-8** – NCT Array Geometry, Plate 15 (LE2, LE3, LE6, LE8)

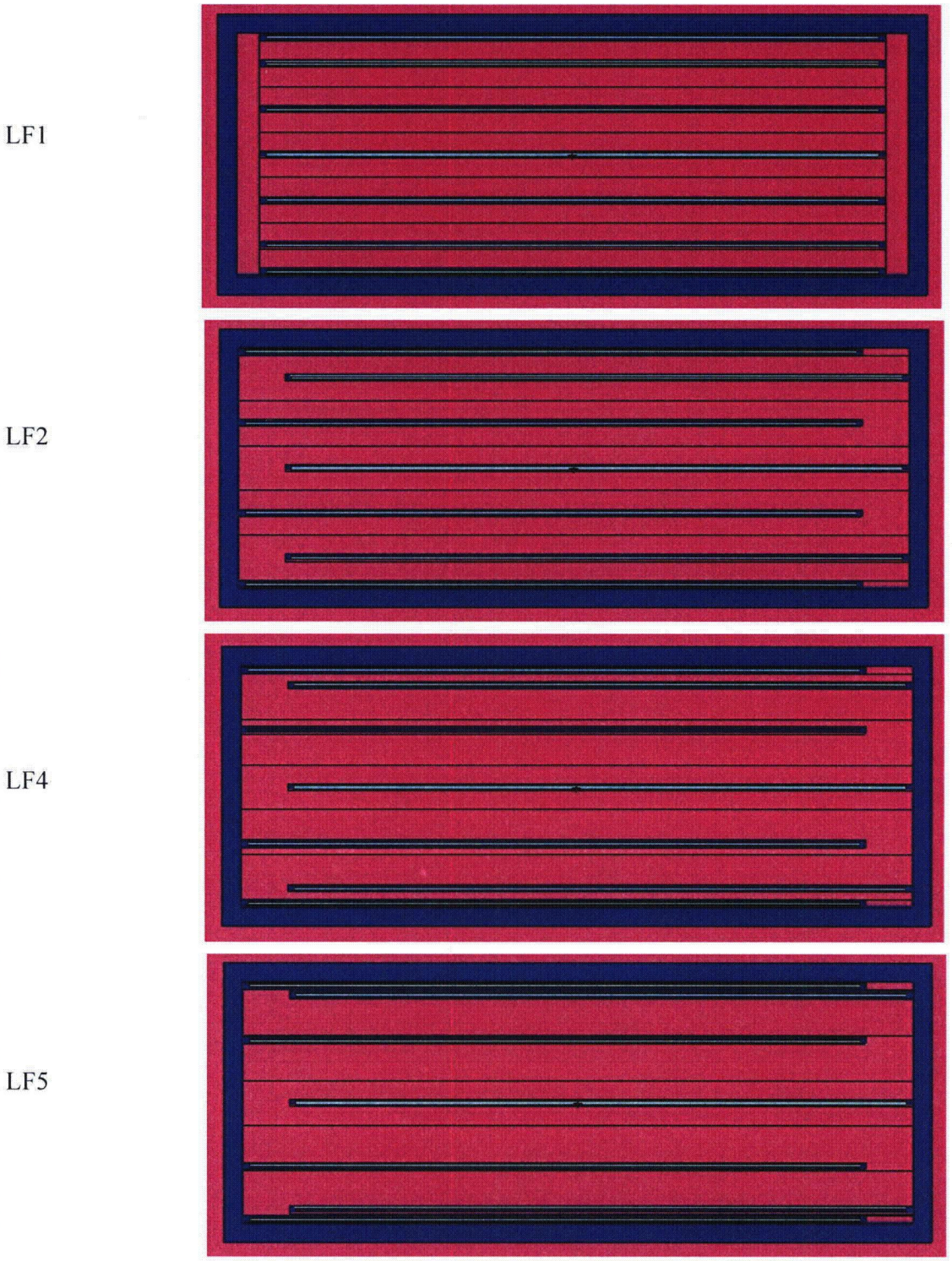


**Figure 6.5-9** – NCT Array Geometry, Plate 3 (LF1, LF2, LF4, LF5)

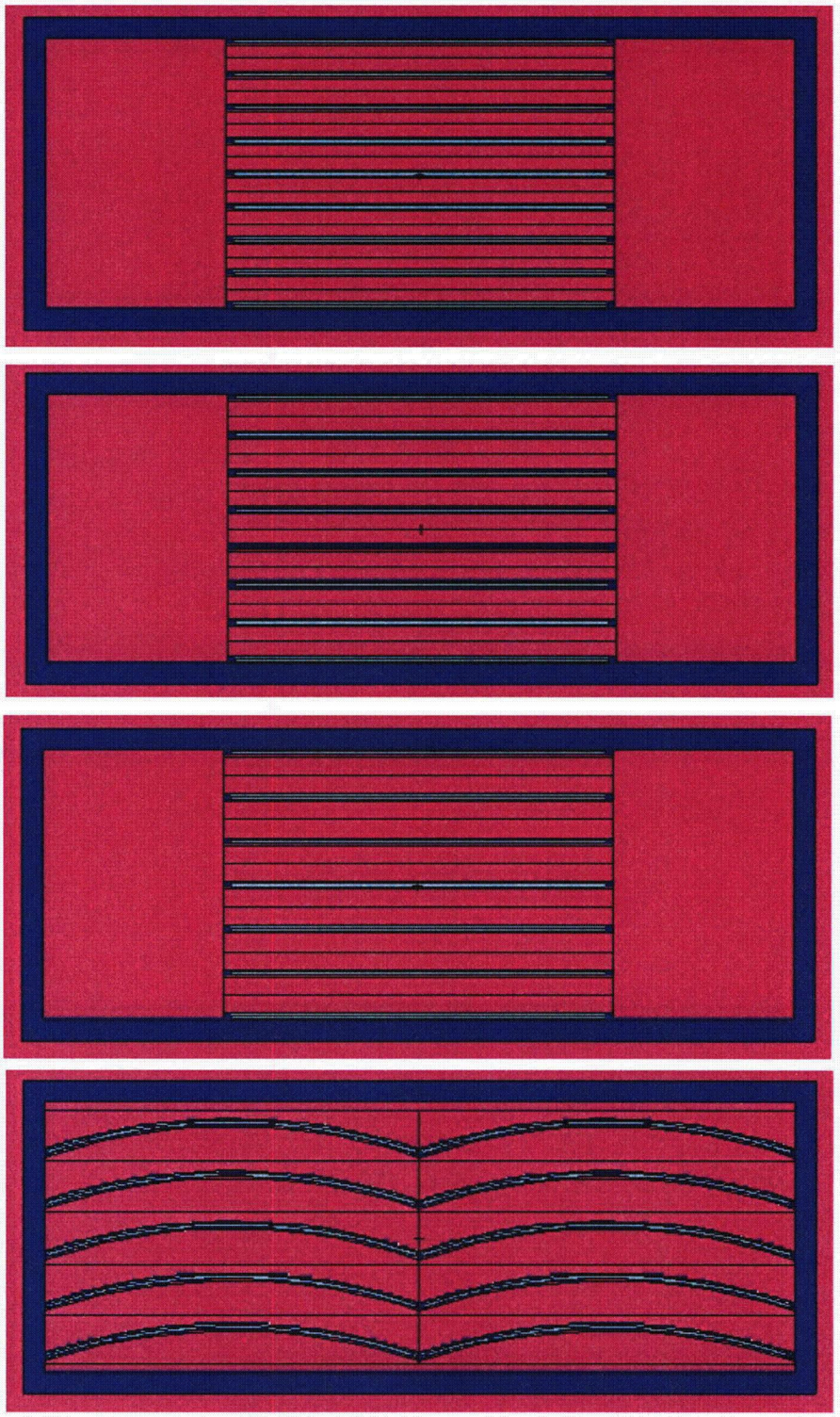


**Figure 6.5-10** – NCT Array Geometry, Miscellaneous (LJ3, LJ4, LJ5, LJ7)

# 6.6 Package Arrays under Hypothetical Accident Conditions

## 6.6.1 HAC Array Configuration

### 6.6.1.1 Fuel Element Payload

The HAC array model is a 5x5x1 array of the HAC single package model. As the FHE is assumed to be damaged, the fuel is free to move laterally within the package. To minimize the distance between the fuel elements, in all HAC array models the fuel elements are rotated and moved toward the center of the array, consistent with the NCT array configuration. The FHE is not modeled, because modeling the FHE in any capacity would push the fuel elements apart and lower the reactivity.

From the HAC single package analysis and NCT array analysis, it is known that reactivity is maximized with full-density water between the fuel plates, because the fuel elements are under moderated. Therefore, all HAC array models have full-density water between the fuel plates. Because the fuel elements may be transported in a plastic bag, it is assumed that the water density between the plates may vary independently from the water density inside the inner tube. This partial moderation effect is similar to the partial moderation effect that could be achieved by modeling the FHE explicitly.

Eight computational series are performed. The variables addressed are (1) water density inside inner tube, (2) water density between tubes, (3) presence of insulation, and (4) presence of FHE neoprene. The geometries of two of these series are shown in Figure 6.6-1, and the geometries of the other configurations are similar. These eight computational series are described in the following paragraphs. The full results are provided in Table 6.6-1.

In Series 1, the water density inside the inner tube is varied from 0 to 1.0 g/cm$^3$, while void is modeled between the tubes. The insulation and FHE neoprene are not modeled. The maximum reactivity occurs for Case F9, with $k_s = 0.72933$. A water density of 0.8 g/cm$^3$ within the inner tube is utilized in the most reactive case.

In Series 2, the most reactive case from Series 1 (Case F9) is modified so that the water density between the tubes is varied between 0 and 1.0 g/cm$^3$, while the water density within the inner tube remains fixed at 0.8 g/cm$^3$. The reactivity reduces as water is added to this region, indicating that the most reactive condition is with void between the tubes.

In Series 3, the water density both inside and between the tubes is assumed to be exactly the same and varied between 0 and 1.0 g/cm$^3$. These cases are less reactive than Case F9 in Series 1.

In Series 4, the moderation conditions of Series 1 are repeated except with the insulation modeled. The maximum reactivity occurs for Case J7 for a water density of 0.6 g/cm$^3$, with a maximum $k_s = 0.73476$. This case is slightly more reactive than Case F9, in which no insulation was modeled.

In Series 5, the most reactive case from Series 4 (Case J7) is modified so that the water density between the insulation and the outer tube is varied between 0 and 1.0 g/cm$^3$, while the water

density within the inner tube remains fixed at 0.6 g/cm$^3$. The reactivity decreases as water is added to this region.

In Series 6, the moderation conditions of Series 1 are repeated except with the FHE neoprene modeled. It was determined in the HAC single package analysis that neoprene will lower the reactivity due to absorption in the chlorine. Therefore, the neoprene is conservatively modeled without chlorine. The maximum reactivity occurs for Case L8, with $k_s = 0.73297$, an increase of 3.6 mk when compared to Case F9. This increase is only slightly above statistical fluctuation, so it may be concluded that the presence of neoprene has at most a small effect on the reactivity. A water density of 0.7 g/cm$^3$ within the inner tube is utilized in the most reactive case. No cases are performed with the neoprene homogeneously mixed into the water because this scenario is already implicitly considered using the variable water density search within the inner tube.

In Series 7, insulation and neoprene are combined in the same model with variable density water inside the inner pipe, as the presence of both insulation and neoprene slightly increased the reactivity when treated separately. The maximum reactivity occurs for Case M8, with $k_s = 0.73599$. This case is slightly more reactive than the cases in which insulation and neoprene are addressed separately.

In Series 8, for completeness, void is modeled in the inner tube, while the water density is allowed to vary between the tubes. Chlorine-free neoprene is utilized to increase moderation in the inner tube, but insulation is ignored to maximize the amount of water between the tubes. The peak reactivity for Series 8 is the lowest of all eight series of calculations.

In conclusion, Case M8 is the most reactive, with $k_s = 0.73599$. This result is below the USL of 0.9209. Case M8 has fully moderated fuel elements, 0.7 g/cm$^3$ water in the inner tube, insulation and chlorine-free neoprene, void between the insulation and outer tube, and fuel elements that have been rotated and moved to the center of the array. Note that this result is lower than the maximum NCT array case because the HAC and NCT array models are quite similar, except the NCT array uses a much larger 9x9x1 configuration.

### 6.6.1.2 Loose Plate Basket Payload

It was established in the criticality analysis for the ATR fuel element that the NCT array calculations bound the HAC array calculations. This result is obtained because a 9x9x1 array is utilized in the NCT calculations, while a smaller 5x5x1 array is utilized in the HAC array calculations. Water moderation is modeled in both the NCT and HAC array calculations within the inner tube, although additional moderation is allowed in the HAC cases between the inner and outer tubes. Therefore, the HAC array calculations are performed only for completeness, as these calculations will not be bounding.

In all the HAC array models, the loose plate basket is filled with full-density water, as it has been established in the NCT array analysis that full-density water moderation within the basket maximizes the reactivity. The internal plate arrangement determined in the NCT array calculations to be the most reactive (Case LC21 for plate type 5) is used in all HAC array models. Also, the loose plate basket is modeled pushed to the center of the array to maximize reactivity, as shown in Figure 6.6-2.

Four series of calculations are performed that utilize different moderations conditions. Results for all cases are provided in Table 6.6-2.

Series 1: In Series 1, the insulation is modeled, and void is modeled between the insulation and the outer tube. The water density between the basket and the inner tube is varied between 0 and 1.0 g/cm$^3$. The maximum reactivity is achieved for Case LK9, with $k_s$ = 0.69792. The water density for this case is 0.8 g/cm$^3$.

Series 2: In Series 2, the most reactive case from Series 1 (Case LK9) is run with variable density water between the insulation and the outer tube. The reactivity decreases when water is added to this region.

Series 3: In Series 3, Series 1 is repeated, except the insulation is replaced with void. The maximum reactivity is close to but bounded by the maximum reactivity from Series 1.

Series 4: In Series 4, the insulation is not modeled, and the same water density is modeled both between the inner and outer tubes, and between the basket and inner tube. The maximum reactivity is significantly less than the maximum reactivity from Series 1.

In conclusion, the maximum reactivity is from Case LK9, with $k_s$ = 0.69792, in which full-density water is modeled within the basket, 0.8 g/cm$^3$ water is modeled between the basket and the inner tube, and void between the insulation and the outer tube. This value is less than the USL of 0.9209.

## 6.6.2 HAC Array Results

Following are the tabulated results for the HAC array cases. The most reactive configuration in each series is listed in boldface.

## Table 6.6-1 – HAC Array Results, Fuel Element

| Case ID | Filename | Water Density Between Tubes ($g/cm^3$) | Water Density Inside Inner Tube ($g/cm^3$) | Water Density Between Plates ($g/cm^3$) | $k_{eff}$ | $\sigma$ | $k_s$ ($k+2\sigma$) |
|---|---|---|---|---|---|---|---|
| **Series 1: Variable water density in inner tube (no insulation, no neoprene)** | | | | | | | |
| F1 | HA_S0P000 | 0 | 0 | 1.0 | 0.57908 | 0.00102 | 0.58112 |
| F2 | HA_S0P010 | 0 | 0.1 | 1.0 | 0.63182 | 0.00112 | 0.63406 |
| F3 | HA_S0P020 | 0 | 0.2 | 1.0 | 0.66922 | 0.00124 | 0.67170 |
| F4 | HA_S0P030 | 0 | 0.3 | 1.0 | 0.69357 | 0.00121 | 0.69599 |
| F5 | HA_S0P040 | 0 | 0.4 | 1.0 | 0.71180 | 0.00116 | 0.71412 |
| F6 | HA_S0P050 | 0 | 0.5 | 1.0 | 0.72106 | 0.00120 | 0.72346 |
| F7 | HA_S0P060 | 0 | 0.6 | 1.0 | 0.72553 | 0.00122 | 0.72797 |
| F8 | HA_S0P070 | 0 | 0.7 | 1.0 | 0.72706 | 0.00112 | 0.72930 |
| **F9** | **HA_S0P080** | **0** | **0.8** | **1.0** | **0.72695** | **0.00119** | **0.72933** |
| F10 | HA_S0P090 | 0 | 0.9 | 1.0 | 0.72116 | 0.00110 | 0.72336 |
| F11 | HA_S0P100 | 0 | 1.0 | 1.0 | 0.71826 | 0.00123 | 0.72072 |
| **Series 2: Case F9 with variable density water between tubes** | | | | | | | |
| **F9** | **HA_S0P080** | **0** | **0.8** | **1.0** | **0.72695** | **0.00119** | **0.72933** |
| G1 | HA_P80S010 | 0.1 | 0.8 | 1.0 | 0.70205 | 0.00112 | 0.70429 |
| G2 | HA_P80S020 | 0.2 | 0.8 | 1.0 | 0.67677 | 0.00125 | 0.67927 |
| G3 | HA_P80S030 | 0.3 | 0.8 | 1.0 | 0.65374 | 0.00113 | 0.65600 |
| G4 | HA_P80S040 | 0.4 | 0.8 | 1.0 | 0.63121 | 0.00114 | 0.63349 |
| G5 | HA_P80S050 | 0.5 | 0.8 | 1.0 | 0.60791 | 0.00104 | 0.60999 |
| G6 | HA_P80S060 | 0.6 | 0.8 | 1.0 | 0.59303 | 0.00111 | 0.59525 |
| G7 | HA_P80S070 | 0.7 | 0.8 | 1.0 | 0.57461 | 0.00109 | 0.57679 |
| G8 | HA_P80S080 | 0.8 | 0.8 | 1.0 | 0.56082 | 0.00110 | 0.56302 |
| G9 | HA_P80S090 | 0.9 | 0.8 | 1.0 | 0.54767 | 0.00102 | 0.54971 |
| G10 | HA_P80S100 | 1.0 | 0.8 | 1.0 | 0.53613 | 0.00108 | 0.53829 |
| **Series 3: Matching water density inside and between tubes** | | | | | | | |
| F1 | HA_S0P000 | 0 | 0 | 1.0 | 0.57908 | 0.00102 | 0.58112 |
| H1 | HA_SP010 | 0.1 | 0.1 | 1.0 | 0.64719 | 0.00115 | 0.64949 |
| **H2** | **HA_SP020** | **0.2** | **0.2** | **1.0** | **0.66047** | **0.00115** | **0.66277** |
| H3 | HA_SP030 | 0.3 | 0.3 | 1.0 | 0.64457 | 0.00112 | 0.64681 |
| H4 | HA_SP040 | 0.4 | 0.4 | 1.0 | 0.62648 | 0.00117 | 0.62882 |
| H5 | HA_SP050 | 0.5 | 0.5 | 1.0 | 0.60286 | 0.00112 | 0.60510 |
| H6 | HA_SP060 | 0.6 | 0.6 | 1.0 | 0.58814 | 0.00116 | 0.59046 |
| H7 | HA_SP070 | 0.7 | 0.7 | 1.0 | 0.57337 | 0.00106 | 0.57549 |
| H8 | HA_SP080 | 0.8 | 0.8 | 1.0 | 0.56082 | 0.00110 | 0.56302 |
| H9 | HA_SP090 | 0.9 | 0.9 | 1.0 | 0.55245 | 0.00122 | 0.55489 |
| H10 | HA_SP100 | 1.0 | 1.0 | 1.0 | 0.54360 | 0.00100 | 0.54560 |

(continued)

Table 6.6-1 – HAC Array Results, Fuel Element (continued)

| Case ID | Filename | Water Density Between Tubes (g/cm$^3$) | Water Density Inside Inner Tube (g/cm$^3$) | Water Density Between Plates (g/cm$^3$) | $k_{eff}$ | σ | $k_s$ (k+2σ) |
|---|---|---|---|---|---|---|---|
| **Series 4: Repeat of Series 1 with insulation** | | | | | | | |
| J1 | HA_DS0P000 | 0 | 0 | 1.0 | 0.58824 | 0.00116 | 0.59056 |
| J2 | HA_DS0P010 | 0 | 0.1 | 1.0 | 0.63716 | 0.00111 | 0.63938 |
| J3 | HA_DS0P020 | 0 | 0.2 | 1.0 | 0.67403 | 0.00118 | 0.67639 |
| J4 | HA_DS0P030 | 0 | 0.3 | 1.0 | 0.69920 | 0.00130 | 0.70180 |
| J5 | HA_DS0P040 | 0 | 0.4 | 1.0 | 0.71665 | 0.00116 | 0.71897 |
| J6 | HA_DS0P050 | 0 | 0.5 | 1.0 | 0.72388 | 0.00117 | 0.72622 |
| **J7** | **HA_DS0P060** | **0** | **0.6** | **1.0** | **0.73230** | **0.00123** | **0.73476** |
| J8 | HA_DS0P070 | 0 | 0.7 | 1.0 | 0.73178 | 0.00112 | 0.73402 |
| J9 | HA_DS0P080 | 0 | 0.8 | 1.0 | 0.72965 | 0.00124 | 0.73213 |
| J10 | HA_DS0P090 | 0 | 0.9 | 1.0 | 0.72638 | 0.00107 | 0.72852 |
| J11 | HA_DS0P100 | 0 | 1.0 | 1.0 | 0.71985 | 0.00113 | 0.72211 |
| **Series 5: Case J7 with variable density water between insulation and outer tube** | | | | | | | |
| **J7** | **HA_DS0P090** | **0** | **0.6** | **1.0** | **0.73230** | **0.00123** | **0.73476** |
| K1 | HA_DP60S010 | 0.1 | 0.6 | 1.0 | 0.72284 | 0.00123 | 0.72530 |
| K2 | HA_DP60S020 | 0.2 | 0.6 | 1.0 | 0.71587 | 0.00120 | 0.71827 |
| K3 | HA_DP60S030 | 0.3 | 0.6 | 1.0 | 0.71029 | 0.00118 | 0.71265 |
| K4 | HA_DP60S040 | 0.4 | 0.6 | 1.0 | 0.70002 | 0.00117 | 0.70236 |
| K5 | HA_DP60S050 | 0.5 | 0.6 | 1.0 | 0.69370 | 0.00122 | 0.69614 |
| K6 | HA_DP60S060 | 0.6 | 0.6 | 1.0 | 0.68266 | 0.00111 | 0.68488 |
| K7 | HA_DP60S070 | 0.7 | 0.6 | 1.0 | 0.67122 | 0.00112 | 0.67346 |
| K8 | HA_DP60S080 | 0.8 | 0.6 | 1.0 | 0.66359 | 0.00115 | 0.66589 |
| K9 | HA_DP60S090 | 0.9 | 0.6 | 1.0 | 0.65393 | 0.00111 | 0.65615 |
| K10 | HA_DP60S100 | 1.0 | 0.6 | 1.0 | 0.64595 | 0.00116 | 0.64827 |
| **Series 6: Repeat of Series 1 with neoprene** | | | | | | | |
| L1 | HA_N2S0P000 | 0 | 0 | 1.0 | 0.60058 | 0.00113 | 0.60284 |
| L2 | HA_N2S0P010 | 0 | 0.1 | 1.0 | 0.64323 | 0.00119 | 0.64561 |
| L3 | HA_N2S0P020 | 0 | 0.2 | 1.0 | 0.68153 | 0.00118 | 0.68389 |
| L4 | HA_N2S0P030 | 0 | 0.3 | 1.0 | 0.70640 | 0.00120 | 0.70880 |
| L5 | HA_N2S0P040 | 0 | 0.4 | 1.0 | 0.71669 | 0.00124 | 0.71917 |
| L6 | HA_N2S0P050 | 0 | 0.5 | 1.0 | 0.72733 | 0.00117 | 0.72967 |
| L7 | HA_N2S0P060 | 0 | 0.6 | 1.0 | 0.72872 | 0.00122 | 0.73116 |
| **L8** | **HA_N2S0P070** | **0** | **0.7** | **1.0** | **0.73069** | **0.00114** | **0.73297** |
| L9 | HA_N2S0P080 | 0 | 0.8 | 1.0 | 0.73081 | 0.00107 | 0.73295 |
| L10 | HA_N2S0P090 | 0 | 0.9 | 1.0 | 0.72692 | 0.00129 | 0.72950 |
| L11 | HA_N2S0P100 | 0 | 1.0 | 1.0 | 0.72371 | 0.00122 | 0.72615 |

(continued)

## Table 6.6-1 – HAC Array Results, Fuel Element (concluded)

| Case ID | Filename | Water Density Between Tubes (g/cm$^3$) | Water Density Inside Inner Tube (g/cm$^3$) | Water Density Between Plates (g/cm$^3$) | $k_{eff}$ | $\sigma$ | $k_s$ (k+2$\sigma$) |
|---|---|---|---|---|---|---|---|
| **Series 7: Repeat of Series 1 with insulation and neoprene** | | | | | | | |
| M1 | HA_DNS0P000 | 0 | 0 | 1.0 | 0.60377 | 0.00107 | 0.60591 |
| M2 | HA_DNS0P010 | 0 | 0.1 | 1.0 | 0.64940 | 0.00107 | 0.65154 |
| M3 | HA_DNS0P020 | 0 | 0.2 | 1.0 | 0.68596 | 0.00110 | 0.68816 |
| M4 | HA_DNS0P030 | 0 | 0.3 | 1.0 | 0.70846 | 0.00115 | 0.71076 |
| M5 | HA_DNS0P040 | 0 | 0.4 | 1.0 | 0.72168 | 0.00122 | 0.72412 |
| M6 | HA_DNS0P050 | 0 | 0.5 | 1.0 | 0.73000 | 0.00124 | 0.73248 |
| M7 | HA_DNS0P060 | 0 | 0.6 | 1.0 | 0.73182 | 0.00122 | 0.73426 |
| **M8** | **HA_DNS0P070** | **0** | **0.7** | **1.0** | **0.73365** | **0.00117** | **0.73599** |
| M9 | HA_DNS0P080 | 0 | 0.8 | 1.0 | 0.73187 | 0.00127 | 0.73441 |
| M10 | HA_DNS0P090 | 0 | 0.9 | 1.0 | 0.73006 | 0.00112 | 0.73230 |
| M11 | HA_DNS0P100 | 0 | 1.0 | 1.0 | 0.72332 | 0.00122 | 0.72576 |
| **Series 8: Case L1 with variable density water between tubes** | | | | | | | |
| L1 | HA_N2S0P000 | 0 | 0 | 1.0 | 0.60058 | 0.00113 | 0.60284 |
| **N1** | **HA_N2P0S010** | **0.1** | **0** | **1.0** | **0.63054** | **0.00107** | **0.63268** |
| N2 | HA_N2P0S020 | 0.2 | 0 | 1.0 | 0.62961 | 0.00118 | 0.63197 |
| N3 | HA_N2P0S030 | 0.3 | 0 | 1.0 | 0.61939 | 0.00113 | 0.62165 |
| N4 | HA_N2P0S040 | 0.4 | 0 | 1.0 | 0.60776 | 0.00108 | 0.60992 |
| N5 | HA_N2P0S050 | 0.5 | 0 | 1.0 | 0.58874 | 0.00108 | 0.59090 |
| N6 | HA_N2P0S060 | 0.6 | 0 | 1.0 | 0.57308 | 0.00109 | 0.57526 |
| N7 | HA_N2P0S070 | 0.7 | 0 | 1.0 | 0.55837 | 0.00107 | 0.56051 |
| N8 | HA_N2P0S080 | 0.8 | 0 | 1.0 | 0.54139 | 0.00101 | 0.54341 |
| N9 | HA_N2P0S090 | 0.9 | 0 | 1.0 | 0.52714 | 0.00106 | 0.52926 |
| N10 | HA_N2P0S100 | 1.0 | 0 | 1.0 | 0.51600 | 0.00114 | 0.51828 |

## Table 6.6-2 – HAC Array Results, Plate 5

| Case ID | Filename | Water Density Between Tubes ($g/cm^3$) | Water Density Inside Inner Tube ($g/cm^3$) | Water Density Between Plates ($g/cm^3$) | $k_{eff}$ | $\sigma$ | $k_s$ ($k+2\sigma$) |
|---|---|---|---|---|---|---|---|
| **Series 1: Variable water density in inner tube, with insulation** | | | | | | | |
| LK1 | HA_N5DS0P000 | 0 | 0 | 1.0 | 0.53784 | 0.00096 | 0.53976 |
| LK2 | HA_N5DS0P010 | 0 | 0.1 | 1.0 | 0.58878 | 0.00098 | 0.59074 |
| LK3 | HA_N5DS0P020 | 0 | 0.2 | 1.0 | 0.62946 | 0.00101 | 0.63148 |
| LK4 | HA_N5DS0P030 | 0 | 0.3 | 1.0 | 0.65858 | 0.00102 | 0.66062 |
| LK5 | HA_N5DS0P040 | 0 | 0.4 | 1.0 | 0.67685 | 0.00100 | 0.67885 |
| LK6 | HA_N5DS0P050 | 0 | 0.5 | 1.0 | 0.68901 | 0.00102 | 0.69105 |
| LK7 | HA_N5DS0P060 | 0 | 0.6 | 1.0 | 0.69483 | 0.00107 | 0.69697 |
| LK8 | HA_N5DS0P070 | 0 | 0.7 | 1.0 | 0.69266 | 0.00120 | 0.69506 |
| **LK9** | **HA_N5DS0P080** | **0** | **0.8** | **1.0** | **0.69576** | **0.00108** | **0.69792** |
| LK10 | HA_N5DS0P090 | 0 | 0.9 | 1.0 | 0.69250 | 0.00105 | 0.69460 |
| LK11 | HA_N5DS0P100 | 0 | 1.0 | 1.0 | 0.68585 | 0.00104 | 0.68793 |
| **Series 2: Case LK9 with variable density water between tubes.** | | | | | | | |
| **LK9** | **HA_N5DS0P080** | **0** | **0.8** | **1.0** | **0.69576** | **0.00108** | **0.69792** |
| LM1 | HA_N5DP80S010 | 0.1 | 0.8 | 1.0 | 0.68989 | 0.00106 | 0.69201 |
| LM2 | HA_N5DP80S020 | 0.2 | 0.8 | 1.0 | 0.67989 | 0.00107 | 0.68203 |
| LM3 | HA_N5DP80S030 | 0.3 | 0.8 | 1.0 | 0.67352 | 0.00098 | 0.67548 |
| LM4 | HA_N5DP80S040 | 0.4 | 0.8 | 1.0 | 0.66658 | 0.00105 | 0.66868 |
| LM5 | HA_N5DP80S050 | 0.5 | 0.8 | 1.0 | 0.65700 | 0.00105 | 0.65910 |
| LM6 | HA_N5DP80S060 | 0.6 | 0.8 | 1.0 | 0.64893 | 0.00118 | 0.65129 |
| LM7 | HA_N5DP80S070 | 0.7 | 0.8 | 1.0 | 0.64141 | 0.00106 | 0.64353 |
| LM8 | HA_N5DP80S080 | 0.8 | 0.8 | 1.0 | 0.63415 | 0.00099 | 0.63613 |
| LM9 | HA_N5DP80S090 | 0.9 | 0.8 | 1.0 | 0.62748 | 0.00103 | 0.62954 |
| LM10 | HA_N5DP80S100 | 1.0 | 0.8 | 1.0 | 0.62100 | 0.00094 | 0.62288 |
| **Series 3: Repeat of Series 1, no insulation** | | | | | | | |
| LN1 | HA_N5S0P000 | 0 | 0 | 1.0 | 0.53334 | 0.00092 | 0.53518 |
| LN2 | HA_N5S0P010 | 0 | 0.1 | 1.0 | 0.58456 | 0.00091 | 0.58638 |
| LN3 | HA_N5S0P020 | 0 | 0.2 | 1.0 | 0.62421 | 0.00108 | 0.62637 |
| LN4 | HA_N5S0P030 | 0 | 0.3 | 1.0 | 0.65402 | 0.00109 | 0.65620 |
| LN5 | HA_N5S0P040 | 0 | 0.4 | 1.0 | 0.67129 | 0.00108 | 0.67345 |
| LN6 | HA_N5S0P050 | 0 | 0.5 | 1.0 | 0.68550 | 0.00108 | 0.68766 |
| LN7 | HA_N5S0P060 | 0 | 0.6 | 1.0 | 0.69042 | 0.00106 | 0.69254 |
| **LN8** | **HA_N5S0P070** | **0** | **0.7** | **1.0** | **0.69145** | **0.00104** | **0.69353** |
| LN9 | HA_N5S0P080 | 0 | 0.8 | 1.0 | 0.69071 | 0.00101 | 0.69273 |
| LN10 | HA_N5S0P090 | 0 | 0.9 | 1.0 | 0.68925 | 0.00102 | 0.69129 |
| LN11 | HA_N5S0P100 | 0 | 1.0 | 1.0 | 0.68493 | 0.00116 | 0.68725 |

(continued)

Table 6.6-2 – HAC Array Results, Plate 5 (concluded)

| Case ID | Filename | Water Density Between Packages ($g/cm^3$) | Water Density Inside Pipe ($g/cm^3$) | Water Density Between Plates ($g/cm^3$) | $k_{eff}$ | $\sigma$ | $k_s$ ($k+2\sigma$) |
|---|---|---|---|---|---|---|---|
| **Series 4: No insulation, matching water densities inside and between tubes** | | | | | | | |
| LN1 | HA_N5S0P000 | 0 | 0 | 1.0 | 0.53334 | 0.00092 | 0.53518 |
| LO1 | HA_N5SP010 | 0.1 | 0.1 | 1.0 | 0.59685 | 0.00097 | 0.59879 |
| **LO2** | **HA_N5SP020** | **0.2** | **0.2** | **1.0** | **0.61533** | **0.00096** | **0.61725** |
| LO3 | HA_N5SP030 | 0.3 | 0.3 | 1.0 | 0.60844 | 0.00108 | 0.61060 |
| LO4 | HA_N5SP040 | 0.4 | 0.4 | 1.0 | 0.59462 | 0.00099 | 0.59660 |
| LO5 | HA_N5SP050 | 0.5 | 0.5 | 1.0 | 0.57802 | 0.00107 | 0.58016 |
| LO6 | HA_N5SP060 | 0.6 | 0.6 | 1.0 | 0.56514 | 0.00107 | 0.56728 |
| LO7 | HA_N5SP070 | 0.7 | 0.7 | 1.0 | 0.55116 | 0.00106 | 0.55328 |
| LO8 | HA_N5SP080 | 0.8 | 0.8 | 1.0 | 0.54262 | 0.00093 | 0.54448 |
| LO9 | HA_N5SP090 | 0.9 | 0.9 | 1.0 | 0.53400 | 0.00102 | 0.53604 |
| LO10 | HA_N5SP100 | 1.0 | 1.0 | 1.0 | 0.52785 | 0.00106 | 0.52997 |

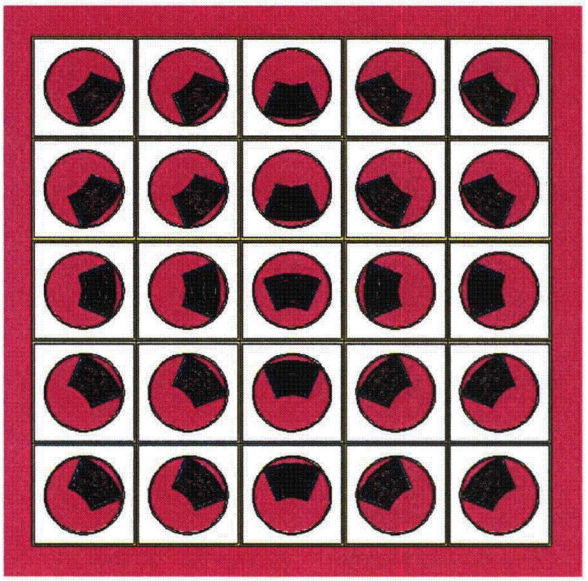

Series 1: Array with variable density water in inner tube, and void between tubes. No insulation modeled.

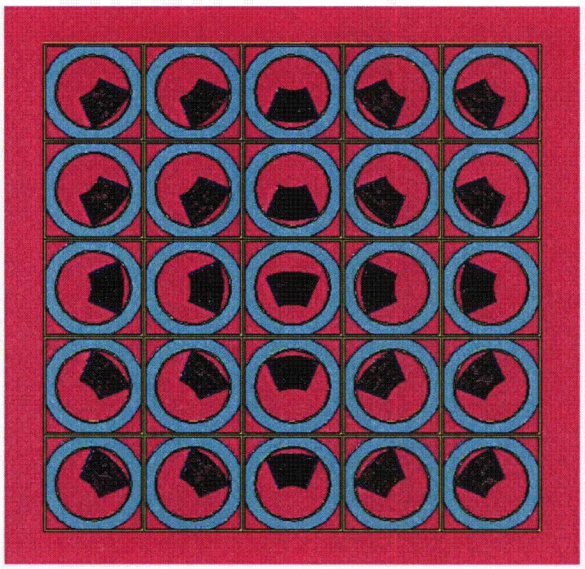

Series 5: Array with 0.6 g/cm$^3$ water in inner tube and variable density water between tubes. Insulation is modeled.

**Figure 6.6-1** – HAC Array Geometry Examples, Fuel Element

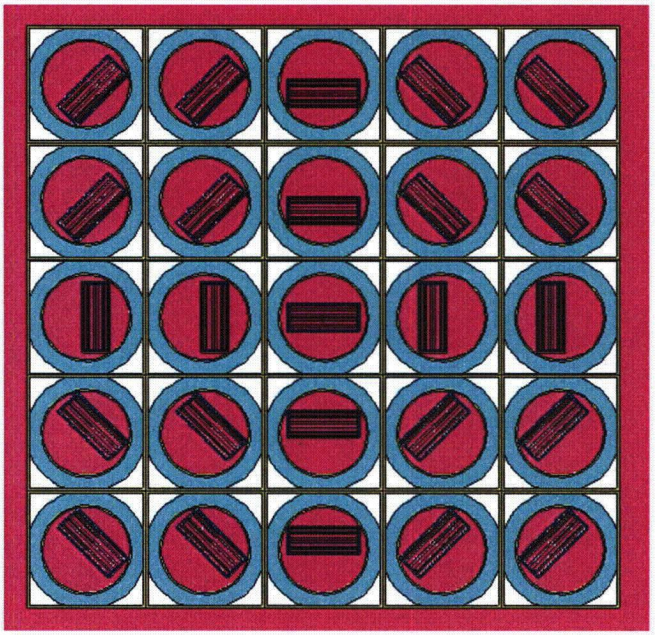

Series 1: Array with variable density water in inner tube, and void between tubes. Insulation is modeled.

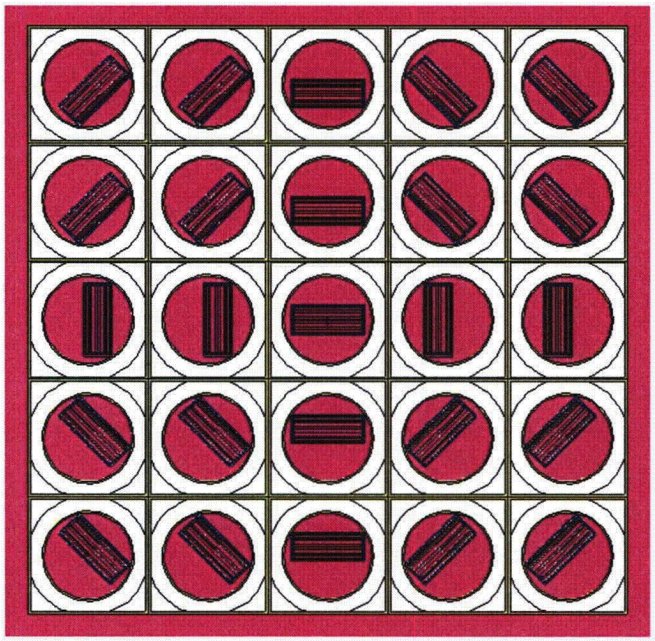

Series 3: Array with variable density water in inner tube, and void between tubes. No insulation modeled.

**Figure 6.6-2** – HAC Array Geometry Examples, Loose Plate Basket

## 6.7 Fissile Material Packages for Air Transport

This section does not apply for the ATR FFSC, because air transport is not claimed.

# 6.8 Benchmark Evaluations

The MCNP, Version 5, Monte Carlo computer code[8] with point-wise ENDF/B-V, -VI, and -VII cross sections has been used extensively in criticality evaluations. The uranium isotopes utilize preliminary ENDF/B-VII cross section data that are considered by Los Alamos National Laboratory to be more accurate than ENDF/B-VI cross sections. ENDF/B-V cross sections are utilized for chromium, nickel, and iron because natural composition ENDF/B-VI cross sections are not available for these elements. The remaining isotopes utilize ENDF/B-VI cross sections. This section justifies the validity of this computation tool and data library combination for application to the ATR FFSC criticality analysis and a bias factor is obtained from these calculations of the critical experiments.

The MCNP code uses room temperature continuous-energy (point-wise) cross sections that are thoroughly documented in Appendix G of the manual. These cross sections are defined with a high-energy resolution that describes each resolved cross section resonance for the isotope. All of the cross-sections used for these analyses were generated from the U.S. Evaluated Nuclear Data Files (ENDF/B).

The validation of the point-wise cross sections is conducted using 35 experimental criticality benchmarks applicable to the ATR FFSC. The statistical analysis of the benchmark experiments results in a USL of 0.9209.

## 6.8.1 Applicability of Benchmark Experiments

The experimental benchmarks are summarized in the OECD Nuclear Energy Agency's *International Handbook of Evaluated Criticality Safety Benchmark Experiments*[9]. Each experiment is discussed in detail in the *Handbook*. It includes estimates of the uncertainty in the measurements, detailed information regarding dimensions and material compositions, comparisons between the multiplication factor calculated by various computer codes, and a list of input files that were used in their calculations.

The critical experiment benchmarks are selected based upon their similarity to the ATR FFSC and contents. The important selection parameters are high-enriched uranium plate-type fuel with a thermal spectrum. Thirty-five (35) benchmarks that meet these criteria are selected from the *Handbook*. The titles for all utilized experiments are listed in Table 6.8-1. Note that the benchmark from HEU-MET-THERM-022 is for the Advanced Test Reactor itself, so the fuel configuration in this benchmark is essentially the same as the fuel modeled in the packaging analysis.

Ideally, benchmarks would be limited to those with a fuel matrix of $UAl_x$ and aluminum, aluminum cladding, and no absorbers, consistent with the ATR criticality models. Experiment set HEU-MET-THERM-006 consists of 23 benchmark experiments. The first 16 experiments are directly applicable, although experiments 17 and 18 utilize thin cadmium sheets, and

[8] MCNP5, "*MCNP – A General Monte Carlo N-Particle Transport Code, Version 5; Volume II: User's Guide*," LA-CP-03-0245, Los Alamos National Laboratory, April, 2003.

[9] OECD Nuclear Energy Agency, *International Handbook of Evaluated Criticality Safety Benchmark Experiments*, NEA/NSC/DOC(95)03, September, 2006.

experiments 19 through 23 utilize uranium in solution in addition to the fuel plates. Experiment set HEU-COMP-THERM-022 consists of 11 benchmark experiments that utilize $UO_2$ powder sintered with stainless steel, and stainless steel cladding. Experiments 1 through 5 do not utilize control rods, while experiments 6 through 11 utilize boron control rods. HEU-MET-THERM-022 is a detailed model of the ATR core using explicit ATR fuel elements very similar to the ATR fuel element model utilized in the criticality analysis. However, this full-core model necessarily contains absorber materials. Despite the presence of absorbers, because this benchmark utilizes ATR fuel, it is considered directly applicable to the ATR criticality analysis.

Therefore, of these 35 benchmarks, 17 benchmarks are directly applicable, while 18 benchmarks are applicable to a lesser degree. To compensate for the benchmarks that are not directly applicable, trending will be performed both on all 35 benchmark experiments and on the subset of 17 directly applicable benchmark experiments. The USL selected is the minimum of both experimental sets.

Benchmark input files are either obtained from the *Handbook* or directly from Idaho National Laboratory (INL). The only changes made to the input files involve changing to a consistent set of cross section libraries, as needed. Review of the input files indicates that standard MCNP modeling techniques are employed. All but one of the input files consists of simple flat plates in various arrangements. The only benchmark that deviates from simple flat plates is the Advanced Test Reactor full-core model, which is directly applicable to the current analysis. These benchmark input files were developed by INL and have been used extensively for their internal criticality evaluations and are considered to be acceptable. Because the geometry and materials are modeled explicitly, any analyst properly modeling the experimental configuration in MCNP5 would obtain the same result within statistical fluctuation.

## 6.8.2 Bias Determination

The USL is calculated by application of the USLSTATS computer program[10]. USLSTATS receives as input the $k_{eff}$ as calculated by MCNP, the total 1-$\sigma$ uncertainty (combined benchmark and MCNP uncertainties), and a trending parameter. Five trending parameters have been selected: (1) Energy of the Average neutron Lethargy causing Fission (EALF), (2) U-235 number density, (3) channel width, (4) ratio of the number of hydrogen atoms in a unit cell to the number of U-235 atoms in a unit cell (H/U-235), and (5) plate pitch.

The uncertainty value, $\sigma_{total}$, assigned to each case is a combination of the benchmark uncertainty for each experiment, $\sigma_{bench}$, and the Monte Carlo uncertainty associated with the particular computational evaluation of the case, $\sigma_{MCNP}$, or:

$$\sigma_{total} = (\sigma_{bench}^2 + \sigma_{MCNP}^2)^{1/2}$$

These values are input into the USLSTATS program in addition to the following parameters, which are the values recommended by the USLSTATS user's manual:

[10] USLSTATS, "*USLSTATS: A Utility To Calculate Upper Subcritical Limits For Criticality Safety Applications,*" Version 1.4.2, Oak Ridge National Laboratory, April 23, 2003.

- P, proportion of population falling above lower tolerance level = 0.995 (note that this parameter is required input but is not utilized in the calculation of USL Method 1)
- 1-$\gamma$, confidence on fit = 0.95
- $\alpha$, confidence on proportion P = 0.95 (note that this parameter is required input but is not utilized in the calculation of USL Method 1)
- $\Delta k_m$, administrative margin used to ensure subcriticality = 0.05.

These data are followed by triplets of trending parameter value, computed $k_{eff}$, and uncertainty for each case. A confidence band analysis is performed on the data for each trending parameter using USL Method 1. The USL generated for each of the trending parameters utilized is provided in Table 6.8-2. All benchmark data used as input to USLSTATS are reported in Table 6.8-3.

In the following sections, the minimum USL computed for each parameter is identified, and the range of applicability is compared to the fuel element and loose plate models.

### 6.8.2.1 Energy of the Average neutron Lethargy causing Fission (EALF)

The EALF is used as the first trending parameter for the benchmark cases. The EALF comparison provides a means to observe neutron spectral dependencies or trends. The data for all 35 experiments are plotted in Figure 6.8-1. Over the range of applicability, the minimum USL is 0.9254 for the full benchmark set, and 0.9212 for the subset of directly applicable benchmarks.

**Range of Applicability, Fuel element models:** All of the single package models and most of the NCT and HAC array models fall within the range of the applicability. The EALF of the most reactive fuel element model (Case D4) has an EALF of 1.44E-07 MeV, which is within the range of applicability. Models with significantly more void spaces or low water densities sometimes exceed the range of applicability (maximum EALF = 2.73E-07 MeV for Case E1), although these cases are not the most reactive. Therefore, the EALF of the most reactive models is acceptably within the range of applicability of the benchmarks.

**Range of Applicability, Loose plate models:** The loose plate analysis is highly moderated, and the EALF of the models fall within the range of applicability of the benchmark experiments with few exceptions. The only cases that fall outside the range of applicability are the very-small pitch cases for Plate 5, because these cases are insufficiently moderated and also thus have low reactivity. Therefore, the EALF is acceptably within the range of applicability of the benchmarks.

### 6.8.2.2 U-235 Number Density

The U-235 number density is used as the second trending parameter for the benchmark cases. The data for all 35 experiments are plotted in Figure 6.8-2. Over the range of applicability, the minimum USL is 0.9240 for the full benchmark set, and 0.9209 for the subset of directly applicable benchmarks.

**Range of Applicability, Fuel element models:** For the optimized fuel element model, the U-235 number densities for plates 1 through 4 and 16 through 19 fall within the range of

applicability, while the number densities for plates 5 through 15 exceed the range of applicability (maximum value = 4.22E-03 atom/b-cm). The maximum range of applicability is 3.92E-03 atom/b-cm, so range is exceeded only slightly. If the minimum USL is extrapolated to this larger number density, the minimum USL of 0.9209 does not change. Also, the average U-235 number density for the fuel element is 3.73E-03 atom/b-cm, which is within the allowable range. Therefore, application of this USL to the fuel element criticality models is considered acceptable.

**Range of Applicability, Loose plate models:** Of the four plate types modeled, the U-235 number densities for plate type 3 fall within the range of applicability, while the number densities for plate types 5, 8, and 15 exceed the range of applicability (maximum value = 4.29E-03 atom/b-cm). The maximum range of applicability is 3.92E-03 atom/b-cm, so the range is exceeded only slightly. If the minimum USL is extrapolated to this larger number density, the minimum USL of 0.9209 does not change. Therefore, application of this USL to the loose plate basket criticality models is considered acceptable.

### 6.8.2.3 Channel Width

The channel width is used as the third trending parameter for the benchmark cases. The data for all 35 experiments are plotted in Figure 6.8-3. Over the range of applicability, the minimum USL is 0.9225 for the full benchmark set, and 0.9209 for the subset of directly applicable benchmarks.

**Range of Applicability, Fuel element models:** The channel width is fixed at 0.085-in for the fuel element models, which exceeds the maximum channel width of 0.078-in of the benchmark experiments. However, this parameter is only slightly larger than the maximum benchmark experiment channel width, and was maximized in order to maximize model reactivity. Extrapolation of the USL to the channel width of 0.085-in yields the same minimum USL of 0.9209. Therefore, application of this USL to the fuel element criticality models is considered acceptable.

**Range of Applicability, Loose plate models:** The maximum channel width of the benchmark models is 0.078-in, while the channel width of the most reactive loose plate model is 0.439-in. Clearly, the loose plate models are well outside the bounds of the benchmark models and extrapolation of the USL would not be appropriate over such a wide range. However, the channel width is directly related to system moderation, and the acceptability of the EALF indicator demonstrates that MCNP is performing acceptably for thermal conditions.

### 6.8.2.4 H/U-235 Atom Ratio

The H/U-235 atom ratio is used as the fourth trending parameter for the benchmark cases. The H/U-235 atom ratio is defined here as the ratio of hydrogen atoms to U-235 atoms in a unit cell. This parameter is computed by the following equation:

NH*C/(NU235*M)

where,

NH is the hydrogen number density

C is the channel width

NU235 is the U-235 number density

M is the fuel meat width

The data for all 35 experiments are plotted in Figure 6.8-4. Over the range of applicability, the minimum USL is 0.9257 for the full benchmark set, and 0.9209 for the subset of directly applicable benchmarks.

**Range of Applicability, Fuel element models:** Using the maximum fuel element plate U-235 number density for the optimized fuel element model, the H/U-235 value may be computed as:

6.687E-02*0.085/(4.224E-03*0.02) = 67.3

Therefore, H/U-235 of the models is acceptably within the range of applicability of the benchmarks.

**Range of Applicability, Loose plate models:** The H/U-235 atom ratio for the most reactive model may be computed as:

6.687E-02*0.439/(4.2887E-03*0.02) = 342

The maximum H/U-235 atom ratio of the benchmark models is 116.5. Clearly, the loose plate models are well outside the bounds of the benchmark models and extrapolation of the USL would not be appropriate over such a wide range. However, the H/U-235 atom ratio is directly related to system moderation, and the acceptability of the EALF indicator demonstrates that MCNP is performing acceptably for thermal conditions.

### 6.8.2.5 Pitch

The fuel plate pitch is used as the fifth trending parameter for the benchmark cases. The data for all 35 experiments is plotted in Figure 6.8-5. Over the range of applicability, the minimum USL is 0.9225 for the full benchmark set, and 0.9209 for the subset of directly applicable benchmarks.

**Range of Applicability, Fuel element models:** The fuel plate pitch is fixed at 0.128-in for all fuel element models (excluding the pitch for plates 1 and 19, which is slightly bigger because these plates are thicker). This pitch falls within the range of the benchmark experiments.

**Range of Applicability, Loose plate models:** The maximum pitch of the benchmark models is 0.128-in, while the pitch of the most reactive loose plate model is 0.487-in (1.236 cm). Clearly, the loose plate models are well outside the bounds of the benchmark models and extrapolation of the USL would not be appropriate over such a wide range. However, the pitch is directly related to system moderation, and the acceptability of the EALF indicator demonstrates that MCNP is performing acceptably for thermal conditions.

### 6.8.2.6 Recommended USL

For the full benchmark set, the minimum USL is 0.9225, while for the subset of directly applicable benchmarks, the minimum USL is 0.9209. Therefore, the USL is trending lower for the subset of directly applicable benchmarks. Note, however, that the average $k_{eff} = 0.992$ for both the full benchmark set and directly applicable subset. The USL could likely be improved

by development of additional benchmark models, but given the large margins to the most reactive case, the lower value (0.9209) is conservatively selected as the USL for this analysis.

**Table 6.8-1** – Benchmark Experiments Utilized

| Series | Title |
|---|---|
| HEU-COMP-THERM-022 | SPERT III Stainless-Steel-Clad Plate-Type Fuel in Water |
| HEU-MET-THERM-006 | SPERT-D Aluminum-Clad Plate-Type Fuel in Water, Dilute Uranyl Nitrate, or Borated Uranyl Nitrate |
| HEU-MET-THERM-022 | Advanced Test Reactor: Serpentine Arrangement of Highly Enriched Water-Moderated Uranium-Aluminide Fuel Plates Reflected by Beryllium |

**Table 6.8-2** – USL Results

| Trending Parameter (X) | Minimum USL Over Range of Applicability | Range of Applicability |
|---|---|---|
| **35 Experiment Set** | | |
| EALF (MeV) | 0.9254 | 5.22210E-08 <= X <= 1.58510E-07 |
| U-235 Number Density (atom/b-cm) | 0.9240 | 1.84900E-03 <= X <= 3.92600E-03 |
| Channel width (in) | 0.9225 | 6.45700E-02 <= X <= 7.80000E-02 |
| H/U-235 | 0.9257 | 65.100 <= X <= 116.50 |
| Pitch (in) | 0.9225 | 0.12457 <= X <= 0.12800 |
| **17 Experiment Set** | | |
| EALF (MeV) | 0.9212 | 5.22210E-08 <= X <= 1.58510E-07 |
| U-235 Number Density (atom/b-cm) | 0.9209 | 1.84900E-03 <= X <= 3.92600E-03 |
| Channel width (in) | 0.9209 | 6.45700E-02 <= X <= 7.80000E-02 |
| H/U-235 | 0.9209 | 66.0 <= X <= 116.50 |
| Pitch (in) | 0.9209 | 0.12457 <= X <= 0.12800 |

## Table 6.8-3 – Benchmark Experiment Data

| No | Case | k | $\sigma_{mcnp}$ | $\sigma_{bench}$ | $\sigma_{total}$ | EALF (MeV) | U-235 (atom/b-cm) | Chanel Width (in) | H/U-235 | Pitch (in) |
|---|---|---|---|---|---|---|---|---|---|---|
| 1 | hct022_c01 | 0.98895 | 0.00060 | 0.0081 | 0.0081 | 9.528E-08 | 3.3155E-03 | 0.06457 | 65.1 | 0.12457 |
| 2 | hct022_c02 | 0.98980 | 0.00061 | 0.0081 | 0.0081 | 9.665E-08 | 3.3155E-03 | 0.06457 | 65.1 | 0.12457 |
| 3 | hct022_c03 | 0.98985 | 0.00063 | 0.0081 | 0.0081 | 9.809E-08 | 3.3155E-03 | 0.06457 | 65.1 | 0.12457 |
| 4 | hct022_c04 | 0.98856 | 0.00060 | 0.0081 | 0.0081 | 9.917E-08 | 3.3155E-03 | 0.06457 | 65.1 | 0.12457 |
| 5 | hct022_c05 | 0.98909 | 0.00063 | 0.0081 | 0.0081 | 9.587E-08 | 3.3155E-03 | 0.06457 | 65.1 | 0.12457 |
| 6 | hct022_c06 | 0.98902 | 0.00059 | 0.0081 | 0.0081 | 9.840E-08 | 3.3155E-03 | 0.06457 | 65.1 | 0.12457 |
| 7 | hct022_c07 | 0.98963 | 0.00056 | 0.0081 | 0.0081 | 9.890E-08 | 3.3155E-03 | 0.06457 | 65.1 | 0.12457 |
| 8 | hct022_c08 | 0.98908 | 0.00057 | 0.0081 | 0.0081 | 9.951E-08 | 3.3155E-03 | 0.06457 | 65.1 | 0.12457 |
| 9 | hct022_c09 | 0.98840 | 0.00056 | 0.0081 | 0.0081 | 9.589E-08 | 3.3155E-03 | 0.06457 | 65.1 | 0.12457 |
| 10 | hct022_c10 | 0.98845 | 0.00060 | 0.0081 | 0.0081 | 9.963E-08 | 3.3155E-03 | 0.06457 | 65.1 | 0.12457 |
| 11 | hct022_c11 | 0.98930 | 0.00060 | 0.0081 | 0.0081 | 1.001E-07 | 3.3155E-03 | 0.06457 | 65.1 | 0.12457 |
| 12 | hmt006_c01 | 0.99240 | 0.00082 | 0.0044 | 0.0045 | 8.481E-08 | 1.8490E-03 | 0.06457 | 116.5 | 0.12457 |
| 13 | hmt006_c02 | 0.99331 | 0.00088 | 0.0040 | 0.0041 | 7.044E-08 | 1.8490E-03 | 0.06457 | 116.5 | 0.12457 |
| 14 | hmt006_c03 | 0.99740 | 0.00072 | 0.0040 | 0.0041 | 6.338E-08 | 1.8490E-03 | 0.06457 | 116.5 | 0.12457 |
| 15 | hmt006_c04 | 0.99282 | 0.00081 | 0.0040 | 0.0041 | 6.185E-08 | 1.8490E-03 | 0.06457 | 116.5 | 0.12457 |
| 16 | hmt006_c05 | 0.99230 | 0.00079 | 0.0040 | 0.0041 | 5.852E-08 | 1.8490E-03 | 0.06457 | 116.5 | 0.12457 |
| 17 | hmt006_c06 | 0.99010 | 0.00071 | 0.0040 | 0.0041 | 5.615E-08 | 1.8490E-03 | 0.06457 | 116.5 | 0.12457 |
| 18 | hmt006_c07 | 0.98783 | 0.00073 | 0.0040 | 0.0041 | 5.432E-08 | 1.8490E-03 | 0.06457 | 116.5 | 0.12457 |
| 19 | hmt006_c08 | 0.98428 | 0.00076 | 0.0040 | 0.0041 | 5.245E-08 | 1.8490E-03 | 0.06457 | 116.5 | 0.12457 |
| 20 | hmt006_c09 | 0.98657 | 0.00072 | 0.0040 | 0.0041 | 5.222E-08 | 1.8490E-03 | 0.06457 | 116.5 | 0.12457 |
| 21 | hmt006_c10 | 0.99885 | 0.00085 | 0.0040 | 0.0041 | 8.220E-08 | 1.8490E-03 | 0.06457 | 116.5 | 0.12457 |
| 22 | hmt006_c11 | 0.98965 | 0.00081 | 0.0040 | 0.0041 | 6.236E-08 | 1.8490E-03 | 0.06457 | 116.5 | 0.12457 |
| 23 | hmt006_c12 | 0.99403 | 0.00070 | 0.0040 | 0.0041 | 5.415E-08 | 1.8490E-03 | 0.06457 | 116.5 | 0.12457 |
| 24 | hmt006_c13 | 1.01283 | 0.00086 | 0.0040 | 0.0041 | 8.231E-08 | 1.8490E-03 | 0.06457 | 116.5 | 0.12457 |
| 25 | hmt006_c14 | 0.98495 | 0.00071 | 0.0061 | 0.0061 | 5.715E-08 | 1.8490E-03 | 0.06457 | 116.5 | 0.12457 |

(continued)

Table 6.8-3 – Benchmark Experiment Data (concluded)

| No | Case | k | $\sigma_{mcnp}$ | $\sigma_{bench}$ | $\sigma_{total}$ | EALF (MeV) | U-235 (atom/b-cm) | Chanel Width (in) | H/U-235 | Pitch (in) |
|---|---|---|---|---|---|---|---|---|---|---|
| 26 | hmt006_c15 | 0.98128 | 0.00077 | 0.0040 | 0.0041 | 5.654E-08 | 1.8490E-03 | 0.06457 | 116.5 | 0.12457 |
| 27 | hmt006_c16 | 0.99241 | 0.00078 | 0.0040 | 0.0041 | 6.330E-08 | 1.8490E-03 | 0.06457 | 116.5 | 0.12457 |
| 28 | hmt006_c17 | 0.98934 | 0.00082 | 0.0040 | 0.0041 | 7.405E-08 | 1.8490E-03 | 0.06457 | 116.5 | 0.12457 |
| 29 | hmt006_c18 | 0.99282 | 0.00087 | 0.0040 | 0.0041 | 8.003E-08 | 1.8490E-03 | 0.06457 | 116.5 | 0.12457 |
| 30 | hmt006_c19 | 0.99360 | 0.00068 | 0.0040 | 0.0041 | 5.243E-08 | 1.8490E-03 | 0.06457 | 113.9 | 0.12457 |
| 31 | hmt006_c20 | 0.99275 | 0.00076 | 0.0040 | 0.0041 | 6.471E-08 | 1.8490E-03 | 0.06457 | 113.7 | 0.12457 |
| 32 | hmt006_c21 | 0.99469 | 0.00077 | 0.0040 | 0.0041 | 6.917E-08 | 1.8490E-03 | 0.06457 | 113.7 | 0.12457 |
| 33 | hmt006_c22 | 0.99670 | 0.00080 | 0.0040 | 0.0041 | 7.407E-08 | 1.8490E-03 | 0.06457 | 113.6 | 0.12457 |
| 34 | hmt006_c23 | 1.00132 | 0.00080 | 0.0040 | 0.0041 | 7.670E-08 | 1.8490E-03 | 0.06457 | 113.5 | 0.12457 |
| 35 | hmt022_c01 | 0.99179 | 0.00013 | 0.0035 | 0.0035 | 1.585E-07 | 3.9260E-03 | 0.078 | 66.0 | 0.12800 |

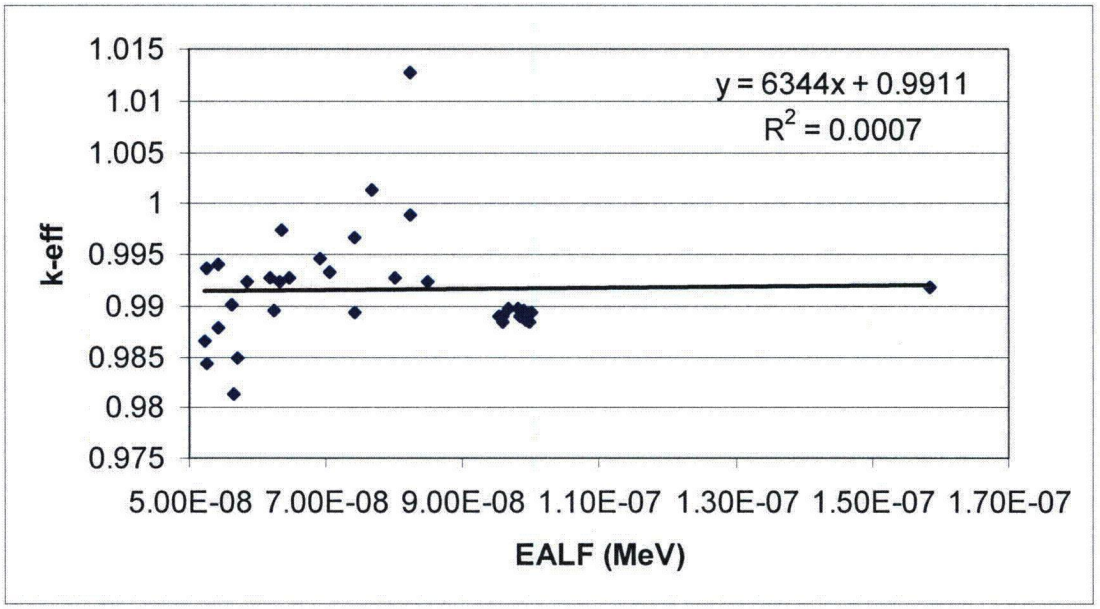


**Figure 6.8-1** – Benchmark Data Trend for EALF

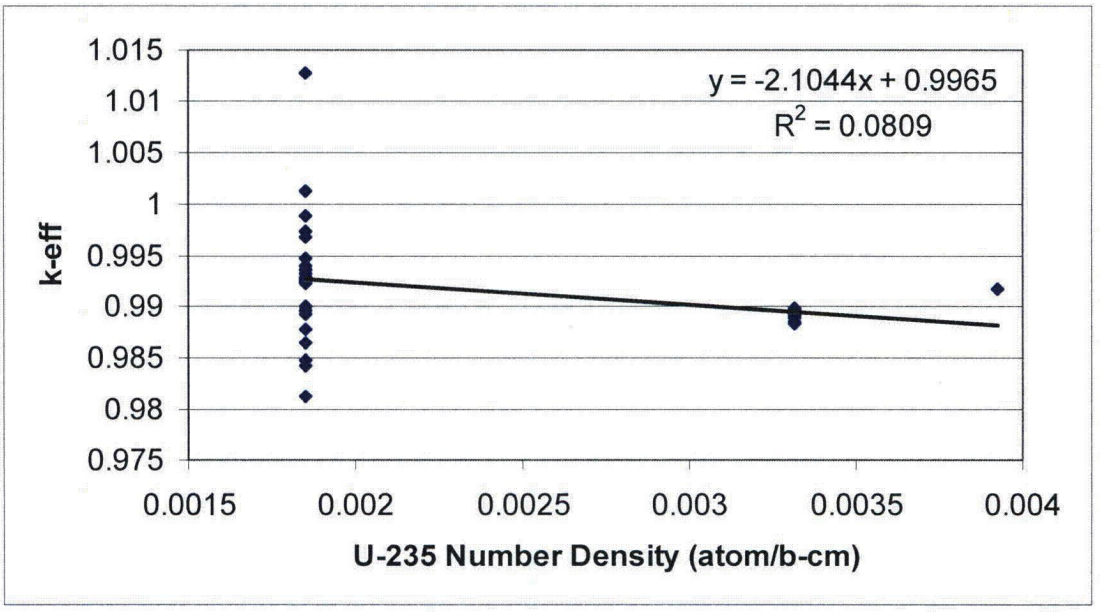


**Figure 6.8-2** – Benchmark Data Trend for U-235 Number Density

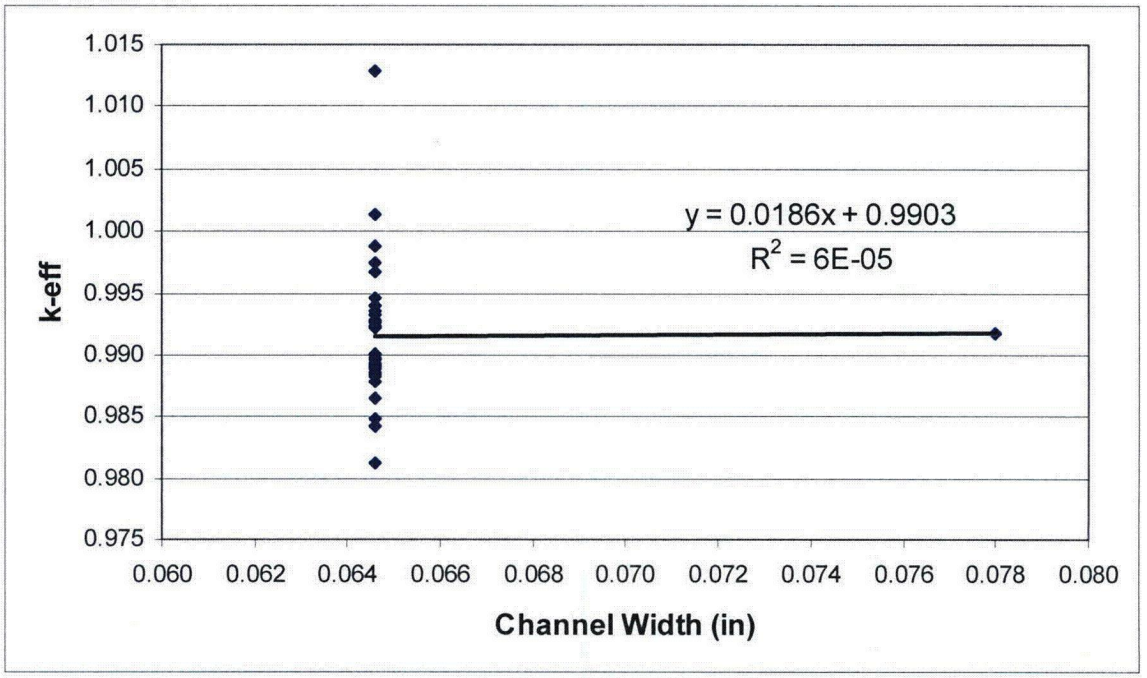


**Figure 6.8-3** – Benchmark Data Trend for Channel Width

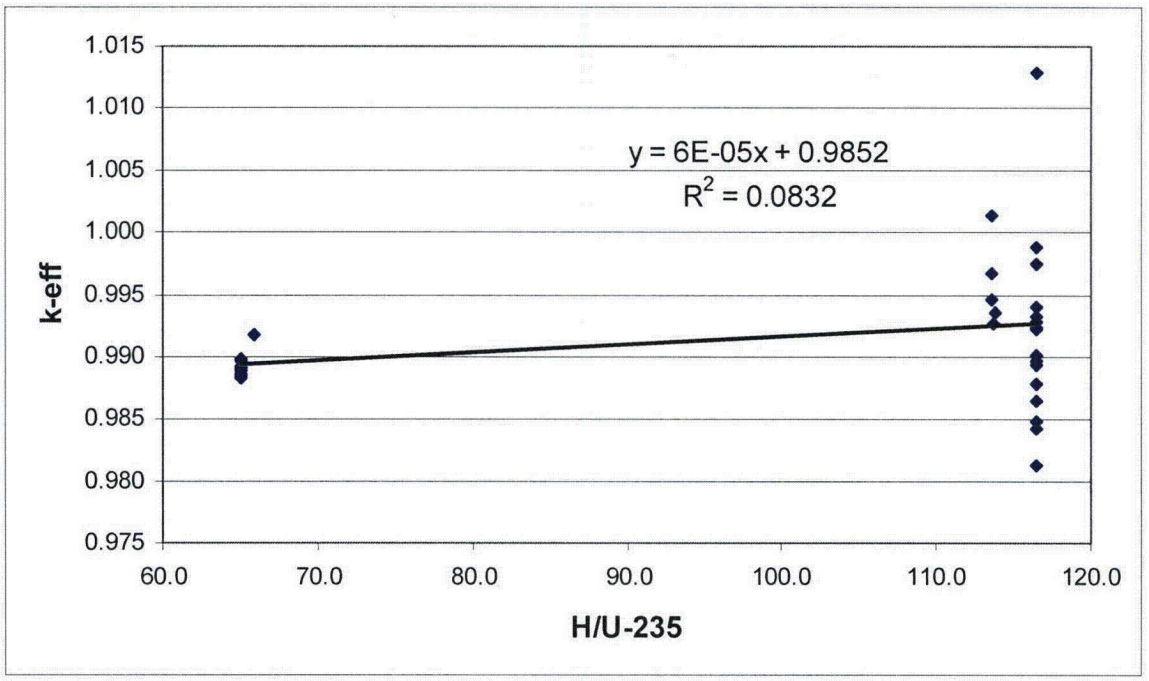


**Figure 6.8-4** – Benchmark Data Trend for H/U-235

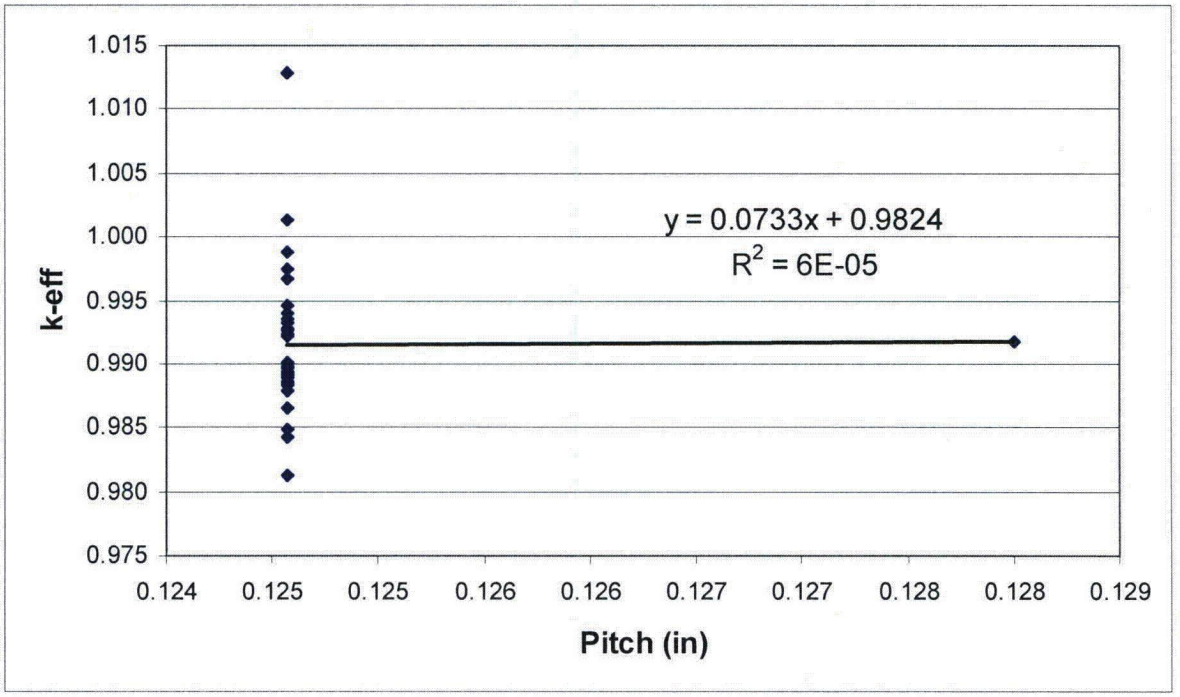


**Figure 6.8-5** – Benchmark Data Trend for Pitch

# 6.9 Appendix

Sample input files are provided for the most reactive NCT array case for both the fuel element payload (Case D4) and the loose plate basket payload (Case LG5).

**Case D4 (NA_P030)**

```
ATR
999     0       -320:321:-322:323:-324:325                  imp:n=0
900     0       310 -311 312 -313 24 -25      fill=3        imp:n=1
901     2 -1.0 (311:-310:313:-312:-24:25) 320 -321 322 -323 324 -325  imp:n=1
c
c       Universe 1: ATR Fuel Element (infinitely long)
c
2       3 -2.7          -6 8 9 -10                  u=1 imp:n=1 $ left Al piece
4       3 -2.7          -5 7 9 -10                  u=1 imp:n=1 $ right Al piece
6       10 5.5010E-02   52 -53 -14 -13              u=1 imp:n=1 $ plate 1
8       3 -2.7          51 -54   -7 -8        #6    u=1 imp:n=1
10      2 -1.00         54 -55   -7 -8              u=1 imp:n=1
12      11 5.4998E-02   56 -57 -16 -15              u=1 imp:n=1 $ plate 2
14      3 -2.7          55 -58   -7 -8        #12   u=1 imp:n=1
16      2 -1.00         58 -59   -7 -8              u=1 imp:n=1
18      12 5.4574E-02   60 -61 -16 -15              u=1 imp:n=1 $ plate 3
20      3 -2.7          59 -62   -7 -8        #18   u=1 imp:n=1
22      2 -1.00         62 -63   -7 -8              u=1 imp:n=1
24      13 5.4583E-02   64 -65 -16 -15              u=1 imp:n=1 $ plate 4
26      3 -2.7          63 -66   -7 -8        #24   u=1 imp:n=1
28      2 -1.00         66 -67   -7 -8              u=1 imp:n=1
30      14 5.4115E-02   68 -69 -16 -15              u=1 imp:n=1 $ plate 5
32      3 -2.7          67 -70   -7 -8        #30   u=1 imp:n=1
34      2 -1.00         70 -71   -7 -8              u=1 imp:n=1
36      15 5.4106E-02   72 -73 -16 -15              u=1 imp:n=1 $ plate 6
38      3 -2.7          71 -74   -7 -8        #36   u=1 imp:n=1
40      2 -1.00         74 -75   -7 -8              u=1 imp:n=1
42      16 5.4102E-02   76 -77 -16 -15              u=1 imp:n=1 $ plate 7
44      3 -2.7          75 -78   -7 -8        #42   u=1 imp:n=1
46      2 -1.00         78 -79   -7 -8              u=1 imp:n=1
48      17 5.4098E-02   80 -81 -16 -15              u=1 imp:n=1 $ plate 8
50      3 -2.7          79 -82   -7 -8        #48   u=1 imp:n=1
52      2 -1.00         82 -83   -7 -8              u=1 imp:n=1
54      18 5.4095E-02   84 -85 -16 -15              u=1 imp:n=1 $ plate 9
56      3 -2.7          83 -86   -7 -8        #54   u=1 imp:n=1
58      2 -1.00         86 -87   -7 -8              u=1 imp:n=1
60      19 5.4092E-02   88 -89 -16 -15              u=1 imp:n=1 $ plate 10
62      3 -2.7          87 -90   -7 -8        #60   u=1 imp:n=1
64      2 -1.00         90 -91   -7 -8              u=1 imp:n=1
66      20 5.4089E-02   92 -93 -16 -15              u=1 imp:n=1 $ plate 11
68      3 -2.7          91 -94   -7 -8        #66   u=1 imp:n=1
70      2 -1.00         94 -95   -7 -8              u=1 imp:n=1
72      21 5.4086E-02   96 -97 -16 -15              u=1 imp:n=1 $ plate 12
74      3 -2.7          95 -98   -7 -8        #72   u=1 imp:n=1
76      2 -1.00         98 -99   -7 -8              u=1 imp:n=1
78      22 5.4083E-02   100 -101 -16 -15           u=1 imp:n=1 $ plate 13
80      3 -2.7           99 -102   -7 -8      #78   u=1 imp:n=1
82      2 -1.00         102 -103   -7 -8            u=1 imp:n=1
84      23 5.4081E-02   104 -105 -16 -15           u=1 imp:n=1 $ plate 14
86      3 -2.7          103 -106   -7 -8      #84   u=1 imp:n=1
88      2 -1.00         106 -107   -7 -8            u=1 imp:n=1
```

```
90      24 5.4075E-02  108 -109 -16 -15          u=1 imp:n=1 $ plate 15
92      3 -2.7         107 -110   -7 -8     #90  u=1 imp:n=1
94      2 -1.00        110 -111   -7 -8          u=1 imp:n=1
96      25 5.4544E-02  112 -113 -16 -15          u=1 imp:n=1 $ plate 16
98      3 -2.7         111 -114   -7 -8     #96  u=1 imp:n=1
100     2 -1.00        114 -115   -7 -8          u=1 imp:n=1
102     26 5.4544E-02  116 -117 -16 -15          u=1 imp:n=1 $ plate 17
104     3 -2.7         115 -118   -7 -8     #102 u=1 imp:n=1
106     2 -1.00        118 -119   -7 -8          u=1 imp:n=1
108     27 5.4949E-02  120 -121 -18 -17          u=1 imp:n=1 $ plate 18
110     3 -2.7         119 -122   -7 -8     #108 u=1 imp:n=1
112     2 -1.00        122 -123   -7 -8          u=1 imp:n=1
114     28 5.4967E-02  124 -125 -14 -13          u=1 imp:n=1 $ plate 19
116     3 -2.7         123 -126   -7 -8     #114 u=1 imp:n=1
c 122     2 -1.00       6:5:-9:10:9 -51 -8 -7:126 -10 -8 -7 u=1 imp:n=1
120     2 -1.00        126 -10 -8 -7              u=1 imp:n=1 $ above 19
121     2 -1.00        9 -51 -8 -7                u=1 imp:n=1 $ below 1
122     5 -0.737       5 -11 9 -10                u=1 imp:n=1 $ right neoprene
123     5 -0.737     -12 6 9 -10                  u=1 imp:n=1 $ left neoprene
125     2 -1.0        12:11:-9:10                 u=1 imp:n=1
c
c       Universe 20: ATR with pipe (center)
c
200     0  -27 -26 22 -23:26 -20 22 -28:27 -21 22 -28  trcl=1
           fill=1  u=20 imp:n=1
201     2 -0.3     #200 -200                    u=20 imp:n=1 $ between ATR/pipe
202     4 -7.94     200 -201                    u=20 imp:n=1 $ pipe
203     6 -0.096    201 -203 250 -251 252 -253 u=20 imp:n=1 $ insulation
204     0           203 250 -251 252 -253       u=20 imp:n=1 $ insulation to
tube
205     4 -7.94     -250:251:-252:253           u=20 imp:n=1 $ tube to inf
c
c       Universe 21: ATR with pipe (down)
c
210     0  -27 -26 22 -23:26 -20 22 -28:27 -21 22 -28  trcl=2
           fill=1  u=21 imp:n=1
211     2 -0.3     #210 -200                    u=21 imp:n=1 $ between ATR/pipe
212     4 -7.94     200 -201                    u=21 imp:n=1 $ pipe
213     6 -0.096    201 -203 250 -251 252 -253 u=21 imp:n=1 $ insulation
214     0           203 250 -251 252 -253       u=21 imp:n=1 $ insulation to
tube
215     4 -7.94     -250:251:-252:253           u=21 imp:n=1 $ tube to inf
c
c       Universe 22: ATR with pipe (up)
c
220     0  -27 -26 22 -23:26 -20 22 -28:27 -21 22 -28  trcl=3
           fill=1  u=22 imp:n=1
221     2 -0.3     #220 -200                    u=22 imp:n=1 $ between ATR/pipe
222     4 -7.94     200 -201                    u=22 imp:n=1 $ pipe
223     6 -0.096    201 -203 250 -251 252 -253 u=22 imp:n=1 $ insulation
224     0           203 250 -251 252 -253       u=22 imp:n=1 $ insulation to
tube
225     4 -7.94     -250:251:-252:253           u=22 imp:n=1 $ tube to inf
c
c       Universe 23: ATR with pipe (right)
c
230     0  -27 -26 22 -23:26 -20 22 -28:27 -21 22 -28  trcl=4
           fill=1  u=23 imp:n=1
231     2 -0.3     #230 -200                    u=23 imp:n=1 $ between ATR/pipe
232     4 -7.94     200 -201                    u=23 imp:n=1 $ pipe
```

```
233     6 -0.096    201 -203 250 -251 252 -253 u=23 imp:n=1 $ insulation
234     0           203 250 -251 252 -253      u=23 imp:n=1 $ insulation to
tube
235     4 -7.94     -250:251:-252:253          u=23 imp:n=1 $ tube to inf
c
c       Universe 24: ATR with pipe (left)
c
240     0  -27 -26 22 -23:26 -20 22 -28:27 -21 22 -28  trcl=5
           fill=1  u=24 imp:n=1
241     2 -0.3     #240 -200                  u=24 imp:n=1 $ between ATR/pipe
242     4 -7.94     200 -201                  u=24 imp:n=1 $ pipe
243     6 -0.096    201 -203 250 -251 252 -253 u=24 imp:n=1 $ insulation
244     0           203 250 -251 252 -253      u=24 imp:n=1 $ insulation to
tube
245     4 -7.94     -250:251:-252:253          u=24 imp:n=1 $ tube to inf
c
c       Universe 25: ATR with pipe (up right)
c
250     0  -27 -26 22 -23:26 -20 22 -28:27 -21 22 -28  trcl=6
           fill=1  u=25 imp:n=1
251     2 -0.3     #250 -200                  u=25 imp:n=1 $ between ATR/pipe
252     4 -7.94     200 -201                  u=25 imp:n=1 $ pipe
253     6 -0.096    201 -203 250 -251 252 -253 u=25 imp:n=1 $ insulation
254     0           203 250 -251 252 -253      u=25 imp:n=1 $ insulation to
tube
255     4 -7.94     -250:251:-252:253          u=25 imp:n=1 $ tube to inf
c
c       Universe 26: ATR with pipe (up left)
c
260     0  -27 -26 22 -23:26 -20 22 -28:27 -21 22 -28  trcl=7
           fill=1  u=26 imp:n=1
261     2 -0.3     #260 -200                  u=26 imp:n=1 $ between ATR/pipe
262     4 -7.94     200 -201                  u=26 imp:n=1 $ pipe
263     6 -0.096    201 -203 250 -251 252 -253 u=26 imp:n=1 $ insulation
264     0           203 250 -251 252 -253      u=26 imp:n=1 $ insulation to
tube
265     4 -7.94     -250:251:-252:253          u=26 imp:n=1 $ tube to inf
c
c       Universe 27: ATR with pipe (down right)
c
270     0  -27 -26 22 -23:26 -20 22 -28:27 -21 22 -28  trcl=8
           fill=1  u=27 imp:n=1
271     2 -0.3     #270 -200                  u=27 imp:n=1 $ between ATR/pipe
272     4 -7.94     200 -201                  u=27 imp:n=1 $ pipe
273     6 -0.096    201 -203 250 -251 252 -253 u=27 imp:n=1 $ insulation
274     0           203 250 -251 252 -253      u=27 imp:n=1 $ insulation to
tube
275     4 -7.94     -250:251:-252:253          u=27 imp:n=1 $ tube to inf
c
c       Universe 28: ATR with pipe (down left)
c
280     0  -27 -26 22 -23:26 -20 22 -28:27 -21 22 -28  trcl=9
           fill=1  u=28 imp:n=1
281     2 -0.3     #280 -200                  u=28 imp:n=1 $ between ATR/pipe
282     4 -7.94     200 -201                  u=28 imp:n=1 $ pipe
283     6 -0.096    201 -203 250 -251 252 -253 u=28 imp:n=1 $ insulation
284     0           203 250 -251 252 -253      u=28 imp:n=1 $ insulation to
tube
285     4 -7.94     -250:251:-252:253          u=28 imp:n=1 $ tube to inf
c
```

```
c       Universe 3: Array of Packages
c
300   0    -300 301 -302 303 imp:n=1 u=3 lat=1 fill=-4:4 -4:4 0:0
             25 25 25 25 22 26 26 26 26
             25 25 25 25 22 26 26 26 26
             25 25 25 25 22 26 26 26 26
             25 25 25 25 22 26 26 26 26
             23 23 23 23 20 24 24 24 24
             27 27 27 27 21 28 28 28 28
             27 27 27 27 21 28 28 28 28
             27 27 27 27 21 28 28 28 28
             27 27 27 27 21 28 28 28 28

5       p  2.4142136 -1 0 -0.2665911 $ right Al outer
6       p -2.4142136 -1 0 -0.2665911 $ left Al outer
7       p  2.4142136 -1 0 -1.474587  $ right Al inner
8       p -2.4142136 -1 0 -1.474587  $ left Al inner
9       cz 7.52856                   $ Al boundary
10      cz 14.015466                 $ Al boundary
11      p  2.4142136 -1 0  0.563076  $ right neoprene
12      p -2.4142136 -1 0  0.563076  $ left neoprene
c
13      p  2.4142136 -1 0 -2.4370013 $ plate 1 & 19 meat
14      p -2.4142136 -1 0 -2.4370013 $ plate 1 & 19 meat
15      p  2.4142136 -1 0 -1.7732672 $ plate 2-17 meat
16      p -2.4142136 -1 0 -1.7732672 $ plate 2-17 meat
17      p  2.4142136 -1 0 -1.9060140 $ plate 18 meat
18      p -2.4142136 -1 0 -1.9060140 $ plate 18 meat
c
20      p  2.4142136 -1 0   0.6      $ right u0 boundary
21      p -2.4142136 -1 0   0.6      $ left u0 boundary
22      cz 7.51                      $ u0 boundary
23      cz 14.02                     $ u0 boundary
24      pz -60.96                    $ bottom of fuel
25      pz  60.96                    $ top of fuel (48")
26      p  2.4142136 -1 0  0.0       $ neoprene notch
27      p -2.4142136 -1 0  0.0       $ neoprene notch
28      cz 13.9                      $ neoprene notch
c
51      cz 7.66699 $ fuel plate 1
52      cz 7.7343
53      cz 7.7851
54      cz 7.85241
c
55      cz 8.06831 $ fuel plate 2
56      cz 8.09752
57      cz 8.14832
58      cz 8.17753
c
59      cz 8.39343 $ fuel plate 3
60      cz 8.42264
61      cz 8.47344
62      cz 8.50265
c
63      cz 8.71855 $ fuel plate 4
64      cz 8.74776
65      cz 8.79856
66      cz 8.82777
c
67      cz 9.04367 $ fuel plate 5
```

```
68      cz 9.07288
69      cz 9.12368
70      cz 9.15289
c
71      cz 9.36879 $ fuel plate 6
72      cz 9.398
73      cz 9.4488
74      cz 9.47801
c
75      cz 9.69391 $ fuel plate 7
76      cz 9.72312
77      cz 9.77392
78      cz 9.80313
c
79      cz 10.01903 $ fuel plate 8
80      cz 10.04824
81      cz 10.09904
82      cz 10.12825
c
83      cz 10.34415 $ fuel plate 9
84      cz 10.37336
85      cz 10.42416
86      cz 10.45337
c
87      cz 10.66927 $ fuel plate 10
88      cz 10.69848
89      cz 10.74928
90      cz 10.77849
c
91      cz 10.99439 $ fuel plate 11
92      cz 11.0236
93      cz 11.0744
94      cz 11.10361
c
95      cz 11.31951 $ fuel plate 12
96      cz 11.34872
97      cz 11.39952
98      cz 11.42873
c
99       cz 11.64463 $ fuel plate 13
100      cz 11.67384
101      cz 11.72464
102      cz 11.75385
c
103      cz 11.96975 $ fuel plate 14
104      cz 11.99896
105      cz 12.04976
106      cz 12.07897
c
107      cz 12.29487 $ fuel plate 15
108      cz 12.32408
109      cz 12.37488
110      cz 12.40409
c
111      cz 12.61999 $ fuel plate 16
112      cz 12.6492
113      cz 12.7
114      cz 12.72921
c
115      cz 12.94511 $ fuel plate 17
```

```
116      cz 12.97432
117      cz 13.02512
118      cz 13.05433
c
119      cz 13.27023 $ fuel plate 18
120      cz 13.29944
121      cz 13.35024
122      cz 13.37945
c
123      cz 13.59535 $ fuel plate 19
124      cz 13.68806
125      cz 13.73886
126      cz 13.83157
c
200      cz 7.3838 $ IR pipe
201      cz 7.6581 $ OR pipe
202      cz 38.1   $ 12" water
203      cz 10.1981 $ 1" insulation
c
250      px  -9.6032 $ square tube
251      px   9.6032
252      py  -9.6032
253      py   9.6032
c
300      px  10.033 $ lattice surfaces/sq. tube
301      px -10.033
302      py  10.033
303      py -10.033
310      px -90.297 $ 9x9 bounds
311      px  90.297
312      py -90.297
313      py  90.297
320      px -120.777 $ outer bounds
321      px  120.777
322      py -120.777
323      py  120.777
324      pz -91.44
325      pz  91.44

m2       1001.62c  2          $ water
         8016.62c  1
mt2      lwtr.60t
m3       13027.62c 1          $ Al
m4       6000.66c   -0.08     $ SS-304
         14000.60c  -1.0
         15031.66c  -0.045
         24000.50c  -19.0
         25055.62c  -2.0
         26000.55c  -68.375
         28000.50c  -9.5
m5       1001.62c  -0.056920  $ neoprene
         6000.66c  -0.542646
c         17000.66c -0.400434
m6       13027.62c  -26.5     $ insulation material
         14000.60c  -23.4
         8016.62c   -50.2
m10      92234.69c 1.7026E-05 $ fuel plate 1
         92235.69c 2.6560E-03
         92236.69c 9.8475E-06
         92238.69c 1.4089E-04
```

```
        13027.62c 5.2187E-02
c       total     5.5010E-02
m11     92234.69c 1.7156E-05 $ fuel plate 2
        92235.69c 2.6763E-03
        92236.69c 9.9226E-06
        92238.69c 1.4196E-04
        13027.62c 5.2153E-02
c       total     5.4998E-02
m12     92234.69c 2.1711E-05 $ fuel plate 3
        92235.69c 3.3869E-03
        92236.69c 1.2557E-05
        92238.69c 1.7966E-04
        13027.62c 5.0974E-02
c       total     5.4574E-02
m13     92234.69c 2.1618E-05 $ fuel plate 4
        92235.69c 3.3724E-03
        92236.69c 1.2503E-05
        92238.69c 1.7889E-04
        13027.62c 5.0998E-02
c       total     5.4583E-02
m14     92234.69c 2.6648E-05 $ fuel plate 5
        92235.69c 4.1571E-03
        92236.69c 1.5413E-05
        92238.69c 2.2051E-04
        13027.62c 4.9696E-02
c       total     5.4115E-02
m15     92234.69c 2.6746E-05 $ fuel plate 6
        92235.69c 4.1724E-03
        92236.69c 1.5470E-05
        92238.69c 2.2132E-04
        13027.62c 4.9670E-02
c       total     5.4106E-02
m16     92234.69c 2.6790E-05 $ fuel plate 7
        92235.69c 4.1791E-03
        92236.69c 1.5495E-05
        92238.69c 2.2168E-04
        13027.62c 4.9659E-02
c       total     5.4102E-02
m17     92234.69c 2.6830E-05 $ fuel plate 8
        92235.69c 4.1854E-03
        92236.69c 1.5518E-05
        92238.69c 2.2201E-04
        13027.62c 4.9649E-02
c       total     5.4098E-02
m18     92234.69c 2.6867E-05 $ fuel plate 9
        92235.69c 4.1911E-03
        92236.69c 1.5539E-05
        92238.69c 2.2232E-04
        13027.62c 4.9639E-02
c       total     5.4095E-02
m19     92234.69c 2.6901E-05 $ fuel plate 10
        92235.69c 4.1965E-03
        92236.69c 1.5559E-05
        92238.69c 2.2260E-04
        13027.62c 4.9630E-02
c       total     5.4092E-02
m20     92234.69c 2.6933E-05 $ fuel plate 11
        92235.69c 4.2015E-03
        92236.69c 1.5577E-05
        92238.69c 2.2287E-04
```

```
        13027.62c 4.9622E-02
c       total     5.4089E-02
m21     92234.69c 2.6963E-05 $ fuel plate 12
        92235.69c 4.2061E-03
        92236.69c 1.5595E-05
        92238.69c 2.2311E-04
        13027.62c 4.9614E-02
c       total     5.4086E-02
m22     92234.69c 2.6990E-05 $ fuel plate 13
        92235.69c 4.2105E-03
        92236.69c 1.5611E-05
        92238.69c 2.2334E-04
        13027.62c 4.9607E-02
c       total     5.4083E-02
m23     92234.69c 2.7017E-05 $ fuel plate 14
        92235.69c 4.2145E-03
        92236.69c 1.5626E-05
        92238.69c 2.2356E-04
        13027.62c 4.9600E-02
c       total     5.4081E-02
m24     92234.69c 2.7077E-05 $ fuel plate 15
        92235.69c 4.2239E-03
        92236.69c 1.5661E-05
        92238.69c 2.2406E-04
        13027.62c 4.9585E-02
c       total     5.4075E-02
m25     92234.69c 2.2037E-05 $ fuel plate 16
        92235.69c 3.4377E-03
        92236.69c 1.2746E-05
        92238.69c 1.8235E-04
        13027.62c 5.0889E-02
c       total     5.4544E-02
m26     92234.69c 2.2037E-05 $ fuel plate 17
        92235.69c 3.4377E-03
        92236.69c 1.2745E-05
        92238.69c 1.8235E-04
        13027.62c 5.0889E-02
c       total     5.4544E-02
m27     92234.69c 1.7683E-05 $ fuel plate 18
        92235.69c 2.7586E-03
        92236.69c 1.0228E-05
        92238.69c 1.4633E-04
        13027.62c 5.2016E-02
c       total     5.4949E-02
m28     92234.69c 1.7487E-05 $ fuel plate 19
        92235.69c 2.7279E-03
        92236.69c 1.0114E-05
        92238.69c 1.4470E-04
        13027.62c 5.2067E-02
c       total     5.4967E-02
c
*tr1     0 -10.8 0                          $ base to center
*tr2     0 7.9 0    180 90 90 90 180 90     $ down
*tr3     0 -7.9 0                           $ up
*tr4    -7.9 0 0    90 180 90 0 90 90       $ right
*tr5     7.9 0 0    90 0 90 180 90 90       $ left
*tr6    -5.6  -5.6 0 45 135 90 45 45 90     $ up/right
*tr7     5.6  -5.6 0 45 45 90 135 45 90     $ up/left
*tr8    -5.6   5.6 0 135 135 90 45 135 90   $ down/right
*tr9     5.6   5.6 0 135 45 90 135 135 90   $ down/left
```

```
c
mode   n
kcode  2500 1.0 50 250
sdef    x=d1 y=d2 z=d3
si1     -90 90
sp1     0 1
si2     -90 90
sp2     0 1
si3     -60 60
sp3     0 1
```

**Case LG5 (NA_N5P050)**

```
ATR
999     0      -320:321:-322:323:-324:325                imp:n=0
900     0      310 -311 312 -313 24 -25     fill=3       imp:n=1
901     2 -1.0 (311:-310:313:-312:-24:25) 320 -321 322 -323 324 -325  imp:n=1
c
c       Universe 5: Plate 5
c
500     14 5.4037E-02   500 -501 502 -503            u=5 imp:n=1 $ fuel meat
501     3 -2.7         (-500:501:-502:503) 510 -511 512 -513  u=5 imp:n=1 $
cladding
502     2 -1.0         -510:511:-512:513                    u=5 imp:n=1 $
water
c
c       Universe 6: Lattice
c
600     0  -531 530  lat=1 fill=-2:2 0:0 0:0
           5
           5(0 -0.2 0)
           5
           5(0 0.2 0)
           5
                           imp:n=1 u=6
c
c       Universe 4: Plates and basket (no pipe)
c
400     0          520 -521 522 -523   fill=6(0 0 0)     imp:n=1 u=4 $ fuel
lattice
401     2 -0.5     (-520:521:-522:523) 400 -401 402 -403 imp:n=1 u=4 $ water
between fuel and basket
402     3 -2.7    -400:401:-402:403        imp:n=1 u=4 $ basket (to infinity)
c
c       Universe 20: Plates with pipe (center)
c
200     0         410 -411 412 -413        fill=4 imp:n=1 u=20 $ fuel/basket
201     2 -0.5    #200 -200            imp:n=1 u=20 $ water between basket and
tube
202     4 -7.94   200 -201                        imp:n=1 u=20 $ tube
203     6 -0.096    201 -203 250 -251 252 -253    imp:n=1 u=20 $ insulation
204     0           203 250 -251 252 -253         imp:n=1 u=20 $ insulation to
tube
205     4 -7.94     -250:251:-252:253             imp:n=1 u=20 $ tube to inf
c
c       Universe 21: Plates with pipe (down)
c
210     0         410 -411 412 -413 trcl=2 fill=4 imp:n=1 u=21 $ fuel/basket
211     2 -0.5    #210 -200            imp:n=1 u=21 $ water between basket and
tube
```

```
212     4 -7.94   200 -201                          imp:n=1 u=21 $ tube
213     6 -0.096    201 -203 250 -251 252 -253      imp:n=1 u=21 $ insulation
214     0           203 250 -251 252 -253           imp:n=1 u=21 $ insulation to
tube
215     4 -7.94     -250:251:-252:253               imp:n=1 u=21 $ tube to inf
c
c       Universe 22: Plates with pipe (up)
c
220     0         410 -411 412 -413 trcl=3 fill=4 imp:n=1 u=22 $ fuel/basket
221     2 -0.5    #220 -200             imp:n=1 u=22 $ water between basket and
tube
222     4 -7.94   200 -201                          imp:n=1 u=22 $ tube
223     6 -0.096    201 -203 250 -251 252 -253      imp:n=1 u=22 $ insulation
224     0           203 250 -251 252 -253           imp:n=1 u=22 $ insulation to
tube
225     4 -7.94     -250:251:-252:253               imp:n=1 u=22 $ tube to inf
c
c       Universe 23: Plates with pipe (right)
c
230     0         410 -411 412 -413 trcl=4 fill=4 imp:n=1 u=23 $ fuel/basket
231     2 -0.5    #230 -200             imp:n=1 u=23 $ water between basket and
tube
232     4 -7.94   200 -201                          imp:n=1 u=23 $ tube
233     6 -0.096    201 -203 250 -251 252 -253      imp:n=1 u=23 $ insulation
234     0           203 250 -251 252 -253           imp:n=1 u=23 $ insulation to
tube
235     4 -7.94     -250:251:-252:253               imp:n=1 u=23 $ tube to inf
c
c       Universe 24: Plates with pipe (left)
c
240     0         410 -411 412 -413 trcl=5 fill=4 imp:n=1 u=24 $ fuel/basket
241     2 -0.5    #240 -200              imp:n=1 u=24 $ water between basket
and tube
242     4 -7.94   200 -201                          imp:n=1 u=24 $ tube
243     6 -0.096    201 -203 250 -251 252 -253      imp:n=1 u=24 $ insulation
244     0           203 250 -251 252 -253           imp:n=1 u=24 $ insulation to
tube
245     4 -7.94     -250:251:-252:253               imp:n=1 u=24 $ tube to inf
c
c       Universe 25: Plates with pipe (up right)
c
250     0         410 -411 412 -413 trcl=6 fill=4 imp:n=1 u=25 $ fuel/basket
251     2 -0.5    #250 -200             imp:n=1 u=25 $ water between basket and
tube
252     4 -7.94   200 -201                          imp:n=1 u=25 $ tube
253     6 -0.096    201 -203 250 -251 252 -253      imp:n=1 u=25 $ insulation
254     0           203 250 -251 252 -253           imp:n=1 u=25 $ insulation to
tube
255     4 -7.94     -250:251:-252:253               imp:n=1 u=25 $ tube to inf
c
c       Universe 26: Plates with pipe (up left)
c
260     0         410 -411 412 -413 trcl=7 fill=4 imp:n=1 u=26 $ fuel/basket
261     2 -0.5    #260 -200           imp:n=1 u=26 $ water between basket and
tube
262     4 -7.94   200 -201                          imp:n=1 u=26 $ tube
263     6 -0.096    201 -203 250 -251 252 -253      imp:n=1 u=26 $ insulation
264     0           203 250 -251 252 -253           imp:n=1 u=26 $ insulation to
tube
265     4 -7.94     -250:251:-252:253               imp:n=1 u=26 $ tube to inf
```

```
c
c       Universe 27: Plates with pipe (down right)
c
270     0         410 -411 412 -413 trcl=8 fill=4 imp:n=1 u=27 $ fuel/basket
271     2 -0.5    #270 -200            imp:n=1 u=27 $ water between basket and
tube
272     4 -7.94   200 -201                          imp:n=1 u=27 $ tube
273     6 -0.096    201 -203 250 -251 252 -253     imp:n=1 u=27 $ insulation
274     0           203 250 -251 252 -253          imp:n=1 u=27 $ insulation to
tube
275     4 -7.94     -250:251:-252:253              imp:n=1 u=27 $ tube to inf
c
c       Universe 28: Plates with pipe (down left)
c
280     0         410 -411 412 -413 trcl=9 fill=4 imp:n=1 u=28 $ fuel/basket
281     2 -0.5    #280 -200            imp:n=1 u=28 $ water between basket and
tube
282     4 -7.94   200 -201                          imp:n=1 u=28 $ tube
283     6 -0.096    201 -203 250 -251 252 -253     imp:n=1 u=28 $ insulation
284     0           203 250 -251 252 -253          imp:n=1 u=28 $ insulation to
tube
285     4 -7.94     -250:251:-252:253              imp:n=1 u=28 $ tube to inf
c
c       Universe 3: Array of Packages
c
300   0    -300 301 -302 303 imp:n=1 u=3 lat=1 fill=-4:4 -4:4 0:0
             25 25 25 25 22 26 26 26 26
             25 25 25 25 22 26 26 26 26
             25 25 25 25 22 26 26 26 26
             25 25 25 25 22 26 26 26 26
             23 23 23 23 20 24 24 24 24
             27 27 27 27 21 28 28 28 28
             27 27 27 27 21 28 28 28 28
             27 27 27 27 21 28 28 28 28
             27 27 27 27 21 28 28 28 28

24      pz -60.96                   $ bottom of fuel
25      pz  60.96                   $ top of fuel (48")
c
200      cz 7.3838 $ IR pipe
201      cz 7.6581 $ OR pipe
203      cz 10.1981 $ 1" insulation
c
250      px  -9.6032 $ square tube
251      px   9.6032
252      py  -9.6032
253      py   9.6032
c
300      px  10.033 $ lattice surfaces/sq. tube
301      px -10.033
302      py  10.033
303      py -10.033
310      px -90.297 $ 9x9 bounds
311      px  90.297
312      py -90.297
313      py  90.297
320      px -120.777 $ outer bounds
321      px  120.777
322      py -120.777
323      py  120.777
```

```
324       pz -91.44
325       pz  91.44
c
400       px -5.7912  $ inner basket surfaces
401       px  5.7912
402       py -2.1336
403       py  2.1336
410       px -6.1214  $ outer basket surfaces
411       px  6.1214
412       py -2.4638
413       py  2.4638
c
500       px -5.7873 $ fuel meat
501       px  5.7873
502       py -0.0254
503       py  0.0254
510       px -5.79   $ fuel cladding
511       px  5.79
512       py -0.06096
513       py  0.06096
520       px -5.791  $ array boundary
521       px  5.791
522       py -2.13296
523       py  2.13296
530       py -0.518    $ lattice bounds
531       py  0.518

m2        1001.62c  2          $ water
          8016.62c  1
mt2       lwtr.60t
m3        13027.62c 1          $ Al
m4        6000.66c   -0.08     $ SS-304
          14000.60c  -1.0
          15031.66c  -0.045
          24000.50c  -19.0
          25055.62c  -2.0
          26000.55c  -68.375
          28000.50c  -9.5
m6        13027.62c  -26.5     $ insulation material
          14000.60c  -23.4
          8016.62c   -50.2
m14       92234.69c 2.7492E-05 $ plate 5
          92235.69c 4.2887E-03
          92236.69c 1.5901E-05
          92238.69c 2.2749E-04
          13027.62c 4.9477E-02
c         total     5.4037E-02
c
*tr2       0  -1.6 0                              $ down
*tr3       0   1.6 0                              $ up
*tr4       1.6 0   0       90 180 90 0 90 90      $ right
*tr5      -1.6 0   0       90 0 90 180 90 90      $ left
*tr6       1.13  1.13 0    45 135 90 45 45 90     $ up/right
*tr7      -1.13  1.13 0    45 45 90 135 45 90     $ up/left
*tr8       1.13 -1.13 0    135 135 90 45 135 90   $ down/right
*tr9      -1.13 -1.13 0    135 45 90 135 135 90   $ down/left
c
mode   n
kcode  2500 1.0 50 250
sdef    x=d1 y=d2 z=d3
```

```
si1     -90 90
sp1     0 1
si2     -90 90
sp2     0 1
si3     -60 60
sp3     0 1
```

# 7.0 PACKAGE OPERATIONS

This section provides general instructions for loading and unloading operations of the ATR FFSC. Due to the low specific activity of neutron and gamma emitting radionuclides, dose rates from the contents of the package are minimal. As a result of the low dose rates, there are no special handling requirements for radiation protection.

Package loading and unloading operations shall be performed using detailed written procedures. The operating procedures developed by the user for the loading and unloading activities shall be performed in accordance with the procedural requirements identified in the following sections. The sequence and wording may be tailored by the user developed procedures such that they become aligned with the user facility terms and processes.

## 7.1 Package Loading

### 7.1.1 Preparation for Loading

Prior to loading the ATR FFSC, the packaging is inspected to ensure that it is in unimpaired physical condition. The packaging is inspected for:

- Damage to the closure locking mechanism including the spring. Inspect for missing hardware and verify the locking pins freely engage/disengage with the package body mating features.
- Damage to the closure lugs and interfacing body lugs. Inspect lugs for damage that precludes free engagement of the closure with the body.
- Deformation of the inner shell (payload cavity) that precludes free entry/removal of the payload.
- Deformed threads or other damage to the fasteners or body of the loose fuel plate basket.
- Damage to the spring plunger or body of the fuel handling enclosure.

Acceptance criteria and detailed loading procedures derived from this section are specified in user written procedures. These user procedures are specific to the authorized content of the package and inspections ensure the packaging complies with Appendix 1.3.2, *Packaging General Arrangement Drawings.*

Defects that require repair shall be corrected prior to shipping in accordance with approved procedures consistent with the quality program in effect.

### 7.1.2 Loading of Contents - ATR Fuel Assembly

1. Remove the closure by depressing the spring-loaded pins and rotating the closure 45° to align the closure locking tabs with the mating cut-outs in the body. Remove the closure from the body.
2. Remove the fuel handling enclosure if present in the payload cavity.

3. Prior to loading, visually inspect the fuel handling enclosure for damage, corrosion, and missing hardware to ensure compliance with Appendix 1.3.2, *Packaging General Arrangement Drawings*.
4. Open the fuel handling enclosure lid and place a fuel element into the holder with the narrow end of the fuel element facing the bottom side of the fuel handling enclosure. As a property protection precaution, the fuel element may optionally be inserted into a plastic bag prior to placement in the fuel handling enclosure.
    a. To open the fuel handling enclosure, release the lid by pulling on the spring plunger located at each end and rotate the lid about the hinged side.
    b. To close the fuel handling enclosure, rotate the lid to the closed position, pull the spring plunger located at each end to allow the lid to fully close, align then release the spring plungers with the receiving holes, gently lift the lid to confirm no movement and that the spring plungers are in the locked position.
5. Insert the fuel handling enclosure into the package.
6. Depress the package closure spring-loaded pins, insert closure onto package body by aligning the closure locking tabs with the mating cut-outs in the body, and rotate the closure to the locked position. Release the spring-loaded pins so that they engage with the mating holes in the package body. Observe the pins to ensure they are in the locked position as illustrated in Figure 7.1-1. The closure is fully locked when both locking pins are compressing the sleeve between the locking pin handle and the closure body.

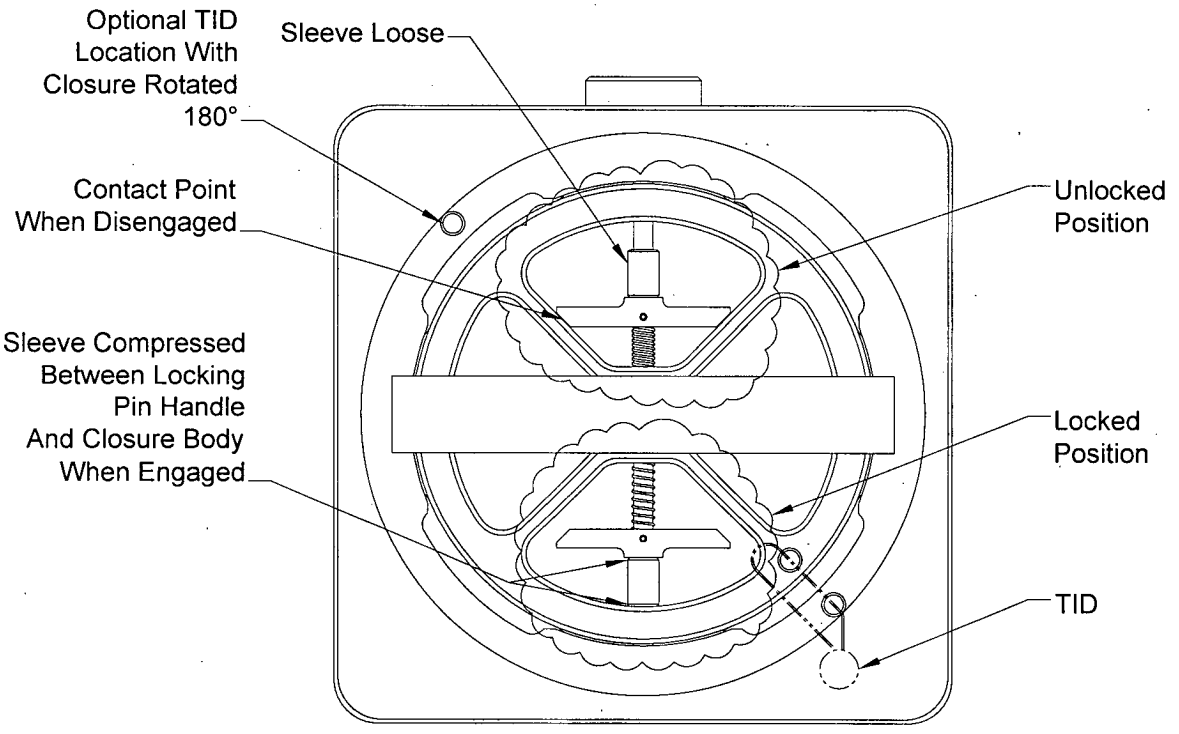


**Figure 7.1-1** - Closure Locking Positions

## 7.1.3 Loading of Contents - Loose Fuel Plates

1. Remove the closure by depressing the spring-loaded pins and rotating the closure 45° to align the closure locking tabs with the mating cut-outs in the body. Remove the closure from the body.
2. Remove the fuel plate basket if present in the payload cavity.
3. Prior to loading, visually inspect the loose fuel plate basket for damage, corrosion, and missing hardware/fastening devices to ensure compliance with Appendix 1.3.2, *Packaging General Arrangement Drawings*.
4. Ensure the combined weight of the loose fuel plates and optional dunnage is 20 lbs or less.
5. Ensure the combined fissile mass of the loose fuel plates does not exceed 600 g uranium-235.
6. Open the loose fuel plate basket by removing the 8 wing nut fasteners securing each half of the basket.
7. Place the fuel plates into one half of the loose fuel plate basket
    a. Flat and curved fuel plates may not be mixed in the same basket.
    b. As a property protection precaution, the fuel plates may optionally be inserted into a plastic bag prior to placement in the fuel plate basket.
    c. Dunnage plates may also be included with the loose fuel plates to reduce any gaps with the basket cavity as a property protection precaution. The dunnage plates may be any aluminum alloy and any size deemed appropriate.
8. Close the fuel plate basket and verify the basket fasteners are installed and finger tight.
    a. With one half of the basket loaded, carefully place the second half over the fuel plates and match the fastener holes.
    b. Insert the 8 spade head screws through the holes and secure with corresponding wing nut (washer optional).
    c. Tighten the 8 wing nut fasteners finger tight.
    d. Visually check the 4 hex head screws located in the center of the basket to verify that they have not loosened. In the event the screws appear to be loose, tighten the fasteners to drawing requirements.
9. Insert the loose fuel plate basket into the package.
10. Depress the package closure spring-loaded pins, insert closure onto package body by aligning the closure locking tabs with the mating cut-outs in the body, and rotate the closure to the locked position. Release the spring-loaded pins so that they engage with the mating holes in the package body. Observe the pins to ensure they are in the locked position as illustrated in Figure 7.1-1. The closure is fully locked when both locking pins are compressing the sleeve between the locking pin handle and the closure body.

### 7.1.4 Preparation for Transport

1. Install the tamper indicating device between the posts on the package closure and body.
2. Perform a survey of the dose rates and levels of non-fixed (removable) radioactive contamination per 49CFR §173.441 and 49CFR §173.443, respectively. The contamination measurements shall be taken in the most appropriate locations to yield a representative assessment of the non-fixed contamination levels.
3. Complete the necessary shipping papers in accordance with Subpart C of 49 CFR §172.
4. Ensure that the package markings are in accordance with 10 CFR §71.85(c) and Subpart D of 49 CFR §172. Package labeling shall be in accordance with Subpart E of 49CFR §172. Package placarding, for either single package transport or the racked configuration, shall be in accordance with Subpart F of 49 CFR §172.
5. Transfer the package to the conveyance and secure the package(s).

## 7.2 Package Unloading

### 7.2.1 Receipt of Package from Conveyance

Radiation and contamination surveys shall be performed upon receipt of the package and the package shall be inspected for damage as required by and in accordance with the user's personnel protection or ALARA program. In addition, the tamper indicating device (TID) shall be inspected. A missing TID or indication of damage to a TID is a Safeguards and Security concern. Disposition of such an incident is beyond the scope of this SAR.

### 7.2.2 Removal of Contents

1. Remove tamper indicating device.
2. Remove the package closure by depressing the spring-loaded pins and rotating the closure 45° to align the closure locking tabs with the mating cut-outs in the body. Remove the closure from the body.
3. Remove the payload container.
4. Open the payload container (fuel handling enclosure or loose fuel plate basket) and remove the contents.
    a. Open the fuel handling enclosure by releasing the spring plunger located at each end and rotate the lid about the hinged side.
    b. Open the loose fuel plate basket by removing the 8 wing nut fasteners securing each half of the basket.
5. Close the fuel handling enclosure lid or loose fuel plate basket as appropriate. If required, return the empty payload container to the package.
    a. To close the fuel handling enclosure, rotate the lid to the closed position, pull the spring plunger located at each end to allow the lid to fully close, align then release

the spring plungers with the receiving holes, gently lift the lid to confirm no movement and that the spring plungers are in the locked position.

b. To close the loose fuel plate basket, place each half of the basket together and align the fastener holes. Insert the 8 spade head screws through the holes and secure with corresponding wing nut (washer optional). Tighten each wing nut finger tight.

6. Depress the package closure spring-loaded pins, insert closure onto package body by aligning the closure locking tabs with the mating cut-outs in the body, and rotate the closure to the locked position. Release the spring-loaded pins so that they engage with the mating holes in the package body. Observe the pins to ensure they are in the locked position as illustrated in Figure 7.1-1. The closure is fully locked when both locking pins are compressing the sleeve between the locking pin handle and the closure body.

## 7.3 Preparation of Empty Package for Transport

Empty packages are prepared and transported per the guidelines of 49 CFR §173.428. The packaging is inspected to ensure that it is in an unimpaired condition and is securely closed.

Any labels previously applied in conformance with subpart E of 49CFR §172 are removed, obliterated, or covered and the "Empty" label prescribed in 49 CFR §172.450 is affixed to the packaging.

## 7.4 Other Operations

This section does not apply.

# 8.0 ACCEPTANCE TESTS AND MAINTENANCE PROGRAM

## 8.1 Acceptance Tests

Per the requirements of 10 CFR §71.85, the inspections and tests to be performed prior to first use of the package are described in this section.

### 8.1.1 Visual Inspections and Measurements

All packaging dimensions, tolerances, general notes, materials of construction, and assembly shall be examined in accordance with the requirements delineated on the drawings in Appendix 1.3.2, *Packaging General Arrangement Drawings*. Source inspections and final release of the packaging will be performed, verifying the quality characteristics were inspected and that the packaging is acceptable. Any characteristic that is out of specification shall be reported and dispositioned in accordance with the quality assurance program in effect.

#### 8.1.1.1 Compression Spring

The compression spring is a component of the closure locking system that maintains the locking pin in the closed position. The compression spring shall be procured to Stock Precision Engineered Components (SPEC) catalog number C0360-035-1120 specification, or equivalent, which includes the following:

- Material shall be approximately 0.035 inch diameter stainless steel wire.
- The nominal outside diameter of the spring shall be approximately 0.36 inches.
- The free length of the spring shall be approximately 1.12 inches.
- The solid height of the spring shall be approximately 0.33 inches.
- The spring shall have a 4.77 (-.1, +.5) lb load at a load length of approximately 0.55 inches.
- The spring rate shall be 8.33 (-.1, +.5) lbs/in.

#### 8.1.1.2 Roll Pin

The roll pin is a component of the closure locking system that maintains the locking pin in the closed position. The roll pin shall be procured to Stock Drive Products/Sterling Instrument (SDP/SI) catalog number A9Y35-0324 specification, or equivalent, which includes the following:

- Material shall be stainless steel.
- The free diameter of the roll pin shall be between 0.099 to 0.103 inches.
- The length of the roll pin shall be approximately 0.75 inches

#### 8.1.1.3 Insulating Blanket

The ceramic fiber insulating blanket is a component of the body and closure assemblies used to reduce heat transfer during thermal events. The insulating blanket shall be procured to Unifrax Durablanket S 6 lb/ft$^3$ specification, or equivalent, which includes the following:

- The material shall be comprised of inorganic ceramic fibers.
- The nominal thickness shall be 0.5 (-0, +.2) inches.
- The nominal density shall be 6 (-15%, +30%) lb/ft$^3$.
- The specific heat shall be 0.25 Btu/lb$_m$-°F minimum.
- The thermal conductivity shall be 0.145 Btu/hr-ft-°F or less at 1200°F.

### 8.1.2 Weld Examinations

All welds shall be examined in accordance with the requirements delineated on the drawings in Appendix 1.3.2, *Packaging General Arrangement Drawings*. Visual examinations are performed in accordance with AWS D1.6[1], Section 6 for stainless steel, AWS D1.2[2], for aluminum, and penetrant examinations are performed under procedures written to ASTM E165-02, *Standard Test Method for Liquid Penetrant Examination*.

### 8.1.3 Structural and Pressure Tests

The packaging does not retain pressure and no pressure testing is required prior to use.

### 8.1.4 Leakage Tests

The packaging contains no seals or containment boundaries that require leakage rate testing.

### 8.1.5 Component and Material Tests

No component or material tests are required for this packaging.

### 8.1.6 Shielding Tests

The packaging does not contain any biological shielding. Shielding tests are not required.

### 8.1.7 Thermal Tests

The material thermal properties utilized in Chapter 3.0, *Thermal* are nominal. However, the thermal analyses in which these values are used are consistently conservative for the Normal

[1] ANSI/AWS D1.6:1999, *Structural Welding Code – Stainless Steel*, American Welding Society (AWS).
[2] ANSI/AWS D1.2:2003, *Structural Welding Code – Aluminum*, American Welding Society.

Conditions of Transport (NCT) and Hypothetical Accident Condition (HAC). Therefore, specific acceptance tests for material thermal properties are not required or performed.

### 8.1.8 Miscellaneous Tests

No other acceptance tests are necessary for the packaging.

## 8.2 Maintenance Program

This section describes the maintenance program used to ensure continued performance of the packaging. The packaging is maintained consistent with a 10 CFR 71 subpart H QA program. Packagings that do not conform to the license drawings are removed from service until they are brought back into compliance. Repairs are performed in accordance with approved procedures and consistent with the quality assurance program in effect.

### 8.2.1 Structural and Pressure Tests

There are no structural or pressure tests that are necessary to ensure continued performance of the packaging.

### 8.2.2 Leakage Rate Tests

No leakage rate tests are necessary to ensure continued performance of the packaging.

### 8.2.3 Component and Material Tests

There is no predetermined replacement schedule for any packaging components and there are no items that would be expected to wear or become damaged during normal usage. The items identified in this section are routinely used during operations and shall be visually inspected prior to each use. Damaged components shall be repaired or replaced prior to further use.

#### 8.2.3.1 Packaging Body and Closure

The closure assembly locking pin spring shall be visually inspected and replaced if it becomes damaged or otherwise fails to function properly (Drawing 60501-10, Item 20, of Appendix 1.3.2, *Packaging General Arrangement Drawings*).

The index lug screws and corresponding tap, or optional wire insert, shall be visually inspected for deformed or stripped threads prior to installation of the screws (Drawing 60501-10, Items 3 and 16).

#### 8.2.3.2 Fuel Handling Enclosure

The spring plunger shall be visually inspected and replaced if it becomes damaged or otherwise fails to function properly (Drawing 60501-30, Item 6, of Appendix 1.3.2, *Packaging General Arrangement Drawings*).

#### 8.2.3.3 Loose Fuel Plate Basket

All threaded components shall be visually inspected as they are installed for deformed or stripped threads (Drawing 60501-20, Items 2, 3, 4, and 5 of Appendix 1.3.2, *Packaging General Arrangement Drawings*).

## 8.2.4 Thermal Tests

No thermal tests are necessary to ensure continued performance of the packaging.

## 8.2.5 Miscellaneous Tests

No miscellaneous tests are required to ensure continued performance of the packaging.

# 9.0 QUALITY ASSURANCE

This chapter defines the Quality Assurance (QA) requirements and methods of compliance applicable to the Advanced Test Reactor Fresh Fuel Shipping Container (ATR FFSC) package. The ATR FFSC package described in this SAR is used to transport single element ATR fuel.

The QA requirements for packagings are described in Subpart H of 10 CFR Part 71 (10 CFR 71). Subpart H is an 18-criteria QA program based on ANSI/ASME NQA-1. Guidance for QA programs for packaging is provided by NRC Regulatory Guide 7.10[1]. The DOE QA requirements for the use of 10CFR71 certified packagings are described in DOE Order 460.1B[2].

The ATR FFSC packaging is designed and built for, and used by Idaho National Laboratory (INL). Procurement, design, fabrication, assembly, testing, maintenance, repair, modification, and use of the ATR FFSC package are all done under QA programs that meet all applicable NRC and DOE QA requirements.

The DOE Idaho Operations Office approved QA program is implemented for all Nuclear Safety activities. Compliance with NRC and DOT packaging and transportation requirements is mandated by DOE Order 460.1B.

This document establishes the programmatic requirements for site-wide implementation and serves as the basis for INL quality assurance program acceptability. It is designed such that implementation of the full scope of requirements as stated in DOE Orders 414.1C, *Quality Assurance* and 460.1B *Packaging and Transport Safety*, constitutes compliance to nuclear safety quality assurance criteria required by 10 CFR 830, Subpart A, *Nuclear Safety Management Quality Assurance Requirements*.

A detailed discussion of the QA program which governs ATR FFSC packaging operations is presented on the following pages to demonstrate compliance with 10 CFR 71, Subpart H.

## 9.1 Organization

### 9.1.1 ATR FFSC Project Organization

This section identifies the organizations involved and describes the responsibilities of and interactions between these organizations.

#### 9.1.1.1 Idaho National Laboratory (INL)

INL Contractor Management has overall responsibility for successfully accomplishing activities. Management provides the necessary planning, organization, direction, control, resources, and support to achieve their defined objectives. Management is responsible for planning, performing, assessing, and improving the work.

---

[1] U.S. Nuclear Regulatory Commission, Regulatory Guide 7.10, *Establishing Quality Assurance Programs for Packaging Used in transport of Radioactive Material, Revision 2*, March 2005.

[2] U.S. Department of Energy Order 460.1B, *Packaging and Transportation Safety*, 4-4-03.

INL Contractor Management is responsible for establishing and implementing policies, plans, and procedures that control the quality of work, consistent with requirements.

INL Contractor Management responsibilities include:

- Ensuring adequate technical and QA training is provided for personnel performing activities.
- Ensuring compliance with all applicable regulations, DOE orders and requirements, and applicable federal, state, and local laws.
- Ensuring personnel adhere to procedures for the generation, identification, control, and protection of QA records.
- Exercising authority and responsibility to STOP unsatisfactory work such that cost and schedule do not override environmental, safety, or health considerations.
- Developing, implementing, and maintaining plans, policies, and procedures that implement the Quality Assurance Program Description (QAPD).
- Identifying, investigating, reporting, and correcting quality problems.
- Achieving and maintaining quality in their respective areas. (Quality achievement is the responsibility of those performing the work. Quality achievement is verified by persons or organizations not directly responsible for performing the work.)
- Empowering employees by delegating authority and decision making to the lowest appropriate level in the organization.

#### 9.1.1.2 Members of the INL Contractor Workforce (at all levels)

- Implement the organization's procedures to meet QA requirements.
- Comply with administrative and technical work control requirements.
- Identify and report issues to the responsible manager for resolution and continuous improvement for the work being performed.
- Seek, identify, and recommend work methods or procedural changes that would improve quality and efficiency.

#### 9.1.1.3 INL Contractor Quality Assurance Management

The INL Contractor QA Management provides independent oversight of all quality related activities.

## 9.2 Quality Assurance Program

### 9.2.1 General

The INL Contractor's QA Program defines and establishes requirements for programs, projects, and activities.

The INL Contractor QA program is developed and maintained through an ongoing process that

selectively applies QA criteria as appropriate to the function or work activity being performed. Applicable QA criteria consist of the following:

- Title 10 CFR Subpart 71, Packaging and Transportation of Radioactive Material
- Title 10 CFR 830.120, Quality Assurance Requirements
- ASME NQA-1-2000, Quality Assurance Requirements for Nuclear Facility Application
- DOE O 414.1C, Quality Assurance
- DOE O 461.1B, Packaging and Transport Safety
- DOE G 414.1-1A, Management Assessment and Independent Assessment

The INL Contractor QA Program is inclusive of applicable requirements from criteria noted above and addresses the following for this SAR:

- Organization
- Quality Assurance Program
- Implementation of the QA Program
- Personnel Qualification and Training
- Quality Improvement
- Documents
- Records
- Work Process
- Procurement
- Inspection and Testing
- Management Assessments
- Independent Assessment

The INL Contractor QA Director is responsible for ensuring implementation of requirements as defined within the QA program and requirements of this SAR, including design, procurement, fabrication, inspection, testing, maintenance, and modifications. Procurement documents are to reflect applicable requirements from 10 CFR 71, Subpart H, ASME NQA-1 and the QA program.

INL Contractor Quality Management assesses the adequacy and effectiveness of the QA program to ensure effective implementation inclusive of objective evidence and independent verification, where appropriate, to demonstrate that specific project and regulatory objectives are achieved.

All INL Contractor personnel and contractors are responsible for effective implementation of the QA program within the scope of their responsibilities. INL Contract packaging and quality engineers are responsible for inspection and testing and are to be qualified, as appropriate, through minimum education and/or experience, formal training, written examination and/or other demonstration of skill and proficiency. Objective evidence of qualifications and capabilities are to be maintained as required. As appropriate, the initial employee training should consist of the following:

- General employee indoctrination
- Program indoctrination
- QA program training
- Applicable NRC and DOT requirements.

**Note:** Only packaging engineers and Quality Engineers with training and/or experience in applicable NRC and DOT requirements and Safety Analysis Reports (SARs) can plan or determine the application of internal INL processes to ensure compliance with Chapter 9 and this SAR.

## 9.2.2 ATR FFSC-Specific Program

The ATR FFSC was designed and tested as described in Chapter 2, *Structural Evaluation,* of this SAR. QA requirements are invoked in the design, procurement, fabrication, assembly, testing, maintenance, and use of the packaging to ensure established standards are maintained. Items and activities to be controlled and documented are described in this chapter.

## 9.2.3 QA Levels

Materials and components of the ATR FFSC are designed, procured, fabricated, assembled, and tested using a graded approach under a 10 CFR 71, Subpart H equivalent QA Program and Regulatory Guide (RG) 7.10. Under that program, the categories critical to safety are established for all ATR FFSC packaging components. These defined quality categories consider the impact to safety if the component were to fail or perform outside design parameters.

### 9.2.3.1 Graded Quality Category A Items:

These items and services are critical to safe operation and include structures, components, and systems whose failure could directly result in a condition adversely affecting public health and safety. The failure of a single item could cause loss of primary containment leading to a release of radioactive material beyond regulatory requirements, loss of shielding beyond regulatory requirements, or unsafe geometry compromising criticality control.

### 9.2.3.2 Graded Quality Category B Items:

These items and services have a major impact on safety and include structures, components, and systems whose failure or malfunction could indirectly result in a condition adversely affecting public health and safety. The failure of a Category B item, in conjunction with the failure of an additional item, could result in an unsafe condition.

### 9.2.3.3 Graded Quality Category C Items:

These items and services have a minor impact on safety and include structures, components, and systems whose failure or malfunction would not significantly reduce the packaging effectiveness and would not be likely to create a situation adversely affecting public health and safety.

### 9.2.3.4 Application of Quality Categories

The design effort and requirements for a QA program are interrelated and are developed simultaneously. To ensure the development of a QA program in which the application of QA requirements is commensurate with their safety significance, engineering personnel perform a systematic analysis of each component, structure, and system to assess the consequences to the health and safety of the public and the environment that would result from malfunction or failure

of such items. This engineering assessment is initiated during the design process and performed in accordance with approved procedures. Establishment of the engineering basis during the design process enables a uniform, consistent application of QA requirements during fabrication, use, and maintenance of packaging.

A logical sequence is established to identifying realistic QA requirements would involve (1) classifying each structure, system, and component (2) grouping items classified as important to safety into quality categories; and (3) specifying the applicable level of QA effort for each category.

The Design Authority (DA) identifies the critical characteristics when they identify design attributes necessary to preserve the safety support function. As necessary, the DA also ensures critical characteristics are included in this SAR by the identification of SSCs and their QA Category designations. Additionally, this SAR includes the safety function, design, and operational attributes necessary for reliable performance. The DA applies design criteria to the design, operation, and maintenance of each critical SSC including recommended codes and standards, as required by RG 7.10. QA requirements shall be applied as necessary to assure the SSCs can perform their function.

The package-specific safety documents identify systems, structures, and components (SSCs) that are important to the safety functions for transportation. As appropriate, the hazard analysis and accident scenarios in the safety basis documents help identify SSCs that must function in order to prevent or mitigate these events. These SSCs are then identified using the classification system found in the NRC QA Category system provided in NRC Regulatory Guide (RG) 7.10. The categories as defined in RG 7.10, and listed below, are analogous to Safety Class, Safety Significant, and General Service that are identified for facility SSCs.

Upon custodianship of the ATR FFSC packages by INL, functional classifications will be used for site operations and activities related to the ATR FFSC. The method of classification is documented as follows.

**Quality Category A:**

Critical impact on safety and associated functional requirements – items or components whose single failure or malfunction could directly result in an unacceptable condition of containment, shielding, or nuclear criticality control. This is functionally equivalent to "safety class" designation used for nuclear facility safety.

**Quality Category B:**

Impact on safety and associated functional requirement – components whose failure or malfunction in conjunction with one other independent failure or malfunction could result in an unacceptable condition of containment, shielding, or nuclear criticality control. This is functionally equivalent to "safety significant" designation used for nuclear facility safety.

**Quality Category C:**

Minor impact on safety and associated functional requirements – components whose failure or malfunction would not result in an unacceptable condition of containment, shielding, or nuclear criticality control regardless of other single failures. This is functionally equivalent to designations given to components that do not meet "safety class or safety significant" criteria used for nuclear facility safety.

The tabulation of this classification process is provided in Tables 9.2-1 and 9.2-2.

**Table 9.2-1** - QA Categories for Design and Procurement of ATR FFSC Subcomponents

| Component | Subcomponent | Category |
|---|---|---|
| Body Assembly | Outer Square Tube | A |
| | Inner Round Tube | A |
| | Bottom End Plate | A |
| | Closure End Plate | A |
| | Stiffening Ribs | A |
| | Thermal Shield Sheet | B |
| | Insulation | B |
| | Tamper Indicating Device Dowel Pin | C |
| | Index Lug Screw | B |
| | Weld Wire | A |
| Closure Assembly | Outer Plate, Closure | A |
| | Inner Plate (Insulation Pocket) | B |
| | Closure Locking Hardware (Pin, Handle, Spring, etc.) | B |
| | Insulation | B |
| | Tamper Indicating Device Dowel Pin | C |
| | Weld Wire | A |
| Fuel Handling Enclosure | Aluminum Body Sheets | C |
| | Aluminum End Plates | C |
| | Fasteners and Hardware | C |
| Loose Fuel Plate Basket | Machined Aluminum Body | A |
| | Screws, Wing Nuts, and Hex Nuts | C |

## Table 9.2-2 - Level of Quality Assurance Effort per QA Element

| 10CFR71 Subpart H QA Element | Level of QA Effort | QA Category | | |
|---|---|---|---|---|
| | | A | B | C |
| 1 (71.103) | **QA Organization (¶9.1)** | | | |
| | • Organizational structure and authorities defined | X | X | |
| | • Responsibilities defined | X | X | |
| | • Reporting levels established | X | X | |
| | • Management endorsement | X | X | |
| 2 (71.105) | **QA Program (¶9.2)** | | | |
| | • Implementing procedures in place | X | X | |
| | • Trained personnel | X | X | |
| | • Activities controlled | X | X | |
| 3 (71.107) | **Design (¶9.3)** | | | |
| | • Control of design process and inputs | X | X | X |
| | • Control of design input | X | X | X |
| | • Software validated and verified | X | X | |
| | • Design verification controlled | X | X | |
| | • Quality category assessment performed | X | X | |
| 4 (71.109) | **Procurement Document Control (¶9.4)** | | | |
| | • Complete traceability | X | X | |
| | • Qualified suppliers list | X | X | |
| | • Commercial grade dedicated items acceptable | X | X | |
| | • Off-the-shelf item | | | X |
| 5 (71.111) | **Instructions, Procedures, and Drawings (¶9.5)** | | | |
| | • Must be written and controlled | X | X | |
| | • Qualitative or quantitative acceptance criteria | X | X | |
| 6 (71.113) | **Document Control (¶9.6)** | | | |
| | • Controlled issuance | X | X | |
| | • Controlled changes | X | X | |
| | • Procurement documents | X | X | X |

| 10CFR71 Subpart H QA Element | Level of QA Effort | QA Category A | QA Category B | QA Category C |
|---|---|---|---|---|
| 7 (71.115) | **Control of Purchased Material, Equipment, and Services (¶9.7)** | | | |
| | • Source evaluation and selection plans | X | X | |
| | • Evidence of QA at supplier | X | X | |
| | • Inspections at supplier, as applicable | X | X | |
| | • Receiving inspection | X | X | |
| | • Objective proof that all specifications are met | X | X | |
| | • Audits/surveillances at supplier facility, as applicable | X | X | |
| | • Incoming inspection for damage only | | | X |
| 8 (71.117) | **Identification and Control of Material, Parts, and Components (¶9.8)** | | | |
| | • Positive identification and traceability of each item | X | X | |
| | • Identification and traceable to heats, lots, or other groupings | X | X | |
| | • Identification to end use drawings, etc. | | | X |
| 9 (71.119) | **Control of Special Processes (¶9.9)** | | | |
| | • All welding, heat treating, and nondestructive testing done by qualified personnel | X | X | |
| | • Qualification records and training of personnel | X | X | |
| | • No special processes | | | X |
| 10 (71.131) | **Inspection (¶9.10)** | | | |
| | • Documented inspection to all specifications required | X | X | |
| | • Examination, measurement, or test of material or processed product to assure quality | X | X | |
| | • Process monitoring if quality requires it | X | X | |
| | • Inspectors must be independent of those performing operations | X | X | X |
| | • Qualified inspectors only | X | X | X |
| | • Receiving inspection | X | X | X |
| 11 (71.123) | **Test Control (¶9.11)** | | | |
| | • Written test program | X | X | |
| | • Written test procedures for requirements in the package approval | X | X | |
| | • Documentation of all testing and evaluation | X | X | |
| | • Representative of buyer observes all supplier acceptance tests if specified in procurement documents | X | | |
| | • No physical tests required | | | X |

| 10CFR71 Subpart H QA Element | Level of QA Effort | QA Category A | QA Category B | QA Category C |
|---|---|---|---|---|
| 12 (71.125) | **Control of Measuring and Test Equipment (¶9.12)** | | | |
| | • Tools, gauges, and instruments to be in a formal calibration program | X | X | |
| | • Only qualified inspectors | X | X | |
| | • No test required | | | X |
| 13 (71.127) | **Handling, Storage, and Shipping (¶9.13)** | | | |
| | • Written plans and procedures required | X | X | |
| | • Routine handling | | | X |
| 14 (71.129) | **Inspection, Test, and Operating Status (¶9.14)** | | | |
| | • Individual items identified as to status or condition | X | X | |
| | • Stamps, tags, labels, etc., must clearly show status | X | X | X |
| | • Visual examination only | | | X |
| 15 (71.131) | **Nonconforming Materials, Parts, or Components (¶9.15)** | | | |
| | • Written program to prevent inadvertent use | X | X | X |
| | • Nonconformance to be documented and closed | X | X | X |
| | • Disposal without records | | | X |
| 16 (71.133) | **Corrective Action (¶9.16)** | | | |
| | • Objective evidence of closure for conditions adverse to quality | X | X | X |
| 17 (71.135) | **QA Records (¶9.17)** | | | |
| | • Design and use records | X | X | |
| | • Results of reviews, inspections, test, audits, surveillance, and materials analysis | X | X | |
| | • Personnel qualifications | X | X | |
| | • Records of fabrication, acceptance, and maintenance retained throughout the life of package | X | X | X |
| | • Record of package use kept for three years after shipment | X | X | |
| | • All records managed by written plans for retention and disposal | X | X | |
| | • Procurement records | X | X | X |
| 18 (71.137) | **Audits (¶9.18)** | | | |
| | • Written plan of periodic audits | X | X | |
| | • Lead auditor certified | X | X | |

# 9.3 Package Design Control

As required by the INL Contractor's Quality Program, design processes shall be established and implemented to satisfy the requirements of the QAPD. These requirements are to be in accordance with:

- 10 CFR 830.122(f), *Criterion 6 – Performance/Design*[3]
- DOE Order 414C, CRD, Attachment 1, 2.b.(2), *Criterion 6 – Design.*

Requirements are implemented to ensure processes and procedures are in place to ensure design features of packaging systems are appropriately translated into specifications, drawings, procedures, and instructions. Design control measures are established for criticality, shielding, thermal, and structural analyses under both normal and accident condition analyses as defined in NRC regulations.

The INL Contractor is responsible for maintaining the package and this SAR. The design documents (e.g., drawings and specifications) are controlled by incorporation into this SAR, which will be reviewed and approved by the NRC.

The design of the ATR FFSC was performed under an NRC-approved QA Program as required by INL. Design inputs consist of an INL statement of work, applicable DOE orders, national standards, specifications, and drawings.

Procedures control design activities to ensure the following occur:

- Design activities are planned, controlled, and documented.
- Regulatory requirements, design requirements, and appropriate quality standards are correctly translated into specifications, drawings, and procedures.
- Competent engineering personnel, independent of design activities, perform design verification. Verification may include design reviews, alternate calculations, or qualification testing. Qualification tests are conducted in accordance with approved test programs or procedures.
- Design interface controls are established and adequate.
- Design, specification, and procedure changes are reviewed and approved in the same manner as the original issue. In a case where a proposed design change potentially affects licensed conditions, the Quality Assurance Program shall provide for ensuring that licensing considerations have been reviewed and are complied with or otherwise reconciled by amending the license.
- Design errors and deficiencies are documented, corrected and corrective action to prevent recurrence is taken.
- Design organization(s) and their responsibilities and authorities are delineated and controlled through written procedures.

[3] DOE, Code of Federal Regulations, 10 CFR 830.122, *Quality Assurance Criteria*, U.S. Department of Energy, Washington, D.C., 2006.

Materials, parts, equipment, and processes essential to the function of items that are important to safety are selected and reviewed for suitability of application.

Computer programs used for design analysis or verification are controlled in accordance with approved procedures. These procedures provide for verification of the accuracy of computer results and for the assessment and resolution of reported computer program errors.

## 9.4 Procurement Document Control

As required by the INL Contractor Quality Program, procurement/acquisition processes and related document control activities are established and implemented to satisfy requirements of the QAPD. Requirements are to be in accordance with:

- 10 CFR 830.122(d), *Criterion 4 – Management/Documents and Records*
- 10 CFR 830.122(g), *Criterion 7 – Performance/Procurement*
- DOE Order 414C, CRD, Attachment 1, 2.a.(4), *Criterion 4 – Documents and Records*
- DOE Order 414C, CRD, Attachment 1, 2.b.(3), *Criterion 7 – Procurement*
- DOE Guide 414.1-3, *Suspect/Counterfeit Items.*

Processes and procedures are in place to ensure appropriate levels of quality are achieved in procurement of material, equipment, and services. Quality Level and Quality Category designations assigned by the Design Authority grade the application of QA requirements for procurements based on radiological material at risk, mission importance, safety of workers, public, environment, and equipment, and other differentiating criteria. Implementing procedures provide the logic process for determining Quality Levels used in procurement of equipment and subcontracting of services. Procedures ensure processes address document preparation and document control, and records management to meet regulatory requirements. Procurement records are kept in a manner that satisfies regulatory requirements.

INL Contractor is responsible for initiating procurement actions for packaging and spare parts from a supplier with a 10 CFR 71, Subpart H QA Program.

Implementing procedures ensure procurement documents are prepared to clearly define applicable technical and quality assurance requirements including codes, standards, regulatory requirements and commitments, and contractual requirements. These documents serve as the principal documents for procurement of structures, systems and components, and related services for use in design, fabrication, maintenance and operation, inspection and testing of storage and/or transportation systems. Procedures ensure purchased material, components, equipment, and services adhere to applicable requirements. Furthermore:

- The assignment of quality requirements through procurement documents is administered and controlled.
- Procurement activities are performed in accordance with approved procedures delineating requirements for preparation, review, approval, and control of procurement documents. Revisions to procurement documents are reviewed and approved by the same cognizant groups as the original document.

- Quality requirements are included in quality-related purchase orders as applicable to the scope of the procurement referencing 10 CFR 71, Subpart H or other codes and standards, as appropriate.
- INL Contractor procurement documents will require suppliers to convey appropriate quality assurance program requirements to sub-tier suppliers.
- INL Contractor procurement documents will include provisions that suppliers either maintain or supply those QA records which provide evidence of conformance to the procurement documents. Additionally, procurement documents shall designate the supplier documents required for submittal to INL for review and/or approval.
- INL shall maintain the right of access to supplier facilities and performance of source surveillance and/or audit activities, as applicable. A statement to this effect is to be included in procurement documents.
- INL shall require the Supplier to warrant that all items furnished under the Contract are genuine (i.e., new, not refurbished, not counterfeit) and match the quality, test reports, markings and/or fitness for intended use as required by the Contract. Any materials furnished as part of the Contract which has been previously found to be suspect/counterfeit by the government or other duly recognized agency, shall not be used.

Procurement documents shall also address the applicability of the provisions of 10 CFR 21 for the Reporting of Defects and Noncompliances.

## 9.5 Instructions, Procedures, and Drawings

As required by the INL Contractor Quality Program, instructions, procedures, and drawing work processes and applicable quality improvement activities shall be established and implemented to satisfy the requirements of the QAPD. These requirements are to be in accordance with:

- 10 CFR 830.122(c), *Criterion 3 – Management/Quality Improvement*
- 10 CFR 830.122(e), *Criterion 5 – Performance/Work Processes*
- DOE Order 414C, CRD, Attachment 1, 2.a.(3), *Criterion 3 – Quality Improvement*
- DOE Order 414C, CRD, Attachment 1, 2.b.(1), *Criterion 5 – Work Processes.*

Requirements are implemented to ensure processes and procedures are in place that achieve quality objectives and ensure appropriate levels of quality and safety are applied to critical components of packaging and transportation systems utilizing a graded approach. The program shall ensure processes and procedures in place to identify and correct problems associated with transportation and packaging activities.

Implementing procedures shall be established to ensure that methods for complying with each of the applicable criteria of 10 CFR 71, Subpart H, as applicable, for activities affecting quality during design, fabrication, inspection, testing, use and maintenance are specified in instructions, procedures, and/or drawings. In addition:

- Instructions, procedures, and drawings shall be developed, reviewed, approved, utilized, and controlled in accordance with the requirements of approved procedures. These

instructions, procedures, and drawings shall include appropriate quantitative and qualitative acceptance criteria.

- Changes to instructions, procedures and drawings, are developed, reviewed, approved, utilized and controlled using the same requirements and controls as applied to the original documents.
- Compliance with these approved instructions, procedures and drawings is mandatory for INL personnel while performing activities affecting quality.

Specific activities by INL regarding preparation of packaging for use, repair, rework, maintenance, loading contents, unloading contents, and transport, must be accomplished in accordance with written and approved instructions, procedures, specifications, and/or drawings. These documents must identify appropriate inspection and hold points and emphasize those characteristics that are important to safety and quality. Transportation package procedures are to be developed and reviewed by technical and quality staff and shall be approved by appropriate levels of management.

### 9.5.1 Preparation and Use

Activities concerning loading and shipping are performed in accordance with written operating procedures developed by the user and approved by the package custodian. Packaging first-time usage tests, sequential loading and unloading operations, technical constraints, acceptance limits, and references are specified in the procedures. A pre-planned and documented inspection will be conducted to ensure that each loaded package is ready for delivery to the carrier.

### 9.5.2 Operating Procedure Changes

Changes in operating procedures that affect the process must be approved at the same supervisory level as the initial issue.

### 9.5.3 Drawings

Controlled drawings are shown in Appendix 1.3.2, *Packaging General Arrangement Drawings*, of this SAR. Implementation of design revisions is discussed in SAR Section 9.3, *Package Design Control.*

## 9.6 Document Control

As required by the INL Contractor Quality Program, document control activities shall be established and implemented to satisfy the requirements of the QAPD. These requirements are to be in accordance with:

- 10 CFR 830.122(d), *Criterion 4 – Management/Documents and Records*
- DOE Order 414C, CRD, Attachment 1, 2.a.(4), *Criterion 4 – Documents and Records.*

Requirements are implemented to ensure processes and procedures are in place to address document, document control, and for the management of records. Records (engineering, test

reports, user instructions, etc.) must be maintained in a manner that conforms to regulatory requirements.

Document control activities related to the design, procurement, fabrication, and testing of ATR FFSC components; and SAR preparation shall be controlled.

Implementing procedures shall be established to control the issuance of documents that prescribe activities affecting quality and to assure adequate review, approval, release, distribution, use of documents and their revisions. Controlled documents may include, but are not limited to:

- Design specifications
- Design and fabrication drawings
- Special process specifications and procedures
- QA Program Manuals/Plans, etc.
- Implementing procedures
- Test procedures
- Operational test procedures and data.

Requirements shall ensure changes to documents, which prescribe activities affecting quality, are reviewed and approved by the same organization that performed the initial review and approval, or by qualified responsible organizations. Documents that prescribe activities affecting quality are to be reviewed and approved for technical adequacy and inclusion of appropriate quality requirements prior to approval and issuance. Measures are taken to ensure that only current documents are available at the locations where activities affecting quality are performed prior to commencing the work.

Package users are responsible for establishment, development, review, approval, distribution, revision, and retention of their documents. Documents requiring control, the level of control, and the personnel responsibilities and training requirements are to be identified.

Packaging documents to be controlled include as a minimum:

- Operating procedures
- Maintenance procedures
- Inspection and test procedures
- Loading and unloading procedures
- Preparation for transport procedures
- Repair procedures
- Specifications
- Fabrication records
- Drawings of packaging and components
- SAR and occurring supplements.

Revisions are handled in a like manner as the original issue. Only the latest revisions must be available for use.

Documentation received from the supplier for each package must be filed by package serial number. These documents are to be retained in the user's facility.

## 9.7 Control Of Purchased Material, Equipment And Services

As required by the INL Contractor Quality Program, the control of purchased material, equipment and services and applicable quality improvement activities shall be established and implemented to satisfy the requirements of the QAPD. These requirements are to be in accordance with:

- 10 CFR 830.122(c), *Criterion 3 – Management/Quality Improvement*
- 10 CFR 830.122(g), *Criterion 7 – Performance/Procurement*
- 10 CFR 830.122(h), *Criterion 8 – Performance/Inspection and Acceptance Testing*
- DOE Order 414C, CRD, Attachment 1, 2.b.(3), *Criterion 3 – Quality Improvement*
- DOE Order 414C, CRD, Attachment 1, 2.b.(3), *Criterion 7 – Procurement*
- DOE Order 414C, CRD, Attachment 1, 2.b.(4), *Criterion 8 – Inspection and Acceptance Testing.*

Requirements are implemented to ensure processes and procedures are in place to ensure appropriate inspections and tests are applied prior to acceptance or use of the packaging or component, and to identify the status of packaging items, components, etc. Requirements shall ensure processes and procedures are in place such that appropriate levels of quality are achieved in the procurement of material, equipment, and services. Quality Level and Quality Category designations by the Design Authority are used to grade the application of QA requirements of procurements based on radiological material at risk, mission importance, safety of workers, public, environment, and equipment, and other differentiating criteria. Requirements shall ensure processes and procedures in place to identify and correct problems associated with transportation and packaging activities.

Activities related to the control of purchased material, equipment and services shall be controlled. Control of purchased material, equipment, and services consist of the following elements:

- Implementing procedures shall be established to assure that purchased material, equipment and services conform to procurement documents.
- Procurement documents shall be reviewed and approved by authorized personnel for acceptability of proposed suppliers based on the quality requirements of the item/activity being purchased.
- As required, audits and/or surveys are conducted to determine supplier acceptability. These audits/surveys are based on one or all of the following criteria: the supplier's capability to comply with the requirements of 10 CFR 71, Subpart H that are applicable to the scope of work to be performed; a review of previous records to establish the past performance of the supplier; and/or a survey of the supplier's facilities and review of the

supplier's QA Program to assess adequacy and verify implementation of quality controls consistent with the requirements being invoked.

- Qualified personnel shall conduct audits and surveys. Audit/survey results are to be documented and retained as Quality Assurance Records. Suppliers are re-audited and/or re-evaluated at planned intervals to verify that they continue to comply with quality requirements and to assess the continued effectiveness of their QA Program. Additionally, interim periodic evaluations are to be performed of supplier quality activities to verify implementation of their QA Program.
- Suppliers are required to provide objective evidence that items or services provided meet the requirements specified in procurement documents. Items are properly identified to appropriate records that are available to permit verification of conformance with procurement documents. Any procurement requirements not met by suppliers shall be reported to INL Contractor Quality Management for assessment of the condition. These conditions are reviewed by technical and quality personnel to assure that they have not compromised the quality or service of the item.
- Periodic surveillance of supplier in-process activities is performed as necessary, to verify supplier compliance with the procurement documents. When deemed necessary, the need for surveillance is noted in approved quality or project planning documents. Surveillances are to be performed and documented in accordance with approved procedures. Personnel performing surveillance of supplier activities are to be trained and qualified in accordance with approved procedures.
- Quality planning for the performance of source surveillance, test, shipping and/or receiving inspection activities to verify compliance with approved design and licensing requirements, applicable 10 CFR 71 criteria, procurement document requirements, or contract specifications is to be performed in accordance with approved procedures.
- For commercial "off-the-shelf" items, where specific quality controls appropriate for nuclear applications cannot be imposed in a practical manner, additional quality verification shall be performed to the extent necessary to verify the acceptability and conformance of an item to procurement document requirements. When dedication of a commercial grade item is required for use in a quality-related application, such dedication shall be performed in accordance with approved procedures.

To ensure compliance with procurement requirements, control measures shall include verification of supplier capability and verification of item or service quality. Procurements of ATR FFSC components are required to be placed with pre-qualified and selected vendors. The vendor's QA Plan must address the requirements of 10 CFR 71, Subpart H and defined requirements. A graded approach is used based on the QA Levels established in Table 9.2-2.

The approach used to control the procurement of items and services must include the following:

- Source evaluation and selection
- Evaluation of objective evidence of quality furnished by the supplier
- Source inspection
- Audit
- Examination of items or services upon delivery or completion.

## 9.8 Identification And Control Of Material, Parts And Components

As required by the INL Contractor Quality Program, activities concerning the identification and control of material, parts, and components shall be established and implemented to satisfy the requirements of QAPD. These requirements are to be in accordance with:

- 10 CFR 830.122(e), *Criterion 5 – Performance/Work Processes*
- 10 CFR 830.122(g), *Criterion 7 – Performance/Procurement*
- 10 CFR 830.122(h), *Criterion 8 – Performance/Inspection and Acceptance Testing*
- DOE Order 414C, CRD, Attachment 1, 2.b.(1), *Criterion 5 – Work Processes*
- DOE Order 414C, CRD, Attachment 1, 2.b.(3), *Criterion 7 – Procurement*
- DOE Order 414C, CRD, Attachment 1, 2.b.(4), *Criterion 8 – Inspection and Acceptance Testing.*

Requirements are implemented to ensure processes and procedures are in place that achieve quality objectives and ensure appropriate levels of quality and safety are applied to critical components of packaging and transportation systems utilizing a graded approach. The program also ensures processes and procedures are in place such that appropriate inspections and tests are applied prior to acceptance or use of the packaging or component, and to identify the status of packaging items, and components. The program shall ensure processes and procedures are in place to ensure appropriate levels of quality are achieved in the procurement of material, equipment, and services.

Activities related to the identification and control of material, parts and components shall be controlled. The requirements for identification and control of material, parts, and components consist of the following elements:

- Implementing procedures are established to identify and control materials, parts, and components. These procedures assure identification of items by appropriate means during fabrication, installation, and use of the items and prevent the inadvertent use of incorrect or defective items.
- Requirements for identification are established during the preparation of procedures and specifications.
- Methods and location of identification are selected to not adversely affect the quality of the item(s) being identified.

- Items having limited shelf or operating life are controlled to prevent their inappropriate use.

Control and identification must be maintained either directly on the item or within documents traceable to the item to ensure that only correct and acceptable items are used. When physical identification is not practical, other appropriate means of control must be established such as bagging, physical separation, or procedural control. Each packaging unit shall be assigned a unique serial number after fabrication or purchase. All documentation associated with subsequent storage, use, maintenance, inspection, acceptance, etc., must refer to the assigned serial number. Verification of acceptance status is required prior to use. Items that are not acceptable must be controlled accordingly. Control of nonconforming items is addressed in Section 9.15, *Nonconforming Parts, Materials, or Components.*

Each ATR FFSC package will be conspicuously and durably marked with information identifying the package owner, model number, unique serial number, and package gross weight, in accordance with 10 CFR 71.85(c).

Replacement parts must be identified to ensure correct application. Minute items must be individually packaged with the package marked with the part identification and traceability information.

## 9.9 Control Of Special Processes

As required by the INL Contractor Quality Program, activities for the control of special processes shall be established and implemented to satisfy the requirements of the QAPD. These requirements are to be in accordance with:

- 10 CRF 830.122(b), *Criterion 2 – Management/Personnel Training and Qualifications*
- 10 CFR 830.122(e), *Criterion 5 – Performance/Work Processes*
- 10 CFR 830.122(g), *Criterion 7 – Performance/Procurement*
- DOE Order 414C, CRD, Attachment 1, 2.a.(2), *Criterion 2 - Personnel Training and Qualifications*
- DOE Order 414C, CRD, Attachment 1, 2.b.(1), *Criterion 5 – Work Processes*
- DOE Order 414C, CRD, Attachment 1, 2.b.(3), *Criterion 7 – Procurement.*

Requirements will be implemented to ensure only trained and qualified personnel perform transportation and packaging activities. The program shall ensure processes and procedures are in place that achieve quality objectives and ensure appropriate levels of quality and safety are applied to critical components of packaging and transportation systems utilizing a graded approach.

Activities related to the control of special processes shall be controlled. The requirements for control of special processes consist of the following elements:

- Implementing procedures shall be established to control special processes used in the fabrication and inspection of storage/transport systems. These processes may include welding, non-destructive examination, or other special processes as identified in procurement documents.

- Special processes are performed in accordance with approved procedures.
- Personnel who perform special processes shall be trained and qualified in accordance with applicable codes, standards, specifications, and/or other special requirements. Records of qualified procedures and personnel are to be maintained and kept current by the organization that performs the special processes.

Package users are responsible to ensure special processes for welding and nondestructive examination of the ATR FFSC during fabrication, use, and maintenance are controlled. Equipment used in conduct of special processes must be qualified in accordance with applicable codes, standards, and specifications. Special process operations must be performed by qualified personnel and accomplished in accordance with written process sheets or procedures with recorded evidence of verification when applicable. Qualification records of special process procedures, equipment, and personnel must be maintained.

Welders, weld procedures, and examination personnel are to be qualified in accordance with the appropriate articles of ASME BPVC, Section IX, "Welding and Brazing Qualifications";[4] and ASME BPVC, Section V, "Nondestructive Examination."[5]

Special processes for QA Level A and B items must be performed by qualified personnel in accordance with documented and approved procedures. Applicable special processes performed by an outside supplier such as welding, plating, anodizing, and heat treating, which are controlled by the suppliers' quality program, are reviewed and/or witnessed in accordance with procurement requirements.

## 9.10 Internal Inspection

As required by the INL Contractor Quality Program, internal inspection activities shall be established to satisfy the requirements of the QAPD. These requirements are to be in accordance with:

- 10 CRF 830.122(b), *Criterion 2 – Management/Personnel Training and Qualifications*
- 10 CFR 830.122(h), *Criterion 8 – Performance/Inspection and Acceptance Testing*
- DOE Order 414C, CRD, Attachment 1, 2.a.(2), *Criterion 2 - Personnel Training and Qualifications*
- DOE Order 414C, CRD, Attachment 1, 2.b.(4), *Criterion 8 – Inspection and Acceptance Testing.*

Requirements are implemented to ensure only trained and qualified personnel perform transportation and packaging activities. The program shall ensure processes and procedures are in place to ensure appropriate inspections and tests are applied prior to acceptance or use of the packaging or component, and to identify the status of packaging items, components, etc.

---

[4] ASME, 2004, American Society of Mechanical Engineers Boiler and Pressure Vessel Code, Section IX, *Welding and Brazing Qualifications*, American Society of Mechanical Engineers, New York, NY

[5] ASME, 2004, American Society of Mechanical Engineers Boiler and Pressure Vessel Code, Section V, *Nondestructive Examination*, American Society of Mechanical Engineers, New York, NY

Activities related to internal inspection shall be controlled. The program requirements for control of internal inspection consist of the following elements:

- Implementing procedures shall be established to assure that inspection or surveillance is performed to verify that materials, parts, processes, or other activities affecting quality conform to documented instructions, procedures, specifications, drawings, and/or procurement documents.
- Personnel performing inspection and surveillance activities shall be trained and qualified in accordance with written approved procedures.
- Inspections and surveillances are to be performed by individuals other than those who performed or supervised the subject activities.
- Inspection or surveillance and process monitoring are both required where either one, by itself, will not provide assurance of quality.
- Modifications and/or repairs to and replacements of safety-related and important-to-safety structures, systems, and components are inspected in accordance with the original design and inspection requirements or acceptable alternatives.
- Mandatory hold points, inspection equipment requirements, acceptance criteria, personnel qualification requirements, performance characteristics, variable and/or attribute recording instructions, reference documents, and other requirements are considered and included, as applicable, during inspection and surveillance planning.

## 9.10.1 Inspections During Fabrication

Specific inspection criteria are incorporated into the drawings for the ATR FFSC packaging. Inspection requirements for fabrication are divided into two responsible areas that document that an accepted ATR FFSC package conforms to tested and certified design criteria. These two areas are:

- In-process inspections performed by the fabricator.
- Independent surveillance of fabrication activities performed by individuals acting on behalf of the purchaser.

The vendor (fabricator) is required to submit Manufacturing/Fabrication Plans prior to the start of fabrication for approval by the customer. These plans shall be used as a tool for establishing witness and hold points. A review for compliance with procurement documents is normally performed as part of the surveillance function at the vendor's facility. The plans shall define how fabrications and inspections are to be performed, processes to be engaged. Inspections must be documented and records delivered in individual data packages accompanying the package in accordance with the procurement specification.

Independent surveillance activities will be performed by qualified personnel selected with approval of the customer.

### 9.10.2 Inspections During Initial Acceptance and During Service Life

Independent inspections are performed upon receipt of the ATR FFSC packaging prior to first usage (implemented by package user procedures) and on an annual basis. Post-loading inspections are also performed prior to shipment. Inspection to be implemented by the package user (by qualified independent inspection personnel) must include the following:

- Acceptance – Ensure compliance with procurement documents. Per Chapter 8, *Acceptance Tests and Maintenance Program* of this SAR, perform (as applicable) first-time-usage inspections, and weld examinations.
- Operation – Verify proper assembly and verify that post-load leak testing (if applicable) is carried out as discussed in Chapter 7, *Package Operations*, of this SAR.
- Maintenance – Ensure adequate packaging maintenance to ensure that performance is not impaired as discussed in Chapter 8, *Acceptance Tests and Maintenance Program* of this SAR.
- Final – Verify proper contents, assembly, marking, shipping papers, and implementation of any special instructions.

## 9.11 Test Control

As required by the INL Contractor Quality Program, test control activities shall be established and implemented to satisfy the requirements of the QAPD. These requirements are to be in accordance with:

- 10 CFR 830.122(e), *Criterion 5 – Performance/Work Processes*
- DOE Order 414C, CRD, Attachment 1, 2.b.(1), *Criterion 5 – Work Processes.*

Requirements are implemented to ensure processes and procedures are in place that achieve quality objectives and ensure appropriate levels of quality and safety are applied to critical components of packaging and transportation systems utilizing a graded approach.

Activities related to test control shall be controlled. The requirements for test control consist of the following elements:

- Implementing procedures shall be established to assure that required proof, acceptance, and operational tests, as identified in design or procurement documents, are performed and appropriately controlled.
- Test personnel shall have appropriate training and shall be qualified for the level of testing which they are performing. Personnel shall be qualified in accordance with approved, written instructions, procedures, and/or checklists.
- Tests are performed by qualified personnel in accordance with approved, written instructions, procedures, and/or checklists. Test procedures are to contain or reference the following information, as applicable:
  - Acceptance criteria contained in the applicable test specifications, or design and procurement documents.
  - Instructions for performance of tests, including environmental conditions.

  - Test prerequisites such as test equipment, instrumentation requirements, personnel qualification requirements, fabrication, or operational status of the items to be tested.
  - Provisions for data recording and records retention.
- Test results are to be documented and evaluated to ensure that acceptance criteria have been satisfied.
- Tests to be conducted after modifications, repairs, or replacements of safety-related and important-to-safety structures, systems, or components are to be performed in accordance with the original design and testing requirements or acceptable alternatives.

Tests are required when it is necessary to demonstrate that an item or process will perform satisfactorily. Test procedures must specify the objectives of the tests, testing methods, required documentation, and acceptance criteria. Tests to be conducted by vendors at vendor facilities must be specified in procurement documents. Personnel conducting tests, test equipment, and procedures must be qualified and records attesting to qualification retained.

### 9.11.1 Acceptance and Periodic Tests

- The fabricator must supply QA documentation for the fabrication of each ATR FFSC packaging in accordance with applicable drawings, specifications, and/or other written requirements.
- The package user must ensure required ATR FFSC packaging inspections and tests are performed prior to first usage.
- Periodic testing, as applicable, will be performed to ensure the ATR FFSC packaging performance has not deteriorated with time and usage. The requirements for the periodic tests are given in the Chapter 8, *Acceptance Tests and Maintenance Program* of this SAR. The results of these tests are required to be documented and maintained with the specific packaging records by the package user.

### 9.11.2 Packaging Nonconformance

Packaging that does not meet the inspection criteria shall be marked or tagged as nonconforming, isolated, and documented in accordance with Section 9.15, *Nonconforming Parts, Materials, or Components*. The packaging must not be used for shipment until the nonconformance report has been properly dispositioned in accordance with Section 9.15.

## 9.12 Control Of Measuring And Test Equipment

As required by the INL Contractor Quality Program, activities pertaining to the control of measuring and test equipment shall be established and implemented to satisfy the requirements of the QAPD. These requirements are to be in accordance with:

- 10 CFR 830.122(h), *Criterion 8 – Performance/Inspection and Acceptance Testing*
- DOE Order 414C, CRD, Attachment 1, 2.b.(4), *Criterion 8 – Inspection and Acceptance Testing.*

Requirements are implemented to ensure processes and procedures are in place to ensure appropriate inspections and tests are applied prior to acceptance or use of the packaging or component, and to identify the status of packaging items, components, etc.

Activities pertaining to the control of measuring and test equipment shall be controlled. The requirements for control of measuring and test equipment shall consist of the following elements:

- Implementing procedures shall be established to assure that tools, gages, instruments and other measuring and testing devices (M&TE) used in activities affecting quality are properly controlled, calibrated and adjusted to maintain accuracy within required limits.
- M&TE are calibrated at scheduled intervals against certified standards having known valid relationships to national standards. If no national standards exist, the basis for calibration shall be documented. Calibration intervals are based on required accuracy, precision, purpose, amount of use, stability characteristics and other conditions that could affect the measurements.
- Calibrations are to be performed in accordance with approved written procedures. Inspection, measuring and test equipment are to be marked to indicate calibration status.
- M&TE are to be identified, labeled or tagged indicating the next required calibration due date, and traceable to calibration records.
- If M&TE is found to be out of calibration, an evaluation shall be performed and documented regarding the validity of inspections or tests performed and the acceptability of items inspected or tested since the previous acceptable calibration. The current status of M&TE is to be recorded and maintained. Any M&TE that is consistently found to be out of calibration shall be repaired or replaced.

Special calibration and control measures on rules, tape measures, levels and other such devices are not required where normal commercial practices provide adequate accuracy.

## 9.13 Handling, Storage, And Shipping Control

As required by the INL Contractor Quality Program, handling, storage, and shipping control activities shall be established and implemented to satisfy the requirements of the QAPD. These requirements are to be in accordance with:

- 10 CFR 830.122(e), *Criterion 5 – Performance/Work Processes*
- DOE Order 414C, CRD, Attachment 1, 2.b.(1), *Criterion 5 – Work Processes.*

Requirements are implemented to ensure processes and procedures are in place that achieve quality objectives and ensure appropriate levels of quality and safety are applied to critical components of packaging and transportation systems utilizing a graded approach.

Activities pertaining to handling, storage, and shipping shall be controlled. The requirements for handling, storage, and shipping control consist of the following elements:

- Implementing procedures shall be established to assure that materials, parts, assemblies, spare parts, special tools, and equipment are handled, stored, packaged, and shipped in a manner to prevent damage, loss, loss of identity, or deterioration.

- When necessary, storage procedures address special requirements for environmental protection such as inert gas atmospheres, moisture control, temperature levels, etc.

Package users shall ensure that components associated with the ATR FFSC are controlled to prevent damage or loss, protected against damage or deterioration, and provide adequate safety of personnel involved in handling, storage, and shipment (outgoing and incoming) operations. Handling, storage, and shipping must be accomplished in accordance with written and approved instructions, procedures, specifications, and/or drawings. These documents must identify appropriate information regarding shelf life, environment, temperature, cleaning, handling, and preservation, as applicable, to meet design, regulatory, and/or DOE shipping requirements.

Preparation for loading, handling, and shipment will be done accordance with approved procedures to ensure that all requirements have been met prior to delivery to a carrier. A package ready for shipment must conform to its shipping paper.

Empty packages, following usage, must be checked and decontaminated if required. Each package must be inspected, reconditioned, or repaired, as appropriate, in accordance with approved written procedures before storing or loading. Empty ATR FFSC packagings are to be tagged with "EMPTY" labels and stored in designated protected areas in order to minimize environmental effects on the containers.

Routine maintenance on the ATR FFSC packaging may be performed as deemed necessary by package users and is limited to cleaning, rust removal, painting, light metal working to restore the original contours and replacement of damaged, worn, or malfunctioning components. Spare components will be placed in segregated storage to maintain proper identification and to avoid misuse.

## 9.14 Inspection, Test, And Operating Status

As required by the INL Contractor Quality Program, inspection, test, and operating status activities shall be established and implemented to satisfy the requirements of the QAPD. These requirements are to be in accordance with:

- 10 CFR 830.122(e), *Criterion 5 – Performance/Work Processes*
- 10 CFR 830.122(h), *Criterion 8 – Performance/Inspection and Acceptance Testing*
- DOE Order 414C, CRD, Attachment 1, 2.b.(1), *Criterion 5 – Work Processes*
- DOE Order 414C, CRD, Attachment 1, 2.b.(4), *Criterion 8 – Inspection and Acceptance Testing.*

Requirements are implemented to ensure processes and procedures are in place that achieve quality objectives and ensure appropriate levels of quality and safety are applied to critical components of packaging and transportation systems utilizing a graded approach. In addition, processes and procedures shall be in place to ensure appropriate inspections and tests are applied prior to acceptance or use of the packaging or component, and to identify the status of packaging items, components, etc.

Activities pertaining to inspection, test, and operating status activities shall be controlled. The requirements for inspection, test, and operating status consist of the following elements:

- Implementing procedures shall be established to assure that the inspection and test status of materials, items, structures, systems, and components throughout fabrication, installation, operation, and test are clearly indicated by suitable means, (e.g., tags, labels, cards, form sheets, check lists, etc.).
- Bypassing of required inspections, tests, or other critical operations is prevented through the use of approved instructions or procedures
- As appropriate, the operating status of nonconforming, inoperative or malfunctioning components of a storage/transport system is indicated to prevent inadvertent operation. The application and removal of status indicators is performed in accordance with approved instructions and procedures.
- Any nonconforming items are identified and controlled in accordance with Section 9.15, *Nonconforming Parts, Materials, or Components*, of this SAR.

Package users shall ensure that the status of inspection and test activities are identified on the item or in documents traceable to the item to ensure that proper inspections or tests have been performed and that those items that do not pass inspection are not used. The status of fabrication, inspection, test, assembly, and refurbishment activities must be identified in documents traceable to the package components.

Measures established in specifications, procedures, and other instructions shall ensure that the following objectives are met:

- QA personnel responsible for oversight of packaging inspections can readily ascertain the status of inspections, tests, and/or operating conditions.
- No controlled items are overlooked.
- Inadvertent use or installation of unqualified items is prevented.
- Documentation is complete.

## 9.15 Nonconforming Materials, Parts, or Components

As required by the INL Contractor Quality Program, control of nonconforming materials, parts, or components shall be established and implemented to satisfy the requirements of the QAPD. These requirements are to be in accordance with:

- 10 CFR 830.122(c), *Criterion 3 – Management/Quality Improvement*
- DOE Order 414C, CRD, Attachment 1, 2.b.(3), *Criterion 3 – Quality Improvement.*

Requirements are implemented to ensure that processes and procedures are in place to identify and correct problems associated with transportation and packaging activities.

Activities pertaining to the control of nonconforming materials, parts, or components shall be controlled. The requirements for nonconforming materials, parts, or components consist of the following elements:

- Implementing procedures shall be established to control materials, parts, and components that do not conform to requirements to prevent their inadvertent use during fabrication or during service.

- Nonconforming items include those items that do not meet specification or drawing requirements. Additionally, nonconforming items include items not fabricated or tested (1) in accordance with approved written procedures, (2) by qualified processes, or (3) by qualified personnel; where use of such procedures, processes, or personnel is required by the fabrication, test, inspection, or quality assurance requirements.
- Nonconforming items are identified and/or segregated to prevent their inadvertent use until properly dispositioned. The identification of nonconforming items is by marking, tagging, or other methods that do not adversely affect the end use of the item. The identification shall be legible and easily recognizable. When identification of each nonconforming item is not practical, the container, package, or segregated storage area, as appropriate, is identified.
- Nonconforming conditions are documented in NCRs and affected organizations are to be notified. The nonconformance report shall include a description of the nonconforming condition. Nonconforming items are dispositioned as use-as-is, reject, repair, or rework.
- Inspection or surveillance requirements for nonconforming items following rework, repair are detailed in the nonconformance reports and approved following completion of the disposition.
- Acceptability of rework or repair of nonconforming materials, parts, and components is verified by re-inspecting and/or re-testing the item to the original requirements or equivalent inspection/testing methods. Inspection, testing, rework, and repair methods are to be documented and controlled.
- The disposition of nonconforming items as use-as-is or repair shall include technical justification and independent verification to assure compliance with design, regulatory, and contractual requirements.
- Items dispositioned as rework or repair are reinspected and retested in accordance with the original inspection and test requirements or acceptable alternatives that comply with the specified acceptance criteria.
- When specified by contract requirements, nonconformances that result in a violation of client contract or specification requirements shall be submitted for client approval.
- Nonconformance reports are made part of the inspection records and are periodically reviewed to identify quality trends. Unsatisfactory quality trends are documented on a Corrective Action Report (CAR) as detailed in Section 9.16, *Corrective Action*, of this SAR. The results of these reviews are to be reported to management.
- Nonconformance reports relating to internal activities are issued to management of the affected organization. The appropriate Quality Assurance Manager shall approve the disposition and performs follow-up activities to assure proper closure.
- Compliance with the evaluation and reporting requirements of 10 CFR 21 related to defects and noncompliances are to be controlled by approved procedures.

## 9.16 Corrective Action

As required by the INL Contractor Quality Program, requirements for corrective action shall be established and implemented to satisfy the requirements of the QAPD. These requirements are to be in accordance with:

- 10 CFR 830.122(c), *Criterion 3 – Management/Quality Improvement*
- DOE Order 414C, CRD, Attachment 1, 2.b.(3), *Criterion 3 – Quality Improvement.*

Requirements are implemented to ensure that processes and procedures are in place to identify and correct problems associated with transportation and packaging activities.

Activities pertaining to corrective actions shall be controlled. The requirements for corrective action consist of the following elements:

- Implementing procedures shall be established to identify significant conditions adverse to quality. Significant and/or repetitive failures, malfunctions and deficiencies in material, components, equipment, and operations are to be promptly identified and documented on a Corrective Action Reports (CARs) and reported to appropriate management. The cause of the condition and corrective action necessary to prevent recurrence are identified, implemented, and followed up to verify corrective action is complete and effective.
- The INL Contractor Quality Assurance Director (DQA) is responsible for ensuring implementation of the corrective action program, including follow up and closeout actions. The DQA may delegate certain activities in the Corrective Action process to others.

## 9.17 Quality Assurance Records

As required by the INL Contractor Quality Program, activities associated with QA records shall be established and implemented to satisfy the requirements of the QAPD. These requirements are to be in accordance with:

- 10 CRF 830.122(b), *Criterion 2 – Management/Personnel Training and Qualifications*
- 10 CFR 830.122(d), *Criterion 4 – Management/Documents and Records*
- 10 CFR 830.122(e), *Criterion 5 – Performance/Work Processes*
- 10 CFR 830.122(h), *Criterion 8 – Performance/Inspection and Acceptance Testing*
- DOE Order 414C, CRD, Attachment 1, 2.a.(2), *Criterion 2 - Personnel Training and Qualifications*
- DOE Order 414C, CRD, Attachment 1, 2.a.(4), *Criterion 4 – Documents and Records*
- DOE Order 414C, CRD, Attachment 1, 2.b.(1), *Criterion 5 – Work Processes*
- DOE Order 414C, CRD, Attachment 1, 2.b.(4), *Criterion 8 – Inspection and Acceptance Testing.*

Requirements are implemented to ensure that only trained and qualified personnel perform transportation and packaging activities. The program shall ensure processes and procedures are

in place to address document preparation, document control, and management of records. In addition, the program ensures processes and procedures are in place which achieves quality objectives and appropriate levels of quality and safety are applied to critical components of packaging and transportation systems utilizing a graded approach. Finally, the program ensures processes and procedures are in place to identify appropriate inspections and tests are applied prior to acceptance or use of the package or component, and to identify the status of packaging items, components, etc.

Quality assurance records shall be controlled. The requirements for quality assurance records consist of the following elements:

- Implementing procedures shall be established to assure control of quality records. The purpose of the Quality Assurance Records system is to assure that documented evidence relative to quality related activities is maintained and available for use by INL Contractor, its customers, and/or regulatory agencies, as applicable.
- Approved procedures identify the types of documents to be retained as QA records, as well as those to be retained by the originating organization. Lifetime and Non-Permanent records are retained by Records Management (RMA) or its customers, as appropriate. Records are identified, indexed, and stored in accessible locations.
- QA Records are maintained for periods specified to furnish evidence of activities affecting the quality of structures, systems, and components that are safety-related or important-to-safety. These records include records of design, procurement, fabrication, assembly, inspection, and testing.
- Maintenance records shall include the use of operating logs; results of reviews, inspections, tests, and audits; results from monitoring of work performance and material analyses; results of maintenance, modification, and repair activities; qualification of personnel, procedures, and equipment; records of calibration of measuring and test equipment; and related instructions, procedures, and drawings.
- Requirements for indexing, record retention period, storage method(s) and location(s), classification, preservation measures, disposition of nonpermanent records, and responsibility for safekeeping are specified in approved procedures. Record storage facilities are established to prevent destruction of records by fire, flood, theft, and deterioration due to environmental conditions (such as temperature, humidity, or vermin). As an alternative, two identical sets of records (dual storage) may be maintained at separate locations.
- INL shall retain required records for at least three (3) years beyond the date of last engagement of activities.

## 9.17.1 General

Sufficient records must be maintained by package users to furnish evidence of quality of items and of activities affecting quality. QA records that must be retained for the lifetime of the packaging include:

- Appropriate production-related records that are generated throughout the package manufacturing and fabrication process

- Records demonstrating evidence of operational capability; e.g., completed acceptance tests and inspections
- Records verifying repair, rework, and replacement
- Audit reports, and corrective actions
- Records that are used as a baseline for maintenance
- Records showing evidence of delivery of packages to a carrier and proof that all DOT requirements were satisfied.

## 9.17.2 Generating Records

Package user documents designated as QA records must be:

- Legible
- Completed to reflect the work accomplished and relevant results or conclusions
- Signed and dated or otherwise authenticated by authorized personnel.

QA records should be placed in a records storage area as soon as is feasible to avoid loss or damage. Individual package QA records must be generated and maintained for each package by the package serial number.

## 9.17.3 Receipt, Retrieval, and Disposition of Records

The RMA has overall responsibility for records management for the ATR FFSC. Package users are responsible for maintaining records while they are in process and for providing completed records to the RMA. A receipt control system shall be established, and records maintained in-house or at other locations are to be identifiable and retrievable and not disposed of until prescribed conditions are satisfied.

Records are to be available for inspection upon request.

**Table 9.17-1** - Quality Assurance Records

| Quality Assurance Record | Retention period |
|---|---|
| Design and Fabrication Drawings | LOP+ |
| Test Reports | LOP+ |
| Independent Design Review Comments | LOP+ |
| Safety Analysis Report for Packaging | LOP+ |
| Vendor Manufacturing and Inspection Plans | LOP+ |
| Material Test Report of Certification of Materials | LOP+ |
| Welding Specifications and Procedures | LOP+ |
| Weld Procedure Qualification Record | LOP+ |
| Welder or Welding Operator Qualification Tests | LOP+ |
| Record of Qualification of Personnel Performing Radiographic and PT Reports | LOP+ |
| Weld Radiographs | LOP+ |
| Liquid Penetrant Reports | LOP+ |
| Dimensional Inspection Report for All Features | LOP+ |
| Visual and Dimensional Inspection upon Receipt of Packaging | LOP+ |
| Package Loading Procedure | S+ |
| Unloading Procedure | S+ |
| Maintenance Procedures | LOP+ |
| Repair Procedures | LOP+ |
| Procurement Specifications | LOP+ |
| Personnel Training and Qualification Documentation | LOP+ |
| Maintenance Log | LOP+ |
| Corrective Action Reports | LOP+ |
| Nonconformance Reports (and resolutions) | LOP+ |
| Incident Reports per 10 CFR 71.95 | LOP+ |
| Preliminary Determinations per 10 CFR 71.85 | S+ |
| Routine Determinations per 10 CFR 71.87 | S+ |
| Shipment Records per 10 CFR 71.91(a), (b), (c), (d) | S+ |
| LOP+ Lifetime of packaging plus 3 years S+ Shipping date plus 3 years | |

# 9.18 Audits

As required by the INL Contractor Quality Program, audit requirements shall be established and implemented to satisfy the requirements of the QAPD. These requirements are to be in accordance with:

- 10 CFR 830.122(i), *Criterion 9 – Assessment/Management Assessment*
- 10 CFR 830.122(j), *Criterion 10 – Assessment/Independent Assessment*
- DOE Order 414C, CRD, Attachment 1, 2.c.(1), *Criterion 9 – Management Assessment*
- DOE Order 414C, CRD, Attachment 1, 2.c.(2), *Criterion 10 – Independent Assessment.*

Requirements are implemented to ensure management assessments are performed on a regular basis. Management assessments are planned and conducted in accordance with written procedures. In addition, the program will be independently assessed periodically in accordance with procedures.

Activities pertaining to audits and assessments shall be controlled. The requirements for audits and assessments consist of the following elements:

- Implementing procedures shall be established to assure that periodic audits verify compliance with all aspects of the Quality Assurance Program and determine its effectiveness. Areas and activities to be audited, such as design, procurement, fabrication, inspection, and testing of storage/transportation systems, are to be identified as part of audit planning.
- INL audits supplier Quality Assurance Programs, procedures, and implementation activities to evaluate and verify that procedures and activities are adequate and comply with applicable requirements.
- Audits are planned and scheduled in a manner to provide coverage and coordination with ongoing Quality Assurance Program activities commensurate with the status and importance of the activities.
- Audits are performed by trained and qualified personnel not having direct responsibilities in the areas being audited and are conducted in accordance with written plans and checklists. Audit results are documented and reviewed by management having responsibility for the area audited. Corrective actions and schedules for implementation are established and recorded. Audit reports include an objective evaluation of the quality-related practices, procedures, and instructions for the areas or activities being audited and the effectiveness of implementation.
- Responsible management shall undertake corrective actions as a follow-up to audit reports when appropriate. The Quality Assurance Management (QAM) shall evaluate audit results for indications of adverse trends that could affect quality. When results of such assessments so indicate, appropriate corrective action will be implemented.

The QAM shall follow up on audit findings to assure that appropriate corrective actions have been implemented and directs the performance of re-audits when deemed necessary.